Université de Montréal

Propriétés anionophores et antibactériennes de sels d'imidazolium et benzimidazolium

par
Claude-Rosny Elie

Département de Chimie
Faculté des arts et des sciences

Thèse présentée à la Faculté des études supérieures et postdoctorales en vue de l'obtention du grade de *philosophiæ doctor* (Ph.D.) en chimie.

juin 2016

Université de Montréal
Faculté des études supérieures et postdoctorales

Cette thèse intitulée:

Propriétés anionophores et antibactériennes de sels d'imidazolium et benzimidazolium

Présentée par :
Claude-Rosny Elie

A été évaluée par un jury composé des personnes suivantes :

Dre. Joelle N. Pelletier, présidente-rapporteure
Dre. Andreea R. Schmitzer, directrice de recherche
Dr. Michel Lafleur, membre du jury
Dr. Normand Voyer, examinateur externe
Dr. Rikard Blunck, représentant de la doyenne de la Faculté des arts et des sciences

Résumé

L'éclosion de bactéries résistantes aux antibiotiques constitue un problème sérieux auquel fait face notre système de santé. L'une des stratégies récemment proposées afin de s'attaquer efficacement et irréversiblement à ces microorganismes multi-résistants est de cibler directement leur membrane via l'action de molécules induisant un débalancement électrolytique de part et d'autre de cette dernière. Parallèlement, ces mêmes agents peuvent aussi avoir des applications dans le traitement de maladies originant des dysfonctions du transport ionique, comme la fibrose kystique. À cet égard, nous présentons dans cette thèse différents sels d'imidazolium et benzimidazolium *N,N*-disubstitués possédant un potentiel à la fois antimicrobien et ionophore. Notre approche se résume d'abord en un volet mécanistique où une série de modifications structurelles ont été apportées à des sels d'imidazolium et benzimidazolium afin d'observer comment ces changements modulent l'efficacité du transport d'anions dans la membrane artificielle d'un liposome. Nous avons à ce titre pu conclure que l'espèce formée de deux bras aromatiques phényléthynylbenzyl, disposées symétriquement de part et d'autre d'un cation imidazolium, induisait le meilleur transport des anions chlorures, au travers d'une membrane de liposomes, à des concentrations de l'ordre du µM. En outre, les monocations imidazolium et benzimidazolium flanqués d'un contre-anion NTf_2^- ont conduit à une activité ionophore plus rapide. Qui plus est, en s'appuyant sur ces résultats, nous avons présenté le premier exemple, à notre connaissance, d'un transporteur d'anions et de cations, contenant le cation benzimidazolium et capable d'agir aussi bien dans des liposomes que dans des bactéries. Dans un second temps, les meilleurs agents ionophores ont été étudiés dans les membranes plus complexes des bactéries et des globules rouges humains pour vérifier leur effet bactéricide et leur innocuité. Le design de nos transporteurs formés d'un espaceur luthidine a ainsi permis d'obtenir un agent antimicrobien efficace dans des bactéries gram positives et négatives (*B. thuringiensis* et *E. coli*) avec une toxicité limitée de l'ordre de 10% sur les globules rouges humains à ses concentrations bactéricides.

Mots-clés : Sel d'imidazolium, sel de benzimidazolium, bactéries, bactéricide, transport anionique, anionophore, transport transmembranaire, auto-assemblage, liposome.

Abstract

The emergence of antibiotic resistant bacteria is a serious problem that our health system faces. One recently proposed strategy to effectively and irreversibly kill these multi-resistant microorganisms is to directly target the integrity of their membrane, using small molecules able to induce an electrolyte imbalance. Moreover, the same molecules may find applications in the treatement od diseases originating from the dysfunction of ion transport, such as cystic fibrosis. Herein we present different imidazolium and benzimidazolium salts N,N-disubstituted with both antimicrobial and ionophoric potential. We first performed mechanistic studies where different structural changes have been made to the imidazolium and benzimidazolium salts to observe how these modifications modulate the efficiency of the anion transport in artificial membrane liposomes. We were able to conclude that the species formed of two aromatic arms phenylethynylbenzyl arranged symmetrically on either side of an imidazolium cation, induced a better transport of chloride anions, through a membrane of liposomes at the micromolar range. In addition, monocations imidazolium and benzimidazolium flanked with an NTf_2^- anion led to faster ionophore activity. Moreover, based on these results we presented the first example, to our knowledge, for an anions and cations benzimidazolium-based transporter, acting as well in liposomes as in bacteria. Secondly, the best anionophore agents were analyzed in more complex bacterias and human red blood cells membranes to study their bactericidal potential and innocuity. Among all the benzimidazolium salts studied, we identified one compound, which presents interesting antibacterial properties as a result of its ability to induce an electrolytic imbalance and to disrupt the integrity and the potential of the bacterial membranes. At the same time this antibacterial agent presented a low toxicity to human cells in bacteriostatic range concentrations.

Keywords: Imidazolium salt, benzimidazolium salt, bacteria, bactericide, anionic transport, anionophore transmembrane transport, self-assembly, liposome.

Table des matières

Tableaux

Liste des figures

Liste des schémas

Liste des abréviations

α-CD	alpha cyclodextrine
ACN	Acétonitrile
ADP	Adénosine diphosphate
ADN	Acide désoxyribonucléique
AMP	Adénosine monophosphate
AO	Acridine orange
ATP	Adénosine triphosphate
CB7	Cucurbit-7-uril
CF	Fibrose kystique (Cystic Fibrosis)
CFTR	Régulateur de conductance transmembranaire associé à la fibrose kystique (Cystic Fibrosis Transmembrane conductance Regulator)
δ	Déplacement chimique
d	Doublet
dd	Doublet de doublets
DisC$_2$5	Iodure de 3,3′-diéthylthiadicarbocyanine (3,3′-diethylthiadicarbocyanine iodine)
DPPC	1,2-Dipalmitoyl-sn-glycéro-3-phosphocholine
DMF	Diméthylformamide
DMSO	Diméthylsulfoxyde
EC$_{50}$	Concentration effective à laquelle la moitié de la réponse maximale est atteinte
ESI (MS)	Spectrométrie de masse à ionisation par électronébuliseur (ElectroSpray Ionization Mass Spectrometry)
EYPC	Phosphatidylcholine issue de jaunes d'œuf (Egg Yolk Phosphatidylcholine)
GUV	Vésicule unilamellaire géante (Giant unilamellar vesicle)
J	Constante de couplage
HPTS	8-Hydroxypyrène-1,3,6-trisulfonate de trisodium
HRMS	Spectrométrie de masse à haute résolution
IC$_{50}$	Concentration inhibitrice médiane (half maximal inhibitory concentration)

logP	Coefficient de partage octanol-eau
LUV	Large vésicule unilamellaire (Large unilamellar vesicle)
m	Multiplet
MAPK	Mitogen-activated protein kinase
MIC	Concentration minimale inhibitrice (Minimal inhibitory concentration)
MLV	Vésicule multilamellaire (Multilamellar vesicle)
MTT	Bromure de 3-(4 5-diméthylthiazol-2-yl)-2 5-diphényltétrazolium
PBS	Tampon phosphate salin (Phosphate buffer saline)
ppm	Partie par million
R	Groupement général
RMN	Résonance magnétique nucléaire
s	Singulet
SEM	Microscopie électronique à balayage (Scanning electron microscopy)
SUV	Petite vésicule unilamellaire (Small unilamellar vesicle)
t	Triplet
td	Triplet de doublets
TBAB	Bromure de tétra-*n*-butylammonium (Tetra-*n*-butylammonium bromide)
THF	Tetrahydrofurane

Remerciements

Je profite de cette opportunité pour tout d'abord remercier ma directrice de recherche, Andreea Schmitzer pour son accueil et ses conseils tout au long de mes quatre années de doctorat et les deux stages d'été, à titre d'étudiant au baccalauréat, que j'ai effectués au sein de son groupe de recherche. Mes sincères remerciements vont également aux autres membres du jury soit : Pre. Joelle N. Pelletier, Pr. Michel Lafleur, Pr. Normand Voyer et Pr. Rikard Blunck, représentant de la doyenne, pour leur temps et pour avoir accepté de corriger et juger ce travail. Je tiens également à souligner l'apport de mes collègues de travail avec qui j'ai cheminé tout au long de cette expérience enrichissante.

Je souhaiterais également exprimer ma gratitude à l'ensemble du corps professoral présent et passé du département de chimie de l'Université de Montréal, de même qu'à toute l'équipe de techniciens pour leur enseignement et leur assistance durant mes années d'étude et mes recherches; en particulier Pre. Joelle N. Pelletier, Pr. Michel Lafleur et Pr. Jefferey Keillor pour m'avoir donné accès à leurs laboratoires et leurs installations.

Enfin, merci à ma famille et amis pour leurs encouragements et leur soutien et tout spécialement à mes parents, ma principale source de motivation.

Chapitre 1   Introduction générale : Transport anionique

1.1. Enjeux socio-épidémiologiques

L'un des plus grands enjeux auquel fait face la médecine moderne est la lutte aux bactéries résistantes. En effet, selon un récent rapport gouvernemental du *Centers for Disease Control and Prevention*, chaque année plus de 2 millions d'américains sont infectés par des souches résistantes aux antibiotiques et 23 000 en meurent, soit plus que le nombre d'homicides répertoriés aux USA.[1] Suite à la découverte de la pénicilline par Fleming au début du XXe siècle, et de la streptomycine en 1952, par Waksman *et al.*, un effort considérable s'est déployé pour fourbir l'arsenal antibactérien commercialement disponible.[1,2,3] Or de nos jours, cet effort est oblitéré par la prescription massive d'antibiotiques à large spectre, tant bien chez l'humain que chez les animaux d'élevage, ce qui concoure à développer de nouvelles souches de microorganismes résistants.[4] Dans cette conjoncture socio-épidémiologique inusitée, de nouvelles alternatives antibactériennes s'imposent, mais à priori il incombe à la communauté scientifique de mieux saisir les processus par lesquels une bactérie contrecarre les effets d'un agent antimicrobien. Parmi les mécanismes connus par lesquels les résistances contre les antibiotiques peuvent principalement se développer citons la modification du récepteur ciblé par l'antibiotique, la modification enzymatique de l'agent antimicrobien par des enzymes bactériennes et enfin le changement de la perméabilité membranaire du microorganisme face au médicament.[5] Ce dernier point a suscité un intérêt grandissant ces dernières années de la part de plusieurs groupes de recherche qui ont tenté de cibler la membrane bactérienne afin de détruire les cellules pathogènes. En effet, l'énergie requise par une bactérie pour reconstruire sa propre membrane endommagée outrepasse largement celle nécessaire aux mécanismes d'inactivation de l'antibiotique ou d'altération de son récepteur.[6] Ce faisant, la voie d'attaque membranaire contre les parasites est une cible de choix dans la lutte aux bactéries multirésistantes.

Parallèlement, une pléthore d'autres pathologies, appelées canalopathies, sont issues des processus dysfonctionnels au niveau de la membrane cellulaire. Citons par exemple la fibrose kystique et les maladies rénales, telles que le syndrome de Bartter.[7-11] Dans le cas de la fibrose kystique, une mutation du gène *Cystic Fibrosis Transmembrane Conductance Regulator* (CFTR) sur le chromosome 7 conduit à une anomalie du canal

anionique CFTR transportant des chlorures. Il en résulte alors un débalancement électrolytique au niveau des cellules du système digestif et respiratoire, provoquant une augmentation, parfois létale, de la viscosité du mucus.[12] Les travaux de Ashcroft, datant d'à peine 15 ans, ont jeté les bases de ce sujet en mettant en lumière le rôle des protéines membranaires transporteuses d'anions.[7] À cet égard, différents groupes de recherche, dont nous survolerons plus loin les travaux, ont subséquemment proposé de nombreuses molécules synthétiques capables de mimer et ainsi compenser l'effet des transporteurs peptidiques naturels dysfonctionnels. En exploitant ainsi les propriétés de perturbateurs de membrane et à la fois de transporteurs d'anions, il devient alors envisageable de conférer à certaines classes de molécules un potentiel sans précédent dans le traitement aussi bien des infections bactériennes que des channelopathies.

1.2.   Description de la membrane phospholipidique

La membrane cellulaire joue le rôle de barrière délimitant le cytoplasme de l'environnement extérieur de la cellule. Elle est par ailleurs le siège d'échanges permanents, entre le milieu interne et externe, assurant la survie des organismes vivants. *Ab initio*, sa composition plutôt complexe et hétérogène, est constituée de phospholipides et de protéines formant une mosaïque souple et fluide. Les phospholipides qui la composent sont des molécules amphiphiles formées d'une tête polaire et de deux chaînes alkyles apolaires.[15,16] Tandis que les têtes hydrophiles des phospholipides s'orientent vers les milieux aqueux, les chaînes hydrophobes, quant à elles, se regroupent dans un enchevêtrement maintenu essentiellement par des interactions hydrophobes. À travers cette structure, certains éléments tels que l'eau, le dioxygène et le dioxyde de carbone peuvent aisément diffuser, alors que les molécules plus larges et les composés chargés, notamment les anions, requirent cependant une médiation, d'où la présence de protéines transporteuses d'anions enclavées dans la membrane cellulaire (Figure 1.1).[15,16]
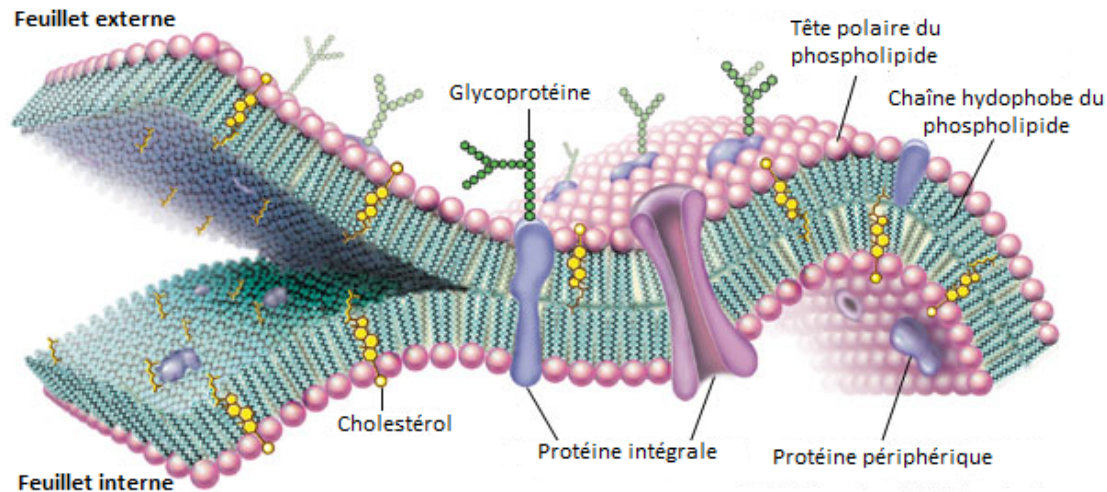
Figure 1.1. Représentation d'une membrane cellulaire (Adapté de Britanica 2007).[17]

Le transport des anions assisté par les protéines transmembranaires peut s'effectuer soit passivement selon un gradient électrochimique ou en sens inverse grâce à un apport énergétique (ex: via l'hydrolyse de l'adénosine triphosphate, ATP).[18] D'un point de vue mécanistique, en outre, qu'il soit passif ou actif le transport ionique se définit également en termes de stœchiométrie et de direction des charges. Ainsi, nous parlons d'un processus uniport lorsque la protéine transporte un seul ion à la fois, d'un processus antiport lorsque deux ions sont transportés en sens opposé par la protéine et finalement d'un mécanisme symport si les deux ions impliqués simultanément dans le transport suivent la même direction. Par abus de langage toutefois le terme symport est souvent associé au mot *co-transport,* bien que ce dernier définisse en réalité les processus aussi bien de symport que d'antiport.
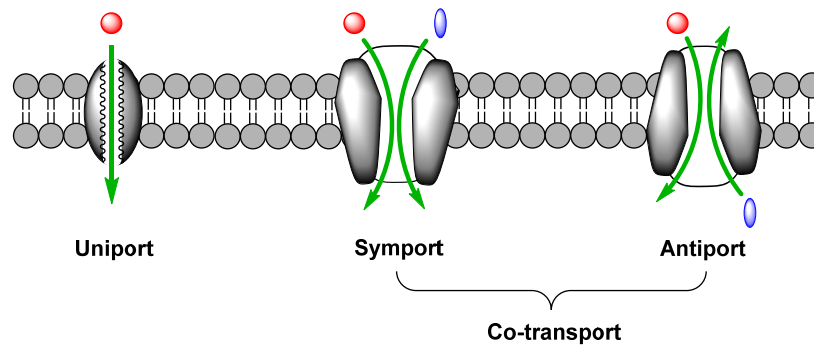
Figure 1.2. Mécanismes de transport ionique dans une bicouche.

1.3.   Techniques analytiques étudiant le transport transmembranaire

1.3.1. Les liposomes

Considérant la grande complexité des membranes cellulaires et les nombreux processus biologiques y ayant lieu, faisant pour certains encore l'objet de conjectures mécanistiques, l'une des méthodes les plus couramment utilisées pour étudier le transport anionique, de façon plus simplifiée, consiste à utiliser des liposomes. Le liposome est une vésicule constituée d'une double couche de phospholipides formant une barrière hydrophobe qui sépare le compartiment aqueux intérieur du milieu hydrophile extérieur. Leur taille varie de quelque nanomètres à plusieurs centaines de nm et permet ainsi de les catégoriser selon leur diamètre en : petits (SUVs), grands (LUVs) et géants (GUVs) pour les liposomes unilamellaires (Figure 1.3), on parle enfin de liposomes multilamellaires (MLVs) lorsque plusieurs couches de phospholipides sont présentes.[19]
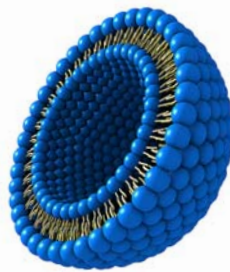
Figure 1.3.   Représentation d'un liposome unilamellaire.

La préparation des liposomes est d'une grande simplicité et se résume à hydrater, avec le solvant ou le tampon qui constitue la phase hydrophile interne, un film de phospholipides. Ensuite, la vésicule est contrainte à adopter une certaine taille par un procédé mécanique appelé extrusion. Puis des cycles de congélation/décongélation favorisent le volume d'encapsulation de la vésicule. Des étapes subséquentes de dialyse ou de passage sur une colonne d'exclusion stérique permettent enfin de séparer les composantes n'ayant pas été trappées dans le liposome.[18] La vaste quantité de phospholipides disponibles sur le marché permet de varier *ad lib* la composition de la membrane du liposome et *de facto* ses propriétés. Au cours des prochains chapitres, nous parlerons essentiellement des liposomes préparés à partir de deux phospholipides soit la

phosphatidylcholine extraite du jaune d'œuf (EYPC) et la 1,2-dipalmitoyl-*sn*-glycéro-3-phosphocholine (DPPC) (Figure 1.4).

R, R' = Chaîne alkyle variable

EYPC   **DPPC**
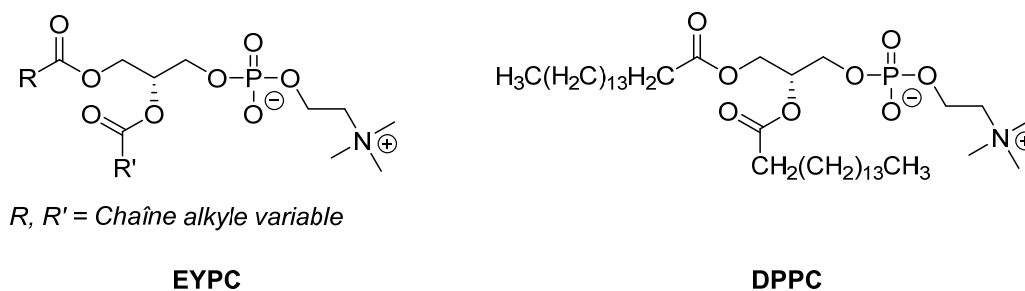
Figure 1.4.   Structure chimique des phospholipides EYPC et DPPC.

Notons, à ce titre que la présence de deux chaînes alkyles dans ces phospholipides donne lieu à une géométrie globalement cylindrique à la molécule, ce qui favorise la formation d'un liposome. Par contraste les tensioactifs n'ayant qu'une seule chaîne alkyle conduisent plutôt à la formation de micelles. En outre, en raison de l'absence d'insaturations sur les deux résidus d'acide palmitique de la DPPC, cette dernière bénéficie d'une stabilisation supplémentaire de ses groupements acyles par des interactions de Van der Waals. Cela confère aux membranes de DPPC une plus grande température de transition gel-fluide de l'ordre de 41 ºC, versus une gamme entre -15 ºC et -7 ºC pour la EYPC, d'où leur plus grande rigidité à température ambiante.[20] Cette propriété des membranes de DPPC sera d'ailleurs exploitée lors des essais que nous verrons ultérieurement. Cependant, il est important de noter que dans l'étude de l'activité des transporteurs aussi bien synthétiques que naturels, des processus d'interactions avec les phospholipides sont à prévoir. En effet, par exemple dans un liposome, la composition en phospholipides, le rapport entre transporteur/lipide et la température sont d'autant d'éléments qui peuvent moduler l'affinité du transporteur pour la bicouche. Dans certains cas de figure le processus exothermique qui favorisent l'association d'une molécule (ex.: une protéine) à une membrane à l'état fluide peut basculer vers un mécanisme endothermique, lorsque la température baisse, créant ainsi une barrière énergétiquement défavorable à la liaison protéine-membrane.[21] Ces facteurs, comme la température, qui peuvent potentiellement influencer l'interpréatation d'analyses effectuées avec certains

phopholipides (ex.: DPPC) nécessitent donc, en cas de doute, d'avoir recours à d'autres méthodes d'appoint, tel que nous le verrons au chapitre 6.

Depuis la première génération de modèle de liposomes décrite par Bangham, d'autres formes plus évoluées de vésicules furent élaborées.[22,23] Ainsi, il est également possible de préparer des mélanges hétérogènes en ajoutant du cholestérol à la membrane, ce qui contribue à modifier sa fluidité et sa perméabilité en fonction de la température. De surcroît, la membrane artificielle peut également contenir des agents de reconnaissance, tels que des anticorps, des immunoglobulines ou des chaînes polyéthylène glycol (PEG) afin d'en améliorer la stabilité et la longévité.[22,23] Dans le cadre de cette thèse, nous n'étudierons que les liposomes de première génération, ayant pour unique composition des phospholipides (EYPC ou DPPC) sans ajout supplémentaire à la membrane.

1.3.2. Modus operandi d'analyse du transport anionique

Le transport d'anions au travers de la membrane est typiquement mesuré par la détection de ces derniers via diverses techniques analytiques. Par exemple, la spectroscopie RMN ^{35}Cl permet de mesurer la translocation de l'espèce anionique chlorure (Cl$^-$) dans les membranes au moyen d'un agent paramagnétique, tel que le Co^{2+}.[18] En effet, ce dernier, imperméable à la membrane lipidique, reste à l'extérieur du liposome en concentration constante, tandis que l'intérieur de la vésicule contient des anions chlorures. Lors de l'efflux de ces anions sous l'effet du transporteur, l'agent paramagnétique produit un changement proportionnel à la concentration extravésiculaire de chlorures sur le profil spectroscopique des signaux RMN associés au ^{35}Cl, par un déblindage et un élargissement de ses pics. Ces derniers peuvent être comparés à un spectre RMN de ^{35}Cl en absence de Co^{2+}, ce qui permet de quantifier la concentration de chlorures ayant diffusé hors du liposome.[18] Il existe également des méthodes potentiométriques, utilisant des électrodes, afin de mesurer les concentrations d'anions transportés. Parmi les différentes catégories de méthodes potentiométriques, mentionnons entre autres la technique de BLM (black lipid membrane) qui se résume à mesurer un courant de part et d'autre d'une membrane artificielle «peinte» sur un orifice au niveau d'un support solide.[24] Bien que cette technique soit fiable et décrite abondamment dans la

littérature des dernières décennies, il n'en demeure pas moins qu'elle requiert une certaine dextérité et est associée à une grande instabilité de la membrane, conjuguée à une forte sensibilité de l'électrode aux moindres interférences électromagnétiques de l'environnement (téléphone, ordinateur etc), ce qui en fait au final une méthode parfois sujette à certains artéfacts expérimentaux.

L'une des techniques les plus utilisées et fiables pour caractériser la diffusion anionique, privilégiée pour sa rapidité, son faible coût et la simplicité de son interprétation demeure la méthode basée sur la fluorescence d'une sonde organique.[18] Elle permet en outre de tirer des informations autant qualitatives que quantitatives sur les processus cinétiques de transport, contrairement à la BLM souvent utilisée qu'à des fins qualitatives. Pour les besoins de notre étude, nous nous pencherons essentiellement sur deux fluorophores soit le 8-hydroxy-1,3,6-pyrènetrisulfonate (HPTS) et le nitrate de bis-*N*-méthylacridinium (lucigénine) (Figure 1.5).
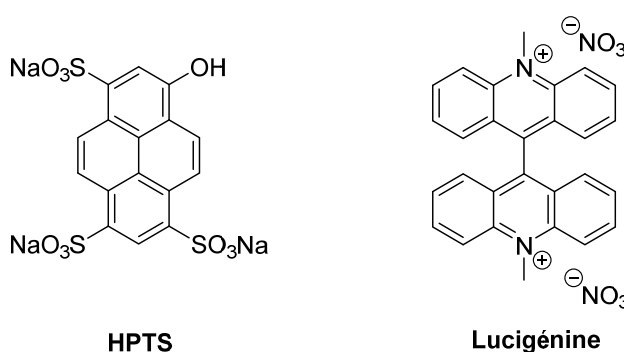
HPTS   **Lucigénine**

Figure 1.5.   Structure chimique des sondes fluorescentes HPTS et lucigénine.

Le HPTS est une molécule qui possède un profil de fluorescence pH-dépendant. Les formes protonnées et déprotonnées du HPTS ont respectivement une longueur d'onde d'excitation à 403 et 460 nm, tandis qu'elles émettent toutes deux à 510 nm.[18] Il est ainsi possible, en mesurant le ratio des intensités des formes déprotonnée (I_0) sur protonnée (I_1), en temps réel, d'évaluer le niveau d'alcalinisation versus d'acidification de l'intérieur du liposome. Le protocole standard consiste à incorporer le HPTS dans des liposomes contenant une solution ionique (e.g: Na^+A^-; A étant un anion inorganique). La diffusion des anions hors du liposome, facilitée par la présence d'un transporteur, entraîne alors

dans leur efflux un proton provenant du HPTS, selon un processus symport A^-/H^+. Cela augmente la fluorescence de l'espèce alcaline du HPTS et donc du ratio (I_0/I_1) des formes déprotonnées sur protonnées. Dans un système de co-transport, l'efflux massif d'anions A^- est dans un second temps compensée par l'entrée d'anions présents dans le milieu extravésiculaire. Le proton suit alors le nouveau gradient, ce qui a pour résultat la reprotonnation du HPTS et conséquemment une diminution du ratio de fluorescence (I_0/I_1) de la molécule. La courbe caractérisant ces deux processus de déprotonnation et reprotonnation du HPTS peut donc être étudiée afin de conclure de l'échange anionique de part et d'autre de la membrane (Figure 1.6a).
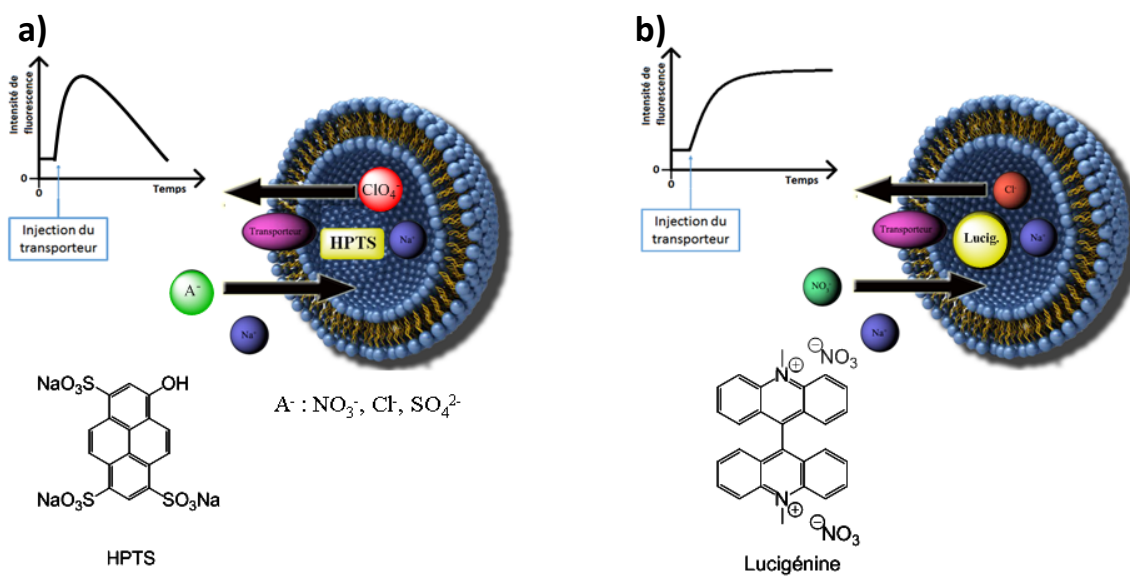
Figure 1.6. Principe expérimental des essais de transport anionique suivi par la fluorescence **a)** du HPTS et **b)** de la lucigénine.

Fonctionnant de façon plus simple, la lucigénine est une autre sonde fluorescente permettant de suivre les échanges anioniques (Figure 1.6b). Elle possède un maximum d'excitation vers 372 nm et sa bande d'émission se situe à 505 nm.[25a] Le principe de cette technique de mesure repose sur le fait que le cation bis-acridinium, formant la lucigénine, subit sélectivement une extinction de fluorescence en présence d'anions halogénures (ex. Cl^-)[18] selon un processus de transfert non radiatif d'électrons. Le mécanisme proposé implique que la lucigénine, à l'état excité, accepte un électron de valence de l'halogénure vers son orbitale fondamentale. Tel qu'illustré à la figure 1.7, les espèces radicalaires

respectives se stabilisent ensuite, tandis que l'électron sur l'orbitale excitée de la lucigénine (Lucigénine^{+}•) est à son tour tranféré vers le niveau fondamental de l'halogénure.[25b]

Relaxations vibrationnelles omises afin de clarifier le diagramme
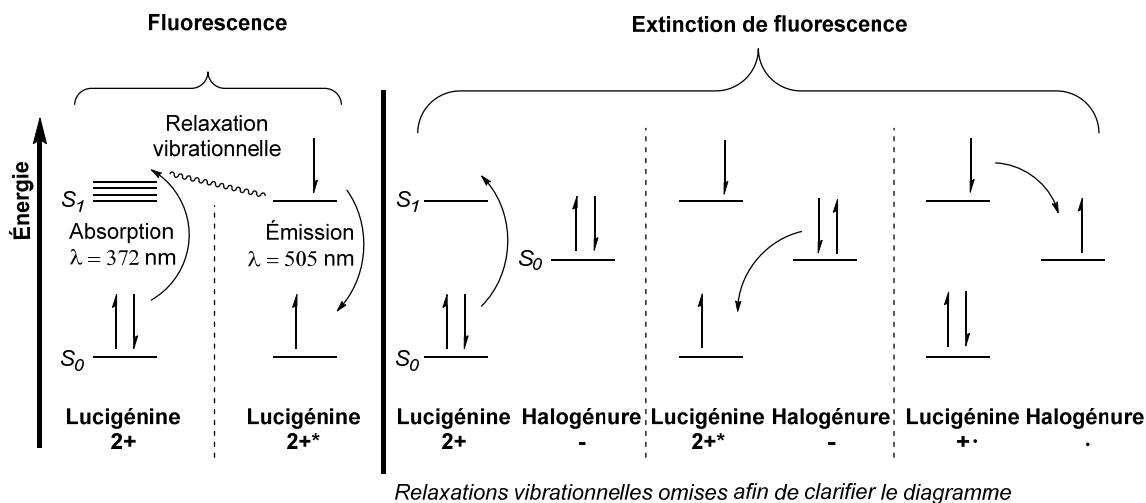
Figure 1.7.   Diagramme de Jablonski illustrant la fluorescence de la lucigénine et son processus d'extinction par un halogénure.

Tirant profit de cette propriété on peut donc incorporer dans un liposome de la lucigénine, baignant dans une solution de NaCl, tandis que le milieu extravésiculaire est constitué par exemple de NaNO$_3$, n'ayant aucun effet sur la fluorescence de la sonde incorporée dans le liposome. Sous l'effet d'un transporteur, l'efflux des Cl$^-$ est associé à une augmentation proportionnelle de la fluorescence de la lucigénine, qui est mesurée en fonction du temps (Figure 1.6b). Enfin, l'intensité maximale de fluorescence peut aussi être exprimée en terme de pourcentage d'efflux total des Cl$^-$ suite à la lyse des liposomes avec un détergent (ex. : Triton, SDS) pour en libérer tout le contenu.

1.4.   Brève revue de littérature sur les transporteurs transmembranaires synthétiques

1.4.1.   Transporteurs mobile versus canaux transmembranaires

Tel qu'évoqué d'entrée de jeu, les défaillances dans le fonctionnement des mécanismes biologiques du transport des anions sont associées à de graves maladies chez

l'humain. En contre-partie, ces mêmes débalancements électrolytiques peuvent être exploités dans une stratégie antimicrobienne si on peut cibler sélectivement des microorganismes pathogènes. Le concept de transport ionique est donc solidaire du criterium de survie des cellules saines tant bien que malignes, ce qui, dans l'observation des manifestations de ce phénomène membranaire, a apporté une riche moisson de données nouvelles aux chimistes supramoléculaires. Il n'en fallu pas plus pour que nombreux furent les chercheurs qui se sont penchés sur le design d'anionophores synthétiques, mimant l'action des protéines transporteuses d'anions, que l'on peut en outre catégoriser en deux familles, soit les transporteurs mobiles et les canaux transmembranaires. Le canal est un échafaudage moléculaire qui s'insère au travers des phopholipides de la membrane, créant de telle sorte un passage favorable à la diffusion des anions de part et d'autre de la bicouche phospholipidique (Figure 1.8a). Un transporteur mobile est quant à lui une structure, souvent moins complexe, capable de lier un anion d'un côté de la membrane, diffuser avec ce dernier au travers de la bicouche sous forme de complexe, puis le relarguer de l'autre côté de la membrane (Figure 1.8b).[18]
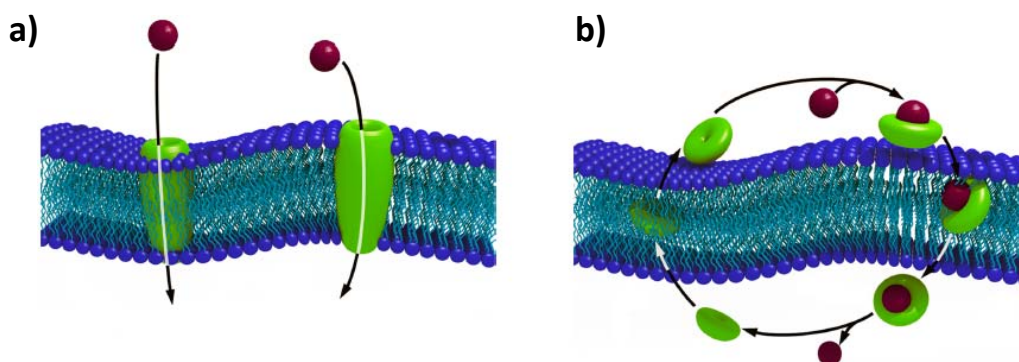
Figure 1.8.   Représentation **a)** du canal transmembranaire et **b)** du transporteur mobile.

1.4.2. Évolution des canaux transmembranaires

L'étude des canaux transmembranaires est antérieure à celle sur les transporteurs mobiles synthétiques. Elle trouve sa genèse dans les travaux de Tomich *et al.* qui élaborèrent un peptide basé sur la structure du récepteur ionotrope de la glycine (GlyR), impliqué dans de nombreuses fonctions du système nerveux central.[26,27] Ils furent en mesure de démontrer, par des tests dans des liposomes, que ce peptide synthétique forme

un oligomère assemblé en canal au travers de la bicouche, permettant ainsi la diffusion des anions chlorures (Figure 1.9 composé **1.1**).[26,27] Dans un même esprit, le groupe de Gokel a synthétisé un peptide constitué d'un cœur polaire de proline flanqué de deux chaînes d'acides aminés hydrophobes, donnant lieu à une molécule analogue à un phospholipide, capable de tailler des pores dans une membrane de liposome (Figure 1.9 composé **1.2**).[28,29] L'équipe du Pr. Voyer s'est quant à elle penchée sur les propriétés d'un peptide synthétique, formé d'éthers couronnes, mimant l'action de l'alpha-hémolysine (Figure 1.9 composé **1.3**).

1.1

1.2

1.3
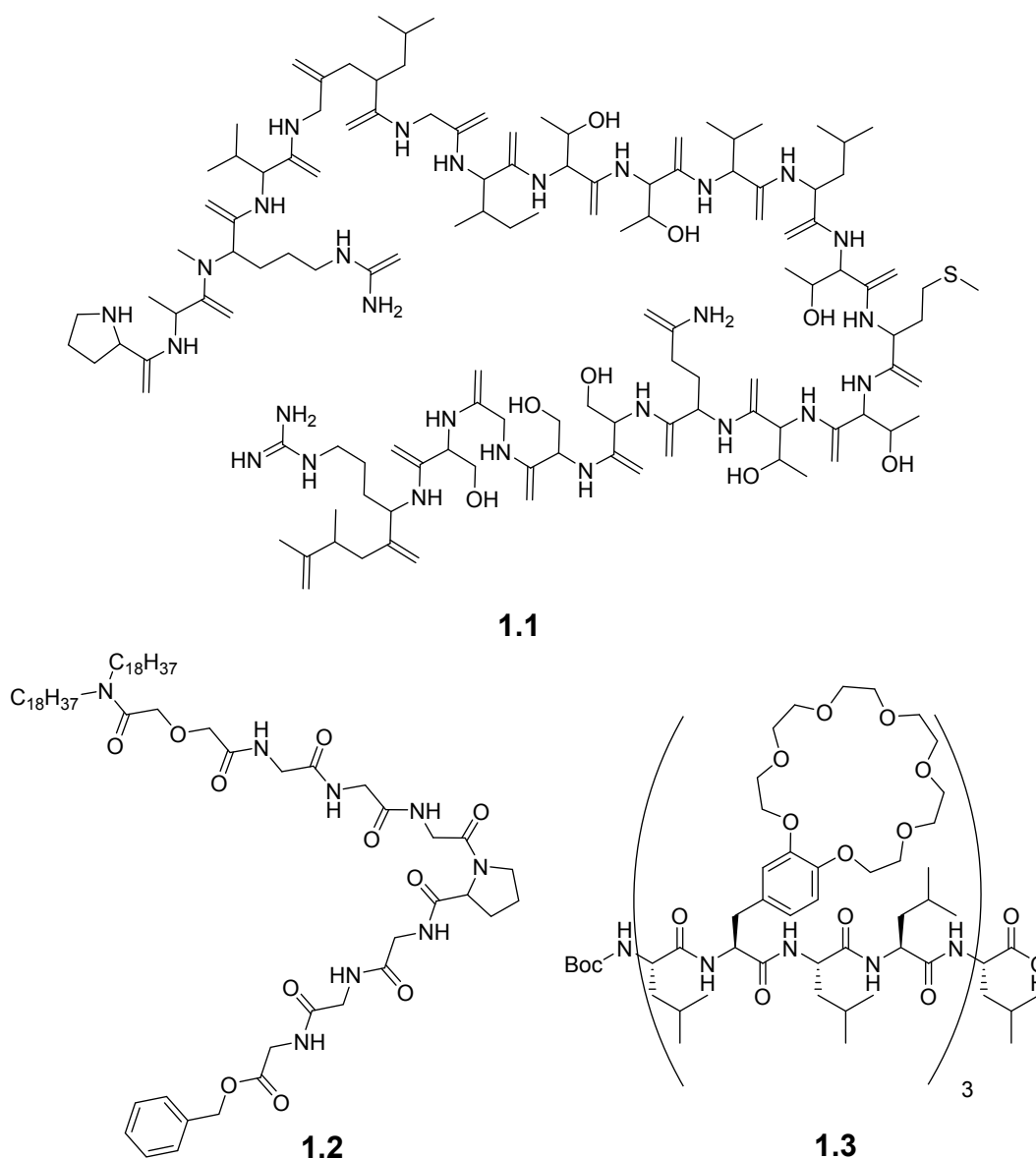
Figure 1.9.   Structure des canaux peptidiques et semi-peptidiques **1.1**, **1.2** et **1.3**.

Capable de se fixer à la surface notamment des cellules cancéreuses et d'en percer la membrane, cet ingénieux auto-assemblage s'avère efficace pour provoquer la lyse des micro-organismes, mais en contre partie présente aussi une certaine toxicité sur les cellules saines.[30] Les peptides présentent tous malheureusement le désavantage d'être sujets à l'action des peptidases bactériennes qui les dégradent. Pour contourner ce mécanisme de défense, le groupe du professeur Matile s'inspira de l'amphotéricine B, un antifongique naturel amphiphile, pour élaborer une chaîne polyène formant une tige rigide perçant les membranes lipidiques (Figure 1.10).[31,32,33] L'évolution de leur modèle vers des canaux plus efficaces, les mena à substituer les groupements hydroxyles de la chaîne par des fluores, un atome reconnu pour sa capacité à induire des ponts hydrogène. Ceci permis à Matile *et al.* d'émettre l'hypothèse que leurs tiges rigides fluoro-aromatiques agissaient à titre de canaux dans les liposomes, promulguant un mécanisme d'échange entre les ions Cl⁻/OH⁻, au cours duquel, par ailleurs, les anions se déplacent par bonds d'un pont hydrogène à l'autre, le long du canal.[31-33]
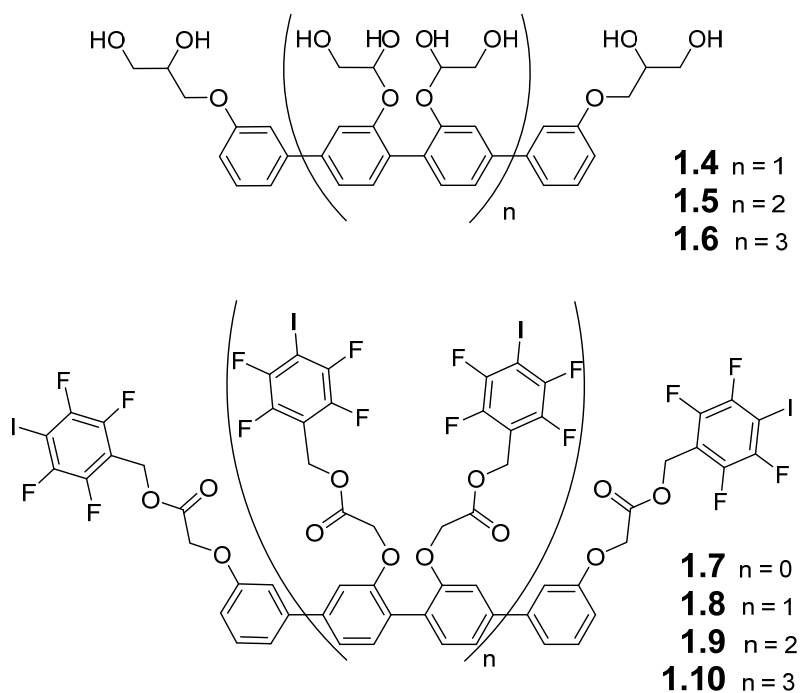
Figure 1.10. Structure des canaux polyènes de Matile *et al.*[31-33]

Dans un effort pour mieux comprendre le mode d'auto-assemblage gouvernant la formation de ces canaux, le même groupe proposa en outre d'intercaler le long des tiges poly-aromatiques des groupements électrodonneurs (Figure 1.11),[31-33] afin de favoriser les interactions supramoléculaires π-π entre le squelette aromatique et l'intercalant dialkoxynaphtalène. Cette structure organisée en forme d'un conduit à quatre faces inséré dans une membrane lipidique créerait ainsi un chemin préférentiel emprunté par les anions Cl⁻/OH⁻. L'équipe de Matile poussa davantage son analyse des interactions π en synthétisant ensuite un squelette rigide formé d'une succession de groupements naphthalènediimides (NDI) entre lesquels s'intercalent un espaceur tétraméthylbenzène.[34-37] Cet agencement singulier donna lieu à la formation de canaux rigides s'insérant dans la membrane d'un liposome et offrant la possibilité aux anions de glisser le long des groupements NDI grâce aux interactions anion- π.
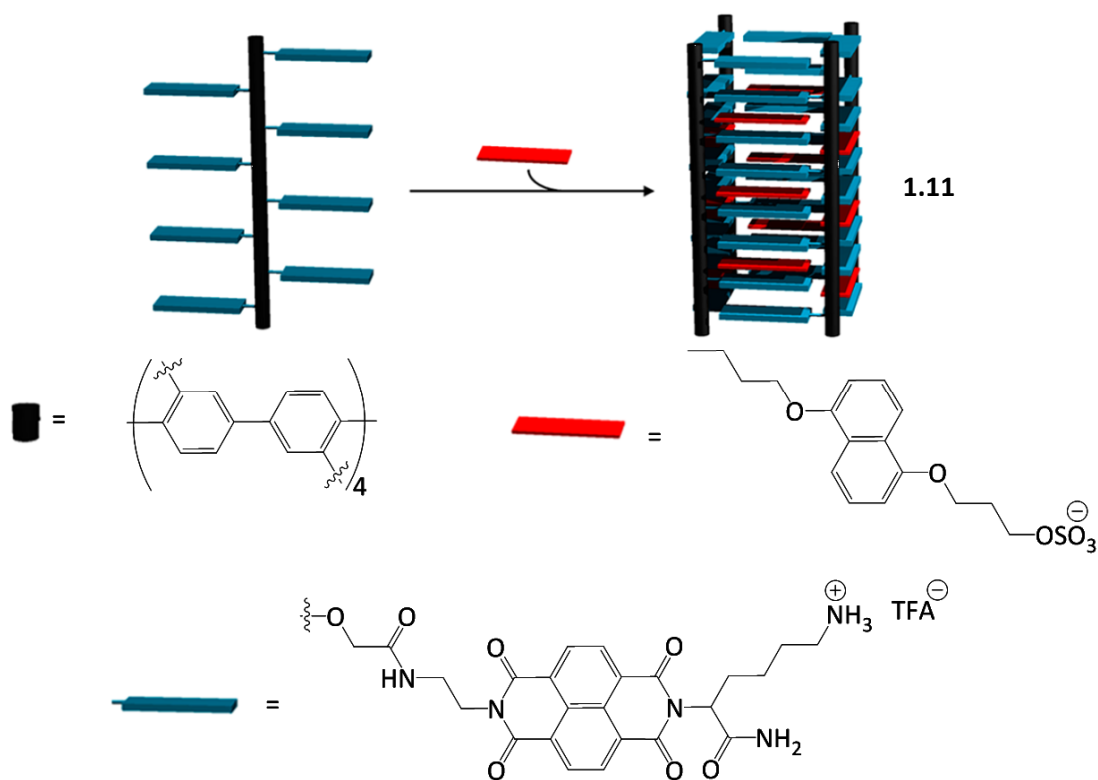
Figure 1.11. Structure du canal rigide de naphthalenediimide **1.11** assemblé par des interactions supramoléculaires π-π.[31-33]

À la suite des travaux de Matile *et al.* et leurs canaux tubulaires, Gin *et al.* ont mis pour leur part au point un canal pH-dépendant basé sur la structure de deux cyclodextrines modifiées pouvant sélectivement faciliter la diffusion des anions par rapport aux cations.[38,39] En effet, en conditions acides, les groupements amino à la base de la cyclodextrine étant protonnés, favorisent des interactions anions-ammonium d'où le transport sélectif (Figure 1.12 composé **1.12**). Similairement, le groupe de Tecilla a pour sa part exploité les propriétés des calixarènes, dont la cavité est toutefois plus petite que les cyclodextrines, afin d'élaborer un canal formé d'un calixarène greffé à une chaîne spermidine.[40] Cette dernière lorsque protonnée au niveau de ses fonctions amines, en milieu acide, génère à l'intérieur du canal une charge positive induisant une force de répulsion des cations et d'attraction des anions. Tecilla *et al.* ont ainsi pu démontrer la sélectivité de leur système par des tests de transport dans des liposomes renfermant la sonde HPTS pH-dépendante (Figure 1.12 composé **1.13**).[40]

$R = NH(CH_2)_3NH_2^+(CH_2)_4NH_3^+$, $R'=CH_2OBn$
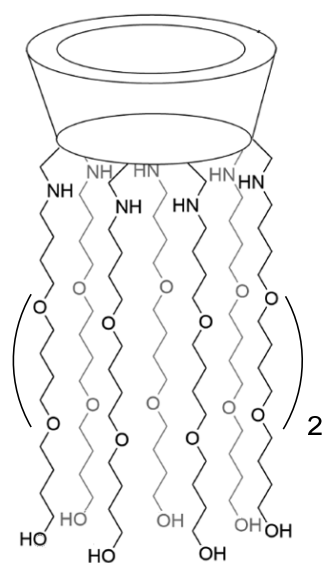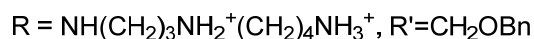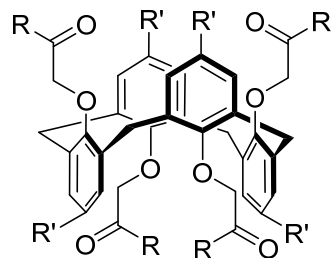
1.12   **1.13**

Figure 1.12. Structure du canal **1.12** à base de cyclodextrine de Gin *et al.*[38,39] et du canal **1.13** à base de calixarène en conformation 1,3-alt de Tecilla *et al.*[40] L'abbréviation Bn définie un groupement benzyle.

Les isophthalamides développées par Gokel *et al.* sont de façon plus inusitée un exemple de canaux transmembranaires formés seulement à haute concentration par un assemblage supramoléculaire, du moins dans le cas du composé **1.17** (Figure 1.13).[41] Son

agencement en agrégats permet la diffusion d'anions au travers de la membrane de liposomes, tel que démontré par des études de transport suivi par la fluorescence de la lucigénine. De surcroît, Gokel *et al.* apportèrent une dimension biologique à leurs transporteurs, en démontrant la capacité des canaux isophthalamides de transporter de l'ADN à l'intérieur de bactéries *E. coli*.[41]

1.14 X = CH, R = CH$_3$
1.15 X = CH, R = H
1.16 X = CH, R = CN
1.17 X = CH, R = NO$_2$
1.18 X = CH, R = OCH$_3$
1.19 X = N, R = H
1.20 X = N, R = NO$_2$
1.21 X = N, R = OCH$_3$
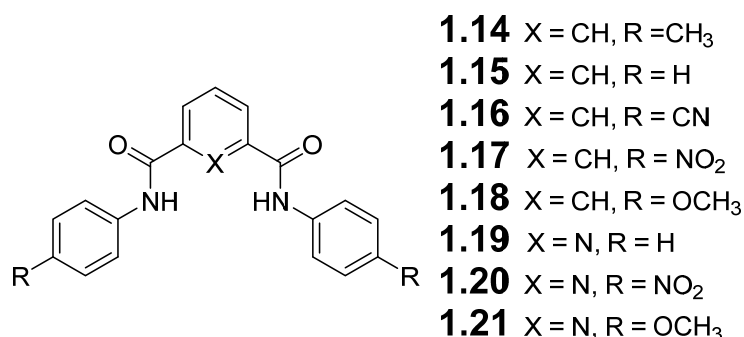
Figure 1.13. Structure des isophthalamides de Gokel *et al.*

A l'instar des isophthalamides formant des canaux à haute concentration et à la fois des transporteurs mobiles à plus basse concentration, le groupe Schmitzer a récemment présenté, dans le cadre de mes travaux, un sel de dibenzimidazolium doté de propriétés antibactériennes et capable de se comporter soit comme un canal ou un transporteur mobile selon la nature du contre-anion de la molécule.[14] Nous aurons à ce propos l'occasion d'élaborer davantage sur le sujet au chapitre 6. Suite au premier modèle supramoléculaire de canal transmembranaire basé sur la structure de l'imidazole que j'ai développé, notre groupe a par la suite apporté une contribution variée en matière d'anionophores principalement axés sur les sels d'imidazolium et benzimidazolium.[13,14,25,42-47] Ces exemples mettant en contexte mes travaux, seront plus amplement discutés au chapitre 5.

1.4.3. Évolution des transporteurs mobiles

Les premiers exemples de transporteurs anioniques dits mobiles étudiés en chimie supramoléculaire se sont largement inspirés de la prodigiosine au début des années

2000.[48,49] Cette molécule naturelle, isolée de souches bactériennes *Streptomyces* et *Serratia*, a démontré d'étonnantes propriétés anticancéreuses et immunosuppressives.[50] Les travaux de Quesada *et al*. ont, à ce titre, mis en lumière le mode d'action de la prodigiosine, formée d'un motif tripyrole faisant office de pince capable de lier des anions (Figure 1.14). En effet, suite à des analyses menées dans des liposomes de 1-palmitoyl-2-oléoyl-*sn*-glycéro-3-phosphocholine (POPC), ils ont observé que la fonction amine du tripyrole lorsque protonnée, en milieu acide, favorise la formation d'un pont hydrogène avec l'anion, ce qui mène à un processus antiport des espèces Cl^-/NO_3^- et Cl^-/HCO_3^-. Ce mécanisme d'échange peut être exploité de façon plus étendue sur des cellules parasites afin d'y provoquer un débalancement électrolytique et ultimement leur lyse. Dès lors, les groupes de Quesada et Sessler étudièrent une banque d'analogues synthétiques de la prodigiosine, dont entre autre l'Obatoclax, un transporteur aux propriétés anticancéreuses actuellement en phase clinique.[51,52]
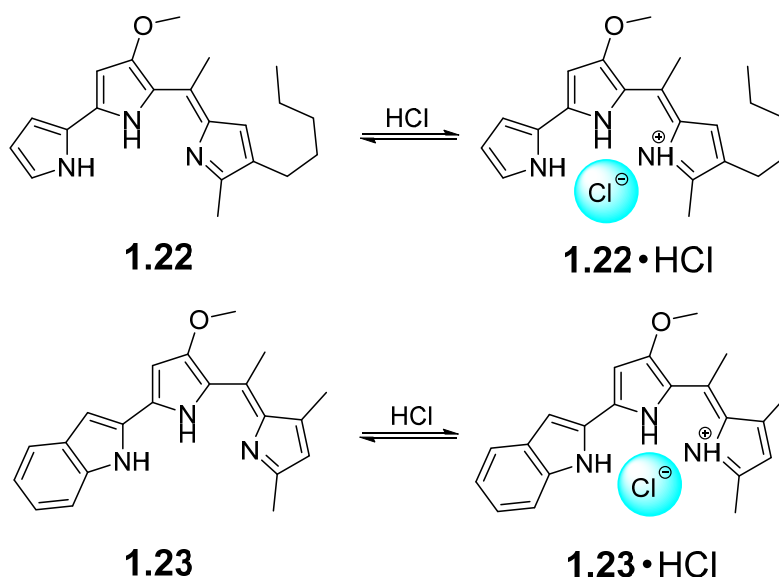
Figure 1.14. Protonation de la prodigiosine **1.22** et de son analogue synthétique Obatoclax **1.23** en milieu acide.

Le potentiel anionophore de la prodigiosine et de ses analogues synthétiques, baptisés tambjamines, ne repose pas seulement sur le degré de protonnation et le pK_a de leur groupement pyrole (qui typiquement se situe à 10 pour les tambjamines versus ~ 7.2

pour la prodigiosine), mais aussi sur l'amphiphilie de la molécule, caractérisée par son *log P*,[53] le coefficient de partition du composé entre l'octanol et l'eau. Plus le *log P* est élevé, plus la molécule se distribue dans la phase organique et à l'inverse, le *log P* est d'autant plus faible que la molécule est hydrophile. Tandis que Quesada *et al.* estimaient au départ que l'amphiphilie optimale des dérivés de la prodigiosine se situait aux alentours d'un *log P* = 4.2,[53] les groupes de Gale et Davis ont pour leur part peaufiné cette théorie en proposant que l'équilibre positionnel entre les groupements hydrophiles et hydrophobes sur un transporteur dictait aussi ses propriétés anionophores.[54] Pour en arriver à ces fins, Davis *et al.* s'intéressa d'abord à la structure de différentes urées et thio-urées, à l'origine greffées à une armature stéroïdienne, nommée cholapode, puis à d'autres analogues synthétiques simplifiés de poids moléculaires plus bas (Figure 1.15, composé **1.24**).[55,56,57] Les cholapodes de Davis *et al.* ont d'abord révélé un puissant effet anionophore pour les processus de transport des ions Cl^-/NO_3^- étudiés dans des liposomes de POPC:cholestérol. Ils observèrent par ailleurs un effet similaire, voire meilleur, pour les cholapodes dont la portion acide cholique fut remplacée par un simple cyclohexane.[58]

R, R' = Chaîne alkyle variable
1.24   **1.25**
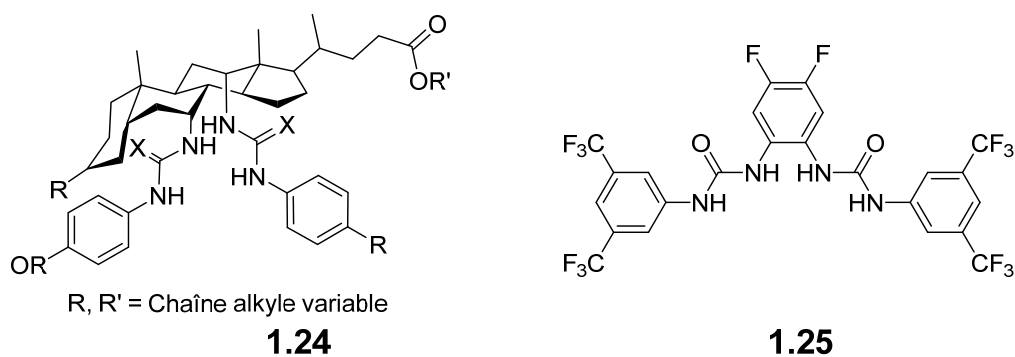
Figure 1.15. Structure générale des cholapodes **1.24** et structure de l'urée aromatique riche en fluore **1.25** proposée par Gale *et al.*[55-57,59]

En réponse à cette découverte et dans une optique de simplifier davantage son modèle, le motif stéroïde, conférant le caractère lipophile aux cholapodes, fut abandonné par Gale et ses collaborateurs au profit de structures aromatiques symétriques et riches en fluores (Figure 1.15, composé **1.25**).[59] Le concept d'halogénation des transporteurs mobiles fait d'ailleurs aujourd'hui largement consensus au sein des chimistes

supramoléculaires comme étant un motif clé capable de complexer les anions pour plusieurs molécules, dont entre autres les calix[4]arenes fluorés de Matile *et al.*[60], les complexes organométalliques fluorés des groupes de Iengo et Tecilla[61] ou encore les transporteurs de Jeong *et al.*[62] Au terme de ces innovations, les travaux subséquents des équipes de Gale et Davis ont enfin permis récemment d'établir une relation structure-activité harmonisée sur les urées, basée d'une part sur la présence de groupements fluorés et d'autre part sur la symétrie de la molécule, tel qu'évoqué précédemment. À cet égard, ils en conclurent qu'il est préférable que les substituants hydrophobes soient optimalement positionnés de part et d'autre du site de liaison polaire de l'anion.[54]

1.5. Description du projet de thèse

1.5.1. Objectif et motivation du projet

Ce projet de thèse avait pour ligne directrice d'élaborer et d'étudier les propriétés de différents sels d'imidazolium et benzimidazolium dans des matrices variées, allant des liposomes aux bactéries, en passant par les globules rouges humains. Au moment de démarrer cette initiative, le motif imidazolium faisait déjà l'objet de recherches intensives dans la littérature à titre de simple récepteur d'anion, principalement grâce aux travaux de Pérez-Garcia *et al.* sur des macrocycles constitués d'unités imidazoliums et d'espaceurs aromatiques (Figure 1.16, composé **1.26**).[63,64] Outre le fait d'avoir un groupement chargé positivement et donc potentiellement capable de se lier à des anions, la synthèse de ces récepteurs imidazoliophanes conduisit à l'observation de ponts hydrogène atypiques avec des halogénures C-H···Cl⁻.
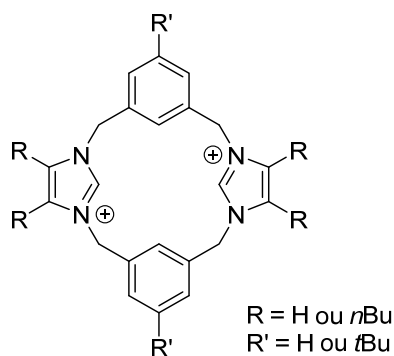
1.26

Figure 1.16. Récepteur d'anion basé sur l'imidazolium par Pérez-Garcia *et al.*

Entre-temps, notre groupe se penchait déjà à l'époque sur les propriétés d'autoassemblage de divers sels d'imidazolium et à l'existence d'interactions supramoléculaires permettant à ces composés amphiphiles de former des agrégats.[65,66,67] Or, la littérature à ce moment ne s'intéressait pas, à notre connaissance, aux possibilités d'aller encore plus loin en terme de propriétés des sels d'imidazolium, par l'élaboration de transporteurs membranaires basés sur ces composés, bien que le transport ionique à des fins biologiques, était – et demeure encore aujourd'hui – un sujet d'intérêt. C'est donc avec cette motivation de rassembler nos connaissances sur les récepteurs d'anions de type imidazolium et la capacité d'agrégation de cette famille de molécules amphiphiles, qu'il nous est venu à l'idée que les sels d'imidazolium pouvaient transporter des anions dans des bicouches au même titre que les ionophores biologiques et synthétiques connus à l'époque. Ainsi, en déconvoluant le design de différents composés partant d'un sel d'imidazolium disubstitué, le rôle de chacun de leurs constituants, soit le noyau cationique, la chaîne aromatique ou aliphatique greffée au noyau, la présence d'un espaceur ou le nombre et la nature des contre-anions ont été étudiés afin de rationaliser, au meilleur de notre connaissance, comment optimiser l'activité ionophore et antibactérienne de la molécule résultante (Figure 1.17). Les sections suivantes présentent en volet le cheminement chronologique de notre analyse telle qu'elle sera traitée dans les chapitres de cette thèse.
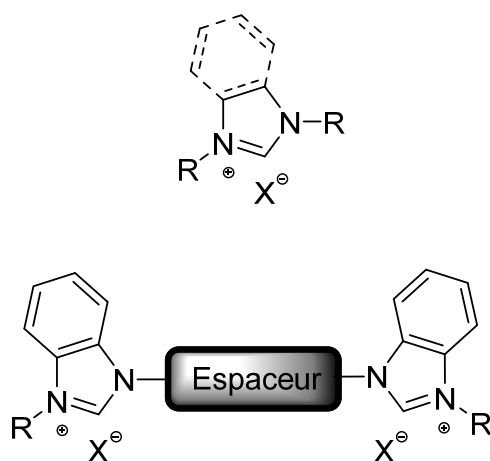
Figure 1.17.   Structure générale des sels d'imidazolium et benzimidazolium étudiés.

1.5.2. Premier exemple de sel d'imidazolium à titre de transporteur d'anions

Nos premiers efforts ont d'abord été orientés de sorte à pouvoir créer un motif amphiphile, basé sur la chimie des imidazoles, capable d'une part de lier et transporter des anions et d'autre part de présenter une distribution adéquate dans les membranes phospholipidiques. Trois bromures d'imidazolium, distincts de par la nature du groupement aliphatique ou aromatique greffé au noyau cationique central, ont été étudiés pour leur capacité à promouvoir la diffusion d'anions chlorures hors d'un liposome. Dès lors, le comportement du composé présentant le meilleur profil ionophore a été inspecté en solution et dans les bicouches grâce à des études spectroscopiques en RMN[1]H, en UV-Vis, en fluorescence et par modélisation informatique. L'hypothèse d'un auto-assemblage du bromure d'imidazolium disubstitué de chaînes aromatiques a également été avancée à la lumière de conclusions d'études computationnelles et par l'observation en solution d'excimères fluorescents caractérisant une agrégation. L'étude a également portée sur la formation de complexes d'inclusion entre un bromure d'imidazolium, une cyclodextrine et un cucurbituril conduisant à l'inactivation progressive du transporteur d'anions. Ces résultats sont présentés au chapitre 2 de cette thèse.

1.5.3. Étude de la relation structure-activité pour différents sels d'imidazolium

Le chapitre 3 de ce manuscrit présente l'influence du contre-anion sur l'activité anionophore de sels d'imidazolium disubstitués. En dérivant par métathèse d'anions le bromure d'imidazolium étudié à la précédente section, nous avons ainsi obtenu quatre nouvelles molécules présentant un profil d'activité différent dans les liposomes. Le meilleur candidat, portant le contre-anion bis(trifluorométhylsulfonyl)amide (NTf_2^-), a fait l'objet d'une analyse plus poussée afin d'en dégager les paramètres cinétiques et thermodynamiques, mais également afin de déduire par quel type de mécanisme ce transporteur d'anion facilitait la translocation des chlorures de part et d'autre d'une bicouche.
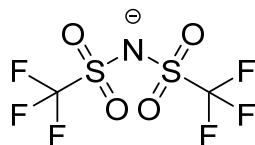
Figure 1.18.   Structure de l'anion bis(trifluorométhylsulfonyl)amide (NTf_2^-).

1.5.4. Étude des propriétés des sels de benzimidazolium et premières applications biologiques

Après avoir rationalisé à la section précédente une relation entre la structure et l'activité ionophore des sels d'imidazolium, basée sur la nature de leur contre-anion, nous avons cherché à étendre nos observations sur une nouvelle famille plus efficace de transporteurs, contenant le noyau benzimidazolium. Il nous est apparu, au regard de tests de transport réalisés dans des liposomes, que cette nouvelle classe d'ionophores possédait une meilleur efficacité que leur analogues imidazolium. Les conclusions tirées au chapitre précédent ont en outre été corroborées encore ici, à savoir qu'une métathèse du contre-anion bromure en NTf_2^- conduisait à un meilleur transporteur. De surcroît, des analyses cinétiques suggérant une coopérativité entre les molécules et les données obtenues en phase cristalline par diffraction de rayons-X sont également venues appuyer

l'idée de départ d'une agrégation des molécules, telles que prédite par modélisation moléculaire au chapitre 2. Enfin, un premier pas a été fait en matière d'application biologique en testant la capacité d'un sel de benzimidazolium à induire la diffusion d'ions calcium à l'intérieur d'une bactérie *E. coli*, grâce à une méthode basée sur la fluorescence d'un biomarqueur présenté au chapitre 4.

1.5.5. Applications biologiques de différentes familles de transporteurs anioniques : revue de littérature

À ce stade de notre cheminement, avant de nous lancer pleinement dans les études dans des milieux biologiques, une rétrospective des travaux dans le domaine du transport anionique s'imposait afin de nous orienter pour la suite des choses. Les résultats concluants présentés au chapitre 4 pavaient désormais la voie à l'élaboration de sels de benzimidazolium dotés d'une capacité ionophore à l'intérieur de liposomes comme chez les bactéries *E. coli*. Dans cette section, nous présentons un éventail d'applications biologiques des molécules transporteuses d'ions, dont entre autres, différentes stratégies employées dans notre groupe et ailleurs dans la littérature afin de circonvenir aux mécanismes de défense de certaines souches bactériennes et pouvoir provoquer leur destruction.

1.5.6. Propriétés antibactériennes d'un sel de benzimidazolium et étude de ces effets membranaires

Le dernier chapitre de la discussion se veut l'une des finalités de nos précédents efforts afin de présenter la preuve de concept d'un transporteur mobile basé sur un sel de benzimidazolium, doté d'un pouvoir antimicrobien et d'une toxicité limitée contre les globules rouges humains. Pour ce faire, parmi une série de molécules candidates, le meilleur agent ionophore a d'abord été sélectionné en fonction de sa concentration effective générant 50% de l'efflux total des chlorure hors d'un liposome (EC_{50}) déterminée dans des liposomes de EYPC. Différents tests ont également été conduits dans des tubes en U et dans des liposomes de DPPC dont la membrane est rigide à température

ambiante, afin d'établir le mécanisme de transport des ions. Après avoir déterminé la concentration minimale inhibitrice (MIC) dans différentes souches bactériennes, le sel de benzimidazolium a été étudié pour ses propriétés de dépolarisation de la membrane bactérienne, ainsi que par microscopie électronique à balayage (SEM) afin d'observer visuellement l'étendue des dommages causés à la membrane d'une souche de *E. coli*.

1.6.   Références

1. Lepri, S., Buonerba, F., Goracci, L., Velilla, I., Ruzziconi, R., Schindler, B.D., Seo, S. M., Kaatz, G. W., Cruciani, G, *J. Med. Chem.* **2016** *59*, 867.

2. Schatz, A., Bugie, E., Waksman A., *Proc. Soc. Exp. Biol, and Med.*, **1944**, *55*, 66.

3. Shinabarger, D. *Expert Opin. Invest. Drugs* **1999**, *8*, 1195.

4. Martínez, J. L. *Science* **2008**, *321*, 365.

5. Dever, L. A., Dermody, T. S. *Arch. Intern. Med.* **1991**, *151*, 886.

6. Goldberg, K., Sarig, H., Zaknoon, F., Epand, R. F., Epand, R. M., *FASEB J.* **2013**, *27*, 3818.

7. Ashcroft, F. M., Ion Channels and Disease Channelopathies: Academic Press: San Diego, **2000**, 481.

8. Planells-Cases, R., Jentsch, T. J., *Biochim. Biophys. Acta, Mol. Basis Dis.* **2009**, *1792*, 173.

9. Cordat E., Casey, J. R., *Biochem. J.*, **2009**, *417*, 423.

10. Maduke, Miller, M. C., Mindell, J. A*., Annu. Rev. Biophys. Biomol. Struct.* **2000**, *29*, 411.

11. Sheppard, D. N., Rich, D. P., Ostedgaard, L. S., Gregory, R. J., Smith A. E., Welsh, M. J., *Nature* **1993**, *362*, 160.

12. O'Sullivan, B. P., Freedman, S. D., *Lancet* **2009**, *373*, 1891.

13. Elie, C.-R., Noujeim, N., Pardin, C., Schmitzer, A. R., *Chem. Commun.* **2011**, *47*, 1788.

14. Elie, C.-R., David, G., Schmitzer, A. R., *J. Med. Chem.* **2015**, *58*, 2358.

15. Campbell, N. A., Reece, J. B., *Biologie* **2007**, 1334.

16. Heller, H., Schaefer, M., Schulten, K., *J. Phys. Chem.* **1993**, *97*, 8343.

17. Image adapté de Encyclopedia Britannica 2007, Internet : https://www.britannica.com/science/cell-membrane, consulté le 2/04/2016.

18. Davis, J. T., Okunola, O., Quesada, R., *Chem. Soc. Rev.* **2010**, *39*, 3843.

19. Philippot J. R, Schuber F., Liposomes as Tools in Basic Research and Industry: CRC Press: Boca Raton, **1995**, 18.

20. (a) Koulov, V., Lambert, T. N., Shukla, R., Jain, M., Bood, J. M., Smith, D. B., Li, H. Y., Sheppard, D. N., Joos, J.-B., Clare, J. P., Davis, A. P., *Angew. Chem. Int. Ed. Engl.* **2003**, *42*, 4931. (b) Krasne, S., Eisenman, G., Szabo, G., *Science* **1971**, *174*, 414.

21. Lassiseraye, D., Courtemanche, L., Bergeron, A., Manjunath, P., Lafleur, M., *Biochim. Biophys. Acta.* **2008**, 1778, 502.

22. Horne, R. W., Bangham, A. D., Whittaker, V. P., *Nature* **1963**, *200*, 1340.

23. Cevc, G., *J. Control. Release* **1993**, *160*, 135.

24. Fyles, T. M., *Chem. Soc. Rev.* **2007**, *36*, 335.

25. a) Chhun, C. Axe et Rotaxane Parapluie, vers de nouveaux transporteurs transmembranaires de chlorures et de médicaments cycliques. Thèse de doctorat, Université de Montréal, Montréal, **2012**. b) Legg, K. D., Hercules, D. M., *J. Phys. Chem.* **1970**, *74*, 2114.

26. Reddy, G. L., Iwamoto, T., Tomich, J. M., Montal, M., *J. Biol. Chem.* **1993**, *268*, 14608.

27. Wallace, D. P., Tomich, J. M., Iwamoto, T., Henderson, K., Grantham, J. J., Sullivan, L. P., *Am. J. Physiol. Cell Physiol.* **1997**, *272*, C1672.

28. Pajewski, R., Ferdani, R., Pajewska, J., Li, R., Gokel, G. W. *J. Am. Chem. Soc.* **2005**, *127*, 18281.

29. Cook, G. A., Pajewski, R., Aburi, M., Smith, P. E., Prakash, O., Tomich, J. M., Gokel, G. W., *J. Am. Chem. Soc.* **2006**, *128*, 1633.

30. Boudreault, P. L., Arseneault, M., Otis, F., Voyer, N., *Chem. Commun.* **2008**, *44*, 2118.

31. Sakai, N., Brennan, K. C., Weiss, L. A., Matile, S., *J. Am. Chem. Soc.* **1997**, *119*, 8726.

32. Weiss, L. A., Sakai, N., Ghebremariam, B., Ni, C., Matile, S., *J. Am. Chem. Soc.* **1997,** *119*, 12142.

33. Vargas Jentzsch, A., Matile, S., *J. Am. Chem. Soc.* **2013**, *135*, 5302.

34. Gorteau, V., Bollot, G., Mareda, J., Perez-Velasco, A., Matile, S., *J. Am. Chem. Soc.* **2006**, *128*, 14788.

35. Gorteau, V., Bollot, G., Mareda, J., Matile, S., *Org. Biomol. Chem.* **2007**, *5*, 3000.

36. Dawson, R. E., Hennig, A., Weimann, D. P., Emery, D., Ravikumar, V., Montenegro, J., Takeuchi, T., Gabutti, S., Mayor, M., Mareda, J., Schalley, C. A., Matile, S., *Nat. Chem.* **2010**, *2*, 533.

37. Mareda, J., Matile, S., *Chem. Eur. J.* **2009**, *15*, 28.

38. Madhavan, N., Robert, E. C., Gin, M. S., *Angew. Chem., Int. Ed.* **2005**, *44*, 7584.

39. Jog, P. V., Gin, M. S., *Org. Lett.* **2008**, *10*, 3693.

40. Izzo, I., Licen, S., Maulucci, N., Autore, G., Marzocco, S., Tecilla, P., De Riccardis, F. *Chem. Commun.* **2008**, 2986.

41. Yamnitz, C. R., Negin, S., Carasel, I. A., Winter, R. K., Gokel, G.W., *Chem. Commun.* **2010**, *46*, 2838.

42. Elie, C.-R., Hebert, A., Charbonneau, M., Haiun, A., Schmitzer, A. R. *Org. Biomol. Chem.* **2013**, *11*, 923.

43. Elie, C.-R., Charbonneau, M., Schmitzer, A. R. *MedChemComm* **2012**, *3*, 1231.

44. Kempf, J., Noujeim, N., Schmitzer, A. R. *RSC Adv*. **2014**, *4*, 42293.

45. Vidal, M., Elie, C.-R., Campbell, S., Claing, A., Schmitzer, A. R. *MedChemComm* **2014**, *5*, 436.

46. Gravel, J., Kempf, J., Schmitzer, A. R. *Chem. Eur. J.* **2015**, *21*, 18642.

47. Elie, C.-R., Gravel, J., Khayat, M., Schmitzer A. R., *Med. Chem. Commun.* **2016**, *7*, 1128.

48. Fürstner, A. *Angew. Chem., Int. Ed.* **2003**, *42*, 3582.

49. Davis, J. T.,Gale, P. A., Dehaen, W., Editions Springer: New York, **2010**, Vol. 24.

50. Perez-Tomas, R., Montaner, B., Llagostera, E., Soto-Cerrato, V. *Biochem. Pharmacol.* **2003**, *66*, 1447.

51. Diaz de Greñu, B., Hernández, P. I., Espona, M., Quiñonero, D., Light, M. E., Torroba, T., Pérez-Tomás, R., Quesada, R. *Chem. Eur. J.* **2011**, *17*, 14074.

52. Sessler, J. L., Eller, L. R., Cho, W.-S., Nicolaou, S., Aguilar, A., Lee, J. T., Lynch, V. M., Magda, D. J. *Angew. Chem., Int. Ed.* **2005**, *44*, 5989

53. Saggiomo, V., Otto, S., Marques, I., Felix, V., Torroba, T., Quesada, R.,*Chem. Commun.* **2012**, *48*, 5274.

54. Valkenier, H., Haynes, C. J. E., Herniman, J., Gale, P. A., Davis, A. P., *Chem. Sci.* **2014**, *5*, 1128.

55. Davis, A. P., Sheppard, D. N., Smith, B. D., *Chem. Soc. Rev.* **2007**, *36*, 348.

56. Valkenier, H., Davis, A. P., *Acc. Chem. Res.* **2013**, *46*, 2898.

57. Brotherhood, P. R., Davis, A. P., *Chem. Soc. Rev.* **2010**, *39*, 3633.

58. Cooper, J. A., Street, S. T. G., Davis, A. P., *Angew. Chem., Int. Ed.* **2014**, *53*, 5609.

59. Karagiannidis, L. E., Haynes, C. J. E., Holder, K. J., Kirby, I. L., Moore, S. J., Wells, N. J., Gale, P. A., *Chem. Commun.* **2014**, *50*, 12050.

60. Vargas Jentzsch, A., Emery, D., Mareda, J., Metrangolo, P., Resnati, G., Matile, S., *Angew. Chem., Int. Ed.* **2011**, *50*, 11675.

61. Milano, D., Benedetti, B., Boccalon, M., Brugnara, A., Iengo, E., Tecilla, P., *Chem. Commun. 2014*, *50*, 9157.

62. Choi, Y. R., Chae, M. K., Kim, D., Lah, M. S., Jeong, K.-S., *Chem. Commun.* **2012**, *48*, 10346.

63. Alcalde, E., Alvarez-Rua, C., Garcia-Granda, S., Garcia-Rodriguez, E., Mesquida, N., Pérez-Garcia, L., *Chem. Commun.* **1999**, *3*, 295.

64. Alcalde, E., Ramos, S., Pérez-Garcia, L., *Org. Lett.* **1999**, *1*, 1035.

65. Leclercq, L., Noujeim, N., Schmitzer, A. R., *Cryst. Growth Des.* **2009**, *9*, 4784.

66. Noujeim, N., Sanon, S., Eberlin, L., Schmitzer, A. R., *Soft Mater.* **2012**, *8*, 10914.

67. Leclercq, L., Schmitzer, A.R., *J. Phys. Chem. B,* **2008***, 112,* 11064.

Chapitre 2   Le motif imidazole: premier exemple d'un transporteur d'anions

2.1. Préface

Antérieurement à nos travaux, la littérature n'offrait, à notre connaissance, aucune information sur le transport membranaire d'anions induit par des sels d'imidazolium. Tel qu'expliqué en introduction, ce motif nous semblait pourtant très attrayant à titre d'agent de reconnaissance des anions, en raison de la charge positive sur le cation imidazolium, mais également parce que de récentes études dans notre groupe, à l'époque, démontraient le potentiel de former des assemblages supramoléculaires à partir de ce motif. Cela nous a donc motivé à chercher à combiner l'hypothétique propriété anionophore des sels d'imidazolium à leur caractère amphiphile afin de développer une nouvelle famille de transporteurs transmembranaires. Le but de cette analyse était également de démontrer l'auto-assemblage en solution de ces transporteurs et la capacité d'en moduler l'activité ionophore par la formation de complexes d'inclusion avec des macrocycles tels que la cyclodextrine et le cucurbituril.

Pour ces travaux publiés en 2011 j'ai fait la synthèse et la caractérisation de toutes les molécules, inspirées et optimisées d'un protocole établit par Christophe Pardin, hormis pour le bromure de butylméthylimidazolium qui est un composé commercial. J'ai également préparé les liposomes et réalisé les tests de transport selon la méthode établie dans la littérature. J'ai également étudié le profil de fluorescence des composés. J'ai réalisé, sous la supervision de Nadim Noujeim, l'analyse en RMN ^{1}H et en UV-Vis du comportement des sels d'imidazolium en présence de différents macrocycles. Enfin, j'ai également assisté la Pre. Andreea Schmitzer dans la rédaction de l'article, qui a par ailleurs effectué toutes les analyses computationnelles. Les informations expérimentales supplémentaires de ce chapitre se trouvent aux pages 139-147 de cette thèse.

2.2.   Article 1 : «Uncovering new properties of imidazolium salts: Cl transport and supramolecular regulation of their transmembrane activity»

Claude-Rosny Elie, Nadim Noujeim, Christophe Pardin and Andreea R. Schmitzer*

Department of Chemistry, Université de Montréal, 2900 Édouard-Montpetit CP 6128 succ. Centre-Ville, Montréal Québec, Canada, H3C 3J7.

2.2.1.   Abstract

We report the Cl⁻ transport activity for three imidazolium-based transporters. We present significant findings regarding the use of α-cyclodextrin and cucurbit[7]uril macrocycles to form inclusion complexes with these salts and to inhibit their membrane activity.

2.2.2.   Introduction

Chloride, an inorganic anion that is completely dissociated and highly solvated in solution,[1] is one of the most abundant anions found in physiological environments. The transport of Cl⁻ in biological systems is crucial to myriad biological processes such as signal transduction, regulation of cell volume, stabilization of resting membrane potential or fluid transport in epithelia.[2] Chloride is transported across cellular membranes by a wide variety of natural anion transport proteins classified as anion exchangers or cation-dependent Cl⁻ co-transporters.[3] Understanding natural ion transport processes and discovering new membrane-active anion transporters have driven the development of synthetic transmembrane ion transporters.[4] For example cystic fibrosis is caused by a mutation in the cystic fibrosis transmembrane conductance regulator protein (CFTR) that facilitates transmembrane Cl⁻ transport. A synthetic sterol analog with polyamine side-chain functions developed by Regen *et al.* has been used to completely restore Cl⁻ transport in cystic fibrosis cells.[5] We report here the Cl⁻ transport activity for three imidazolium-based Cl⁻ transporters. We present significant findings regarding the use of water-soluble α-cyclodextrin (**α-CD**) and cucurbit[7]uril (**CB7**) to form inclusion complexes with these salts in order to inhibit their membrane activity. To the best of our knowledge this is the first example of imidazolium cations that induce anion transport across a biomembrane, where activity can be controlled by the formation of inclusion complexes.

The biocompatibility of the imidazole ring provides a scaffold for biomimetic applications.[6] Among the imidazolium salt's most promising attributes are antimicrobial action[7] and molecular self-assembly into liquid crystals.[8] While the imidazole ring affords a wealth of biophysical-related applications, it has previously been incorporated

in the structure of transport carriers by Gale *et al.*[9] Imidazolium salts represent a new and completely unexplored class of potential anion transporters. They adopt self-organized structures mainly through H-bonds that induce structural directionality, contrary to classical salts which mainly form aggregates through electrostatic interactions.[10] Further supramolecular interactions developed by imidazolium salts are π-stacking interactions, aliphatic interactions, and dipolarizability/polarizability.[11] We have recently designed and synthesized imidazolium salts to maximize stacking interactions by the introduction of aromatic groups on the imidazolium moiety.[12]

The imidazolium salts we studied as anion transporters are shown in Scheme 2.1. They differ in the substitution pattern of the two nitrogen atoms of the imidazolium ring, but more importantly, in their self-association properties in aqueous solution and capacity to partition in the bilayer. Recently, Matile *et al.* elaborated the concept to exploit anion-π interactions for this purpose and suggested that π-acidic aromatics can be linked together to produce unbendable scaffolds with multiple binding sites for anions to move along, across a lipid bilayer membrane.[13] In the case of compounds **2.2** and **2.3** the intrinsic anion-π interaction is even stronger, due to the imidazolium positive charge close to the aromatic system.
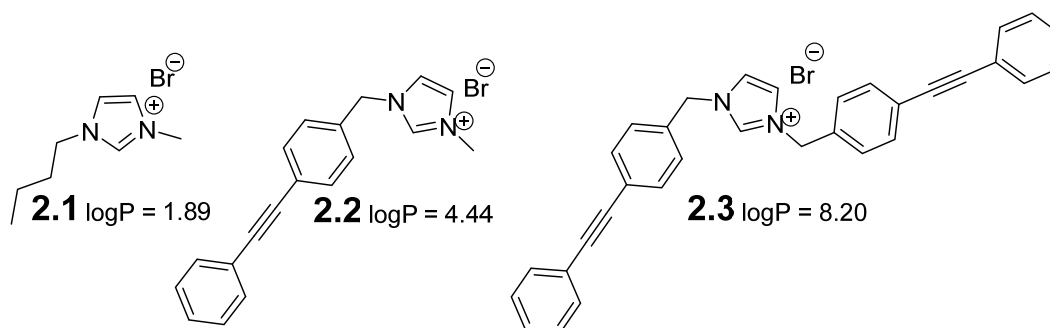
Scheme 2.1.   Imidazolium salts studied for transmembrane Cl⁻ transport activity.

2.2.3.   Results and Discussion

Compounds **2.1-2.3** were tested for Cl⁻ transport activity using liposome assays previously reported.[14] Liposomes loaded with the Cl⁻ sensitive dye, lucigenin, were subjected to a Cl⁻ gradient in the intravesicular solution. A cartoon representation of the

liposome assay sequence is shown in the insert of Figure 2.1. Direct measurement of Cl⁻ efflux by using lucigenin depicted in Figure 2.1, confirms that only compound **2.3** induces Cl⁻/NO₃⁻ exchange in lipid vesicles while analogs **2.1** and **2.2** are completely inactive.
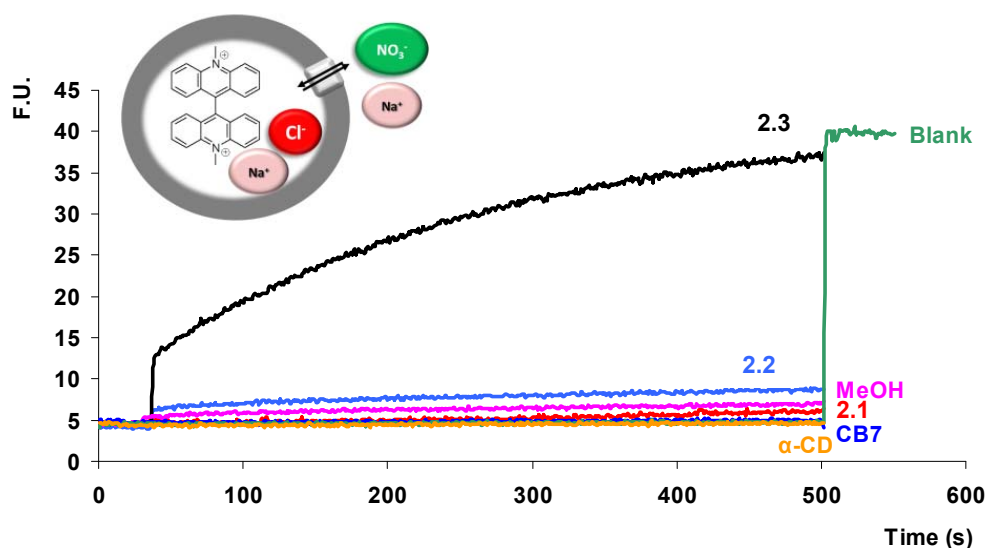
Figure 2.1. Relative activity of compounds **2.1-2.3** in the lucigenin-based Cl⁻ transport assay. Intravesicular 100 mM NaCl, 10 mM phosphate buffer, extravesicular 100 mM NaNO₃, 10 mM phosphate buffer (pH 6.4). 0.25 mM solutions of **2.1-2.3** were injected at t = 35 s to give a final concenration of 40 μM (see annexe 1 for details) ; the Blank: aqueous 10% Triton-X was injected at t = 500 s. The liposome lyse for other assays is not shown. Each curve represents the average of three trials.

Fluorescence spectra recorded under the same conditions as the anion transport assays, provide strong evidence of the partition of compounds **2.2** and **2.3** into the less polar liposomal bilayer (Annexe 1). Emission spectra of **2.2** and **2.3** indicate the existence of the excimers of the aromatic rings, suggesting that the aromatic-aromatic interactions are pronounced in the presence of liposomes. The self-association of **2.1** in the solid state has been well described,[15] and its solubility in aqueous solution does not suggest any self-assembly under the transport assay conditions. To gain better insight into the geometrical parameters of more hydrophobic compounds **2.2** and **2.3** in aqueous solution, we performed a computational study using the PM6/SCF-MO method, at the restricted Hartree-Fock level, applying COSMO parameters in MOPAC2009™.[16] As shown in

Figure 2.2, the effective π- π interactions of the aromatic arms result in formation of a planar bilayer in the aggregates. In compounds **2.2** and **2.3**, in addition to forming electrostatic interactions with the bromide anions, the imidazolium rings form a localized positive charge close to this aromatic part. However, in the case of **2.2**, the aromatic interactions are predicted to form in only one direction. For compound **2.3**, the imidazolium units, separated by the aromatic spacers, do not provide an enclosed binding site for the anions, but the aggregation process is predicted to achieve aggregates with the right length for hydrophobic matching with the lipid bilayer membrane. Compound **2.3** does not bind the inorganic anion but rather forms transient channels with a positively charged and aromatic interior allowing permeation of the inorganic anion and transport through anion-π interactions. Since the imidazolium unit is positively charged, independently of the pH, the anion-π interactions may be strong enough to allow Cl⁻ to cross the aromatic channel. Even if compounds **2.1-2.3** look similar to the carriers previously reported by Sessler and Gale,[17] they act rather as channel forming transporters than carriers, as compound **2.2** is completely inactive.
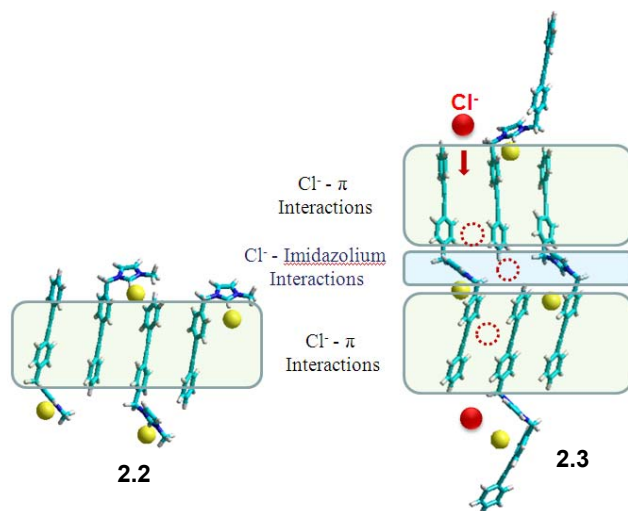
Figure 2.2. Self-assembly of **2.2** and **2.3** modeled by PM3 geometry optimization and proposed anion-π interactions favouring Cl⁻ transport by **2.3**. The π- π interactions and anion-π interactions are shown is green, the anion-cation interactions are shown in light blue (Br⁻ are shown in yellow and Cl⁻ in red).

We previously reported that we can control the equilibria of different imidazolium aggregates in aqueous solution in the presence of **CDs**.[12a)] In this study we set out to determine if the inclusion complexes formed by these salts can be used to block the transport of the active compound. It was not unexpected that both **α-CD** and **CB7** form inclusion complexes with **2.3**, by accommodating the aromatic arms into their hydrophobic cavity. As can be seen in Figure 2.3, 1 or 2 equivalents of **CB7** partially inhibit the transport properties of compound **2.3**. However, 2 equivalents of **α-CD** completely inhibit the Cl⁻ transport. These results suggest that the nature of the inclusion complex may play a fundamental role on the transport properties. To the best of our knowledge this is the first example of simple anion transporter across a model biomembrane whose activity can be controlled by the formation of inclusion complexes. The formation of the inclusion complexes with **α-CD** or **CB7** may result in the assembly of more highly water-soluble complexes and in the displacement of the partition equilibrium of **2.3** towards the aqueous phase. As less self-assembled aggregates of **2.3** are present in the bilayer, transport inhibition is observed.
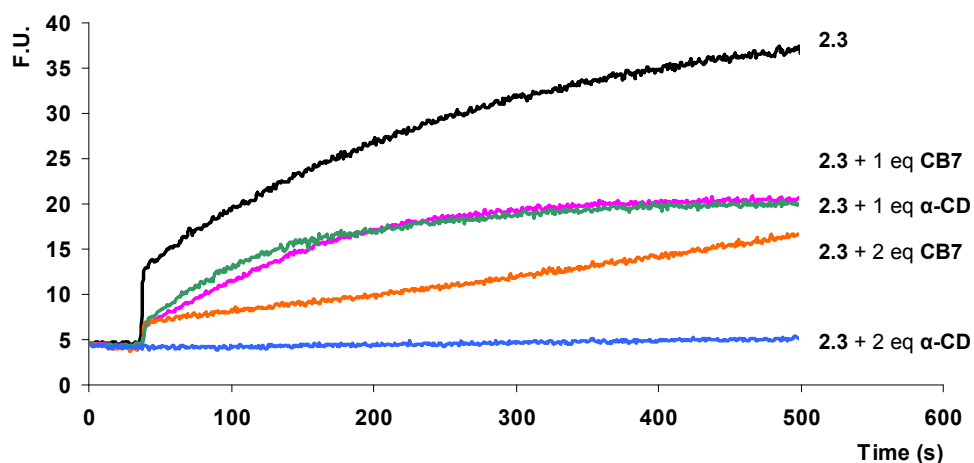
Figure 2.3.   Relative activity of compound **2.3** in the presence of α-CD and CB7: Intravesicular 100 mM NaCl, 10 mM phosphate buffer, extravesicular 100 mM NaNO$_3$, 10 mM phosphate buffer (pH 6.4). The experimental details are given in annexe 1.

This affirmation allows us to emphasize the importance of the hydrophobicity of the anion transporter, as the more hydrophilic compounds **2.1** and **2.2** do not transport. The shape of the transporter as well as its self-assembly properties are other parameters to consider for this new class of imidazolium-based synthetic anion transporters. The formation of the inclusion complexes was observed by ^{1}H NMR and UV spectroscopy studies of compound **2.3** in the presence of different concentrations of **CB7** (Figure 2.4) and **α-CD** (Annexe 1). The ^{1}H NMR spectrum in the presence of **CB7** shows complexed and uncomplexed broad peaks for the aromatic protons, suggesting rapid association rate or the presence of multiple complexes. The titration isotherms and Jobs' plots (Annexe 1) obtained by UV spectroscopy, confirmed that the complexation involves multiple equilibria, where more than two species are present at equilibrium.
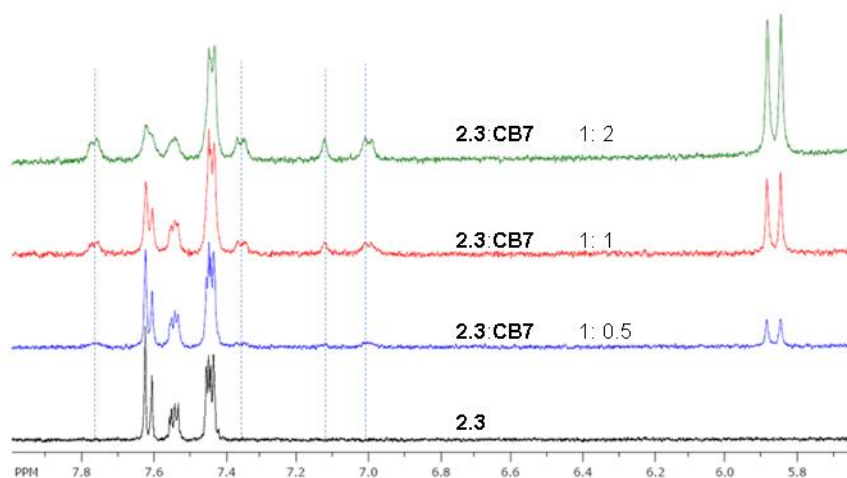
Figure 2.4.   Partial ^{1}H NMR spectra of **2.3** in the presence of different amounts of CB7 in D$_2$O/CD$_3$OD (50/50 V/V), [**2.3**] = 0.25 mM.

For the specific application as chloride transmembrane transporters, the active compounds must be sufficiently water-soluble for delivery, but also be sufficiently lipophilic for insertion into the biomembrane. Therefore, our strategy to use amphiphilic molecules that are only partially soluble in water, but are also able to form inclusion complexes with non-toxic macrocycles, allows us to control their partition and diffusion across membranes. Self-assembly of **2.3** cannot be demonstrated in aqueous solution by ^{1}H NMR study at 0.25 mM. At this low concentration aggregates are already formed. The

self-association results in the formation of water-insoluble aggregates, that precipitate. Even if the self-aggregation of compound **2.3** is too complex to determine the thermodynamic parameters and the binding constants with **α-CD** and **CB7**, we demonstrate here that we can regulate the Cl⁻ transport by the formation of inclusion complexes at only 2 equivalents of **α-CD**. The insertion of **2.3** in the phospholipid bilayer and its extraction by the macrocycle towards the aqueous phase can be observed by fluorescence (Figure 2.5). The fluorescence spectra in the presence of 2 equivalents of **α-CD** and **CB7** are completely different and confirm the hypothesis that **α-CD** act more rapidly on the disruption of the aggregate.
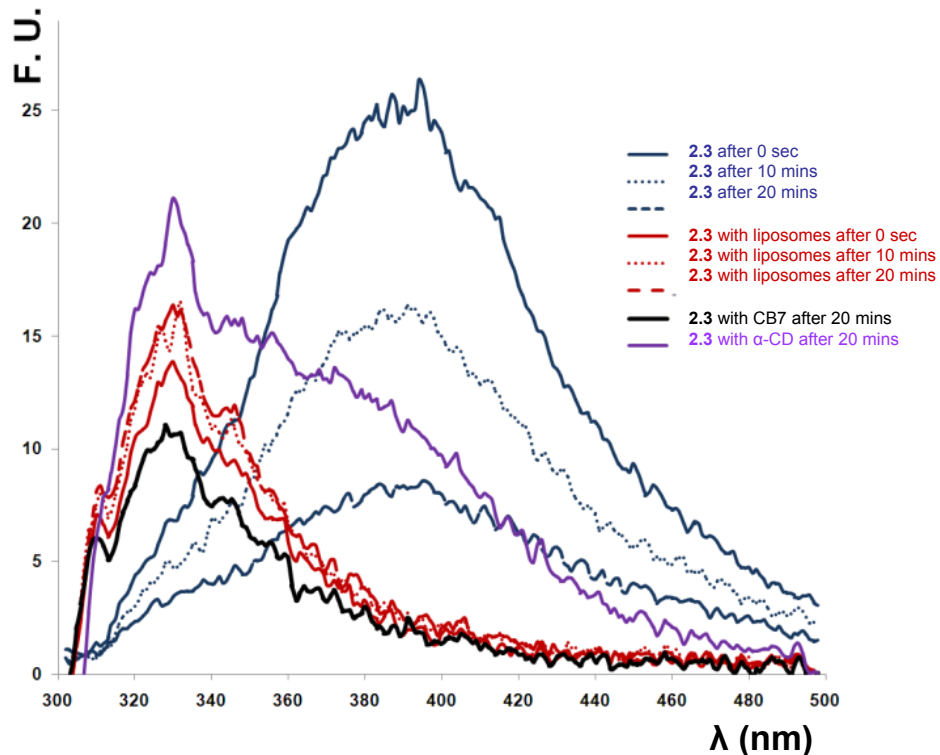
Figure 2.5.   Fluorescence spectra of **2.3** recorded in the same conditions as the anion transport experiment. Without liposomes after 1, 10, 20 min; In the presence of liposomes after 1, 10 and 20 mins. Two equivalents of CB7 or α-CD were added after 10 min and the spectra was recorded at t = 20 min (excitation at 290 nm).

Depending on the size of its cavity, the macrocycle can bind and accommodate the aggregate without disrupting it, as in the case of **CB7**. **α-CD** can accommodate only

the monomer in its cavity, which results in the disruption of the aggregate and the complete disappearance of the conductive channels (Figure 2.6 and annexe 1 for the molecular modeling results).
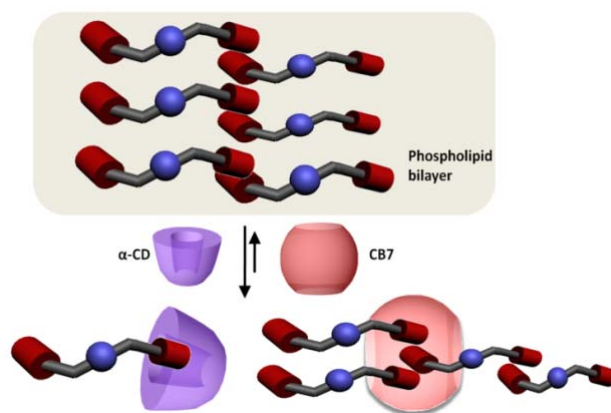
Figure 2.6.   Schematic representation of the formation of inclusion complexes of **2.3** with CB7 and α-CD and displacement of the transporter from the bilayer.

2.2.4.   Conclusion

The ease of and the low concentration (μM) range at which the imidazolium salt **2.3** transports Cl⁻ make it an attractive candidate for developing therapies for Cl⁻ transport-related deficiencies such as cystic fibrosis. The imidazolium salts can delocalize their positive charge into the heterocyclic ring, which may reduce the cytotoxic effect associated with some of the currently known cationic anion transporters. We present here a new property of imidazolium salts which can act as powerful anion tranporters. We also demonstrate the possibility to regulate the transport activity of imidazolium-based compounds by the formation of different inclusion complexes with water-soluble macrocycles. The imidazolium-based compounds obviously exhibit a great potential as anion transporters, which provide a pathway for the design of novel transporters with high efficiency and good opportunities for the development of imidazolium-based compounds for biomedical applications. Further studies on the mechanism and the anion transport as well as the synthesis of other imidazolium-based compounds for anion transport are currently underway in our group.

2.2.5.   Notes and references

1. Bianchi, A., Bowman-James, K., Garcia-Espana, E., in *Supramolecular Chemistry of Anions*. Wiley-VCH: New York, **1997**, 461.

2. Suzuki, M., T. Morita, Iwamoto, T., *Cell. Mol. Life Sci.* **2005**, *63*, 12.

3. a) Hille, B., in *Ionic Channels of Excitable Membranes*, 3rd edn Sinauer Associates, Sunderland **2001**. b) Sheth, T. R., Henderson, R. M., Hladky, S. B., Cuthbert, A.W., *Biochim. Biophys. Acta.* **1992**, *1107*, 179. c) Jeong, E. J. , Kang, E. J., Sung, L. T., Hong, S. K., Lee, E., *J. Am. Chem. Soc.* **2002**, *124*, 14655. d) Davis, J. T., Okunola, O., Quesada, R., *Chem. Soc. Rev.* **2010**, *39*. 3842.

4. a) Li, X., Wu, Y.-D., Yang, D., *Acc. Chem. Res.* **2008,** *41*, 1428.b) McNally, B.A., Leevy, W. M., Smith, B. D., *Supramol. Chem.* **2007,** *19*, 29.c) Sisson, A. L., Shah, M. R., Bhosale, S., Matile, S., *Chem. Soc. Rev.* **2006,** *35*, 1269. d) Gale, P. A., *Chem. Soc. Rev.* **2010,** *39*, 3746. e) Gokel, G. W., Barkey, N., *New J. Chem.* **2009,** *33*, 947. f) Bates, G. W., Gale, P. A., *Struct. Bonding* **2008,** *129*, 1.

5. a) Deng, G., Dewa, T., Regen, S. L., *J. Am. Chem. Soc.* **1996**, *118*, 8975. b) Jiang, C. W., Lee, E. R., Lane, M. B., Xiao, Y.-F., Harris, D. J., Cheng, S. H*., Am. J. Physiol* **2001**, *281*, L1164.

6. Anderson, E. B., Long, T. E., *Polymer* **2010**, *12*, 2447.

7. a) De Luca, L., *Curr. Med. Chem.* **2006**, *13*, 1. b) Demberelnyamba, D., Kim, K.-S., Choi, S., Park, S.-Y., Lee, H., Kim, C.-J., *Bioorg. Med. Chem.* **2004,** *12*, 853.

8. a) Batra, D., Hay, D.N.T., Firestone, M.A., *Chem Mater* **2007**, *19*, 4423. b) Batra, D., Seifert, S., Firestone, M.A., *Macromol. Chem. Phys.* **2007**, *208*, 1416.

9. Gale, P.A., Garric, J., Light, M.E., McNally, B.A., Smith, B.D., *Chem. Commun.* **2007**, 1736.

10. a) Szejtli, J., *Chem. Rev.* **1998**, *98*, 1743-1754. b) Uekama, K., Hirayama, F., Irie, T., *Chem. Rev.* **1998**, *98*, 2045. c) Li, S., Purdy, W. C., *Chem. Rev.* **1992**, *92*, 1457.

11. Gao, Y.A., Zhao, X., Dong, B., Zheng, L., Li, N., Zhang, S., *J. Phys. Chem. B* **2006**, *110*, 8576.

12. a) Leclercq, L., Schmitzer, A.R., *J. Phys. Chem. B,* **2008***, 112,* 11064. b) Leclercq, L.*,* Noujeim, N., Schmitzer, A. R., *Cryst. Growth Des.* **2009**, *9*, 4784.

13. a) Mareda, J., Matile, S., *Chem.-Eur. J.,* **2009,** *15*, 28**.** b**)** Dawson, R.E.**,** Hennig, A., Weimann, D. P., Emery, D., Ravikumar, V., Montenegro, J., Takeuchi, T., Gabutti, S., Mayor, M., Mareda, J., Schalley, C., Matile, S., *Nat. Chem.* **2010**, *2*, 533.

14. a) Davis, A. P., Sheppard, D. N., Smith, B.D., *Chem. Soc. Rev.* **2007** *36*, 348. b) Sidorov, V., Kotch, F. W., Kuebler, J. L., Lam, Y. F., Davis, J. T., *J. Am. Chem. Soc.* **2003,** *125*, 2840. c) McNally, B.A., Koulov, A.V., Smith, B. D., Joosb, J. B., Davis, A. P., Harrell Jr., W. A., Bergmeyer, M. L., Zavalij, P. Y., Davis, J. T., *Chem. Commun.*, **2010**, *46*, 3950. d) McNally, B. A., Koulov, A. V., Smith, B. D., Joos, J. B., Davis, A. P., *Chem. Commun.,* **2005**, 1087.

15. a) Sheldon, R. A., *Chem. Commun.* **2001**, 2399. b) Wasserscheid, P., Keim, W., *Angew. Chem., Int. Ed.* **2000**, *39*, 3772. c) Dupont, J., de Souza, R. F., Suarez, P. A. Z., *Chem. Rev.* **2002**, *102*, 3667. d) Song, C. E. , *Chem. Commun.* **2004**, 1033.

16. Stewart, J. J. P., in *Stewart Computational Chemistry*; Version 7.213W

17. a) Sessler, J. L., Eller, L.R., Cho, W. S., Nicolaou, S., Aguilar, A., Lee, J. T., Lynch, V. M., Magda, D. J., *Angew. Chem., Int. Ed.* **2005**, *44*, 5989. b) Gale, P. A., Light, M. E., McNally, B., Navakhun, K., Sliwinski, K. E., Smith, B. D., *Chem. Commun.* **2005**, *30*, 3773.

Chapitre 3   Étude de la relation structure-activité pour différents sels d'imidazolium

3.1. Préface

Au terme de nos précédentes analyses ayant mis en lumière l'efficacité d'un bromure d'imidazolium à titre de transporteur d'anions, nous avons cherché à établir une première relation entre la structure et l'efficacité de cette nouvelle famille de composés.

A ce titre, nous avons modifié les contre-anions appariés au cation imidazolium afin d'en comparer l'effet sur le transport. Nous nous sommes également intéressés aux paramètres thermodynamiques et cinétiques de ces nouvelles molécules. Puis une approche expérimentale a été proposée afin de déterminer le mécanisme d'action de nos composés dans les membranes lipidiques. Ainsi la caractérisation du transport ionique et sa sélectivité dans des liposomes de EYPC et de DPPC a été faite par des méthodes analytiques variées faisant appel à des sondes fluorescentes telles que la lucigénine et le HPTS.

J'ai été l'instigateur principal de ce projet en faisant la synthèse et la caractérisation de toutes les molécules étudiées, ainsi qu'en conduisant l'ensemble des tests analytiques. Mathieu Charbonneau, mon stagiaire de l'époque, a participé sous ma supervision au développement de la méthode utilisée pour préparer les liposomes de DPPC et a également aidé à l'analyse des résultats et à la révision de l'article, que j'ai écrit en entier. Pre. Andreea Schmitzer a dirigé et supervisé l'ensemble des travaux de cette recherche et a procédé à la révision de l'article. Les informations expérimentales supplémentaires de ce chapitre se trouvent aux pages 148-160 de cette thèse.

3.2. Article 2: « An anion structure-activity relationship of imidazolium-based synthetic transporters »

Claude-Rosny Elie, Mathieu Charbonneau and Andreea R. Schmitzer*

Department of Chemistry, Université de Montréal, 2900 Édouard-Montpetit CP 6128 succ. Centre-Ville, Montréal Québec, Canada, H3C 3J7.
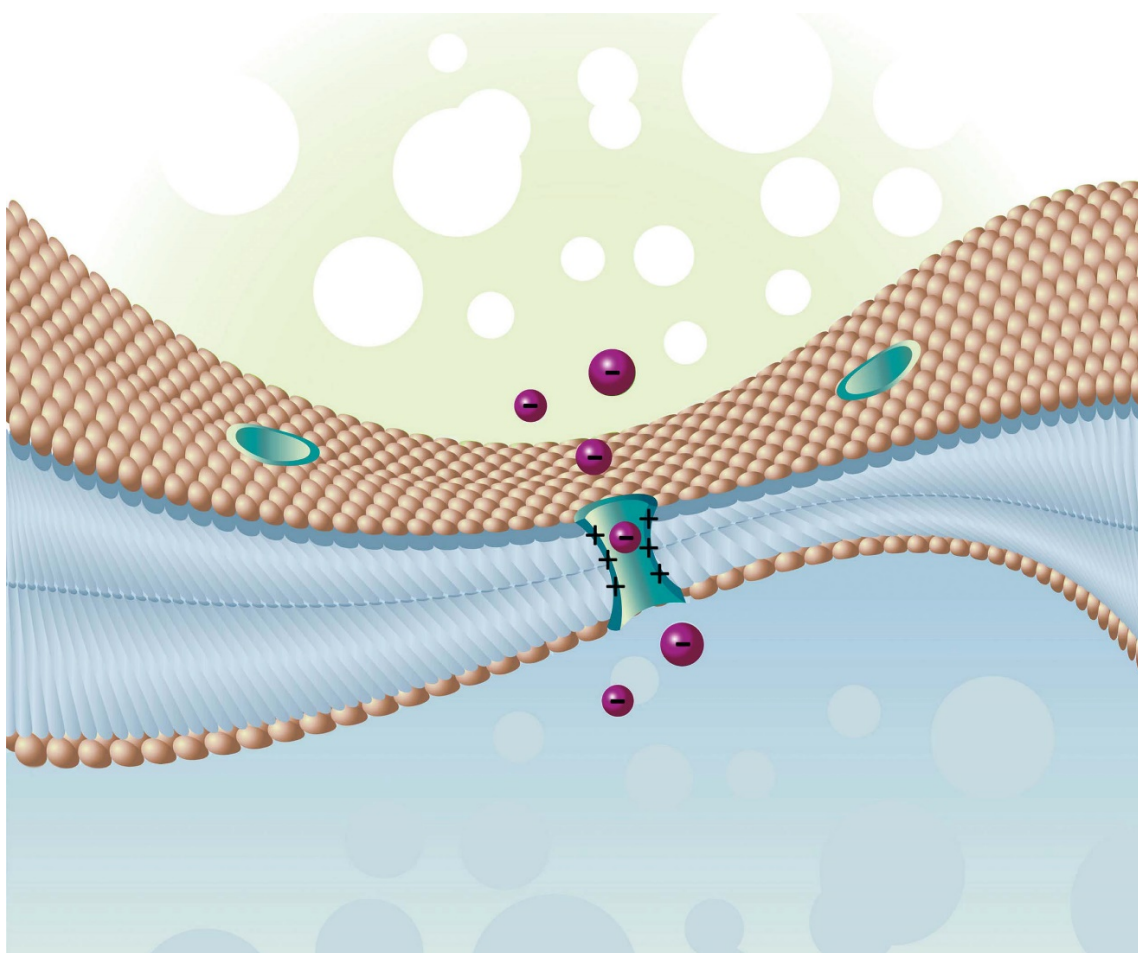
Figure 3.1.   Table of contents graphic

3.2.1.   Abstract

We have developed imidazolium-based salts as a new recognition motif with strong anionophoric properties across phospholipid bilayers. We present here factors intrinsic to the imidazolium salts that allow the modulation of their ionophoric properties. We also report the kinetic and thermodynamic parameters of the most active imidazolium salt.

3.2.2.   Introduction

Recent advances in the biomedical world have highlighted the growing number of diseases that have a pathogenesis based on the dysfunction of transmembrane ion

channels.[1] A lot of studies were carried out to explain problems associated with the transport of positive ions, such as sodium or potassium.[1] However, diseases described in more recent studies, such as osteoporosis, kidney stones and deafness, originate from the dysfunction of chloride channels.[2] Cystic fibrosis (CF) is a typical example, where the diffusion of chloride ions through the lipidic membranes is altered by the mutation of the CFTR protein, causing an electrolyte imbalance.[3] The study of the mechanisms of transport of anions in general and particularly those relative to Cl⁻, which is important for the development of new classes of antibiotics, antineoplastics and other treatments, is progressively gaining pertinence.[4] In this respect, a certain number of synthetic peptides with selective anionophoric properties on chloride were recently reported.[1] For example, Gokel *et al.* proved that modified peptides can form chloride channels.[5] In addition, Gale, Smith and Sessler *et al.*[6,7] showed that a prodigiosin analogue, a metabolite isolated from *Serratia marcescens*, with anticancerous properties,[8,9] possesses chloride transport properties. These synthetic peptides have complex structures and only a few non-peptidic synthetic channels, chloride selective, have been described in the literature. In particular, Matile *et al.* suggested that a polyol scaffold may be able to assure anionic transport.[10] We previously demonstrated that imidazolium salts with low molecular weights possess anionophoric properties.[11] We also showed that it was also possible to modulate the Cl⁻ transport across the bilayer by complexing the imidazolium salt with cyclodextrins and cucurbituril.[11] In the case of these supramolecular switches, the anionic diffusion through the membrane can be activated or inhibited.

We report here the factors, this time intrinsic to the imidazolium salt, that are responsible for the ionophoric activity of these salts (scheme 3.1). Therefore, our current study deals primarily with the influence of the nature of the imidazolium counter-anion on its anionophoric activity across the membrane of egg yolk phosphatidylcholine (EYPC) liposomes, using the lucigenin method (figure 3.2). Secondly, we describe the efflux of different anions using the pH-sensitive *8-hydroxypyrene-1,3,6-trisulfonic acid trisodium salt* (HPTS) method (figure 3.3) in the presence of the imidazolium transporters, as well as a detailed mechanistic study to elucidate whether they act as mobile ion transporters or rather form a transmembrane

channel. Finally, the kinetic parameters of the most active imidazolium salt, the EC_{50} and the rate constant characterizing the efflux of the Cl⁻ are presented.
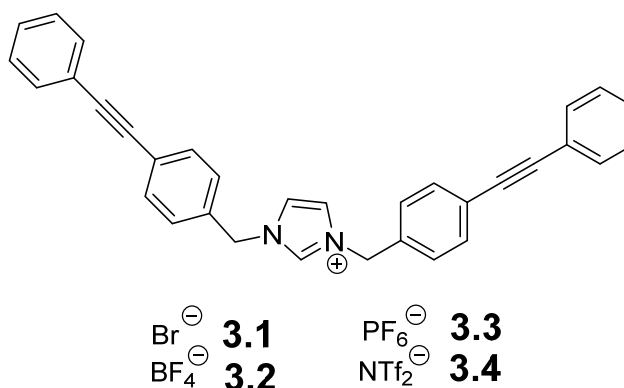
Scheme 3.1. Imidazolium salts studied for chloride transmembrane transport.
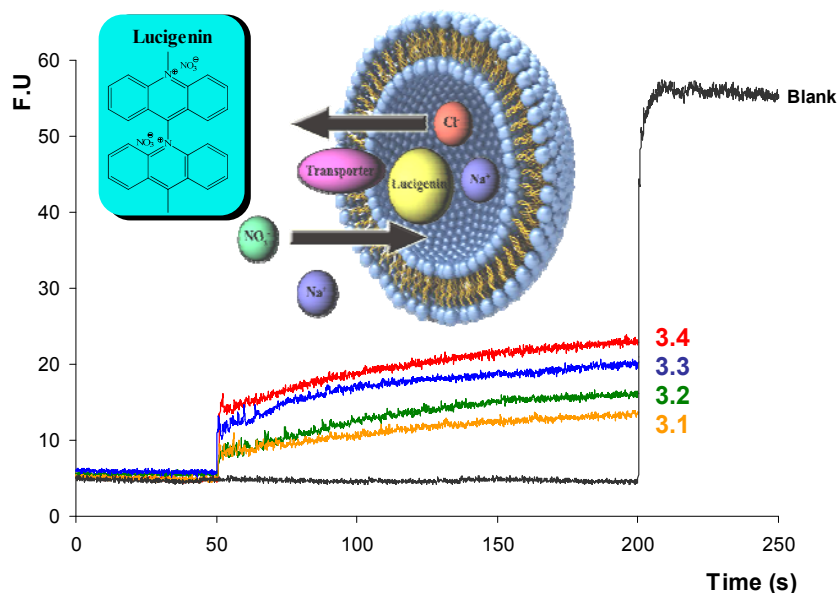
Figure 3.2. Relative activity of compounds **3.1**-**3.4** in the lucigenin-based Cl⁻ transport assay. Intravesicular conditions: 100 mM NaCl, 10 mM phosphate buffer, 2 mM lucigenin; extravesicular conditions: 100 mM NaNO₃, 10 mM phosphate buffer (pH 6.4). 0.1 mM solutions of **3.1**-**3.4** were injected at t = 50 s to give a final concenration of 16 µM (see annexe 2 for details); aqueous 10% Triton X-100 was injected at *t* = 500 s for **3.1**-**3.4** (not shown). For the Blank: aqueous 10% Triton-X was injected at t = 200 s. Each curve represents the average of three trials.
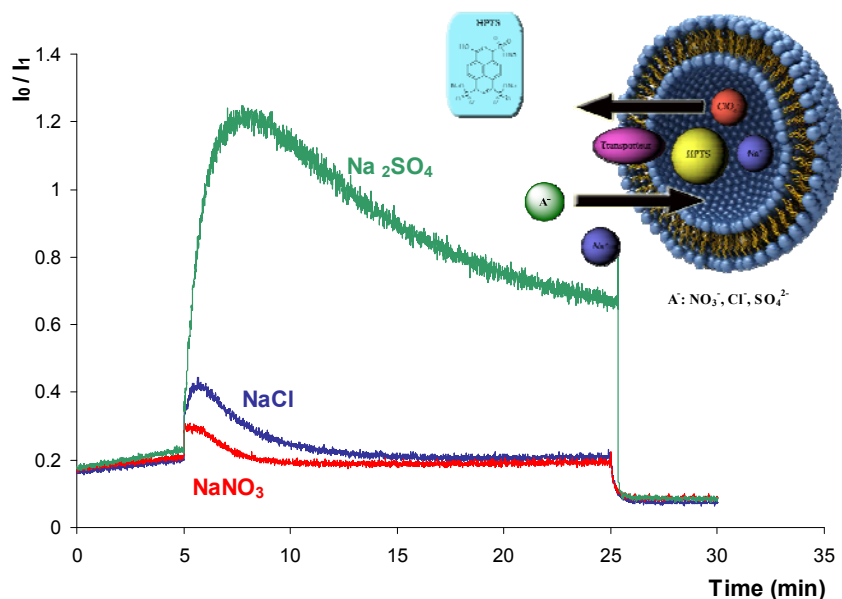
Figure 3.3. HPTS-based transport assay. Intravesicular: 100 mM $NaClO_4$, 10 mM phosphate buffer (pH = 6.2). Extravesicular: 100 mM Na^+ A^- (A^- = NO_3^-, Cl^-) or 75 mM Na_2SO_4, 10 mM phosphate buffer (pH = 6.3). 1.5 mM solution of **3.4** in MeOH was injected at t = 5 min to give a final concentration of 50 µM, ratio **3.4**/EYPC = 0.10 (see annexe 2 for details). Aqueous 10% Triton-X was injected at t = 25 min. Temperature was set to 37 ℃. The *Y*-axis "Ratio" refers to the ratio of HPTS fluorescence emission at 510 nm (I_0/I_1) where I_0 is the excitation at 460 nm (basic form of HPTS) and I_1 is the excitation at 403 nm (acidic form of HPTS). Each curve represents the average of three trials.

3.2.3.   Results and Discussion

All imidazolium salts were prepared following the same procedure involving first a reduction of a halogenated benzoic acid to the corresponding alcohol (annexe 2). The 4-iodobenzyl alcohol was coupled by a Sonogashira reaction with a terminal alkyne (annexe 2), then subjected to bromination, leading to the (4-phenylethynyl)benzyl bromide. The latter was then grafted onto an imidazole ring, in a succession of two nucleophilic attacks to obtain the *N,N'*-diphenylethynylbenzylimidazolium bromide **3.1**. The imidazolium salts **3.2–3.4** were obtained through anion metathesis of bromide (annexe 2). The Cl⁻ transmembrane transport activities of **3.1–3.4** were evaluated by fluorimetry, as previously reported.[11,12] Chloride efflux out of EYPC vesicles containing the fluorescent probe lucigenin, for which fluorescence is inhibited by the presence of halides,[12e] was measured and the fluorescence traces show the change in emission when

the transporter is added. As shown in Figure 3.2, the efflux of the Cl^- increases significantly in the presence of the ionophores **3.1–3.4**. The vesicles were lysed by addition of detergent Triton-X at an arbitrary moment, provoking the end of the chloride efflux. The first 150 s of the transport process, following injection of imidazolium, were then analysed. The Cl^- transport activity of imidazolium salts **3.1–3.4** follows the Hofmeister sequence,[13] according to the following order: $Br^- < BF_4^- < PF_6^- < NTf_2^-$.

This suggests that the counter-anion of the imidazolium salt has a direct impact on its anionophoric activity. This is due to the fact that counter-anions possessing a kosmotropic nature are strongly solvated by the water molecules.[14,15] The preferential hydration of Br^- is due to its capacity to establish interactions with water molecules. The resulting hydrated salt is less susceptible to self-aggregate and to distribute into the hydrophobic bilayer. Conversely, molecules with highly chaotropic counter-anions (*e.g.*: NTf_2^-), which are less hydrated, tend to penetrate and aggregate more easily into the bilayer. Ionophore **3.4** is the most active in the Cl^- transmembrane transport as a result of its distribution and self-aggregation in the liposome bilayer, thus the Cl^-/NO_3^- transmembrane exchange increases.

To gain insights into the transport mechanism of **3.4** and to corroborate the results obtained in the lucigenin-based assays, compound **3.4** was also studied using liposomes loaded with HPTS (Fig. 3.3). Three series of measurements were performed using anions with different permeabilities in the extravesicular medium and the same $NaClO_4$ solution as the intravesicular medium. The nitrate (ΔG_{hyd} = -300 kJ mol^{-1}) is a more hydrophobic species than chloride (ΔG_{hyd} = -340 kJ mol^{-1}) and sulfate (ΔG_{hyd} = -1080 kJ mol^{-1}).[16] The results shown in Fig. 3.3, analyzed according to Davis *et al.*,[17] show that the efflux of the intra-vesicular anions, under the effect of the transporter, causes the deprotonation of the HPTS and results in the alkalinization of the intravesicular medium, inducing an increase of the I_0/I_1 fluorescence ratio. Then, the translocation of the extravesicular anions towards the inside of the liposome leads to the symport migration of the protons following the anionic gradient. This results in acidification of the intravesicular medium and, as a result, a decrease of the I_0/I_1 fluorescence ratio. In the presence of the imidazolium salt **3.4**, the anionic exchange on

both sides of the liposome membrane takes approximately 8, 10 and over 25 minutes for the couples NO_3^-/ClO_4^-, Cl^-/ClO_4^- and SO_4^{2-}/ClO_4^- respectively.

It should be noted that this selectivity for the anionic transport, induced by the imidazolium salt **3.4**, follows once again the Hofmeister's sequence,[13] *i.e.* $NO_3^- > Cl^- > SO_4^{2-}$. The I_0/I_1 fluorescence ratio can be explained by the simultaneous alkalinization and acidification processes. When these processes overlap in time, the I_0/I_1 ratio indicates a low peak due to the fast deprotonation of the HPTS, compensated by a massive entry of protons, according to anionic migration. The alkalinization process can be more accurately visualized in the case of an extravesicular anion that is not very permeable (*e.g.*: SO_4^{2-}), which leads to a slow acidification. The rapid alkalinization of the inside of the liposome in the case of the NO_3^-/ClO_4^- couple suggests that it is easier to translocate the ClO_4^- anion encapsulated in the liposome in the presence of a very permeable extravesicular anion such as NO_3^-. When replacing NO_3^- with the less permeable SO_4^{2-}, the acidification process is considerably slowed down. It can also be observed that the liposomes remain intact during the transport process, until their lysis with Triton-X at 25 minutes.

In order to elucidate the mechanism governing the anionic transport of these imidazolium-based transporters, we studied the capacity of **3.4** either to act as a mobile ionic transporter or rather to form a transmembrane channel. To distinguish the possible mechanisms, we measured the efflux of the Cl^- outside 1,2-dipalmitoyl-*sn*-glycero-3-phosphocholine (DPPC) liposomes using the lucigenin-based assay, at temperatures above and below DPPC's transition phase (41 °C). Details of the procedure are given in the annexe 2. The effectiveness of a mobile anionic transporter, limited by its diffusion through the membranes, is generally considerably reduced when the DPPC liposome bilayer is maintained in a gel-state (< 41 °C),[18,19] whereas in the case of a transmembrane channel formation, no or only a small alteration of its effectiveness is observed below the bilayer's gel-to-liquid crystalline phase transition temperature.[18,19] As shown in figure 3.4, in the presence of 7 mol.% imidazolium salt **3.4** (relative to the DPPC concentration), the efflux of the Cl^- ion is only partially affected in the five assays from 25 °C to 45 °C. Fig. 3.4b clearly shows that, after 300 seconds, there is a quasi-linear variation of the

anionophoric activity of **3.4** with the temperature. These results prove that imidazolium **3.4** forms a transmembrane channel, corroborating our previous molecular modeling results,[11] where the aromatic arms self-assemble by π–π interactions, forming transient channels. The rigid scaffold of these channels promotes the diffusion of the anions through the bilayer, by anion–π interactions. [11]
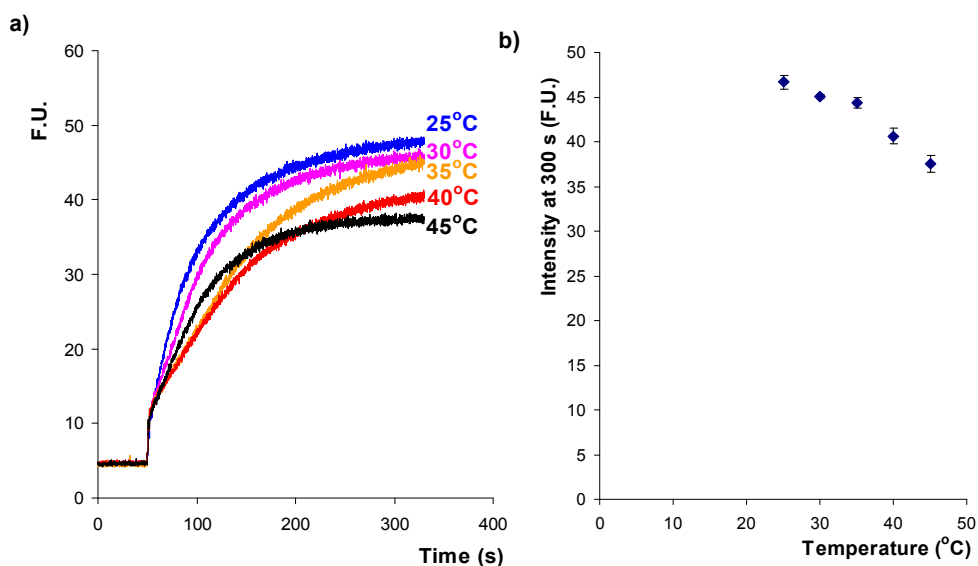
Figure 3.4. Chloride efflux out of DPPC liposomes at 25 ºC, 30 ºC, 35 ºC, 40 ºC and 45 ºC. The data at each temperature are obtained by using 7 mol.% of **3.4** (relative to DPPC concentrations). The data at each temperature are the average of three series of measurements.

A detailed kinetic study of the anionic transport of the Cl⁻ initiated by **3.4** in EYPC liposomes was performed using the lucigenin-based assay. Firstly, the initial rate was calculated from different **3.4**/EYPC molar ratios, varying from 1% to 30%. The Stern–Volmer equation illustrates the quenching extinction mechanism relative to the lucigenin fluorescence in the presence of its quencher, the chloride ion: [20]

$$\left(\frac{F_0}{F}\right) = 1 + K_{sv}[Cl^-] \tag{3.1}$$

where F_0 is the maximum fluorescence intensity in the absence of the quencher, determined by injecting Triton-X; F is the fluorescence measured at a specific moment;

K_{sv} is the Stern–Volmer constant; K_{sv} = 142 M^{-1} and [Cl⁻] is the intravesicular concentration of chloride ions. Eqn (3.2) was obtained by taking the derivative of eqn (3.1) to give the initial rate:

$$-\left(\frac{d[Cl^-]}{dt}\right) = \left(\frac{F_0}{K_{sv}}\right) \bullet \left(\frac{1}{F^2}\right) \bullet \left(\frac{dF}{dt}\right)_{t=0} = V_0 \tag{3.2}$$

The initial rate (V_0) was measured after the injection of the transporter, at less than 10% of the maximum fluorescence intensity where the efflux of chloride follows the Michaelis– Menten kinetics:

$$\text{aggregates} \xrightleftharpoons{K_{diss}} n \text{ monomer} \tag{3.3}$$
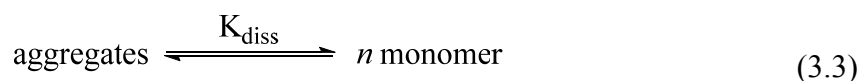
$$K_{diss} = \frac{[monomer]^n}{[aggregates]} \tag{3.4}$$

$$V_0 = k_{obsd}[Cl^-]_{t=0} = k_2[aggregates][Cl^-]_{t=0} \tag{3.5}$$

$$k_{obsd} = \frac{k_2[monomer]^n}{K_{diss}} \tag{3.6}$$
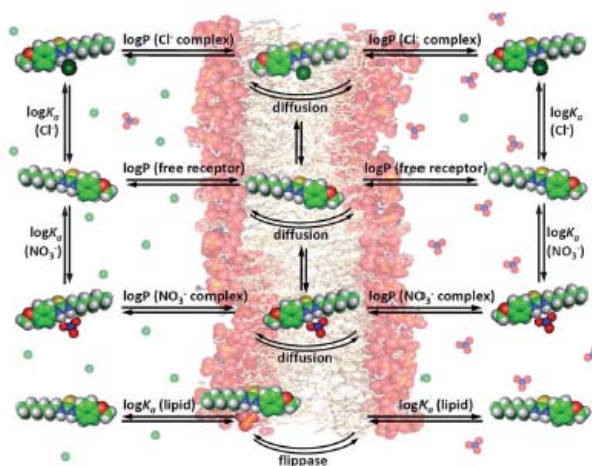
Figure 3.5.   Cartoon depicting equilibria occurring during transmembrane anion transport process.[21] Reproduced with permission of Royal Society of Chemistry.

In the self-aggregation process of **3.4**, there is an equilibrium between the monomeric and aggregated forms (eqn (3.4)). The term «monomer» should not be seen as necessarily a single molecule, but as an elemental unit. It represents with respect to eqn (3.4) a level of organisation of the imidazolium, inferior to the aggregation level. However, we should mention that transport process is a complex one, where multiple equilibria are involved such as partitioning of the free imidazolium and the anion complex into the bilayer, the formation, diffusion and insertion mechanism of the aggregates as well as the translocation of anions through the channel-like ionophore and interactions of ions from the buffer.[21] Our efforts to deconvoluate all these parameters aren't enough successful at this point to allow us to express the individual rates of all these processes independently into our simplified model. They are included into the expression of the rate constant we shall see. However one can note that some other factors such as flippase activity on phospholipids can be neglected here as there are no such proteins in our liposomes.

The initial rate is expected to obey eqn (3.5), as a function of a pseudo-first order constant, k_{obsd}. In addition, k_{obsd} is the result of the rate constant k_2 being directly related to the concentration of the active aggregates. By combining eqn (3.4) and (3.5), it is possible to express the aggregate concentration in terms of monomer concentration and the dissociation constant (K_{diss}), which defines the equilibrium between the two species. Eqn (3.6) shows that k_{obsd} varies according to the monomer concentration to the nth power. The monomer, as an elemental unit, plays a role in the transport. The result of this mathematical calculation shows that k_{obsd} follows first-order kinetics relative to monomer **3.4** concentrations, as depicted in Fig. 3.6.
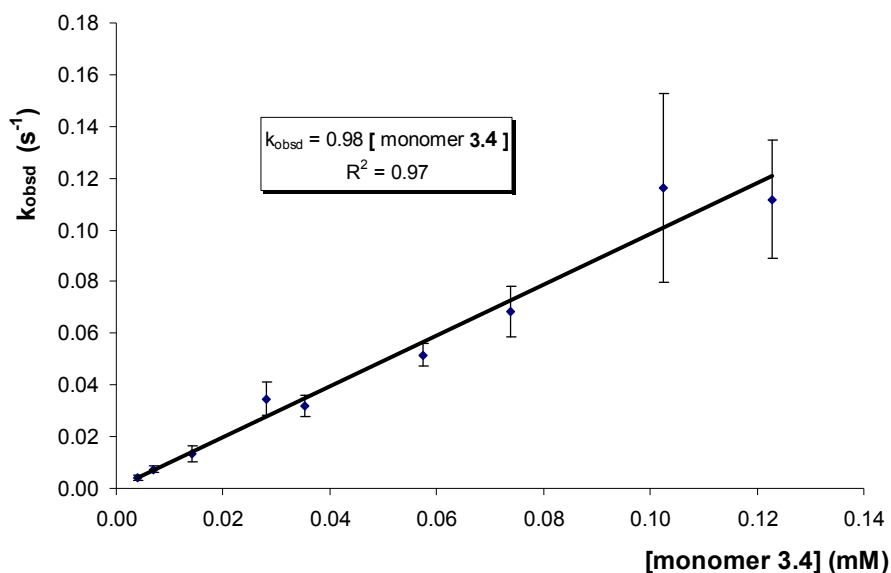
Figure 3.6. Plot of k_{obsd} according to the monomer concentration of the imidazolium **3.4**. The solid line represents a linear fit of the data according to eqn (3.6). The data at each concentration of **3.4** are the average of 3 series of measurements.

The graph's slope (0.98 mM^{-1} s^{-1}) shown in figure 3.6 corresponds to the ratio k_2/K_{diss} (eqn (3.6)). This term resembles a specificity constant describing the transporter's ability to facilitate the diffusion of a given anion, and is directly related to the aggregation of **3.4**. The parameter k_2/K_{diss} contains two terms: one is the rate constant and the other is the dissociation constant of the self-association process. Unfortunately, we have not been able to separate these kinetic and thermodynamic constants. However, since the ratio is around 1, it is reasonable to assume that the rate constant k_2 and the dissociation constant K_{diss} are in the same range. A detailed Hill analysis under denaturating conditions may reveal the exact stoichiometry of the active aggregate. [22]

Finally, the effectiveness (*i.e.* its EC$_{50}$ value) of the imidazolium **3.4** for chloride transport across the bilayer was calculated. The EC$_{50}$ value of compound **3.4** in a Cl^{-}/NO$_3^{-}$ system is 5.74 mol.% (relative to the EYPC concentration). This result is comparable to the EC$_{50}$ obtained for the phenylthioureas (3.05 mol.%)[23] described by Gale *et al.*, and considered to be a very effective class of transporters. This suggests that

further structural improvements of the imidazolium skeleton can be made to improve its anionophoric effectiveness and reduce its EC_{50}.

3.2.4.   Conclusions

In conclusion, we demonstrated that imidazolium salts **3.1–3.4** are molecules with anionophoric properties. The assays carried out through direct measurement of the efflux of Cl⁻ outside the EYPC liposomes and followed by the fluorescence of the lucigenin proved the superior activity of compound **3.4** compared to the other studied imidazolium salts. Its activity is comparable to other known ionophores. We also showed that imidazolium **3.4** assures anionic diffusion through the formation of trans-membrane channels. This is a major breakthrough in terms of highlighting the mechanism, so far unsolved, of the behaviour of the imidazolium ionophores in a bilayer. Finally, the kinetics governing the aggregation of the imidazolium molecules in the channels and their effectiveness in terms of promoting the efflux of the Cl⁻ ions have been characterized by the specificity constant k_2/K_{diss} equal to 0.98 $mM^{-1}s^{-1}$. This parameter is a very useful tool which may, in the future, be used to measure the specificity of a transporter for a given anion.

3.2.5.   Experimental Section

All the reagents were purchased from Aldrich. They were all used without further purification. L-α-Phosphatidylcholine was purchased from Avanti Polar Lipids. Liposome fluorimetric assays were recorded using a Varian Cary Eclipse fluorescence spectrophotometer. NMR experiments were recorded on a Bruker Advance 300 or 400 instrument. Chemical shifts are given in ppm (δ) and measured relative to TMS. High-resolution mass spectra (HRMS) were recorded on a TSQ Quantum Ultra (Thermo Scientific) triple quadrupole with accurate mass option (Université de Montréal Mass Spectrometry Facility).

3.2.6.   Notes and references

1. Reddy, G. L., Iwamoto, T., Tomich, J. M., Montal, M., *J. Biol. Chem.* **1993**, 268, 14608. (b) Oblatt-Montal, M., Reddy, G. L., Iwamoto, T., Tomich, J. M., Montal, M., *Proc. Nat. Acad. Sci.* **1994**, *91*, 1495. (c) Wallace, D. P., Tomich, J. M., Eppler, J. W., Iwamoto, T., Grantham, J. J., Sullivan, L. P., *Biochim. Biophys. Acta (Biomembranes)* **2000**, *1464*, 69. (d) Mitchell, K. E., Iwamoto, T., Tomich, J., Freeman, L. C, *Biochim. Biophys. Acta (Biomembranes)* **2000**, *1466*, 47. (e) Broughman, J. R., Mitchell, K. E., Sedlacek, R. L., Iwamoto, T., Tomich, J. M. Schultz, B. D., *Am. J. Physiol.: Cell Physiol.* **2001**, *280*, C451.

2. Jentsch, J.T., Maritzen, T., Zdebik, A., *J Clin Invest.* **2005**, *115*, 2039.

3. Deng, G., Dewa, T., Regen, S. L., *J. Am. Chem. Soc.* **1996**, *118*, 8975. (b) Jiang, C. W., Lee, E. R., Lane, M. B., Xiao, Y.-F., Harris, D. J., Cheng, S. H., *Am. J. Physiol.* **2001**, *281*, L1164.

4. Matile, S., Vargas Jentzsch, A., Montenegro, J., Fin, A., *Chem. Soc. Rev.* **2011**, *40*, 2453. (b) Fernandez-Lopez, S., Kim, H. S., Choi, E. C., Delgado, M., Granja, J. R., Khasanov, A., Kraehenbuehl, K., Long, G., Weinberger, D. A., Wilcoxen, K. M., Ghadiri, M. R. *Nature* **2001**, *412*, 452. (c) Porter, E. A., Wang, X. F., Lee, H. S., Weisblum, B., Gellman, S. H., *Nature* **2000**, *404*, 565. (d) Hamuro, Y., Schneider, J. P., DeGrado, W. F., *J. Am. Chem. Soc.* **1999**, *121*, 12200. (e) Yamashita, K., Janout, V., Bernard, E. M., Armstrong, D., Regen, S. L., *J. Am. Chem. Soc.* **1995**, *117*, 6249.

5. Schlesinger, P. H., Ferdani, R., Liu, J., Pajewska, J., Pajewki, R., Saito, M., Shabany, H., Gokel, G.W., *J. Am. Chem. Soc.* **2002**, *124*, 1848.

6. Gale, P.A., Light, M. E., McNally, B., Navakhum, K., Sliwinski, K. E., Smith, B. D., *Chem. Commun.*, **2005**, *30*, 3773.

7. Sessler, J. L., Eller, L. R., Cho, W.-S., Nicolaou, S., Aguilar, A., Lee, J. T., Lynch, V. M., Magda, D. J., *Angew. Chem., Int. Ed.* **2005**, *45*, 5985.

8. Furstner, A., *Angew. Chem., Int. Ed.* **2003**, *42*, 3582.

9. Manderville, R. A., *Curr. Med. Chem.: Anti-Cancer Agents* **2001**, *1*, 195.

10. Weiss, L. A., Sakai, N., Ghebremariam, B., Ni, C., Matile, S., *J. Am. Chem. Soc.* **1997**, *119*, 12142.

11. Elie, C.-R., Noujeim, N., Pardin, C., Schmitzer, A. R., *Chem. Commun.* **2011**, *47*, 1788.

12. Davis, P., Sheppard, D. N., Smith, B. D., *Chem. Soc. Rev.* **2007**, *36*, 348 (b) Sidorov, V., Kotch, F. W., Kuebler, J. L., Lam, Y.-F., Davis, J. T., *J. Am. Chem. Soc.* **2003**, *125*, 2840. (c) McNally, B. A., Koulov, A. V., Smith, B. D., Joosb, J. B., Davis, A. P., Harrell Jr, W. A., Bergmeyer, M. L., Zavalij, P. Y., Davis, J. T., *Chem. Commun.* **2010**, *46*, 3950. (d) McNally, B. A., Koulov, A. V., Smith, B. D., Joos, J-B., Davis, A. P., *Chem. Commun.* **2005**, 1087. (e) McNally, B. A., Koulov, A. V., Lambert, T. N., Smith, B. D., Joos, J-B., Sisson, A. L., Clare, J. P., Sgarlata, V., Judd, L. W., Magro, G., Davis, A. P., *Chem.-Eur. J.* **2008**, *14*, 9599.

13. Hofmeister, F., *Arch. Exp. Pathol. Pharmacol.* **1888**, *24*, 247.

14. Collins, K.D., *Biophys. J.* **1997**, *72*, 65.

15. Hribar, B., Southall, N. T., Vlachy, V., Dill, K. A., *J. Am. Chem. Soc.* **2002**, *124*, 12302.

16. Marcus, Y., *J. Chem. Soc. Faraday Trans.* **1991**, *87*, 2995.

17. Sidorov, V., Kotch, F. W., Abdrakhmanova, G., Mizani, R., Fettinger, J. C., Davis, J. T., *J. Am. Chem. Soc.* **2002**, *124*, 2267.

18. Koulov, V., Lambert, T. N., Shukla, R., Jain, M., Bood, J. M., Smith, B. D., Li, H. Y. D., Sheppard, N., Joos, J-B., Clare, J. P., Davis, A. P., *Angew. Chem., Int. Ed.* **2003**, *42*, 4931.

19. Krasne, S., Eisenman, G., Szabo, G., *Science* **1971**, *174*, 414.

20. (a) Wissing, F., Smith, J. A. C., *J. Membrane Biol.* **2000**, *177*, 199. (b) Chhun, C. Axe et Rotaxane Parapluie, vers de nouveaux transporteurs transmembranaires de chlorures et de médicaments cycliques. Thèse de doctorat, Université de Montréal, Montréal, **2012**.

21. Busschaert, N., Bradberry, S. J., Wenzel, M., Haynes, C. J. E., Hiscock, J. R., Kirby, I. L., Karagiannidis, L. E., Moore, S. J., Wells, N. J., Herniman, J., Langley, G. J., Horton, P. N., Light, M. E., Marques, I., Costa, P. J., Felix, V., Frey, J. G., Gale, P. A. *Chem. Sci.* **2013**, *4*, 3036.

22. Bhosale, S., Matile, S., *Chirality* **2006**, *18*, 849.

23. Andrews, N. J., Haynes, C. J. E., Light, M. E., Moore, S. J., Tong, C. C., Davis, J. T., Harrell Jr., W. A., Gale, P. A., *Chem. Sci.* **2011**, *2*, 256.

Chapitre 4   **Étude des propriétés ionophores des sels de benzimidazolium et premières applications biologiques**

4.1.   Préface

Les résultats observés dans le cadre du chapitre 3 de cette thèse nous ont conduits à établir une relation entre la structure et l'activité ionophore des sels d'imidazolium basée sur la nature de leurs contre-anions respectifs. Ayant démontré que les contre-anions plus chaotropiques, tels que le bis(trifluoromethylsulfonyl)amide, donnaient lieu à des canaux plus aptes à pénétrer les membranes et induire un transport ionique plus important, nous nous sommes intéressés à faire varier la nature du cation, en remplacant le cation imidazolium par un benzimidazolium. En effet, l'utilisation du motif benzimidazole visait à augmenter l'aromaticité du cation et ses interactions avec les anions, tout en gardant son autoassemblage dans les bicouches, par des empilements π des groupements latéraux.

En comparant la concentration effective générant 50% de l'efflux des ions chlorures hors d'un liposome (EC$_{50}$) de cette nouvelle famille de transporteurs, nous pûmes effectivement observer une nette amélioration de l'efficacité relative des transporteurs de type benzimidazolium par rapport à l'ancienne génération des sels d'imidazolium. Une équation cinétique a également été développée pour dégager des constantes de vitesses initiales apparentes (k_{obsd}) toujours en gardant à l'esprit l'existence d'équilibres multiples du transporteur, tel qu'évoqué au chapitre 3. Il est cependant important de mentionner que l'expression de la vitesse initiale et la valeur du EC$_{50}$ sont deux éléments totalement différents. En effet une vitesse initiale faible ne se traduit pas nécessairement par un faible EC$_{50}$. En outre, nous discutons également dans cet article du coefficient de Hill, un paramètre dont l'interprétation a également beaucoup évoluée dans la littérature et selon les auteurs qui l'emploient, qu'ils soient du domaine d'expertise de la chimie supramoléculaire ou de la biochimie. Ces trois éléments (k_{obsd}, EC$_{50}$ et coefficient de Hill) formant les piliers des théories sur la relation quantitative structure-activité (QSAR), n'ont pas fait l'objet ici d'un rapprochement par des équations mathématiques, bien que la littérature propose parfois des formules complexes qui tentent d'unifier ces trois paramètres.

Enfin, nous nous sommes intéressés à la capacité des sels de benzimidazolium d'induire le transport d'ions calcium à l'intérieur d'une bactérie *E. coli* (Dh5α, citrine-pBad) surexprimant un marqueur biologique des ions Ca^{2+}.

J'ai piloté l'ensemble du projet en faisant la synthèse et la caractérisation de toutes les molécules étudiées ainsi qu'en effectuant et supervisant toutes les étapes des tests analytiques et les analyses *in cellulo* en compagnie de mes stagiaires Adam Haiun et Audrey Hébert. Mathieu Charbonneau a également participé sous ma supervision à la synthèse des sels de benzimidazolium et m'a assisté dans la révision de l'article que j'ai écrit en entier. Pre. Andreea Schmitzer a dirigé et supervisé l'ensemble des travaux de cette recherche et a procédé à la révision finale de l'article. Les informations expérimentales supplémentaires de ce chapitre se trouvent aux pages 161-183 de cette thèse.

4.2. Article 3 : « Benzimidazolium-based synthetic chloride and calcium transporters in bacterial membranes »

Claude-Rosny Elie[a], Audrey Hébert[a], Mathieu Charbonneau[a], Adam Haiun[b] and Andreea R. Schmitzer*[a].

[a]Department of Chemistry, Université de Montréal, 2900 Édouard-Montpetit CP 6128 succ. Centre-Ville, Montréal Québec, Canada, H3C 3J7.
[b]John Abbott College, Sainte-Anne-de-Bellevue, Québec, Canada

Figure 4.1.   Table of Contents Graphic

Herein, we present the first example of a benzimidazolium-based artificial transmembrane chloride transporter and a synthetic calcium ionophore that can regulate intracellular calcium concentrations into bacteria.

4.2.1.   Introduction

Ion transport across cell membranes is the basis for generation of membrane potentials and provides the osmotic gradients for transmembrane and paracellular fluid transport. Chloride transport in the human apical epithelial cell membrane is mainly mediated by the cAMP dependent Cystic Fibrosis Transmembrane Conductance Regulator [CFTR] chloride channel, which can move chloride into and out of the cell, and the calcium-activated chloride channels. Calcium activated chloride channels

complement the function of CFTR in transmembrane chloride transport[1,2] where they seem to regulate each other's activity. It was previously demonstrated that in biological systems, changes in ion concentration induced by opening a certain ion channel invariably affects the behavior of other ion channels.[3,4]

To the best to our knowledge, the first and single example of an artificial chloride channel that can regulate intracellular calcium concentrations and the contraction of smooth muscle cells *via* modulating cell membrane potentials in living cells and tissues was reported by Yang *et al.*[5] The ability of synthetic chloride channels to perturb functions of natural ion channels open new perspectives for the applications of other synthetic ion channels in biological systems.

Research into synthetic ion transporters has led to the development of complex families of molecules[6,7,8] that rely on weak interactions[9] such as hydrogen bonds, cation-π and anion-π- interactions.[10] We previously exploited the anion-π-type interactions in the development of imidazolium-based synthetic chloride transporters.[11] In this case, anion-π interactions are due to the electron-withdrawing effect of imidazolium on the aromatic rings.[12,13] The effective anionic transport properties of these compounds were attributed to the formation of dimeric channel architectures into the liposome lipid membranes.[11,14] Nevertheless, the presence multiple binding sites for ions along the dimer offer the possibility of multi-ion hopping as seen in biological ion channels responsible for fast and selective transport processes.[15] Our interest in improving the effectiveness of these imidazolium-type transporters in terms of different parameters (e.g. EC_{50} and specificity constant) led us to develop new compounds by replacing the imidazolium unit with a benzimidazolium moiety (figure 4.2). These low molecular weight compounds still possess good amphiphilic character for spanning the lipid membranes and the presence of the benzimidazolium cation maximizes the supramolecular π-stacking properties. We describe here how this benzimidazolium cation has an impact on the efficiency of the chloride transport activity. We demonstrate that these benzimidazolium transporters can also ensure the transport of cations across the membranes of living *E. coli*, showing their "ditopic" properties: the ability to operate as an anion and cation symport mechanism. These new properties may be of interest to simultaneously transport $Ca^{2+}/2Cl^-$ in order to efficiently compensate the CFTR dysfunction.
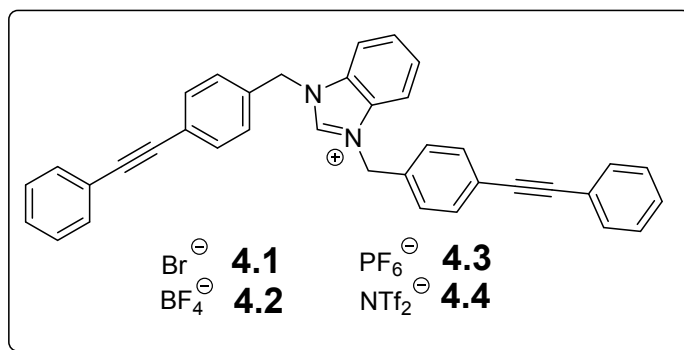
Figure 4.2.   Imidazolium salts studied for chloride transmembrane transport.

4.2.2.   Results and Discussion

Benzimidazolium ionophores were synthesised by the reaction of benzimidazole and sodium hydride with (4-phenylethynyl)benzyl bromide[11,14] followed by the reaction with an equivalent of (4-phenylethynyl)benzyl to afford benzimidazolium **4.1** in 63% yields (scheme 4.1). The other compounds were obtained through anion metathesis of bromide affording **4.2**, **4.3** and **4.4** in 90%, 99% and 90% yields, respectively (scheme 4.2).
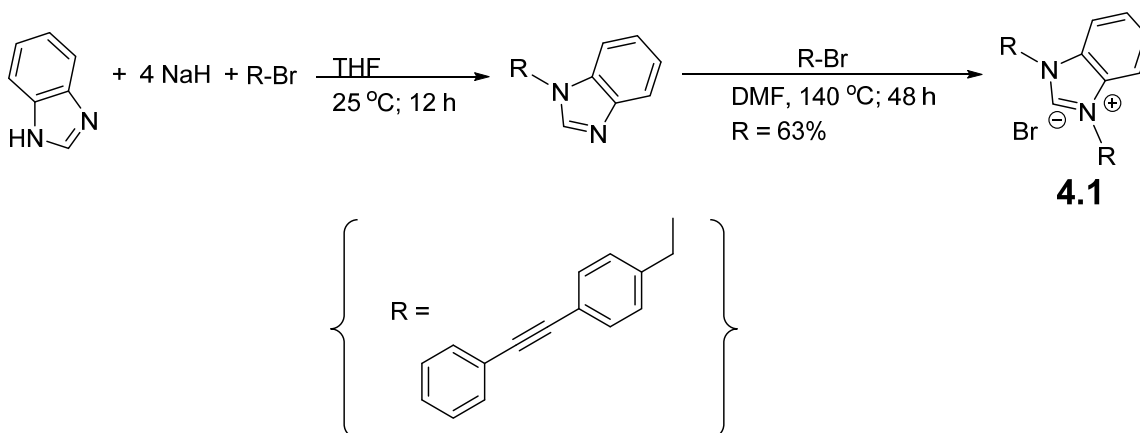
Scheme 4.1.   Synthesis of compound **4.1**.
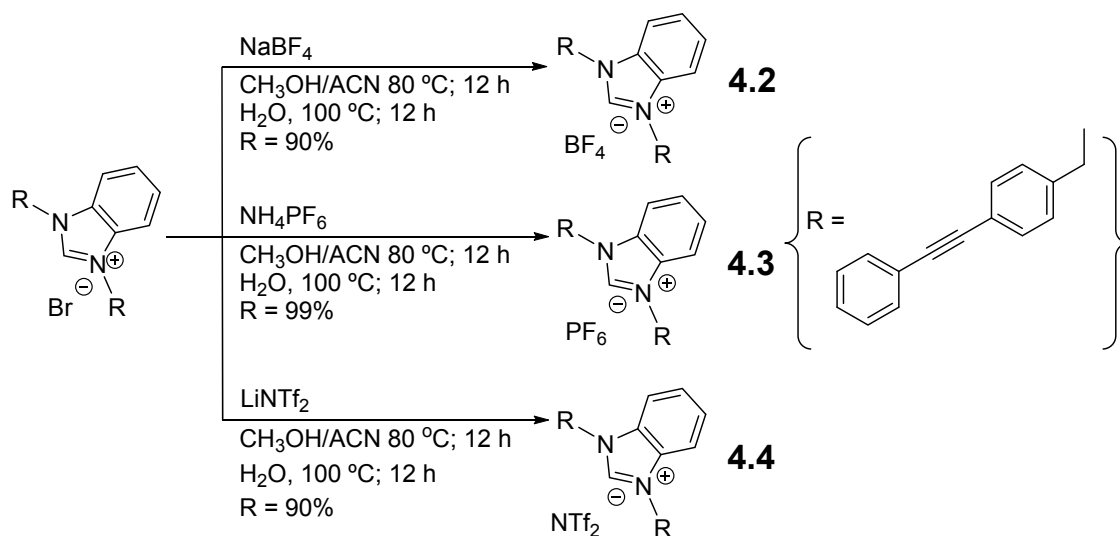
Scheme 4.2.   Synthesis of compounds **4.2–4.4.**

The benzimidazolium salts **4.1-4.4** were first studied for their ability to promote the transport of Cl⁻ across egg yolk phosphatidylcholine (EYPC) bilayers by directly monitoring the flow of ions in the presence of lucigenin.[11,14,16] Chloride efflux out of EYPC vesicles containing lucigenin,[17] was measured and the fluorescence traces show the change in emission when an aliquot of transporter is added to the lucigenin-containing vesicles. A cartoon representation of the liposome assay sequence is shown in the inset of figure 4.3. It appears, as depicted in this figure, that the injection of compound **4.4** induces an earlier increase of fluorescence. Benzimidazolium salts **4.2** and **4.3** present a similar activity, whereas the bromide (compound **4.1**) leads to a slower fluorescence increase, suggesting a weaker efflux of Cl⁻. Furthermore, the Cl⁻ transport activity of salts **4.1-4.4** follows the same trend as we had previously observed for the imidazolium salts, according to the Hofmeister series. The preferential hydration of Br⁻ is due to its capacity to establish interactions with water molecules,[18] compared to BF₄⁻, PF₆⁻ or NTf₂⁻. The resulting hydrated salt is less susceptible to self-aggregate and to penetrate into the hydrophobic bilayer. Molecules with a highly chaotropic counter-anion (e.g.: NTf₂⁻), which are less hydrated, are more subject to distribute into the liposome membrane and thus be more effective in the chloride transport process.
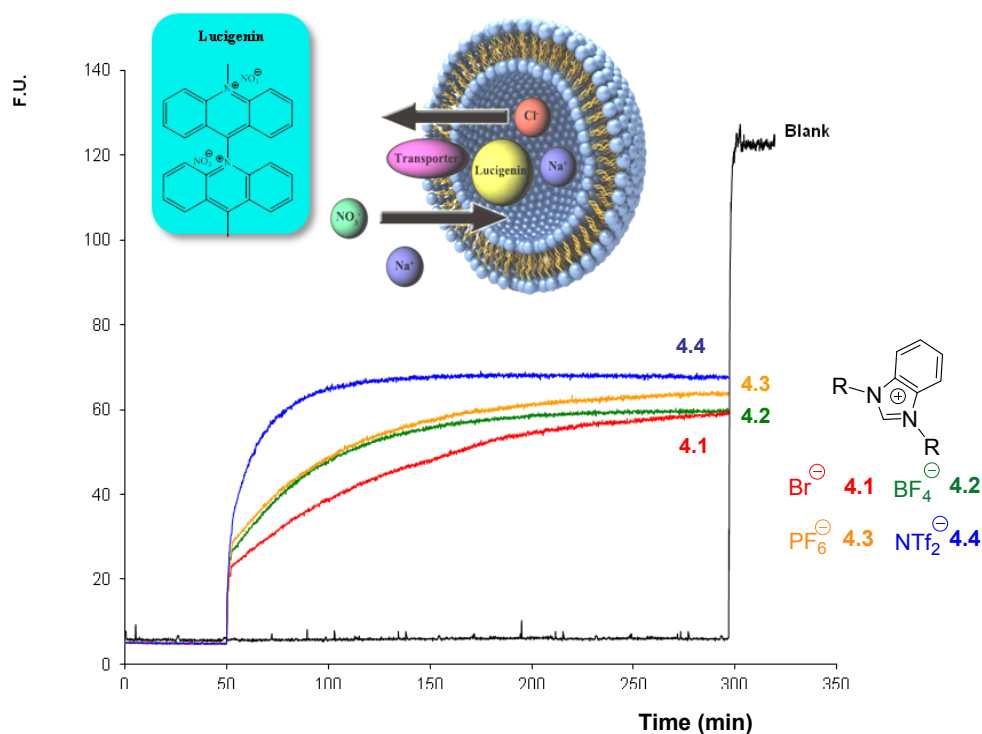
Figure 4.3. Relative activity of compounds **4.1-4.4** in the lucigenin-based Cl⁻ transport assay. Intravesicular conditions: 100 mM NaCl, 10 mM phosphate buffer, 2 mM lucigenin; extravesicular conditions: 100 mM NaNO₃, 10 mM phosphate buffer (pH 6.4).). 0.25 mM solutions of **4.1-4.4** were injected at t = 50 s to give a final concenration of 40 μM (see annexe 3 for details); aqueous 10% Triton X-100 was injected at t = 300 s. Each curve represents the average of three trials. R = 4-phenylethylbenzyl.

We also examined the extent of Cl⁻ efflux out of fluid-phase EYPC vesicles as a function of time and ionophore content. By using similar procedures to those we previously described,[14] the mole percentages of **4.4** were varied from 1% to 12.5% corresponding respectively to 3 μM to 43 μM of transporter. The effectiveness of benzimidazolium **4.4** was characterized in the chloride transport process across the bilayer by its EC_{50} values, using dose-response analysis (Annexe 3) based over data shown in figure 4.4a. The EC_{50} value for compound **4.4** in a Cl⁻/NO₃⁻ system was 2.99 mol.% (relative to the EYPC concentration), a value slightly lower than the EC_{50} obtained for our previous imidazolium transporter (5.74 mol.%) or the phenylthioureas (3.05

mol.%) described by Gale *et al.*, and considered to be very effective synthetic transporters.[14,19]
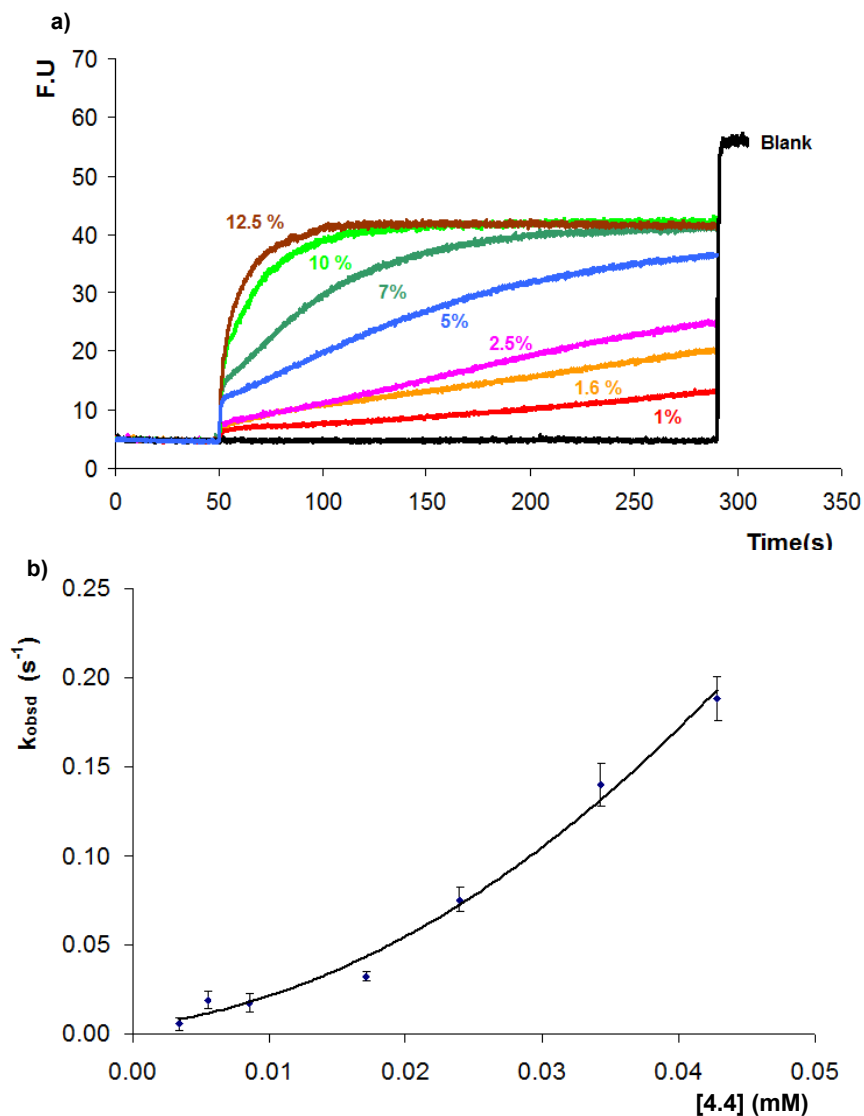
Figure 4.4.   (a) Efflux of Cl⁻ out of EYPC vesicles containing 1.0, 1.6, 2.5, 5, 7, 10 and 12.5 mol % of **4.4** (increasing rates, respectively) as a function of time at 37 °C. Each curve represents the average of three trials. (b) Plot of k_{obsd} versus concentration of **4.4**; the solid line represents a nonlinear least-squares fit of the data according to eqn (4.1), where *n* = 2.0. The data at each concentration of **4.4** is the average of 3 series of measurements.

Analysis of internal Cl$^-$ efflux for different mole percentages of **4.4**, as a function of time yielded the kinetic profiles depicted in Fig. 4.4b. The observed pseudo-first-order rate constants (k_{obsd}) were found to have a second-order dependency on the concentration of **4.4** (figure 4.4b). Based on the mathematical approach we previously developed,[14] we can show here that:

$$k_{obsd} = \frac{k_2 \left[\text{monomer} \right]^n}{K_{diss}} + k_0 \qquad (4.1)$$

where K_{diss} is the equilibrium constant for dissociation of an assembly of n ionophore molecules into monomers, k_2 is an intrinsic rate constant and k_0 is the rate constant for ion transport in the absence of an ionophore. The linear correlation that was found between k_{obsd} and $[\textbf{4.4}]^2$ supports the hypothesis of transport-active dimers. Since thermodynamically stable systems might sometimes be undervalued,[18,20] the value of the Hill coefficient n, corresponding to the stoichiometry of the transport active aggregate was also estimated with a curve fitting (GraphPad Prism 6.0, GraphPad Software, Inc.) at 2.09. This is again, consistent with a dimerization process, responsible for chloride transport.

According to our kinetic model, the value of k_2/K_{diss} (the slope), the effectiveness of transporter **4.4** increases 100 times compared to the previously reported imidazolium salt.[14] This ratio resembles a specificity constant, describing the transporter's ability to facilitate the diffusion of a given anion and the aggregation of **4.4**. Although it was not possible to us to separate the two terms in k_2/K_{diss}, their high ratio strongly suggests either a very high rate constant (k_2) or a very low dissociation process (K_{diss}). This last scenario is in agreement with the lower EC$_{50}$, supporting the idea according to which the EC$_{50}$ and K_{diss} have proportional values.[18]

The organization of benzimidazolium transporters in the solid state was confirmed by X-ray diffraction. Crystals of **4.1** were grown by slow evaporation from acetonitrile and chloroform. The structure elucidated by single crystal X-ray diffraction is shown in Fig. 4.5 (see Annexe 3 for details).

42.998 Å

5.987 Å
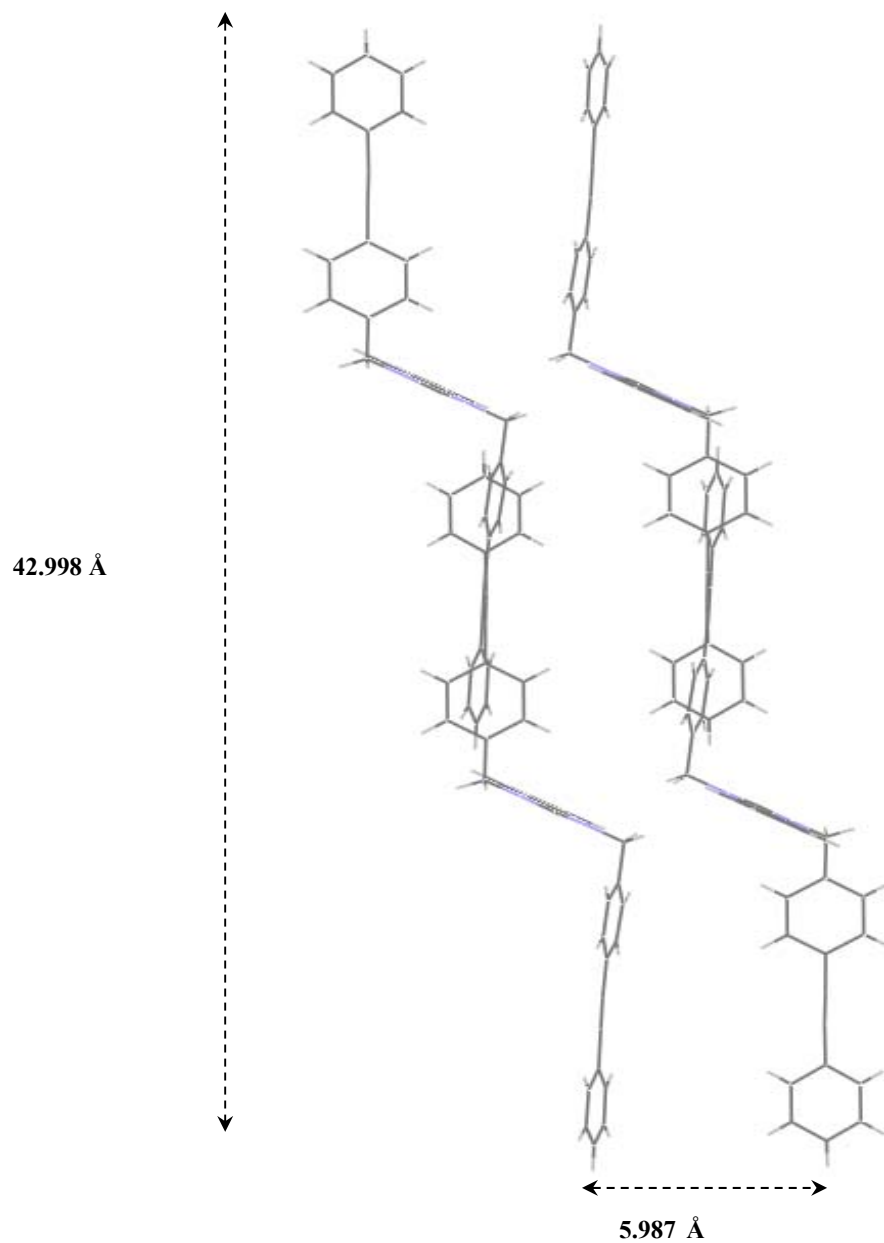
Figure 4.5.   Packing motif of **4.1** illustrating the dimerization process in the solid state.
Br⁻ counter-anions not shown for clarity.

Crystal organization of the benzimidazolium cations is in close agreement with the theoretical organization predicted by molecular modeling.[11,14] The structure observed for **4.1** reveals the formation in one plane of a channeled structure, where the repeating unit is the benzimidazolium dimer. The supramolecular complex is self-assembled by C-H···π interactions. The dimeric structure forms a membrane-spanning channel which can promote the diffusion of the ions through the lipid bilayer. Remarkably, the dimer's length in the crystal structure is 42.998 Å, which corresponds to the thickness of an EYPC liposome bilayer (around 40 Å).[21] Additionally, the channel is flanked on its sides by two bent molecules having aromatic edge-to-face orientation at 5.987 Å distance. Benzimidazolium cations and bromide anions are held together by ionic interactions and H-bonds.

We have not been able to obtain crystals of compound **4.4**, but we believe bigger counter-anions (e.g.: NTf_2^-) should yield larger channel diameters, as the bromide anions are positioned between the benzimidazolium rings. The activity of the transporter is probably not only due to the desolvation of the counter-anion, but also to the variable diameter of the channel, governed by the anion's size.
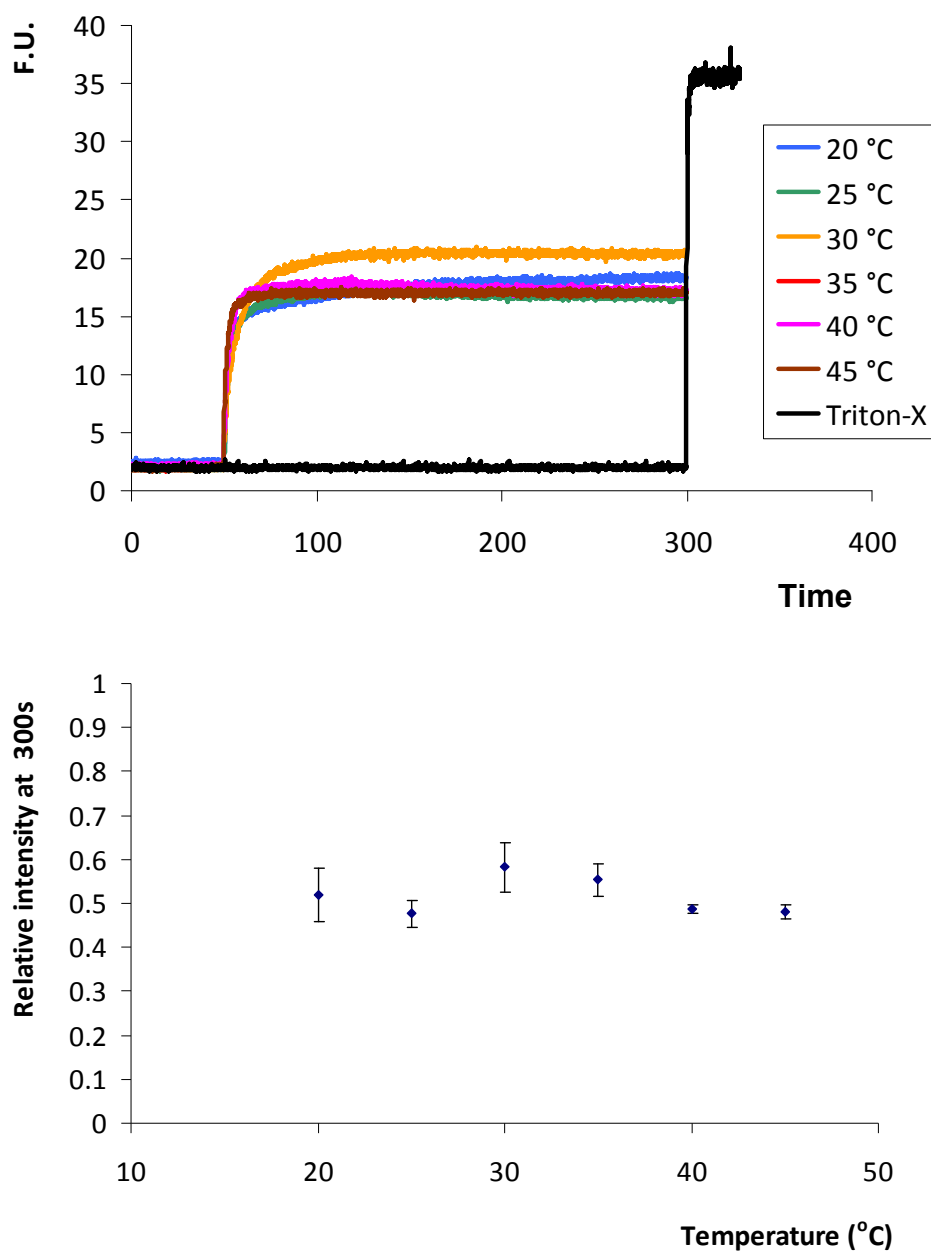
Figure 4.6. Chloride efflux out of DPPC liposomes at 20 ºC, 25 ºC, 30 ºC, 35 ºC, 40 ºC and 45 ºC. The data at each temperature is obtain by using 7 mol.% of **4.4** (relative to DPPC concentrations). The data at each temperature is the average of three series of measurements.

In order to support the transmembrane channel hypothesis versus a mobile ionic transport mechanism, we measured the ionophoric activity of compound **4.4** in gel and

fluid phase membranes.[22] For this purpose, we measured the efflux of the Cl$^-$ out of 1,2-dipalmitoyl-*sn*-glycero-3-phosphocholine (DPPC) liposomes using the lucigenin-based assay, at temperatures above and below DPPC's transition phase (41°C). As shown in figure 4.6, in the presence of 7 mol% **4.4** (relative to the DPPC concentration), the results support a membrane-spanning mechanism, since the anionophoric activity of **4.4** remains independent on the fluidity of the DPPC membrane.

As mentioned earlier, the benzimidazolium salts studied here possess the structural requirements to favour anion-π and cation-π interactions. With all the kinetic and structural information on the chloride transmembrane transport, we further studied the capacity of our benzimidazolium salts to promote a Ca^{2+}/ 2 Cl$^-$ symport processes, in respect to the interest to compensate CFTR dysfunction. To explore the potential applications of compound **4.4** in biological and pharmacological sciences, we investigated whether compound **4.4** can modulate bacterial cell permeability for calcium cations.

For these studies, we used *E. coli* (DH5α, citrine-pBad) strains, overexpressing a mutant protein with post-translational modifications[22] (see annexe 3 for details and resource informations). This protein is a genetically encoded Ca^{2+} indicator located in the subcellular environment. In this way, it was used as a non-ratiometric indicator of the increase in intracellular calcium concentrations as its fluorescence increases in the presence of Ca^{2+}. The mutant we used possessed a Q69M mutation, presenting improved properties in particular with regard to its photostability, its pH sensitivity and its expression at 37 °C.[22] Transport tests were carried out in a quartz cuvette by adding a 1.6 mL aliquot of the *E. coli* bacterial culture and CaCl$_2$ (1 mM). The fluorescence intensity of citrine was then recorded as a function of time. After 2 minutes, an aliquot of 150 μL of the ionophore **4.4**, or of MeOH was injected (see annexe 3 for details).
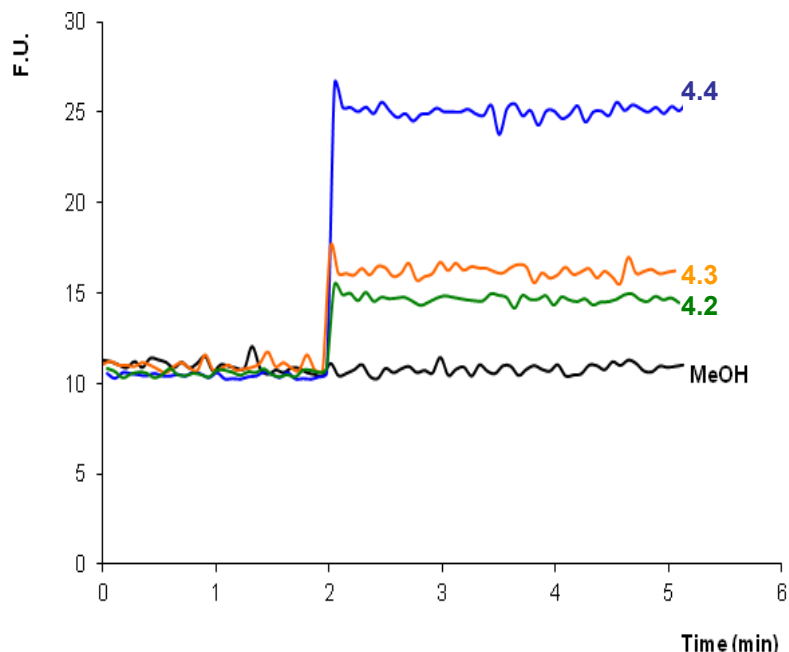
Figure 4.7. Fluorescence changes in *E. coli* cells expressing cytosolic calcium-bioindicator after given stimulations with MeOH, **4.2**, **4.3** and **4.4** (0.24 mM as final concentration) in the presence of extracellular $CaCl_2$ (0.38 mM as final concentration). (λ_{ex} = 516 nm; λ_{em} = 529 nm). See annexe 3 for details.

Figure 4.7 clearly shows a sudden increase in cytosolic citrine fluorescence when compounds **4.2-4.4** are added, compared to the control (MeOH). This fluorescence increase represents a massive influx of calcium into the *E. coli* under the effect of the ionophores. This supports the hypothesis that benzimidazolium transporter is able to facilitate the diffusion of Ca^{2+} cations across *E. coli* membranes, similar to the symport process observed in liposomes. Calcium transport efficiency follows the same order in bacteria as in liposomes, with compound **4.4** being the most active Ca^{2+} transporter. This could be directly related to the size of the channel opening. Moreover, their ability to transport ions through bacterial membranes provides an additional support to channel formation. As explained above, the transport efficiency of a channel is virtually independent of the nature of the membrane (gel/fluid state) in which it is inserted. The increase in fluorescence is not due to bacterial lysis, which would have had, as a consequence, a decrease of the optical density. The measure of the bacterial population,

better known as optical density or O.D.$_{600}$ of an aliquot of *E. coli* in presence **4.4** indicates the same value as an aliquot of living bacteria (O.D.$_{600}$ = 1.3) (see Annexe 3 for details).

4.2.3.   Conclusion

In summary, we herein described the ability of small benzimidazolium compounds to act as good ionophores and identified one lead compound **4.4** that functions in liposomes and living bacteria. This latter combines a higher k_2/K_{diss} constant and lower EC$_{50}$ than its previous imidazolium analogue.[14] We have also presented the first example of a benzimidazolium-based compound that can transport anions and cations across liposomes, as well as bacterial membrane, *via* a channel formation pathway. The ability of **4.4** to drill transient channels through the robust wall of bacterial cells should make it attractive as a paradigm for designing future antibiotic transporters across resistant bacteria membranes. Characterization of the membrane-spanning channel's size and its ability to transport other molecules need further insights and are currently being investigated in our laboratory.

4.2.4.   Acknowledgements

4.2.5.   References

1. Eggermont, J., *Proc. Am. Thorac. Soc.* **2004**, *1*, 22.

2. Hartzell, C., Putzier, I., Arreola, J., *Ann. Rev. Physiol.* **2005**, *67*, 719.

3. Armstrong, C. M., Hille, B., *Neuron* **1998**, *20*, 371.

4. Hille, B., *Ion channels of excitable membranes,* Sunderland, MA : Sinauer Associates **2001**.

5. Li, X., Shen, B., Yao, X.-Q., Yang, D., *J. Am. Chem. Soc.* **2009**, *131*, 13676.

6. Lawal, O., Iqbal, K. S. J., Mohamadi, A., Razavi, P., Dodd, H. T., Allen, M. C. , Siddiqui, S., Fucassi, F., Cragg, P. J., *Supramol. Chem.* **2009**, 21, 55.b) Iglesias-Sanchez, J. C., Wang, W., Ferdani, R., Prados, P., de Mendoza, J., Gokel, G. W., *New J. Chem.* **2008**, *32*, 878. c) O. A. Okunola, J. L. Seganish, K. J. Salimian, P. Y. Zavalij, J. T. Davis, *Tetrahedron* **2007**, *63*, 10743.d) Tanaka, Y., Kobuke, Y., Sokabe, M., *Angew. Chem.* **1995**, *107*, 717 .

7. a) Chui, J. K., Fyles, T. M., *Beilstein J. Org. Chem.,* 2011, **7**, 1562. b) Matile, S. Vargas Jentzsch, A., Fin, A., Montenegro, J., *Chem. Soc. Rev.* **2011**, *40*, 2453 c) Devi, U., Brown, J. R., Almond, A., Webb, S. J., *Langmuir* **2011**, *27*, 1448 .d) Otis, F., Racine-Berthiaume, C., Voyer, N., *J. Am. Chem. Soc.* **2011**, *133*, 6481. e) Cho, H., Widanapathirana, L., Zhao, Y., *J. Am. Chem. Soc.* **2011**, *133*, 141. f) Davis, J. T., Gale, P. A., Okunola, O. A., Prados, P., Iglesias-Sanchez, J. C., Torroba, T., Quesada, R., *Nat. Chem.* **2009**, *1*, 138. g) Davis, A. P., Sheppard, D. N., Smith, B. D. , *Chem. Soc. Rev.* **2007**, *36*, 348.

8. Reddy, G. L., Iwamoto, T., Tomich, J. M., Montal, M., *J. Biol. Chem.* **1993**, *268*, 14608. (b) Oblatt-Montal, M., Reddy, G. L., Iwamoto, T., Tomich, J. M., Montal, M., *Proc. Nat. Acad. Sci., U.S.A* **1994**, *91*, 1495. (c) Wallace, D. P., Tomich, J. M., Eppler, J. W., Iwamoto, T., Grantham, J. J., Sullivan, L. P., *Biochim. Biophys. Acta (Biomembranes).* **2000**, *1464*, 69. (d) Mitchell, K. E., Iwamoto, T., Tomich, J., Freeman, L. C., *Biochim. Biophys. Acta (Biomembranes)* **2000**, *1466*, 47. (e) Broughman, J. R., Mitchell, K. E., Sedlacek, R. L., Iwamoto, T., Tomich, J. M., Schultz, B. D., *Am. J. Physiol.: Cell Physiol.* **2001**, *280*, C451.

9. a) Dawson, R. E., Hennig, A., Weimann, D. P., Emery, D., Gabutti, S., Montenegro, J., Ravikumar, V., Mayor, M., Mareda, J., Schalley, C. A., Matile, S., *Nat. Chem.* **2010**, *2*, 533. b) Mšek, J., Vargas Jentzsch, A., Sakurai, S., Emery, D., Mareda, J., Matile, S., *Angew. Chem.* **2010**, *122*, 7846.

10. a) Walter, S., Kniep, F., Herdtweck, E., Huber, S., *Angew. Chem.* **2011**, *123*, 7325; *Angew. Chem. Int. Ed.* **2011**, *50*, 7187. b) Dordonne, S., Crousse, B., Bonnet-Delpon, D., Legros, J., *Chem. Commun.* **2011**, *47*, 5855 c) Kraut, D. A., Churchill, M. J., Dawson, P. E., Herschlag, D., *ACS Chem. Biol.* **2009**, *4*, 269. d) Bruckmann, A., Pena, M. A., Bolm, C., *Synlett* **2008**, *6*, 900.

11. Elie, C.R., Noujeim, N., Pardin, C., Schmitzer, A.R., *Chem. Commun.* **2011**, *47*, 1788.

12. Dykeman, R.R., Yan, N., Scopelliti, R., Dyson, P. J., *Inorg. Chem.* **2011**, *50*, 717.

13. a) Frontera, A., Gamez, P., Mascal, M., Mooibroek, T. J., Reedijk, J., *Angew. Chem.,* **2011**, **123**, 9736 ; *Angew. Chem. Int. Ed.* **2011**, *50*, 9564. b) Salonen, L. M., Ellermann, M., Diederich, F., *Angew. Chem.* **2011**, *123*, 4908; *Angew. Chem. Int. Ed.* **2011**, *50*, 4808. c) Chifotides, H. T., Schottel, B. L., Dunbar, K. R., *Angew. Chem.* **2010**, *122*, 7360; *Angew. Chem. Int. Ed.* **2010**, *49*, 7202. d) Berryman, O. B., Bryantsev, V. S., Stay, D. P., Johnson, D. W., Hay, B. P., *J. Am. Chem. Soc.* **2007**, *129*, 48. e) QuiÇonero, D., Garau, C., Rotger, C., Frontera, A., Ballester, P., Costa, A., Deya, P. M., *Angew. Chem.* **2002**, *114*, 3539; *Angew. Chem. Int. Ed.* **2002**, *41*, 3389. f) Mascal, M., Armstrong, A., Bartberger, M. D., *J. Am. Chem. Soc.* **2002**, *124*, 6274. g) Alkorta, I., Rozas, I., Elguero, J., *J. Am. Chem. Soc.* **2002**, *124*, 8593.

14. Elie, C. R., Charbonneau, M., Schmitzer, A. R., *Med. Chem Commun.* **2012**, *3*, 1231.

15. Galligan, J. P., Dougherty, D. A., *Proc. Natl. Acad. Sci. USA* **1999**, *96*, 9459. b) Mecozzi, S., West, A. P., Dougherty, D. A., *Proc. Natl. Acad. Sci. USA* **1996**, *93*, 10566. c) Ma, J. C., Dougherty, D. A., *Chem. Rev.* **1997**, *97*, 1303.

16. Davis, P., Sheppard, D. N., Smith, B. D., *Chem. Soc. Rev.* **2007**, *36*, 348. b) Sidorov, V., Kotch, F. W., Kuebler, J. L., Lam, Y. F., Davis, J. T., *J. Am. Chem. Soc.* **2003**, *125*, 2840. c) McNally, B. A., Koulov, A. V., Smith, B. D., Joosb, J.

B., Davis, A. P., Harrell Jr., W. A., Bergmeyer, M. L., Zavalij, P. Y., Davis, J. T., *Chem. Commun.* **2010**, *46*, 3950. d) McNally, B. A., Koulov, A. V., Smith, B. D., Joos, J. B., Davis, A. P., *Chem. Commun.* **2005**, *8*, 1087.

17. McNally, B. A., Koulov, A. V., Lambert, T. N., Smith, B. D., Joos, J-B., Sisson, A. L., Clare, J. P., Sgarlata, V., Judd, L. W., Magro, G., Davis, A. P., *Chem.-Eur. J.* **2008**, *14*, 9599.

18. Matile, S., Sakai, N., in *Analytical Methods in Supramolecular Chemistry* 2ᵉ ed. (ed. Schalley, C. A.) 711. (Wiley, Weinheim, **2012**).

19. Andrews, N. J., Haynes, C. J.E., Light, M. E., Moore, S. J., Tong, C. C., Davis, J. T., Harrell Jr., W. A., Gale, P. A., *Chem. Sci.* **2011**, *2*, 256.

20. Bhosale, S., Matile, S., *Chirality* **2006**, *18*, 849.

21. Sabin, J., Prieto1, G., Ruso1, J. M., Hidalgo-Alvarez, R., Sarmiento, F., *Eur. Phys. J. E*, **1998**, *20*, 401.

22. a) Krasne, S., Eisenman, G., Szabo, G. *Science* **1971**, *174*, 413. b) Boheim, G., Hanke, W., Eibl, H., *Proc. Natl. Acad. Sci.*, *U.S.A.* **1980**, *77*, 3403. c) Koulov, V., Lambert, T. N., Shukla, R., Jain, M., Bood, J. M., Smith, B. D., Li, H. Y., Sheppard, D. N., Joos, J-B., Clare, J. P., Davis, A. P., *Angew. Chem., Int. Ed.*, 2003, **42**, 4931. d) Krasne, S., Eisenman, G., Szabo, G., *Science*, **1971**, *174*, 414. e) Griesbeck, O., Baird, G. S., Campbell, R. E., Zacharias, D. A., Tsien, R. Y. *J. Biol. Chem.* **2001**, *276*, 29188.

Chapitre 5   **Applications biologiques de différentes familles de transporteurs anioniques : revue de littérature**

5.1. Préface

Cet avant-dernier article de la thèse vient mettre en perspective mes travaux au milieu d'une vaste étendue d'exemples de transporteurs anioniques de l'époque, présentant un intérêt biologique. Nous avions été approché pour écrire cette revue scientifique, tandis que j'entamais alors mes recherches sur les propriétés des sels de benzimidazolium sur les souches bactériennes *E. coli* et *Bacillus thurigiensis*. D'autres membres du groupe débutaient également des travaux connexes sur d'autres molécules, contenant des cations imidazolium, afin de tester leur potentiel ionophore.

L'article dont fait l'objet ce chapitre fait donc un tour d'horizon des différentes applications biologiques des transporteurs mobiles et des canaux transmembranaires synthétiques, dont entre autres ceux récemment développés dans notre groupe. Ce travail est un effort collectif de tous les co-auteurs. Quant à la facture et la disposition de la revue, auxquelles j'ai activement participé, de même que la restauration de plusieurs images tirées de la littérature elles ont été effectuées sous la supervision de la Pre. Andreea Schmitzer. L'essentiel du papier a été rédigé par la Pre. Schmitzer et j'ai contribué en partie à la révision de la version finale.

5.2. Article 4 :«Biologically active synthetic anionophores»

Claude-Rosny Elie, Marc Vidal, Mathieu Charbonneau, Audrey Hébert, Andreea R. Schmitzer*.

Department of Chemistry, Université de Montréal, 2900 Édouard-Montpetit CP 6128 succ. Centre-Ville, Montréal Québec, Canada, H3C 3J7.

Figure 5.1. Table of Contents Graphic

5.2.1. Abstract

The physiological importance of proteins that can regulate ion balance and transmembrane transport is highlighted by different diseases where ion channel dysfunction is observed. During the past two decades, considerable effort has been devoted to develop synthetic ionophores that can insert into or cross cell membranes and restore the dysfunction of highly complex protein channels.

Notwithstanding the remarkable structural advances made, only a few classes of synthetic ionophores were studied in complex with pro- and eukaryotic cells in order to obtain information about their biological activity and potential application in ion channel replacement therapy, anti-cancer therapy or antimicrobial treatments. However, only a few synthetic ionophores showed promising biological activity in cellular assays. This review aims to show the utility of synthetic ionophores for different biological applications, including: restoring ion concentration, inducing cell death in different cancer cells, and protecting against a variety of pathogenic microbes. Because the

activities of these ionophores depend primarily on their overall physicochemical properties and structure, we discuss here specific functional units and scaffolds that are important for obtaining selective, non-toxic transporters for specific biological applications.

5.2.2. Introduction

The cell membrane is a dynamic barrier composed of proteins and phospholipids. It functions as a barrier between intracellular and extracellular environments for the cell and its organelles, thus compartmentalizing cellular functions.[1] Membrane composition varies between plasma and organelle membranes and its selective permeability allows small hydrophilic species (O_2, CO_2, N_2) and small uncharged polar molecules (water, urea) to cross, while it is generally impenetrable to large uncharged molecules (*i.e.* glucose) and ions (H^+, K^+, Cl^-). This impermeability is in part due to the energetic cost of the dehydration required to penetrate into the hydrophobic core of the phospholipid bilayer. Different proteins embedded in the cell membrane facilitate the passage of ions and polar molecules by acting as carriers and channels. They actively or passively transport both polar molecules and ions through the membrane and maintain cellular concentration gradients, which are vital for signaling pathways and cellular processes.[2] Active transport against a concentration gradient is energetically driven by ATP hydrolysis, while use of an electrochemical gradient allows for passive transport.[3]

Anion channels, in particular, function to maintain a range of cellular processes in eukaryote cells, including: resting membrane potential, trans-epithelial transport, cell volume regulation and acidification of organelles.[3] Chloride channels, for example, are involved in cellular processes such as endocytosis, where the cell membrane pinches inward from the extracellular medium by forming an endosome. The disruption of chloride channel function results in numerous diseases.[4] One well-known example of a chloride channel-related disease is the cystic fibrosis transmembrane conductance regulator (CFTR) dysfunction.[5] An important function of anion channels is their ability to control cell morphology, which has a direct impact on cell death.[3, 6, 7] A dramatic reduction of ion concentration has been shown in apoptotic cells that exhibit a shrunken morphology, although cell death can be inhibited without the necessary change in cell

morphology. This was demonstrated by the ability of chloride and potassium channel inhibitors to partially or completely inhibit cell death induced by staurosporine. [8] Furthermore, maintaining the normal physiological intracellular concentration of monovalent ions inhibits the activation and activity of the death cascades.[9] Despite the well-known biological activity of hydraphiles as synthetic transmembrane channels in bacteria,[10] less interest has been noted for the activity of anion transporters in bacteria.

In the last few years, particular attention has been devoted to the development of synthetic anion transporters (anionophores) that show promising activity in model systems, such as liposomes. [11] A complete and exquisitely detailed account of small synthetic compounds designed, synthesized and studied to bind and transport anions across synthetic lipid bilayers was recently published.[12] The rationale behind developing anion receptors as well as their basis for design as transmembrane transporters can be found there and in the other recent reviews.[13] More recently, several research groups have begun to consider the potential of using synthetic anion ionophores for biological applications, applications that will be discussed in this review.

In general, it is difficult to determine whether transport occurs *via* mobile carrier diffusion or a self-assembled channel (Figure 5.2a). One approach relies on mechanistic experiments, which often measure transport as a function of ionophore concentration and membrane fluidity. Ionophore concentration studies that result in a linear or non-linear relationship are assigned to a mobile carrier[14,15] or self-assembled channel mechanism[16]. Membrane fluidity experiments utilize the gel (solid) to fluid (liquid) lipid phase change of 1,2-dipalmitoylphosphatidylcholine (DPPC) vesicle membranes at 41 ºC, and have been able to differentiate between a mobile carrier and channel transporter.[17] A channel spans the membrane to form a conduit for ions to flow through, and produces similar fluxes in both DPPC gel and fluid phases because the channel interior is unaffected by lipid phases. In contrast, a mobile carrier diffuses through the membrane, thus its activity is dramatically decreased in the more viscous gel phase.
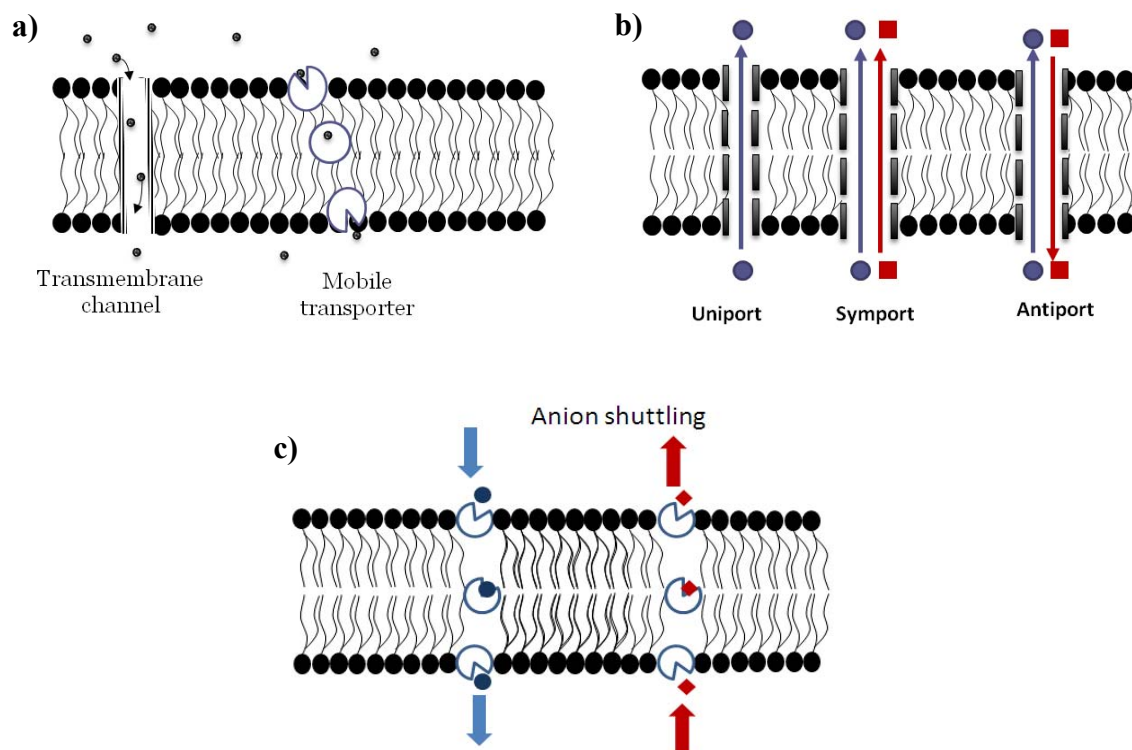
Figure 5.2. Mechanisms in transmembrane transport: a) Self-assembled transmembrane channel vs. mobile transporter; b) Types of active transport in channels; c) Anion shuttling carrying two different anions.

Transport of ions by synthetic transmembrane channels usually only occurs *via* passive transport mechanisms in which the charge balance across the membrane is maintained. This can be achieved by either a symport mechanism, where both an anion and a cation are transported, or by an antiport or shuffling mechanism, where two anions are transported or exchanged across the membrane in opposite directions (Figure 5.2b). In the case of mobile carriers, they diffuse across the bilayer, dissipating the transmembrane gradient for the carried anion. If the anionophore can carry different anions, then it can dissipate the gradient for a second ion as it moves back across the membrane, appearing to act as a global anti-porter.

Notwithstanding the transport mechanism, intramolecular hydrogen bonding and self-association are crucial to organize the anion binding site and to control the three-dimensional arrangement of an anionophore. To date, most reported biologically active anionophores generally contain polarized N–H groups, mostly from amides and

analogues. Urea is an interesting building block for anion transporter design because it can establish two relatively strong hydrogen bonds with the anion. The two N–H groups can interact with a single acceptor atom or with two adjacent oxygen atoms of an oxyanion.[18] The imidazolium cation also possesses anion recognition properties, due to the three divergent hydrogen bond donors and the positive charge delocalized in the ring,[19] and as such, they have been exploited in the past years for the development of imidazolium-based anion receptors. Many imidazolium-based receptors have recently found applications for sensing various anions.[19] The ease of functionalizing the nitrogen atoms of the imidazolium ring makes them interesting candidates for the synthesis of different families of salts, where different interactions can be introduced to obtain self-assembled systems. Moreover, they are endowed with an amphiphilic nature; their lipophilic properties allow them to cross membranes, whilst retaining the ability to interact with anions *via* the imidazolium ring. Thirdly, the inherent biocompatibility of the imidazolium cation makes it such that it can be easily incorporated into biological applications.[20]

5.2.3. Urea and isophthalamides in cystic fibrosis

Cystic fibrosis (CF) is a lethal inherited disorder resulting from ion transport abnormalities in airway epithelia, resulting in mucus accumulation and bacterial colonization. CF is caused by mutations in the CFTR gene that encodes a transmembrane chloride channel located primarily in the apical membrane of epithelial cells. Although transfection of normal CFTR remains a therapeutic goal, currently, treatment of symptoms and the use of antibiotics are considered the predominant therapeutic strategies against CF. Novel pharmacological approaches should be developed to restore Cl^- transport in CF, including incorporation of artificial Cl^- transporters into the cell membranes.

Cholapods[13] are a particular class of synthetic chloride transporters derived from cholic acid, having a lipophilic backbone and four positions that can be derivatized with different substituents (Figure 5.3).[21] The anion binding pocket is formed by arylureas at positions *7* and *12*, which effectively shield the transported anion. The ionophore's

lipophilicity and anion binding affinity can be adjusted by changing the functional groups at positions *3*, *7* and *12*.[22]
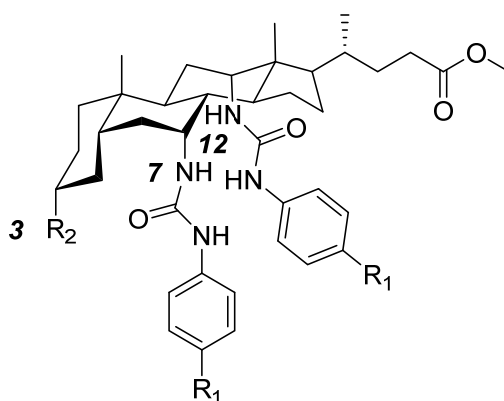
Figure 5.3.   Cholapods studied in Madin Darby canine kidney MDCK epithelia

Epithelial cells lose their usual polarization during carcinogenesis. Cholapod-mediated chloride transport was demonstrated in live cells using Madin Darby canine kidney (MDCK) epithelia cells[14] and Ussing chamber technique. The method involves growing an oriented layer of cells on a filter support and placing it between current- and voltage-measuring electrodes.[23] Endogenous active transport systems will generate a potential difference across the cell membrane. Addition of the cholapod ionophore causes discharge of the electrochemical gradient, which can be detected as a current. This class of ionophores was proposed to be used in the treatment of cystic fibrosis where chloride transport across the cell membrane is impaired because of the formation of a mucous layer on epithelial cells.[21]

More recently, Yang *et al.* demonstrated that an α-aminoxy-containing ionophore (Figure 5.3) forms functional Cl⁻ channels not only in lipid bilayer membranes of liposomes, but also in those of MDCK live cells, as revealed by both single-channel and whole-cell patch clamp experiments. [24] Synthetic Cl⁻ channels formed by these isophtalamide-containing α-amino acids can shift resting membrane potential toward Cl⁻ equilibrium potential in living cells by increasing the Cl⁻ permeability of their membranes. [25] The synthetic Cl⁻ channels result in depolarization of the membrane potential, and are able to regulate the physiological functions of relevant natural ion channel proteins in a biological system. Yang *et al.* also showed that these isophtalamide

transporters regulate natural voltage-gated ion channels, intracellular calcium (Ca^{2+}) concentrations, and the contraction of smooth muscle cells by modulating cell membrane potentials in living cells and tissues.[26] In light of these observations, this compound may have therapeutic potential for the treatment of CF lung disease or other diseases that would benefit from increased chloride transport.
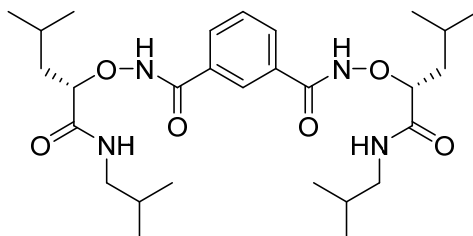
Figure 5.4.   α-aminoxy isophthalamide form transmembrane channels modulating cell membrane potential by increasing Cl⁻ permeability in MDCK cells.

The synthetic ionophores described in this section have the potential to be employed as chemical tools for the treatment of CF. Future cell studies should investigate and determine that they can dissipate electrical and/or chemical gradients. An ambitious goal is to produce lead compounds for channel replacement therapies. Following delivery to the lungs by inhalation, the anionophores must insert into the cell membrane, replace missing CFTR activity and restore, for a period, normal mucus transport. To prove the feasibility of this approach, suitable anionophores must present high activities (so that small amounts can be used), and the ionophores must have proven effectiveness in live cells, as opposed to synthetic model membranes. More than that, the anionophores may be selective enough towards lungs cells. Compounds that demonstrate optimal deliverability and anion transport activity should then be subjected to further biological testing using cells that line the air passages of CF lungs. Additionally, the possibility of these ionophores to restore salt and water transport to the cells should be investigated. Then, the capacity of these anionophores to promote mucus transport should be assessed. Finally, tests for toxicity and pharmacokinetics properties to assess whether the anionophores are likely to succeed as drugs should be performed. In the specific case of cystic fibrosis, there is the possibility of the direct delivery of a synthetic transporter to the lung by inhalation, but penetration of the thick sticky mucus that blocks air passages remains a formidable technical challenge.

5.2.4. Urea/thiourea in cancer therapy

Cell death is an important biological consequence of exposure to extrinsic agents, and has been claimed to be modulated or triggered when the intracellular pH (pH$_i$) drops below 7.[27] Matsuyama and co-workers proposed that pH$_i$ regulatory mechanisms may offer new approaches for tumor therapy.[28] Consequently, Gale *et al.* developed small urea-containing systems based on tris-(2-aminoethyl)amine scaffolds (Figure 5.5),[29] which induced cell death in human cancer cells *in vitro*.[30]

First, vesicle and U-tube experiments using ion-selective electrodes and fluorescent dyes indicate that compounds **5.1–5.10** function as ion carriers that can mediate the transport of anions predominantly *via* an anion exchange mechanism, including chloride/nitrate, chloride/bicarbonate and a small amount of chloride/sulfate antiport or dual anion shuffling, even though H$^+$/Cl$^-$ co-transport can also occur. The authors proposed that the main reason for the superior transport activity observed for the fluorinated receptors was due to their high lipophilicity, rather than to the differences in anion binding that were observed using ^{1}H NMR titrations and single-crystal X-ray crystallography.

5.1 X = O, R = Ph   **5.6** X = S, R = Ph
5.2 X = O, R = p-C$_6$H$_4$F   **5.7** X = S, R = p-C$_6$H$_4$F
5.3 X = O, R = C$_6$F$_5$ **5.8** X = S, R = C$_6$F$_5$
5.4 X = O, R = p-C$_6$H$_4$(CF$_3$)   **5.9** X = S, R = p-C$_6$H$_4$(CF$_3$)
5.5 X = O, R = [3,5-bis(CF$_3$)phenyl]   **5.10** X = S, R = [3,5-bis(CF$_3$)phenyl]
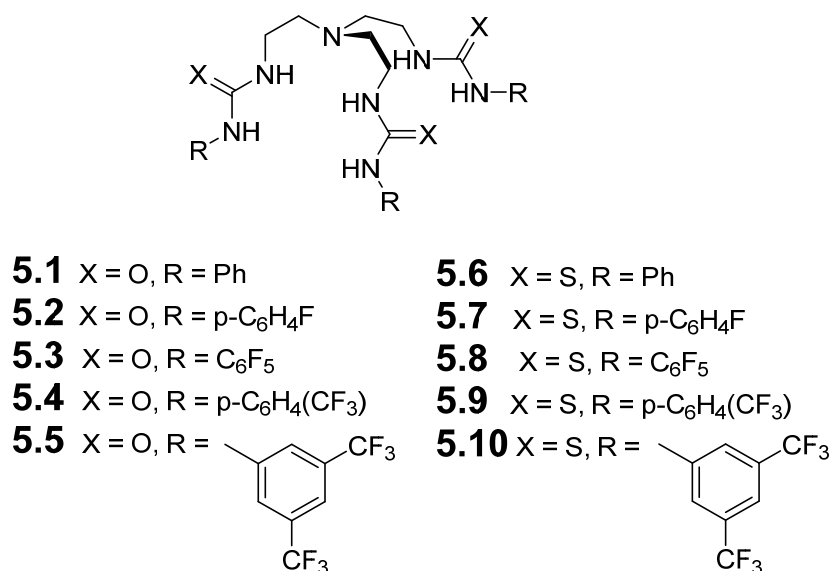
Figure 5.5.   Tris-(2-aminoethyl)amine-based ureas and thioureas

The biological activity of ureas **5.1–5.5** and thioureas **5.6–5.10** was shown in different tumor cell lines using three methods: evaluation of cell viability, estimation of

the pH changes in acidic cell compartments by acridine orange staining, and by nuclear Hoechst staining for assessment of apoptotic cell death induction. The pH_i in transformed or cancerous cells generally remains neutral or slightly more alkaline compared to normal cells, and is regulated by a variety of pH_i homeostatic mechanisms, including: Na^+/H^+ co-transport, Na^+-dependent and -independent Cl^-/HCO_3^- exchange, vacuolar type H^+-ATPase (V-ATPase), among other mechanisms.[31] The *in vitro* cytotoxic activity of receptors **5.1–5.10** was tested on a collection of cancer cell lines of diverse origins. All thioureas -in particular, **5.8**, **5.9**, and **5.10** - displayed a widespread cytotoxic effect across the panel of cell lines used, which might be due to the inherent higher toxicity of thioureas compared to ureas.[32] The mechanism by which receptors **5.1–5.10** display cytotoxic effects and the *in vitro* ionophore activity of the tripodal receptors on GLC4 cell lines was studied using vital staining with acridine orange (AO). This cell-permeable dye accumulates in acidic compartments, such as lysosomes, exhibiting a characteristic orange fluorescence emission in its protonated state, whereas it emits green fluorescence at higher pH.[33] When GLC4 cells were stained with AO, granular orange fluorescence was observed in the cytoplasm, suggesting that the orange fluorescence is due to acidified lysosomes. Cells treated with ionophores **5.4**, **5.7**, **5.8**, and **5.9** showed a complete disappearance of orange emission, indicating that these receptors can alter the intracellular pH.

Combining the results obtained in the vesicle assays with the *in vitro* AO staining suggests that an anion exchange mechanism, such as Cl^-/HCO_3^-, could be responsible for the increase in internal pH, although other mechanisms such as H^+/Cl^- co-transport processes were not ruled out. If lipophilicity is the main determining factor for activity, then the most lipophilic compounds are also the best anionophores. Indeed, this appears to be the case for compounds **5.1–5.10**, since the most lipophilic compounds also contain the most acidic (thio)urea functionalities and are therefore likely to be good H^+/Cl^- co-transporters. It was proposed that the cytotoxicity displayed by ionophores **5.1–5.10** was due to apoptosis, which is induced by changes in the internal pH regulation due to the chloride/bicarbonate exchange or H^+/Cl^- co-transport. However, the perfect correlation between the transport activity in liposomes and that in cells suggests that the observed

anticancer activity could be due to an increase of the cytosolic chloride level and an apoptosis-induced cellular death.

Structurally less complex transporters related to ureas/thiourea-based anion ionophores are indole-based transporters developed more recently by Gale *et al.* (Figure 5.6).[34] Apopotosis provoked by changes in nuclear morphology including nuclear condensation, fragmentation and formation of apoptotic bodies was evidenced by Hoechst 33342 staining in the presence of the indole-based compounds, which allowed for their preliminary identification as anion transporters. It was shown that in the presence of compounds **5.13**, **5.14**, **5.17**, **5.21** and **5.22,** nuclear condensation and apoptotic body formation were responsible for cell death. The *in vitro* ionophoric activity of these cytotoxic compounds was demonstrated again in A375 melanoma cells using AO. Cells in basal conditions were stained with AO and showed typical granular orange fluorescence, corresponding to cellular acidic compartments such as lysosomes. After cell exposure to cytotoxic compounds **5.13**, **5.14**, **5.17**, **5.21**, and **5.22**, orange fluorescence completely disappeared in all cases, indicating the increase of pH in the acidic organelles through the acidification of the cytoplasm.

5.11 X = O, R' = H, R" = H
5.12 X = S, R' = H, R" = H
5.13 X = O, R' = CF_3, R" = ^nBu
5.14 X = S, R' = CF_3, R" = ^nBu

5.15 X = O, R = H
5.16 X = S, R = H
5.17 X = O, R = CF_3
5.18 X = S, R = CF_3

5.19 X = O, R = H
5.20 X = S, R = H
5.21 X = O, R = CF_3
5.22 X = S, R = CF_3
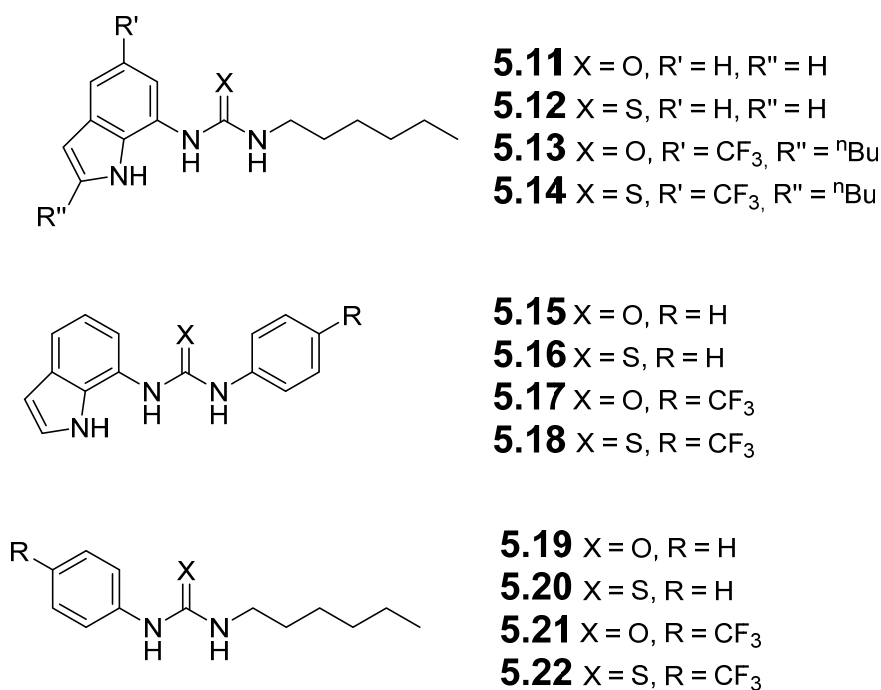
Figure 5.6.   Indolylurea/thiourea transporters

The potent anion transport activity and *in vitro* cytotoxicity towards a range of cancerous cell lines of *ortho*-phenylenediamine-based ureas was also recently reported (Figure 5.7).[35]

5.23 R' = H
5.24 R' = F
5.25 R' = Cl

5.26 R" = *p*-CN
5.27 R" = *p*-CF$_3$
5.28 R" = *p*-NO$_2$
5.29 R" = *m*-NO$_2$
5.30 R" = *o*-NO$_2$

5.31 R'" = CN
5.32 R'" = CF$_3$
5.33 R'" = NO$_2$
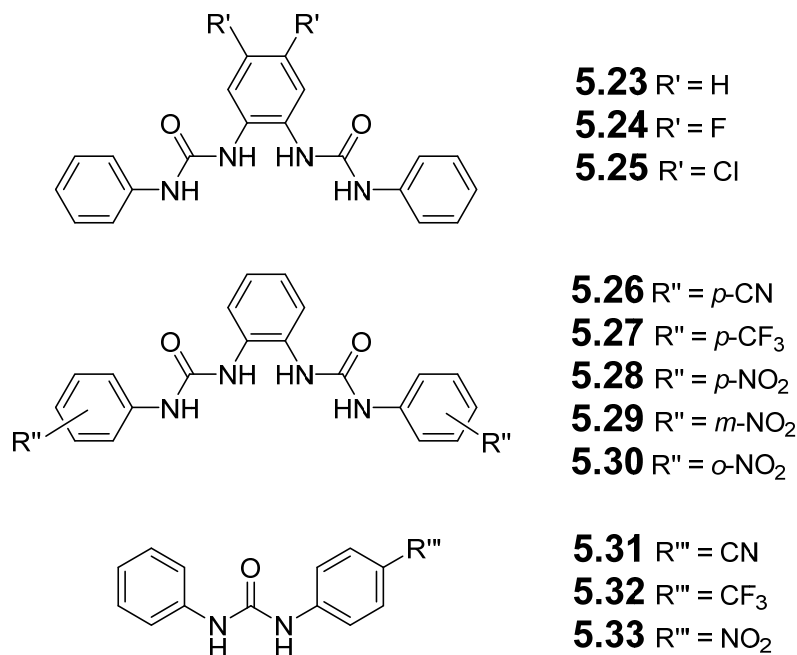
Figure 5.7. *Ortho*-phenylenediamine-based bisureas **and** monoureas

A single-point cell viability assay utilizing MTT (3-(4,5-dimethylthiazol-2-yl)-2,5-diphenyltetrazolium bromide was performed with compounds **5.23–5.30** (10 μM) on a selection of cancer cell lines of diverse origins. Cell viability was assessed 48 h after exposure to each of the compounds. Compounds **5.22**, **5.27** and **5.30** display significant cytotoxicity towards the tested cancerous cell lines. In comparison, compounds **5.25**, **5.28** and **5.29** were less toxic, whilst compounds **5.23** and **5.26** were the least toxic in the series. Compounds **5.24**, **5.25**, **5.27**, **5.28**, **5.29** and **5.30** are toxic in a range of cancer cell lines. With the exception of compound **5.30**, all of the cytotoxic compounds were found to facilitate Cl$^-$/NO$_3^-$ and Cl$^-$/HCO$_3^-$ transport in vesicle-based ion transport assays.[13a] In an AO assay, these ureas were found to alter pH$_i$ in A375 cells, and the formation of apoptotic bodies was clearly observed with the most cytotoxic compounds (**5.24**, **5.27** and **5.30**) using Hoechst 33342 staining in A375 cells. Compounds **5.24** and **5.27** facilitated cell death in A375 cells, likely through sustained changes in pH$_i$ as a consequence of *in vitro* ion transport. Compound **5.27** was shown to reduce the viability of the cell lines to a

greater extent than compound **5.28** whilst compound **5.28** was the most effective anion transporter of the two. This could be due to differences between the model membrane used for the vesicle studies and the biological membranes present in the cells. All these urea-containing ionophores displayed promising activity in the tested cancerous cell lines. However, half maximal inhibitory concentration (IC_{50}) values of the ionophores are approximately 10-fold lower for normal cells than those obtained for cancerous lines.[36] Considering this, more evidence for selectivity over non-malignant cells should be demonstrated before they can be considered the next generation of anticancerous compounds. Toxicity may also be an issue for this functional group, and its replacement by isosteric groups was proposed. Squaramides have lately been developed as urea and thiourea analogues, with lower lipophilicity and higher chloride affinity.[37] However, their biological applications have not yet been reported. Isophtalamides, further urea and thiourea analogues, are also able to complex anions via their NH groups of their amide bonds, and merit further exploration.[38]

5.2.5. Pyrol-containing anionophores in cancer therapy

The tripyrrolic metabolite prodigiosin stands out as the best studied natural ionophores, being able to promote Cl^-/HO^- exchange. Prodigiosins, isolated mostly from Gram negative bacteria, are characterized by a common pyrryldipyrrylmethene structure with varying side-chains (Figure 5.8).[39] The mode of action of prodigiosin in cells rests on various functions, including: pH modulation, cell cycle inhibition, DNA cleavage and regulation of mitogen-activated protein kinases (MAPK).[40] Prodigiosin mimics consisting of pyrrole and pyridine transporters contain two hydrogen-bond donor groups and a protonation site. Upon protonation, the binding affinity is enhanced, and increases chloride transport. Depending on the conditions, these mobile carriers promote both anion exchange and chloride co-transport.

R$_1$: H, *n*-pentyl
R$_2$: methyl, ethyl, *n*-undecyl
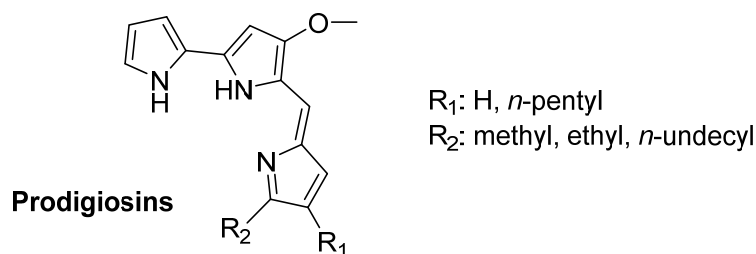
Figure 5.8.   Natural prodigiosins

The number of reported synthetic prodigiosin derivatives has increased substantially over the past years. Research efforts have focused on identifying their mechanism of action, optimizing their activity, and cytotoxicity. Sessler *et al*. reported that the anticancer activity of polypyrrolic molecules (Figure 5.9) can be closely related to their anion transport efficiency.[41] Anticancer activity was evaluated *in vitro* in cancerous cell lines and the order of anticancer efficacy was directly related to the order of transport efficiency (**5.36** > **5.34** > **5.35** > **5.37**).
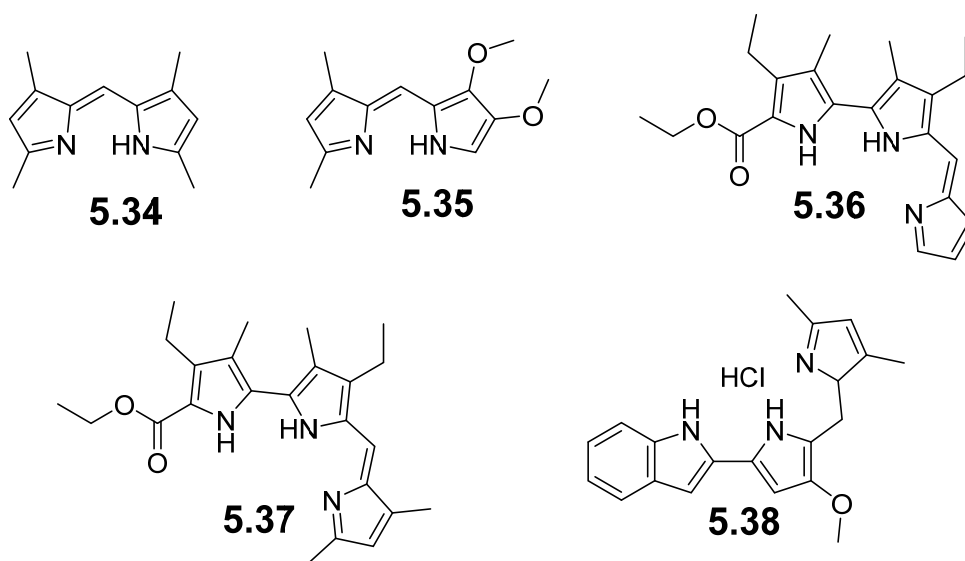
Figure 5.9.   Polypyrrolic molecules with anticancer activity.

Further studies have shown that removal of the methoxy group reduced prodigiosin cytoxicity in tumor cells.[42] Moreover, there is no correlation between the pK_a of the pyrrolylpyrromethene unit and chloride affinity of some prodigiosin derivatives with their cytotoxicity in HL-60 leukemia cells,[43] or their ability to inhibit cell proliferation in A549 human lung and PC3 prostate cancer cells. Mechanistic ion

transport studies in vesicle systems identified prodigiosin as an anion exchanger.[44] Prodigiosin functions naturally in cell systems as an HCl co-transporter, to de-acidify organelles by uncoupling the proton pump V-ATPase.[45]

Bipyrrole-containing tambjamine derivatives[46] have also demonstrated ionophore activity and showed *in vitro* activity using a lung cancer cell line, increasing the lysosomal pH by facilitating influx of bicarbonate into the lysosomes. Synthetic prodigiosin analogues such as Obatoclax **5.38** are of particular interest, and are in clinical trials for cancer treatment.[47] These indole-containing prodigiosin analogues provided further evidence that anticancer activity of prodigiosins is due to their anion transport activity, controlling cell death by discharging pH gradients in living cells. Even if these compounds have IC$_{50}$ values only 10-fold lower on non-malignant cells,[37] their decreased toxicity encourages further exploration as the ionophores that modulate pH in cells could be employed for therapeutic purposes, by controlling different cell death pathways *in vivo*. However, the selectivity of these compounds for inducing cancer cells death over non-cancer cells must be elucidated in detail before further biological development can occur. There are pharmacokinetic factors to be considered, such as undesired toxicity, metabolic instability, tissue selectivity and target membrane residence time.

It is also interesting to compare the biological performance of the two classes of synthetic transporters: channels and carriers. One might anticipate higher biological activity following the corresponding transport rates for the channels and higher selectivity for the carriers. Regarding selectivity, most of the synthetic anion channels seem to co-transport cations to some extent; carriers appear to be more specific towards which anions they transport, as observed in the anti-cancer activity of small anion carriers. There is no evidence that the cholapods or the prodigiosin family either transport or co-transport metal cations. Regarding transport activity, it is difficult to make comparisons between various studies because of differences in the reporting of concentrations; sometimes only ratios are listed, sometimes overall concentrations. However, there is no clear indication that the synthetic anion channels give higher transport rates than the carriers.

5.2.6. Imidazolium and benzimidazolium-based anionophores as antimicrobials

Cation-selective ionophores are regularly used as antibiotics, but their anion analogs are much less common. However, once a transmembrane channel is inserted in the bilayer, it may transport anions towards the exterior of the bacteria, creating an imbalance in the ion homeostasis. As mentioned previously, chloride transport in epithelial cell membranes is mainly mediated by a channel regulator activated by a calcium-regulated protein. The transfer of information between these two regulated proteins was also observed in other ion channel-associated diseases.[48] Calcium co-transport *via* benzimidazolium salts was demonstrated in bacterial strains by over-expressing a mutant citrine fluorescent protein as a genetically encoded Ca^{2+} indicator. A massive influx of calcium into the *E. coli* cytosol was observed when ionophores were added to the bacterial suspension. Calcium transport efficiency followed the Hofmeister series for different anions, illustrating a symport process. The capacity of **39** to self-assemble and form transmembrane ion channels in the bacterial cell membranes (Figure 5.10) encouraged the development of other imidazolium salts as ionophores with antimicrobial properties.
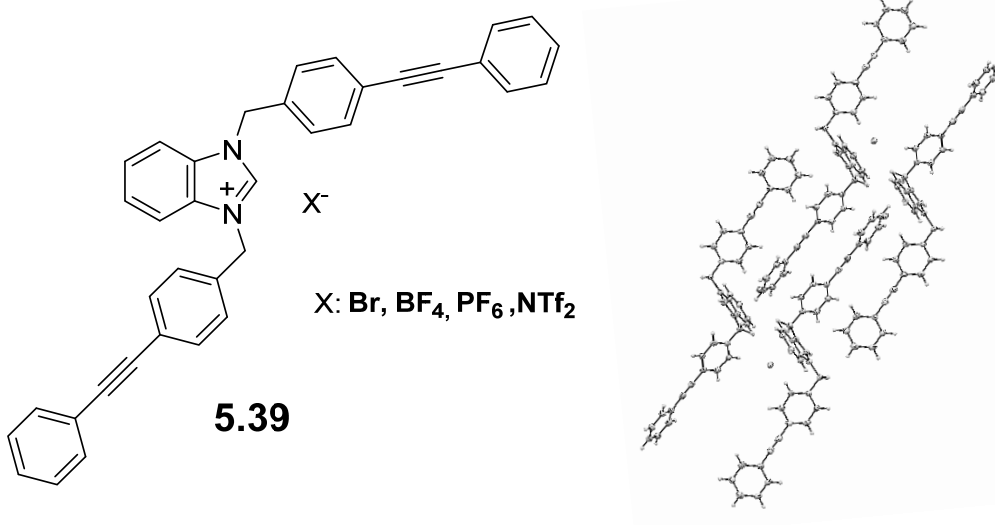
Figure 5.10. Self-association of benzimidazolium salts. Ortep diagram of benzimidazolium ionophore **5.39** showing its assembly into dimers forming a transient channel.

The transmembrane activity of binol-functionalized ionophores **5.40** and **5.41** (Figure 5.11) was first demonstrated in liposomes, and then their activities in Gram-negative and Gram-positive bacteria were reported.[20]

n = 1, X: NTf$_2$ **5.40**
n = 5, X: NTf$_2$ **5.41**
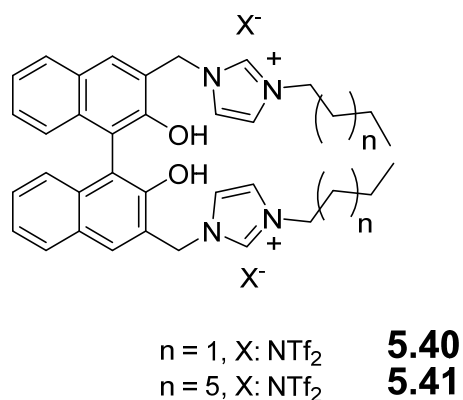
Figure 5.11.   Imidazolium-functionalized binols with antibacterial properties

Antibacterial tests were performed against *E. coli* (Gram-negative) and *Bacillus thuringiensis* (Gram-positive). Bacterial growth rates were monitored after exposure to these compounds. As shown in Figure 5.12, at 10 µM, compound **5.41** completely inhibited bacterial growth, while compound **5.40** causes a growth delay of *E. coli*.
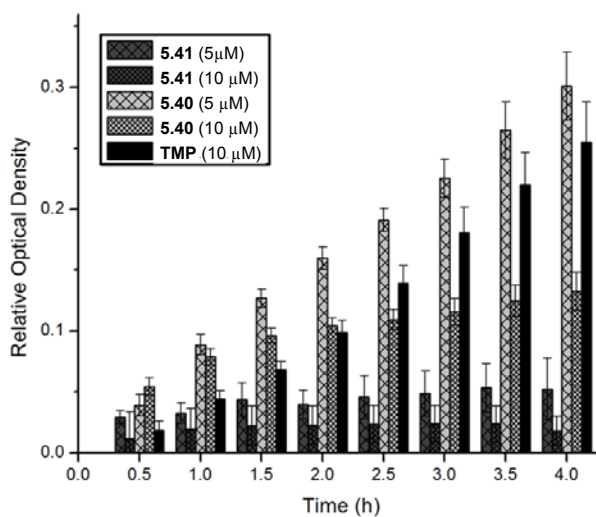
Figure 5.12.   Relative antibacterial activities of compounds **5.40** and **5.41** in Gram-negative bacteria *E. coli* grown at 37 °C over 4 h. The antibiotic trimethoprim (TMP) at 10 µM served to compare the efficacy of growth inhibition.

Compound **5.41** showed strong antibacterial activity at 2 μM in *B. thuringiensis*, while compound **5.40** was less selective for this Gram-positive strain (Figure 5.13). The difference in the cell membrane structure for these two bacterial strains is likely the cause of the different specificity observed.
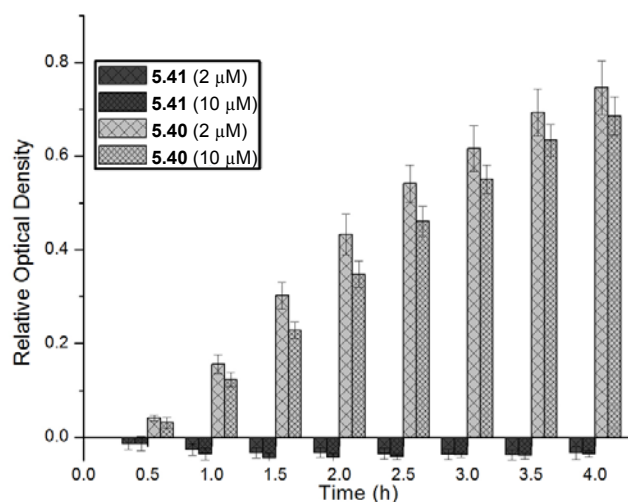
Figure 5.13.   Relative antibacterial activity of compounds **5.40** and **5.41** in Gram-positive *B. thuringiensis* (*HD73*) grown at 37 °C over 4 h.

Mechanistically, there are two major steps that may contribute to the antimicrobial activity of these imidazolium salts. First, the imidazolium cationic head group may approach the negatively charged cell membrane of microbes *via* an electrostatic interaction. This interaction is also entropically favored due to the release of a large number of counterions. Next, the hydrophobic tail of the molecule could undergo self-promoted transport across the cell membrane, resulting in disruption in the bilayer and the release of the intracellular constituents, leading to cell death. In this step, an optimum hydrophobicity of the amphiphile would allow **5.41** to easily enter and diffuse in the non-polar environment created by the lipid bilayers of the cell membrane.

The imidazolium-based anionophores, acting as transmembrane ion-channels or mobile carriers depending on their structure, are the first synthetic transporters showing efficiency and specificity as antimicrobial agents. Their ability to penetrate bacterial membranes and to disturb ion homeostasis predicts promising applications as therapeutic agents. The question remains: would the combination of an imidazolium-based

anionophore and an FDA-approved antibiotic result in an altered function, rather than each being administered independently? We surmise that as transmembrane pore formation occurs, membrane penetration is enhanced. This inference is possible, and any possible interactions between antibiotics and ionophores have yet to be determined, and are currently under investigation.

Finally, there is the topic of transporters for anions other than Cl^-. For example, an interesting target with potential biological utility is a synthetic transport system for bicarbonate. A specific goal would be a mimic of chloride/bicarbonate exchangers, which play important roles in red blood cells and epithelial tissues. The challenge in this case is to produce an ionophore that can extract the very hydrophilic bicarbonate anion, and allow it to pass into the lipophilic interior of a bilayer membrane.

5.2.7. Conclusions

Over the few past years, interesting biological applications have been discovered for a variety of synthetic ionophores. With every new biological-activity/structure relationship obtained from these anionophores, researchers get closer to more sophisticated structures presenting useful biological properties. The application of these systems as treatment for diseases caused by malfunction of chloride, calcium or other natural protein-based ion channels may depend on their metabolic properties, but their anticancer and antibacterial activity and specificity may open the door to a new avenue to alter cell membrane integrity for specific purposes.

5.2.8. Acknowledgements

5.2.9. Biographical Information

Claude-Rosny Elie received his B.Sc. in Chemistry from Université de Montréal, Canada and he is pursuing his Ph.D at the same institution under the guidance of Professor A.R. Schmitzer as NSERC scholarship. His research interests involve the investigation of imidazolium and benzimidazolium salts for transmembrane transport properties.

Marc Vidal received his Engineering degree and M.Sc. in Chemistry from Ecole Nationale Supérieure de Chimie de Caen, France and he is pursuing his Ph.D at the Université de Montréal under the guidance of Professor A.R. Schmitzer. His research interests involve the investigation of imidazolium-functionalized binol salts for transmembrane transport properties.

Mathieu Charbonneau received his B.Sc. in Chemistry from Université de Montréal, Canada and he is pursuing his M.Sc at the same institution under the guidance of Professor A.R. Schmitzer. His research interests involve the investigation of imidazolium-functionalized peptides for transmembrane transport properties.

Audrey Hébert is pursuing her B.Sc. at the Université de Montréal and she worked under the guidance of Professor A.R. Schmitzer during the summer of 2012 and 2013 as NSERC scholarship.

Andreea R. Schmitzer is Professor of Chemistry at the Université de Montréal, Canada. She was awarded three Ichikizaki Fund for Young Chemists Awards, a CNC IUPAC Travel Award and a Thieme Chemistry Journals Award. Her research program focuses on using synthetic organic chemistry to engineer the interface between chemistry and biology, and spans the areas of transmembrane transporters, catalysis and biological applications of supramolecular assemblies.

5.2.10. References

1. Daleke, D.L., *J. Lipid Res.* **2003**, *44*, 233-242.

2. a) Kunzelmann, K., *J. Membr. Biol.* **2005**, *205*, 159. b) Dubyak, G.R., *Adv. Phys. Ed.* **2004**, *28*, 143.

3. a) Jentsch, T.J., *J. Phys.-London* **2007**, *578*, 633. b) Grabe, M., Oster, G., *J. Gen. Phys.* **2001**, *117*, 329. c) Jentsch, T.J., Stein, V., Weinreich, F., Zdebik, A.A., *Phys. Rev.* **2002**, *82*, 503.

4. a) Jentsch, T.J., Maritzen, T., Zdebik, A.A., *J. Clin. Invest.* **2005**, *115*, 2039-2046. b) Puljak, L., Kilic, G. *Biochim. Biophys. Acta.-Molecular Basis Of Disease* **2006**, *1762*, 404. c) Jentsch, T.J., Neagoe, L., Scheel, O., *Curr. Opp. Neurobiol.* **2005**, *15*, 319.

5. Moskowitz, S.M., Gibson, R.L., Effmann, E.L. *Ped. Radiol.* **2005**, *35*, 739.

6. a) Remillard, C.V., Yuan, J.X.J., *Am. J. Physiol.- Lung Cell. Mol. Physiol.* **2004**, *286*, L49. b) Heimlich, G., Bortner, C.D., Cidlowski, J.A., *Cell Vol. Sign.* **2004**, *559*, 189. c) Okada, Y., Shimizu, T., Maeno, E., Tanabe, S., Wang, X., Takahashi, N., *J. Membr. Biol.* **2006**, 209, 21. d) Takahashi, N., Wang, X.M., Tanabe, S., Uramoto, H., Jishage, K., Uchida, S., Sasaki, S., Okada, Y., *Cell. Physiol. Biochem.* **2005**, *15*, 263.

7. Green, D.R., Reed, J.C., *Science* **1998**, *281*, 1309.

8. a) Bortner, C.D., Cidlowski, J.A., *Biochem. Pharmacol.* **1998**, *56*, 1549. b) Bortner, C.D., Cidlowski, J.A., *Pflugers Archiv-Eur. J. Physiol.* **2004**, *448*, 313. c) Heimlich, G., Cidlowski, J.A., *J. Biol. Chem.* **2006**, *281*, 2232.

9. Lang, F., Hoffmann, E.K., *Compr. Physiol.* **2012**, *2*, 2037.

10. Gokel, W.G., Negin, S., *Acc. Chem. Res.* **2013**, *46*, 2824.

11. a) Busschaert, N., Gale, P.A., *Angew. Chem. Int. Ed.* **2013**, *52*, 1374. b) Davis, A.P., Sheppard, D.N., Smith, B.D., *Chem. Soc. Rev.* **2007**, *36*, 348.

12. Gale, P.A., *Acc. Chem. Res.* **2011**, *44*, 216.

13. a) Davis, J.T., Okunola, O., Quesada, R., *Chem.Soc. Rev.* **2010**, *39*, 3843. b) Brotherhood, P.R., Davis, A.P., *Chem. Soc. Rev.* **2010**, *39*, 3633. c) Mareda, J., Matile, S., *Chem. Eur. J.* **2009**, *15*, 28. d) Gokel, G.W., Barkey, N., *New J. Chem.* **2009**, *33*, 947. e) Li, X., Wu, Y.D., Yang, D., *Acc. Chem. Res.* **2008**, *41*, 1428.

14. Koulov, A.V., Lambert, T.N., Shukla, R., Jain, M., Boon, J.M., Smith, B.D., Li, H.Y., Sheppard, D.N., Joos, J.B., Clare, J.P., Davis, A.P., *Angew. Chem. Int. Ed.* **2003**, *42*, 4931.

15. Benz, R., Stark, G., *Biochim. Biophys. Acta*. **1975**, *382*, 27.

16. a) Bandyopadhyay, P., Janout, V., Zhang, L.H., Regen, S.L., *J. Am. Chem. Soc.* **2001**, *123*, 7691. b) De Riccardis, F., Di Filoppo, M., Garrisi, D., Izzo, I., Mancin, F., Pasquato, L., Scrimin, P., Tecilla, P., *Chem. Commun.* **2002**, *24*, 3066. c) Otto, S., Osifchin, M., Regen, S.L., *J. Am. Chem. Soc.* **1999**, *121*, 7276.

17. Krasne, S., Eisenman, G., Szabo, G., *Science* **1971**, *174*, 412.

18. Amendola, V., Fabbrizzi, L., Mosca, L., *Chem. Soc. Rev.* **2010**, *39*, 3889.

19. Xu, Z., Kim, S.K., Yoon, J., *Chem. Soc. Rev*. **2010**, *39*, 1457.

20. Vidal, M., Elie, C.R., Campbell, S., Claing, A., Schmitzer, A.R., *Med. Chem. Comm.* **2014**, *5*, 436.

21. a) Davis, A.P., *Coord. Chem. Rev.* **2006**, *250*, 2939.

22. Clare, J.P., Ayling, A.J., Joos, J.B., Sisson, A.L., Magro, G., Perez-Payan, M.N., Lambert, T.N., Shukla, R., Smith, B.D., Davis, A.P., *J. Am. Chem. Soc.* **2005**, *127*, 10739.

23. Sheppard, D.N., Carson*,* M.R., Ostedgaard*,* L.S., Denning*,* G.M., Welsh, M.J., *Am. J. Physiol.* **1994***, 266,* L405.

24. Ma, B., Zha, H., Li, N., Yang, D., Lin, G. *Mol. Pharm*. **2011**, *8*, 1073.

25. Li, X., Shen, B., Yao, X.Q., Yang, D., *J. Am. Chem. Soc.* **2009**, *131*, 13676.

26. Shen, B., Li, X., Wang, F., Yao, X., Yang, D. *PLoS One* **2012**, *7*, e34694.

27. a) Thangaraju, M., Sharma, K., Leber, B., Andrews, D.W., Shen, S.-H., Srikant, C.B., *J. Biol. Chem*. **1999**, *274*, 29549. b) Thangaraju, M., Sharma, K., Liu, D., Shen, S.-H., Srikant, C. B., *J. Biol. Chem.* **1999**, *59*, 1649.

28. Matsuyama, S., Llopis, J., Deveraux, Q.L., Tsien, R.Y., Reed, J.C., *Nat. Cell Biol.* **2000**, *2*, 318.

29. Busschaert, N., Gale, P.A., Haynes, C.J., Light, M.E., Moore, S.J., Tong, C.C., Davis, J.T. , Harrell, W.A. Jr., *Chem. Commun.* **2010**, *46*, 6252.

30. Busschaert, N, Wenzel, M., Light, M.E., Iglesias-Hernández, P., Pérez-Tomás, R., Gale. P.A., *J. Am. Chem. Soc.* **2011**, *133*, 14136.

31. Shrode, L.D., Tapper, H., Grinstein, S., *J. Bioenerg. Biomembr.* **1997**, *29*, 393.

32. a) Smith, P.B., Crespi, C., *Biochem. Pharmacol.* **2002**, *63*, 1941. b) Onderwater, R.C.A., Commandeur, J.N.M., Groot, E.J., Sitters, A., Menge, W.M.P.B, Vermeulen, N.P.E. *Toxicology* **1998**, *125*, 117. c) Svarovsky, S.A., Simoyi, R.H., Makarov, S.V.A., *J. Phys. Chem. B* **2001**, *105*, 12634.

33. Allison, A.C., Young, M.R., *Lysosonzes in Biology and Pathology*, Dingle, J. T. and Fell, H. B. ed. **1969**, Amsterdam, Vol. 12, 601.

34. a) Andrews, N.J., Haynes, C.J.E., Light, M.E., Moore, S.J., Tong, C.C., Davis, J.T., Harrell, W.A. Jr., Gale, P.A. *Chem. Sci.* **2011**, *2*, 256. b) Moore, S.J., Wenzel, M., Light, M.E., Morley, R., Bradberry, S.J., Gómez-Iglesias, P., Soto-Cerrato, V., Pérez-Tomás, R., Gale, P.A. *Chem. Sci.* **2012**, *3*, 2501.

37. Moore, S.J., Haynes, C.J.E., González, J., Sutton, L.J., Brooks, S.J., Light, M.E., Herniman, J., Langley, G.J., Soto-Cerrato, V., Pérez-Tomás, R., Marques, I., Costa, P.J., Félix, V., Gale, P.A., *Chem. Sci.* **2013**, *4*, 103.

36. Gale, P.A., Tomás, R.P., Quesada, R., *Acc. Chem. Res.* **2013**, *46*, 2801.

37. Busschaert, N., Kirby, I.L., Young, S., Coles, S.J., Horton, P.N., Light, M.E., Gale, P.A., *Angew. Chem. Int. Ed.* **2012**, *51*, 4426.

38. Carasel, I.A., Yamnitz, C.R., Winter, R.K., Gokel, G.W., *J. Org. Chem.* **2010**, *75*, 8112.

39. a) Davis, J.T. **2010**, Gale, P. A. and Dehaen, W. ed., Springer-Verlag: Berlin Heidelberg, 24, 145-176.

40. a) Benz, R., Frohlich, O., Lauger, P., *Biochim. Biophys. Acta.* **1977**, *464*, 465. b) Ramoneda, B. M., Perez-Tomas, R., *Biochem. Pharmacol.* **2002**, *63*, 463.

41. Sessler, J.L., Eller, L.R., Cho, W.S., Nicolaou, S., Aguilar, A., Lee, J.T., Lynch, V.M., Magda, D.J., *Angew. Chem. Int. Ed.* **2005**, *44*, 89.

42. Manderville, R.A., *Curr. Med. Chem. Anticancer Agents* **2001**, *1*, 195.

43. Melvin, M.S., Tomlinson, J.T., Park, G., Day, C.S., Saluta, G.R., Kucera, G.L., Manderville, R.A., *Chem. Res. Toxicol.* **2002**, *15*, 734.

44. Seganish, J.L., Davis, J.T., *Chem. Commun.* **2005**, *46*, 5781.

45. a) Beutler, J.A., McKee, T.C., *Curr. Med. Chem.* **2003**, *10*, 787. b) Sato, T., Konno, H., Tanaka, Y., Kataoka, T., Nagai, K., Wasserman, H.H., Ohkuma, S., *J. Biol. Chem.* **1998**, *273*, 21455. c) Ohkuma, S., Sato, T., Okamoto, M., Matsuya, H., Arai, K., Kataoka, T., Nagai, K., Wasserman, H.H., *Biochem. J.* **1998**, *334*, 731. d) Konno, H., Matsuya, H., Okamoto, M., Sato, T., Tanaka, Y., Yokoyama, K., Kataoka, T., Nagai, K., Wasserman, H.H., Ohkuma, S., *J. Biochem.* **1998**, *124*, 547.

46. Iglesias Hernández P., Moreno, D., Javier, A.A., Torroba, T., Pérez-Tomás, R., Quesada, R., *Chem. Commun.* **2012**, *48*, 1556.

47. Díaz de Greñu, B., Iglesias Hernández, P., Espona, M., Quiñonero, D., Light, M. E., Torroba, T., Pérez-Tomás, R., Quesada, R., *Chem. Eur. J.* **2011**, *17*, 14074.

48. a) Elie, C.-R., Noujeim, N., Pardin, C., Schmitzer, A. R., *Chem. Commun.* **2011**, *47,* 1788. b) Elie, C.-R., Hébert, A., Charbonneau, M., Haiun, A., Schmitzer, A. R., *Org. Biomol. Chem.* **2013,** *11*, 923.

Chapitre 6   Propriétés antibactériennes d'un sel de benzimidazolium et étude de son effet sur la membrane cellulaire

6.1. Préface

À ce stade du projet nous étions parvenus à synthétiser différentes familles de transporteurs anioniques et à en cerner la plupart des caractéristiques cinétiques et thermodynamiques sur lesquelles nous nous basions afin d'améliorer notre modèle. L'une des finalités ultimes de toute cette recherche était, depuis le début, au-delà du développement d'un transporteur d'anion basé sur les sels d'imidazolium, la capacité d'en dégager une application biologique. Nos observations encourageantes présentées au chapitre 4, ouvraient déjà la porte à une telle perspective, tandis que nous étions parvenus à décrire la translocation d'ions calcium à l'intérieur d'une bactérie *E. coli*, sous l'effet d'un de nos transporteurs. Dès lors, il nous semblait approprié d'exploiter ce paradigme dans une optique antibactérienne en cherchant à provoquer un débalancement ionique et une perturbation de la membrane cellulaire d'une souche microbienne, afin d'en provoquer la lyse. Bien qu'étant conscients que nos molécules candidates puissent agir selon une pléthore de mécanismes sur les bactéries et les autres organismes vivants, comme c'est d'ailleurs le cas pour plusieurs molécules biologiquement actives, nos efforts se concentrèrent ici, au meilleur de nos moyens et capacités, sur l'action des sels de benzimidazolium au niveau des bicouches de liposomes, des membranes bactériennes et sur celles des globules rouges. Pour ce faire, une série de tests bioanalytiques (détermination des EC_{50} et concentration minimale inhibitrice) ont d'abord été effectués en présence de liposomes et de bactéries, dans le but de sélectionner notre meilleur transporteur et agent antibactérien. Les résutats ont convergé vers un même sel de dibenzimidazolium. Ce dernier fut étudié pour ses propriétés de dépolarisation de la membrane bactérienne, ainsi que par microscopie électronique à balayage (SEM) afin d'observer visuellement les dommages causés à la membrane d'une souche de *E. coli*.

Toutes les synthèses, analyses et caractérisations ont été réalisées par moi-même, assisté du support de mon stagiaire Guillaume David pour les tests en présence de liposomes et en microscopie. J'ai rédigé l'article en totalité avant de le soumettre à la révision de la Pre. Andreea Schmitzer, qui a également supervisé et piloté tout le projet. Les informations expérimentales supplémentaires de ce chapitre se trouvent aux pages 184-221 de cette thèse.

6.2. Article 5 : « Strong antibacterial properties of anion transporters: a result of depolarization and weakening of the bacterial membrane»

Claude-Rosny Elie, Guillaume David and Andreea R. Schmitzer*

Department of Chemistry, Université de Montréal, 2900 Édouard-Montpetit CP 6128 succ. Centre-Ville, Montréal Québec, Canada, H3C 3J7.

ABSTRACT. The development of low molecular weight anionophores is an emerging topic in chemistry as the need for these compounds increases with the continuous discovery of pathologies involving anomalies in anion transport processes. Development of new concepts to initiate anion imbalance in living cells while fighting multidrug resistant bacteria is a paramount topic. In this study, three series of compounds including *N,N'*-diphenylethynylbenzyl benzimidazolium salts (**6.1-6.2**), 1,1'- (pyridine-2,6-diyl) bis(3 - (4-(phenylethynyl)benzyl) -1H-benzo[d]imidazol-3-ium) salts (**6.3 - 6.5**) and 1,1'- (pyridine-2,6-diylbis(methylene)) bis(3-(4-(phenyl ethynyl)benzyl)-1H-benzo[d]imidazol-3-ium) salts (**6.6-6.8**) displaying high antimicrobial activity and low toxicity against human cells were designed, synthesized and studied. The most potent compound displayed micromolar minimal inhibitory concentrations (MICs) in different gram-negative and gram-positive bacteria, while its hemolytic activity remained around 10% or less, even after a prolonged period of exposure. The mechanism of action of these benzimidazolium salts on bacterial membrane was assessed by bioanalytical techniques including assays in model membrane liposomes, membrane depolarization studies and scanning electron microscopy (SEM) in living bacteria.

6.2.1. Introduction

The study of synthetic anion transporters remains an important subject in medical research today. This interest comes from the considerable number of diseases originating in dysfunctions of natural anion channels.[1] In 1999, Sessler and Allen were the first to hypothesize that restoring the efflux of chloride ions in cell membranes through a synthetic channel may be useful to treat cystic fibrosis.[2] This assumption marked the beginning of many breakthroughs in this field. Voyer *et al.* described later on a peptide-based chloride transporter, able to penetrate the cell membrane in a non-selective way.[3] In the same vein, Gale *et al.* developed prodigiosin analogs, natural amphiphilic products extracted from microorganisms such as *Streptomyces* and *Serratia*, that have showed anticancer activity, linked to a transport process of chloride ions across cell membranes.[4] More recently Quesada *et al.* also reported the *in vivo* cytotoxic effects of synthetic tambjamine analogs and they established a relationship between the cancer cell death and

the membrane disruption, as a result of an electrolyte imbalance mechanism, involving nitrate and chloride anions.[5] The anionophoric properties of these natural compounds are obvious, but still poorly understood from a mechanistic, kinetic and thermodynamic perspective. Even if these synthetic transporters main application envisages the death of cancer cells, other types of pathogens, such as bacteria, could be targeted, knowing that 70% of nosocomial infections are becoming resistant to the commonly prescribed antibiotics in hospitals.[6] Several synthetic amphiphilic transporters described in the literature are inspired by the natural antimicrobial peptides (AMPs), well known for their activity in bacteria, viruses, fungi and even cancer cells.[7] However, the synthesis of antimicrobial peptides often requires several synthetic steps and generally results in poor yields.[8] Moreover, their poor stability towards proteases is a clear concern. Besides, the major challenge to successfully mimic these antimicrobial peptides remains their low toxicity *in vivo*.[8a,b] For all these reasons we have developed synthetic anionophores based on benzimidazolium salts (Scheme 6.1), possessing the amphiphilic characteristics of AMPs, endowed with a powerful antibacterial activity and low toxicity for normal human cells. Since these salts do not contain peptidic bonds, they may be insensitive to the action of peptidases and therefore they should retain their biological activity under physiological media. Herein we demonstrate their anion transport properties and we provide evidence of their antibacterial action by membrane depolarization assays and SEM imaging of bacteria in the presence of these salts. Based on the amphiphilic scaffold of compounds **6.1** and **6.2** we had previously reported as potent anionophores,[9,10] new analogs were designed, synthesized and studied, all possessing the benzimidazolium unit and the phenylethylbenzyl substituents. Since other biscationic antimicrobials generally show a lower cytoxicity than the monocationic analogs,[8b,c] we decided to couple two benzimidazolium cations through a pyridyl or a lutidine unit. The pyridyl and lutidine units can act as protonation sites, but could also participate in binding of different anions in aqueous medium. Details of the synthesis of these new compounds are provided in Schemes 6.2 and 6.3 and the annexe 4.

Scheme 6.1. Benzimidazolium salts studied for transmembrane anionophoric properties

X=Br = **6.1**
X=NTf₂ = **6.2**

X=Br = **6.3**
X=NTf₂ = **6.4**
X=OTf = **6.5**

X=Br = **6.6**
X=NTf₂ = **6.7**
X=OTf = **6.8**

≡ R
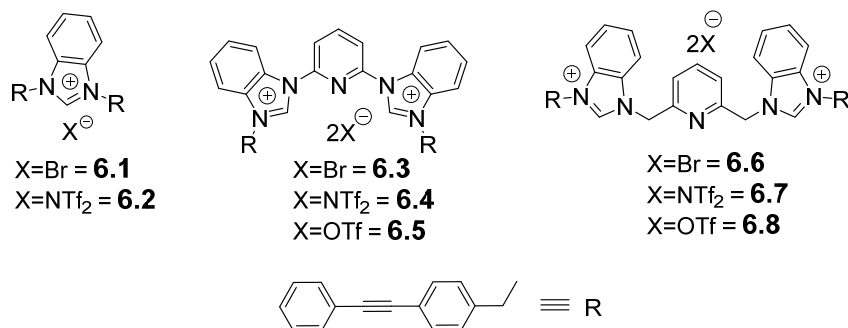
Scheme 6.2. Synthesis of pyridine-bridged bis-benzimidazolium salts **6.3-6.5**[*]

≡ R
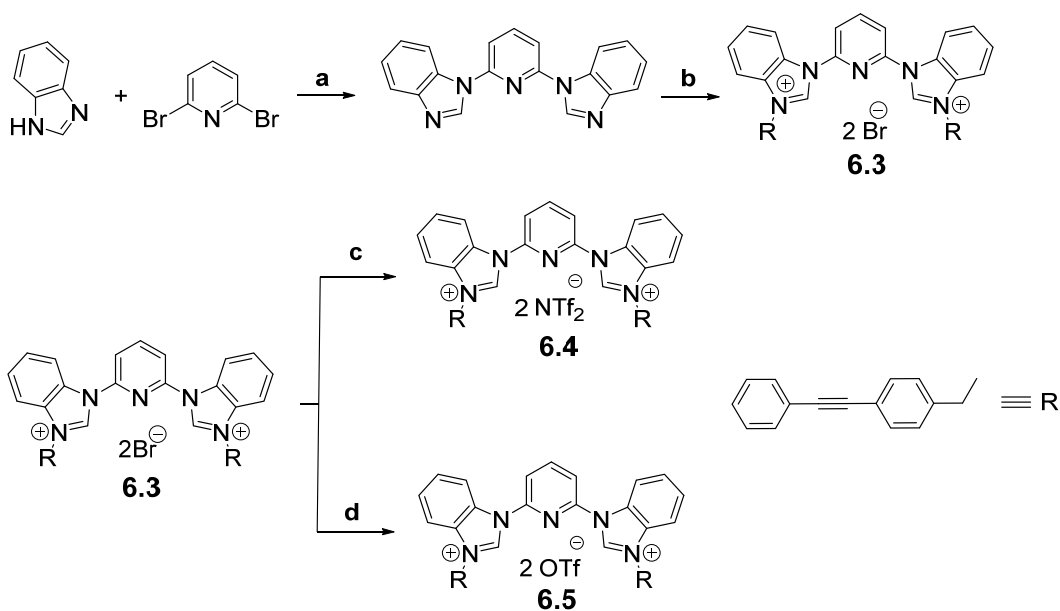
*Reagents and conditions: (a) NaH, DMF (anh), 155 °C, 96 h. (b) R-Br, ACN, 85 °C, 72 h. (c) (1) LiNTf₂, MeOH/ACN, 85 °C, 12 h; (2) H₂O, 100 °C, 12 h. (d) LiOTf, MeOH/ACN, 85 °C, 12 h; (2) H₂O, 100 °C, 12 h.

Scheme 6.3. Synthesis of lutidine-bridged bis-benzimidazolium salts **6.6-6.8**[**]
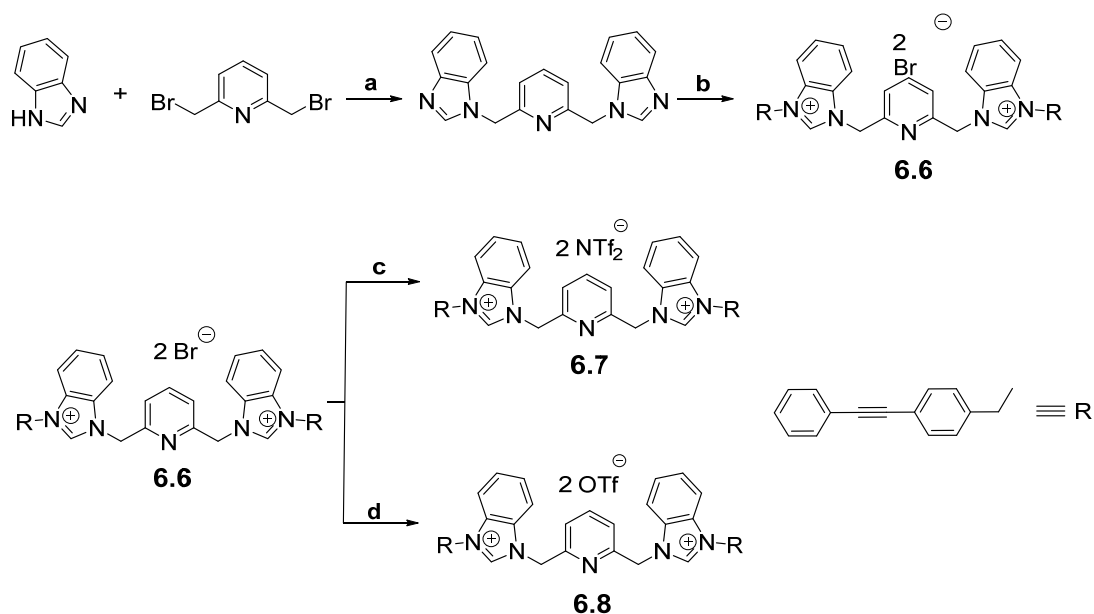
**Reagents and conditions: (a) KOH, TBAB, toluene/H_2O, 25 °C, 12 h. (b) R-Br, ACN, 85 °C, 72 h. (c) (1) LiNTf2, MeOH/ACN, 85 °C, 12 h; (2) H_2O, 100 °C, 12 h. (d) LiOTf, MeOH/ACN, 85 °C, 12 h; (2) H_2O, 100 °C, 12 h.

6.2.2. Results and discussion

Anion transport assays

The chloride transport ability of all synthetic benzimidazolium salts was first evaluated in egg yolk phosphatidylcholine (EYPC) liposomes. The transmembrane anion transport activity of the compounds was evaluated by fluorimetry, as previously reported.[8-14] EYPC vesicles containing 2 mM lucigenin, which fluorescence is inhibited by the presence of chloride anions, were loaded with a NaCl solution and suspended in a NaNO3 buffer. The chloride efflux from the liposomes was followed over 300 seconds by monitoring lucigenin's fluorescence when the transporter, dissolved in MeOH, was added to the extravesicular medium. At the end of the assay, the liposomes were lysed with Triton-X, in order to normalize the 100% efflux of chloride. A dose-dependent relationship was observed between the activity of the benzimidazolium salts and their concentration, thus making possible to calculate an EC_{50} reported in Table 6.1. Salts **6.6**,

6.7 and **6.8** possess better transport properties, with lower EC_{50} compared with their benzimidazolium salts analogs with a pyridyl spacer. In particular, compound **6.8** induces a 50% chloride ion efflux at a ratio of 0.46 mol% (with respect to the lipid). The presence of the methylene groups increases the flexibility of compounds **6.6**, **6.7** and **6.8**, which may allow them to adopt different conformations during the transport process when they penetrate the bilayer.

Table VI-1. Transport data determined by Hill analysis. EC_{50} represents the concentration (mol.% with respect to lipid) of ionophore required to mediate 50% chloride efflux after 250 sec.

Compounds	Counter-anion	$EC_{50,250s}$ (mol.%)
6.1	Br$^-$	14.8
6.2	NTf$_2$$^-$	5.8*
6.3	Br$^-$	24
6.4	NTf$_2$$^-$	6.9
6.5	OTf$^-$	12.0
6.6	Br$^-$	14
6.7	NTf$_2$$^-$	5.6
6.8	OTf$^-$	0.46

*the value of 2.9% previously reported for **6.2** was calculated in different lipid concentration conditions[15c]

We then investigated the transport mechanism of the benzimidazolium salts with lutidyl spacer **6.6-6.8**, which present a better potency than their analogue with pyridyl spacer for a given counter-anion. First, the chloride ion efflux outside of 1,2-dipalmitoyl-sn-glycero-3-phosphocholine (DPPC) liposomes was followed using the same lucigenin fluorescence assay, as previously reported in the literature.[10, 15] The DPPC liposomes were first loaded with a solution of NaCl containing lucigenin (2 mM), and then

suspended in a nitrate solution. The benzimidazolium salt, diluted in methanol, was added to the extravesicular solution and the efflux of Cl^- from the liposomes at temperatures above and below DPPC's transition phase (41 ºC) was monitored. The 100% chloride release was calibrated by lysing the liposomes with Triton-X, after 300 seconds. The efficiency of a mobile anion transporter, limited by its diffusion through the membranes, is generally considerably reduced when the DPPC liposome bilayer is maintained in the gel-state (at temperatures inferior to 41 ºC), whereas in the case of the formation of a transmembrane channel, no or only a small alteration of its efficiency is observed below the bilayer's gel-to-liquid crystalline phase transition temperature.[10,15]
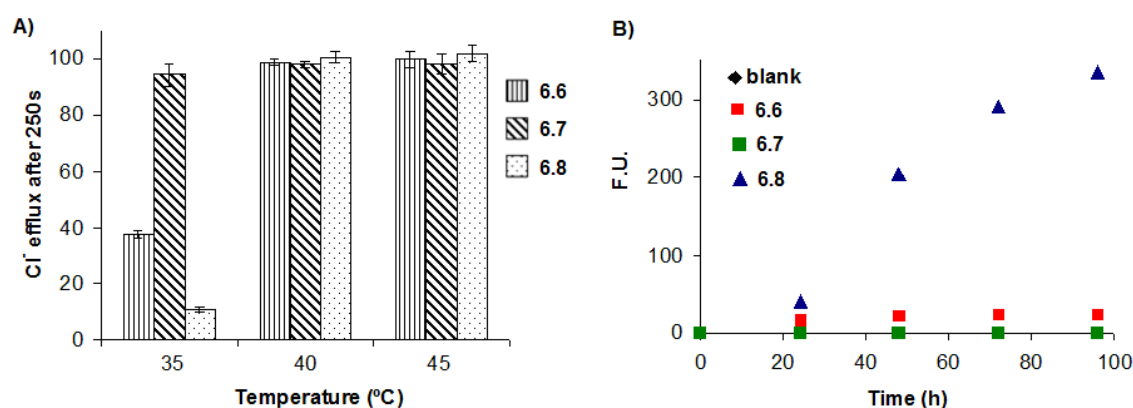
Figure 6.1.   A) Chloride efflux in DPPC liposomes at 35 ºC, 40 ºC and 45 ºC. The data at each temperature are obtained by using 10 mol% of benzimidazolium salts **6.6-6.8** (relative to 6.25 mM DPPC concentration). The data at each temperature are the average of three series of measurements. B) Increase of the lucigenin's fluorescence in U-tube tests in the presence of compounds **6.6-6.8** (a zoom is provided for **6.6**, **6.7** and the blank in the annexe 4).

Based on a method previously reported in the literature[15a] and our results shown in Figure 6.1A, it can be conclude that compound **6.8** shows a behaviour characteristic of a mobile carrier. It is interesting to note that in this regard, the OTf^- salt (**6.8**) that shows a temperature dependent activity acts as a mobile carrier, while the NTf_2^- salt (**6.7**) for which the transport activity is only partially affected by the temperature, rather forms

transmembrane channels for the same benzimidazolium cation. The bromide salt (**6.6**) appears meanwhile to obey an intermediate mechanism, half away between a mobile carrier and a transmembrane channel, suggesting that the nature of the counter-anion of these benzimidazolium salts alone may be sufficient to change the transport mechanism. Gokel *et al.* have also previously reported a switch from a transmembrane synthetic channel anion transport mechanism to mobile carriers over a certain concentration range of dipicolineamides.[16] At the same time, the change of the transport mechanism of these benzimidazolium salts could be due to chaotropic and chosmotropic factors modulated by the nature of the counter-anions, as well as different partition coefficients of the monomer, the aggregates and the association equilibrium in water and in the phospholipid bilayer. We have already discussed, in chapter 3 of this thesis, the very unpredictable impact of these factors related to multiple equilibria observed during transmembrane anion transport process (see figure 3.5, chapter 3). Nevertheless a broader range of counter-anions is under investigation in order to get a better insight of the influence of the nature of the counter-anion on the mechanism.

Among different other studies that can confirm the mechanism of transport,[17] we decided to perform additional U-tube tests for compounds **6.6**-**6.8**, as previously described by our group.[18] The transport of nitrate as lucigenin's counter-anion in a U-tube involves the translocation of the lucigenin across the organic phase that separates two aqueous phases. The U-tube experiments were performed with compounds **6.6**-**6.8** incorporated in the chloroform phase, by monitoring the increase of lucigenin's fluorescence in the receiving phase. As the formation of transmembrane channels is impossible in the bulk organic chloroform phase, the translocation of lucigenin from one aqueous to the other aqueous phase is the result of a mobile transport mechanism of the nitrate anions, and thus of the lucigenin. As shown in Figure 6.1B, compound **6.8** actively transports nitrate anions, while a very slow transport mechanism and an intermediate process can be observed for compounds **6.7** and **6.6** respectively. These results allow us to affirm that **6.8** acts as an active mobile anion transporter.

Antibacterial studies

      Liposomes are model membranes that historically have been indispensable for the development of our understanding of biological membranes. Nevertheless, bacterial cell membranes are structurally much more complex than liposomes, with lipid bilayers containing other components such as proteins, lipopolysaccharides and many other materials that can interfere with the activity of the studied compound. The antibacterial activity of the benzimidazolium salts was thus evaluated in the presence of gram-negative *E. coli* and gram-positive *B. thuringiensis* strains. The minimal inhibitory concentrations (MICs), presented in Table 6.2, have been determined as described in the annexe 4. At a first glance, the benzimidazolium salts **6.6-6.8** have a more pronounced antibacterial activity. In this respect, following the same pattern as the activity in liposomes, compound **6.8** showed an improved antibacterial activity towards *E. coli*. The limited activity of the other benzimidazolium salts against *E. coli* (DH5α) could however come from the presence of an efflux pump protein (TolC) in this stain, which may limit the mass aggregation and accumulation of the ionophore in the bacteria.[19, 20] Indeed, it is well known that this transmembrane protein plays a role of protection, by limiting the accumulation of intruding molecules in the bacteria, including toxins and antimicrobial agents, through their expulsion from the bacteria.[19, 20] In order to verify whether inhibiting this protective mechanism by disabling the TolC protein, it is possible to increase the activity of the benzimidazolium salts, we performed the same study in a mutant *E. coli* (SK037) strain, for which TolC has been deactivated.[21] As shown in Table VI-2, *E. coli* (SK037) presents an increased sensitivity to the benzimidazolium salts with MICs 2.5 to 10 times lower than those required to inhibit the growth of the wild type *E. coli* (DH5α) strain. Furthermore, the gram-positive strain *B. thuringiensis* (HD73) presents even a greater sensitivity to all the benzimidazolium salts tested. The membrane of *B. thuringiensis* (HD73) is devoid of an outer wall and efflux pumps, which seems to explain how, with a less robust and less protected membrane, this bacterial strain, can possess a higher sensitivity to the antibacterial effects of the studied ionophores.[22] Compounds **6.6-6.8** possess MICs in the micromolar range, compared to all the imidazolium-based dications reported in the literature with structural similarity which present antimicrobial properties, but in the milimolar ranges[8b].

Table VI-2. Antibacterial activity against gram negative and gram positive bacteria

Compounds	Minimal Inhibitory Concentrations (µM)		
	E. coli		*B. thuringiensis*
	DH5α	SK037	HD73
6.1	>100	>100	10
6.2	>100	25	10
6.3	>100	>100	10
6.4	>100	>100	10
6.5	>100	>100	10
6.6	100	10	10
6.7	50	10	10
6.8	25	10	2

Haemolytic assays

The antibacterial results are even more encouraging when they are associated with the very low cytotoxicity of these benzimidazolium salts to human cells. Haemolysis assays were performed over 1 hour and 24 hours (Figure 6.2). It is interesting to notice that compound **6.8**, which shows the best antibacterial potential in all the strains studied (MIC 2-25 µM) also has a haemolytic activity inferior to 10% after 1 hour and only 10 % after 24 hours on human red blood cells at a concentration of 25 µM. The toxicity of **6.8** on human cells therefore remains very low in its bacteriostatic concentrations, even after a prolonged exposure period of 24 hours.
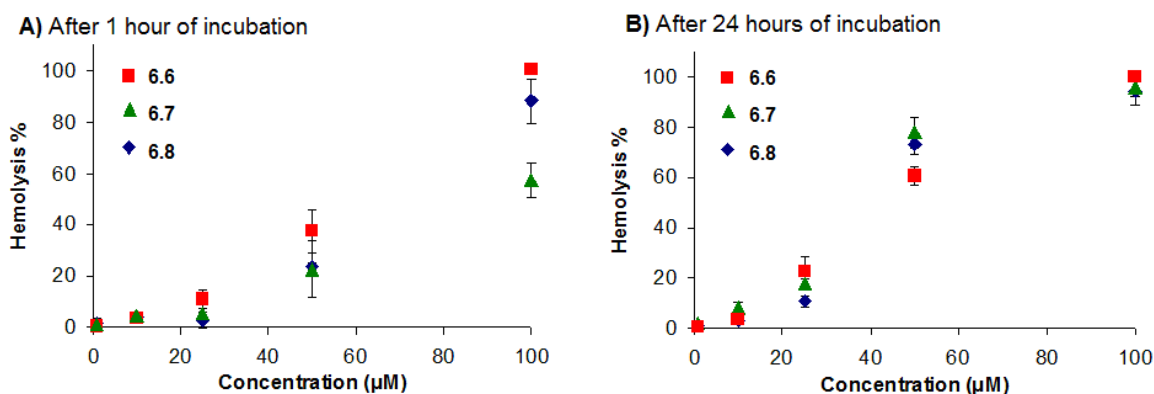
Figure 6.2. Haemolytic activities of compounds **6.6**, **6.7** and **6.8** after A) 1 hour of incubation and B) 24 hours of incubation. The points represent the average of six independent measurements.

Depolarization of the bacterial membrane

Having demonstrated the bacteriostatic capacity of these benzimidazolium salts, we decided to get better insights into the mechanism of the bacterial growth inhibition induced by these ionophores. The starting hypothesis was that an alteration of the permeability of the membrane of the bacteria causes an efflux of ions, such as observed in the liposomes. This ion imbalance should lead to a change in the membrane potential that provides the necessary energy and ensures the proper distribution, on both sides of the membrane, of the growth factors involved in the cell division of the bacteria.[20,23,24] Therefore, the depolarization of the cell membrane would be sufficient to seriously impair or inhibit the bacterial growth. Furthermore, given that the transmembrane potential of the bacteria is high (-120 to -200 mV) compared with the potential of eukaryotic cells (-60 to -80 mV) and erythrocytes (-8.4 mV), it may be possible to target bacterial growth selectively through their depolarization, without affecting dramatically the integrity of the eukaryotic cells and red blood cells[20,23,24]. Moreover, the transmembrane potential perturbation in bacteria is associated with the modification of vital mechanisms, including cell division, emergence of resistance and energy production (ATP).[20,23,24] In order to verify this hypothesis we incorporated a sensitive fluorescent dye 3,3′-diethylthiadicarbocyanine iodine (diSC$_2$5) in the outer membrane of *E. coli* (SK037) bacteria. The diSC$_2$5 is a fluorophore possessing the particularity of having a quenched fluorescence in the intact and polarized lipid membranes, and which becomes fluorescent

upon returning to the aqueous extracellular medium, when the membrane is irreversibly damaged and depolarized.[23] In other words, while the decrease of fluorescence of diSC$_2$5 signifies a membrane permeabilization, and hence the incorporation of the dye into the bilayer, the increase of the fluorescence signal is associated with a depolarization of the membrane and therefore the bacterial death.[20,26-28] The first step of this assay consisted of incubating a suspension of bacteria with diSC$_2$5 in order to allow its incorporation in the outer membrane of the bacteria, until the fluorescence decreases to a stable baseline. Then, upon the addition of a solution of benzimidazolium salt in DMSO at different concentrations, the fluorescence of diSC$_2$5 was followed over a period of ~2 hours. In figure 6.3, compounds **6.2** and **6.6** cause, even at a concentration corresponding to 40 times their MICs, only a slight decrease in the fluorescence of diSC$_2$5. This result suggests that these benzimidazolium salts transiently increase the permeability of the outer membrane of the bacteria, allowing the incorporation of a small fraction of diSC$_2$5. This increase in membrane permeability is however not associated with the depolarization of the membrane and thus does not lead to the death of the bacteria, even at high concentration of the anionophore after 2 hours. This result leads us to believe that **6.2** and **6.6** induce transient damage of the bacterial membrane, damage that the cell can quickly repair in order to prevent cytolysis. This hypothesis could allow the use these benzimidazolium salts and another antibacterial agents in synergy at a low dose, to temporarily weaken the bacteria, while acting concurrently on other targets, leading to the death of the microorganism. In the case of **6.7** and **6.8**, compounds having shown the best EC$_{50}$ and MIC, it is not surprising to observe a strong modification of the membrane during the depolarization tests. The fluorescence of diSC$_2$5 previously incubated with the *E. coli* (SK037) increases upon addition of **6.7** and **6.8**, which suggests a sustained membrane permeabilization, also accompanied by the depolarization of the membrane and probably the cell death. The depolarization tests show that irreversible damage can be caused to the membrane of the pathogenic bacteria *E. coli*, especially in the presence of compound **6.8**.
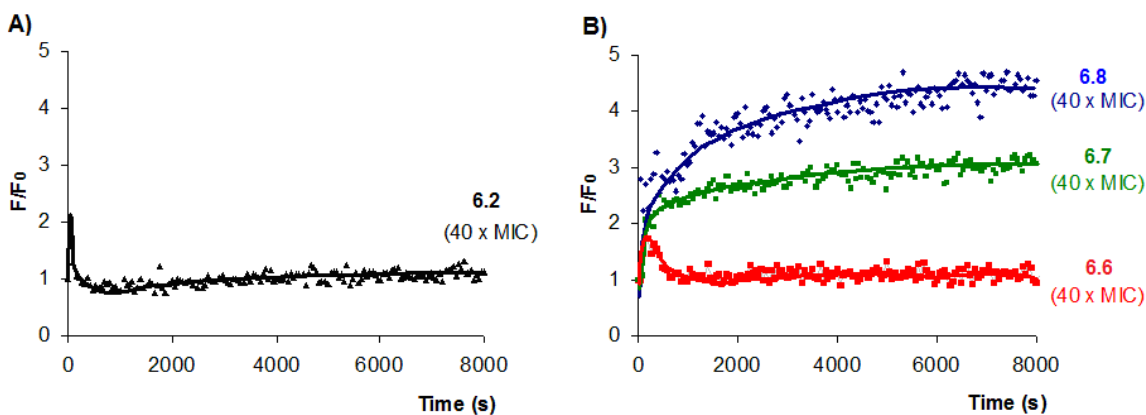
Figure 6.3. Effects of the antimicrobial benzimidazolium salts on the fluorescence intensity of diSC$_2$5 in the presence of the *E. coli* (SK037). A) Benzimidazolium salts were added at 70 s, at a final concentration of 1 mM for **6.2** and B) 0.4 mM for **6.6**, **6.7** and **6.8** corresponding to 40 times their MIC with respect to *E. coli* (SK037).

Modification of membrane morphology

The modification of *E. coli* (SK037) membrane in the presence of anionophore **6.8** was followed by SEM microscopy. As shown in Figure 6.4 (i, ii), untreated bacteria, which typically take the form of elongated cells, have a firm surface and a swollen appearance, and show an external membrane with a visible texture and surface, with multiple exocellular appendages forming a complex biofilm. In the presence of **6.8**, at a concentration corresponding to 0.5 time their MIC, the appearance and distribution of bacteria after 12 and 24 hours change drastically (Figure 6.4 iii and iv). The size and the diameter of the bacteria are reduced, and concave collapses in the membrane can be observed while a large amount of debris, presumably the cell contents, are present around the few intact bacteria (Figure 6.4 iii, arrows in Figure 6.4 iv). This suggests that compound **6.8** provokes the leakage of the bacterial content to the extracellular area. It can also be observed that the surface of the bacteria is less well defined and a modification of the contour and the texture can be observed. The dose-dependent damage of the bacteria was confirmed with samples treated with higher concentrations of **6.8**, corresponding to the MIC (with respect to inoculums concentration), as more accentuated

morphology changes were observed after 12 h and 24 h (Figure 6.4 v, arrows in Figure 6.4 vi).
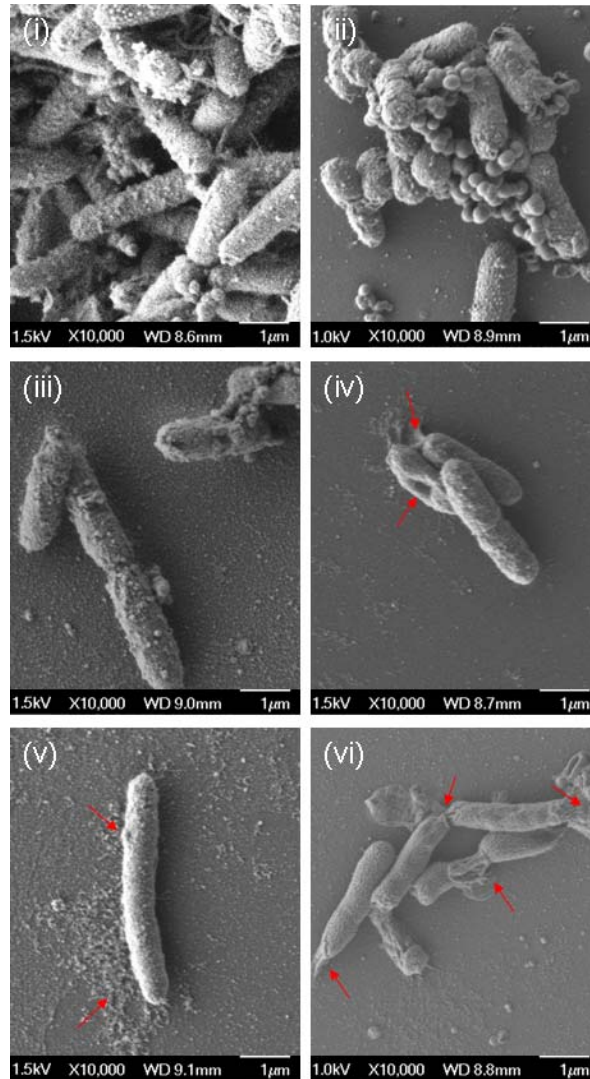
Figure 6.4.   Change of the cell morphology and membrane damage by field emission scanning electron microscope. *E. coli* (*SK037*) after 12 h (i) and 24 h (ii) (control). Treatment with **6.8** at a 0.5xMIC concentration after 12 h (iii) and 24 h (iv). Treatment with **6.8** at the MIC concentration after 12 h (v) and 24 h (vi).

6.2.3. Conclusion

In conclusion, we present here a class of small synthetic antimicrobial molecules, containing in their structure a benzimidazolium unit, and which are able to mimic the natural process of the anionic transport through both transmembrane channel and simultaneous mobile carrier mechanisms, depending on the nature of their counter-anion. Among the benzimidazolium salts studied here, we identified compound **6.8**, which presents interesting antibacterial properties as a result of its ability to induce an electrolytic imbalance and to disrupt the integrity and the potential of the bacterial membranes. At the same time this compound presents a low toxicity to human cells in bacteriostatic range concentrations, representing a new potential antimicrobial agent and an interesting paradigm that could be further optimized for therapeutic purposes.

6.2.4. Experimental section

General Procedures. All chemicals were purchased from Aldrich Chemicals in their highest purity and used without further purification. Methanol-d_4, dimethyl sulfoxide-d_6 or chloroform-d_3 were also purchased from Aldrich Chemicals. All solvents were purchased from EDM and liquid reagents were degassed by bubbling nitrogen for 15 min before each use. NMR experiments were recorded on Bruker Avance spectrometers at 400 MHz or 300 MHz. All NMR experiments were obtained by the use of the sequence commercially available on Bruker spectrometer. Coupling constants are given in Hertz (Hz) and chemical shifts are given in ppm (δ) measured relative to residual solvent. Data are reported as follows: chemical shift, multiplicity (br = broad, s = singlet, d = doublet, t = triplet, q = quartet, quin = quintuplet, m = multiplet). Mass spectra analyses were obtained at the Université de Montréal Mass Spectrometry Facility and were recorded on a Mass spectrometer LC-LCQ Advantage (Ion trap) Thermo Scientific with ESI ionization source (direct injection), a mass spectrometer LC-TOF Agilent Technologies with ESI ionization source (direct injection) and on a mass spectrometer LC-MS Thermo Scientific. The purity of the compounds was determined by high performance liquid chromatography (HPLC). Purity of all final compounds was 95% or

higher. The instrument was a Thermo Scientific system, on a Kinetex C8 (Phenomenex), 2.6 μm particle size (50 mm × 3.0 mm), eluent A: H_2O + 0.1% formic acid and eluent B: MeOH. The gradient started at 50% B and 95% B was reached in 7 minutes, kept for 1 minute at 95% B and go back to 50% within 0.5 min, for a total analysis time of 12 minutes. The flow rate was 0.35 mL/min and the detection performed at 300 nm. Fluorimetric studies were performed on a Varian Cary Eclipse Fluorescence spectrophotometer equipped with a temperature controller. The antimicrobial and haemolytic assays were performed on a Fluostar Optima plate reader. The *E. coli* (*DH5α* and *SK037*) and Baccilus thuringiensis (*HD73*) strains were provided by prof. J. Pelletier, Chemistry Department, Université de Montréal.

2,6-bis(1H-benzo[d]imidazol-1-yl)pyridine: Under nitrogen atmosphere, to a suspension of 1.5 g (13 mmoles) of benzimidazole and 0.43 g (18 mmoles) of NaH in DMF (anh), 1.5 g (6.3 mmoles) of dibromopyridine solution in DMF (anh) are added and the mixture is heated under reflux for 72 h. Then the mixture is cooled to room temperature and 100 mL of distilled water is added to the solution. The residue obtained is filtered and washed with isopropanol. The crude product is dried in an oven to obtain 0.77 g (Yield 40%) of an orange solid. ESI-MS: m/z [M+H]+ (C19H6N5)+ calc.311.3, found 312.3. ^{1}H NMR (400 MHz, Methanol-d4) δ ppm = 8.99 (s, 2 H), 8.32 (t, J=8.2 Hz, 1 H), 8.28-8.26 (m, 2 H), 7.91 (d, J=8 Hz, 2 H), 7.63-7.61 (m, 2 H), 7.45-7.43 (m, 4 H).

1,1'-(pyridine-2,6-diyl)bis(3-(4-(phenylethynyl)benzyl)-1H-benzo[d]imidazol-3-ium) dibromide (6.3): 0.1935 g (0.623 mmoles) of 2,6-bis(1H-benzo[d]imidazol-1-yl)pyridine and 0.3551 g (1.31 mmoles) of (4-phenylethynyl)benzyl bromide are dissolved in 30 mL of ACN. The mixture is stirred under reflux for 72 h and the resulting precipitate is filtered, washed with 10 mL of ACN and dried in vacuuo. 0.32 g (61% Rdt) of a white powder was obtained. ESI-MS: m/z [M-H]+ (C49H34N5)+ calc. : 692.3, found : 692.3. ^{1}H NMR (400 MHz, Methanol-d4) δ ppm = 8.73 (t, *J*=8 Hz, 1 H), 8.52-8.50 (m, 2 H), 8.40 (d, *J*=8 Hz, 2 H), 8.05-8.04 (m, 2 H), 7.82-7.80 (m, 4 H), 7.66-7.65 (m, 8H), 7.51 (m, 4H), 7.40-7.39 (m, 6H), 6.02 (s, 4H). ^{13}C NMR (75 MHz, Dimethyl sulfoxide-d6): δ ppm = 143.50, 138.25, 134.83, 132.40, 131.67, 131.86, 131.60, 129.46,

129.26, 129.19, 127.35, 123.17, 122.45, 122.08, 117.82, 114.57, 114.47, 113.56, 90.56, 89.14, 50.23.

1,1'-(pyridine-2,6-diyl)bis(3-(4-(phenylethynyl)benzyl)-1H-benzo[d]imidazol-3-ium) bis(trifluoromethane)sulfonimide (6.4): 100 mg (0.12 mmoles) of **6.3** are dissolved in a mixture of MeOH/ACN (50 :50). Then, 258 mg (0.90 mmoles) of LiNTf$_2$ are added to 10 mL of methanol before being poured onto the solution containing the imidazolium salt. The resulting mixture is then brought to 85 °C and stirred with a magnetic stir bar during 12 hours. After evaporating the solvent under reduced pressure, 40 mL of distilled water are added to the powder obtained. The mixture is heated to 100 ºC for 12 hours under magnetic stirring, and then filtered on a fritted glass. The raw product is then dried in an oven, in order to obtain 96 mg of a white powder (95% yield). ESI-MS: m/z [M]$^-$ (C$_2$F$_6$NO$_4$S$_2$)$^-$ calculated : 280.1, founded : 280.0. ^{1}H NMR (400 MHz, Chloroform-d$_3$) δ ppm = 10.23 (s, 2 H), 8.55 (s, 1 H), 8.21 (q, J=8 Hz, 4 H), 7.77 (t, J=8 Hz, 2 H), 7.67-7.52 (m, 15 H), 7.37-7.36 (m, 5 H), 7.18 (s, 4 H), 5.81 (s, 4 H). ^{13}C NMR (75 MHz, Dimethyl sulfoxide-d$_6$): δ ppm = 146.89, 145.04, 145.00, 134.30, 132.35, 131.89, 130.29, 129.49, 129.38, 129.27, 128.54, 128.04, 126.33, 122.43, 122.07, 118.53, 117.80, 116.45, 113.53, 90.82, 89.12, 50.77.

1,1'-(pyridine-2,6-diyl)bis(3-(4-(phenylethynyl)benzyl)-1H-benzo[d]imidazol-3-ium) bis(trifluoromethane)sulfonate (6.5): 200 mg (0.23 mmoles) of **6.3** are dissolved in a mixture of MeOH/ACN (50 :50). Then, 270 mg (1.76 mmoles) of LiOTf are added to 10 mL of methanol before being poured onto the solution containing the imidazolium salt. The resulting mixture is then brought to 85 °C and stirred with a magnetic stir bar during 12 hours. After evaporating the solvent under reduced pressure, 40 mL of distilled water are added to the powder obtained. The mixture is heated to 100ºC for 12 hours under magnetic stirring, and then filtered on a fritted glass. The raw product is then dried in an oven, in order to obtain 220 mg of a rosy brown powder (96% yield). ESI-MS: m/z [M]$^-$ (CF$_3$O$_3$S)$^-$ calculated : 149.6, found : 149.0. ^{1}H NMR (400 MHz, Methanol-d$_4$) δ ppm = 8.72 (t, J=8 Hz, 1 H), 8.52 (s, 2 H), 8.39 (d, J=8 Hz, 2 H), 8.03 (s, 2 H), 7.80 (s, 4 H), 7.64 (s, 8H), 7.52 (s, 4H), 7.49 (m, 8H), 6.00 (s, 4H). ^{13}C

NMR (75 MHz, Dimethyl sulfoxide-d$_6$) δ ppm = 146.88, 145.01, 143.94, 134.31, 132.36, 131.88, 131.69, 130.30, 129.50, 129.39, 129.28, 129.54, 128.05, 123.30, 122.43, 118.99, 118.54, 116.47, 114.87, 90.62, 89.15, 50.77.

2,6-bis((1H-benzo[d]imidazol-1-yl)methyl)pyridine: To a suspension of 0.44 g (3.76 mmoles) of benzimidazole and 0.84 g (15.0 mmoles) of KOH in water 0.0417 g (0.13 mmoles) of TBAB solution in toluene are added and the mixture is stirred vigorously before adding 0.5 g (1.88 mmoles) of 2,6-dibromomethylpyridine. Then the mixture is left to room temperature overnight before evaporate toluene. Then 100 mL of water is added to the residue before stirring 5 more minutes, then filtered and washed with water. The crude product is dried in an oven to obtain 0.905 g (71% yield) of an white solid. ^{1}H NMR (400 MHz, Methanol-d$_4$) δ ppm = 8.35 (s, 2 H), 7.74 (t, J=8 Hz, 1 H), 7.66 (d, *J*=8 Hz, 2 H), 7.40 (d, *J*=8 Hz, 2 H), 7.20 - 7.11 (m, 6 H), 5.55 (s, 4 H).

1,1'-(pyridine-2,6-diylbis(methylene))bis(3-(4-(phenylethynyl)benzyl)-1H-benzo[d]imidazol-3-ium) dibromide (6.6) : 0.50 g (1.47 mmoles) of 2,6-bis(1H-benzo[d]imidazol-1-yl)pyridine and 0.879 g (3.24 mmoles) of (4-phenylethynyl)benzyl bromide are dissolved in 30 mL of ACN. The mixture is stirred under reflux for 72 h and the resulting precipitate is filtered, washed with 10 mL of ACN, and dried in vacuo. 0.91 g (86% Rdt) of a white powder was obtained. ESI-MS: m/z [M-H]$^+$ (C$_{51}$H$_{38}$N$_5$)$^+$ calc. 721.4, found 720.3. ^{1}H NMR (400 MHz, Methanol-d$_4$) δ ppm 8.01 (t, *J*=8 Hz, 1 H), 7.86 (d, *J*=8 Hz, 2 H), 7.66 – 7.36 (m, 26 H), 5.82 (s, 4 H), 5.65 (s, 4 H). ^{13}C NMR (75 MHz, Dimethyl sulfoxide-d$_6$) δ ppm = 153.57, 143.55, 139.40, 134.95, 132.34, 131.86, 131.69, 130.89, 129.46, 129.27, 129.17, 129.17, 127.03, 123.12, 123.08, 122.41, 114.33, 114.16, 90.54, 89.13, 51.26, 50.00.

1,1'-(pyridine-2,6-diylbis(methylene))bis(3-(4-(phenylethynyl)benzyl)-1H-benzo[d]imidazol-3-ium) bis(trifluoromethane)sulfonimide (6.7) : 0.712 g (0.82 mmoles) of **6.6** are dissolved in a mixture of MeOH/ACN (50 :50). Then, 1.76 g (6.11 mmoles) of LiNTf$_2$ are added to 10 mL of methanol before being poured onto the solution containing the imidazolium salt. The resulting mixture is then brought to 85 °C

and stirred with a magnetic stir bar during 12 hours. After evaporating the solvent under reduced pressure, 40 mL of distilled water are added to the powder obtained. The mixture is heated to 100ºC for 12 hours under magnetic stirring, and then filtered on a fritted glass. The raw product is then dried in an oven, in order to obtain 0.94 g of a white powder (90% yield). ESI-MS: m/z [M]-$(C_2F_6NO_4S_2)^-$ calc. 280.1, found 280.0. ^{1}H NMR (400 MHz, Methanol-d^4) δ ppm 8.01 (t, J=8 Hz, 1 H), 7.85 (d, J=8 Hz, 2 H), 7.64 – 7.38 (m, 28 H), 5.82 (s, 4 H), 5.65 (s, 4 H). ^{13}C NMR (75 MHz, Dimethyl sulfoxide-d$_6$): δ ppm = 153.61, 143.61, 139.43, 134.77, 132.39, 131.84, 130.98, 129.25, 129.04, 127.21, 127.05, 123.20, 123.01, 122.41, 122.08, 117.81, 114.24, 114.11, 113.55, 90.59, 89.05, 51.35, 50.08.

1,1'-(pyridine-2,6-diylbis(methylene))bis(3-(4-(phenylethynyl)benzyl)-1H benzo[d]imidazol-3-ium) bis(trifluoromethane)sulfonate (6.8) : 100 mg (0.12 mmoles) of **6.6** are dissolved in a mixture of MeOH/ACN (50 :50). Then, 140 mg (0.90 mmoles) of LiOTf are added to 10 mL of methanol before being poured onto the solution containing the imidazolium salt. The resulting mixture is then brought to 85 °C and stirred with a magnetic stir bar during 12 hours. After evaporating the solvent under reduced pressure, 40 mL of distilled water are added to the powder obtained. The mixture is heated to 100 ºC for 12 hours under magnetic stirring, and then filtered on a fritted glass. The raw product is then dried in an oven, in order to obtain 0.90 g of a white powder (76% yield). ESI-MS: m/z [M]- $(CF_3O_3S)^-$ calc. 149.6, found 149.0. ^{1}H NMR (400 MHz, Methanol-d$_4$) δ ppm = 8.02 (t, J=8 Hz, 1 H), 7.88-7.86 (m, 2H), 7.66-7.63 (m, 4 H), 7.50-7.46 (m, 10 H), 7.40-7.37 (m, 8 H), 5.82 (s, 4H), 5.67 (s, 4H). ^{13}C NMR (75 MHz, Dimethylsulfoxide-d$_6$): δ 153.60, 143.59, 139.45, 134.80, 132.40, 131.85, 131.77, 130.95, 129.27, 129.05, 127.22, 127.06, 123.27, 123.17, 123.02, 122.40, 119.00, 114.25, 114.12, 90.59, 89.07, 51.33, 50.06.

Preparation of EYPC large unilamellar vesicles (LUVs) for lucigenin based assays. A lipid film is formed by evaporating a chloroform solution containing 50 mg of EYPC under reduced pressure at 25 °C. The lipid film is then dried in vacuo at room temperature for at least 2 hours. The lipid film is then hydrated with 1 mL of a 2 mM

lucigenin solution containing NaCl (100 mM), and sodium phosphate salt (10 mM, pH = 6.4). The obtained suspension is subjected to 20 freeze/thaw cycles (1 cycle = 1 minute at -20°C followed by 1 minute at 37 °C). The mixture is vortexed for 1 minute after every cycle to help the hydration. The solution is then extruded through a 100 nm cylindrical pores polycarbonate membrane 21 times until the solution is transparent and passed down a Sephadex G-25 column to remove extravesicular lucigenin dye. The eluant is a solution containing 100 mM of NaCl and 10 mM of sodium phosphate salt. 10.4 mL of liposome suspension is isolated after gel filtration. The stock solution is 6.25 mM in lipid, assuming all EYPC is incorporated into the liposomes.

Preparation of DPPC large unilamellar vesicles (LUVs) for lucigenin based assays. A lipid film is formed by evaporating a chloroform solution containing 50 mg of DPPC under reduced pressure at 25 °C. The lipid film is then dried under vacuum at 45 ºC for at least 2 hours. The lipid film is then hydrated with 1 mL of a 2 mM lucigenin solution containing NaCl (100 mM), and sodium phosophate salt (10 mM, pH = 6.4). The obtained suspension is subjected to 15 freeze/thaw cycles (1 cycle = 1 minute at -4 °C followed by 1 minute at 45 ºC). The mixture is vortexed for 1 minute after every cycle to help the hydration. The solution is then extruded through a 100 nm cylindrical pores polycarbonate membrane 21 times at temperature between 45-55 ºC (fluid state lipid) until the solution is transparent and passed down a Sephadex G-25 column to remove extravesicular lucigenin dye. The eluant is a solution containing 100 mM of NaCl and 10 mM of sodium phosphate salt. 10.4 mL of liposome suspension were isolated after gel filtration. The stock solution was 6.25 mM in lipid, assuming all DPPC is incorporated into the liposomes. A small aliquot of liposomes suspension was taken from time to time, in order to verify the DPPC concentration by Stewart *et al.* method.[29]

Chloride transport assays with DPPC and EYPC LUVs. A 20 μL aliquot of the stock solution of DPPC LUVs is added to a 2.5 mL gently stirred thermostated buffer solution containing 10 mM sodium phosphate salt (pH = 6.4), and 100 mM NaCl. The lucigenin fluorescence was monitored by excitation at λex = 372 nm and the emission is recorded at λem = 503 nm. At t = 50 s, 100 μL of solution of transporter in MeOH is

added to give a solution of 10 mol.% (relative to lipids) in benzimidazolium. Finally at t = 300 s, 100 μL of a Triton-X 1% solution is added in order to lyse the liposomes. The temperature is set to 35 °C, 40 °C and 45 °C. For assays in EYPC liposomes, at t = 50 s of the experiment, 100 μL of solution of transporter at different concentrations in MeOH is added. Finally at t = 300 s, 100 μL of a Triton-X 1% solution is added in order to lyse the liposomes. The temperature is set to 37 °C. Experiments are repeated in triplicate and all traces reported are the average of the three trials.

U-tube experiment. In the U-shaped glass tube experiment the lipid bilayer is mimicked by chloroform, a dense hydrophobic solvent. We assume that the formation of an ion channel is virtually impossible in such conditions. The organic phase consists of 10 mL chlorofom and contained 1 mM of ionophore. A control experiment is performed with neat chloroform. 5 ml of aqueous lucigenin solution (0.1 mM) and water are placed in each arm of the U-tube, as donating and receiving aqueous phase respectively. Lucigenin (bis-*N*-methylacridinium nitrate) present initially in the donating phase should pass through the bulky hydrophobic chloroform phase paired to the nitrate anions, transported by a mobile carrier, in order to reach the receiving phase. The increase of lucigenin's concentration in the receiving phase is monitored by fluorimetry. The experiments is conducted at room temperature and the lucigenin's fluorescence is monitored by excitation at λex = 372 nm and the emission was recorded at λem = 503 nm.

Minimal inhibitory concentration (MIC) determination. 5 mL of lysogeny broth (LB) medium is inoculated with *E. coli* (*DH5α* and *SK037* strains) or Bacillus thuringiensis (*HD73* strain). The precultures is grown overnight at 37 °C under stirring, and resuspended in 75 mL of a fresh LB medium. The cultures are grown at 37 °C until the optical density (O.D.$_{600}$) = 0.5 and then rediluted in fresh LB medium until O.D.$_{600}$ = 0.1. Assays are performed in 96-well culture plates. Each well is filled with 185 μL bacterial culture, 10 μL MiliQ water and 5 μL DMSO or compounds in DMSO solution, as the final volume in each well is 200 μL and the concentration in DMSO max 2.5 % (v/v). The plates are stirred in an thermostated incubator at 37°C and the optical density (O.D.$_{600}$) is monitored at t = 0 h, 4 h, 8 h and 24 h. Every experiment is performed in

triplicates in independent bacterial cultures. The MICs are determined as the minimal concentration at which no bacterial growth was detected.

Measurement of haemolytic activity. Haemolytic activity is tested against erythrocytes from human blood. Fresh human red blood cells (blood type O) are centrifuged for 10 minutes at 1000 rpm, then washed three times with PBS buffer and diluted to a concentration of 2% (v/v) in PBS buffer. 10 µL of two-fold serial dilutions of compounds **6.6**, **6.7** and **6.8** in DMSO are added to 96-well plates, after which 190 µL of erythrocyte suspension are added. After 1 or 24 h of incubation at 37 °C with gentle shaking, the plates are centrifuged for 10 minutes at 2000xg. 50 µL of supernatant of each well are transferred to a fresh plate and the release of hemoglobin is monitored by measuring the absorbance at 405 nm. The values for 0% and 100% hemolysis are determined by incubating erythrocytes with PBS or with 0.5% (v/v) Triton X-100. The hemolysis percentage is calculated using the following equation:

$$\text{Hemolysis (\%)} = \frac{A - A_0}{A_{100} - A_0} \times 100$$

where A is the absorbance of supernatant **6.6**, **6.7** and **6.8** solutions, A_0 is the absorbance of supernatant with PBS and A_{100} is the absorbance of supernatant with 0.5% Triton X-100. Data are the mean of three separate experiments.

Membrane depolarization with Gram-negative strain. Preparation of bacterial suspensions is the same as in the anti-bacterial activity assay for *E. coli* (*SK037*). Bacterial cultures are grown overnight in LB broth at 37 °C. Cells are harvested by centrifugation three times at 500xg and washed in a buffer containing 20 mM glucose and 5 mM HEPES (pH 7.3). Then, after the washing, pellets are resuspended in the same HEPES buffer. Fractions from each cell suspension are diluted into a cuvette to an optical density (O.D.$_{600}$) of 0.15 along with the dye diSC$_2$5 at a final concentration of 1 µM in the buffer. The mixture is allowed to equilibrate for 1 h to a stable baseline at 37 °C. The diSC$_2$5 fluorescence is monitored by excitation at λex = 600 nm and the emission is recorded at λem = 660 nm. Samples are stirred during the measurement at a constant

temperature of 37 ºC. At t = 50 s, 63 µL of solution of transporter in DMSO is added to a 2.5 mL of suspension to give a solution of 1 mM in **6.2** or 0.4 mM in **6.6**, **6.7** and **6.8**.

Field emission SEM. Preparation of bacterial suspensions is the same as in the anti-bacterial activity assay with *E. coli (SK037)*. Cell suspensions are centrifuged, washed three times and re-suspended in the same volume of 10 mM of PBS (pH 7.4). Fractions from each cell suspension are diluted to an optical density (O.D.$_{600}$) of 1.20. Subsequently, 1 mL cell suspensions (9 x 10^8 colony-forming units per mL, CFU/mL) are transferred along with 10 µL of solution of transporter in DMSO to give solutions of 0.04 mM and 0.08 mM in **6.8** to poly-lysine-coated glass slides previously placed in the wells of polystyrene culture dishes. The plates are kept at 37 ºC for 12 h or 24 h to allow the adhesion of treated *E. coli* cells to the glass slides. After required time, slide-immobilized cells are washed with PBS three times, then fixed with 2.5% (v ∕ v) glutaraldehyde in 10 mM PBS, washed three times with the same buffer and stained with 1% (v∕v) OsO$_4$ in 10 mM PBS. Samples are then dehydrated with a graded ethanol series. After critical-point drying and carbon coating, the samples are observed with a JEOL JSM-7400F field emission microscope SEM (JEOL Ltd, Tokyo, Japan).

ASSOCIATED CONTENT

Supporting Information. Synthetic details, NMR and MS spectra for all compounds, anion transport assay, U-tube experiment, antibacterial assay, measurement of haemolytic activity, membrane depolarization assay and crystallographic data tables. This material is available free of charge via the Internet at http://pubs.acs.org.

AUTHOR INFORMATION

Corresponding Author

* Email: ar. schmitzer@umontreal.ca

Author Contributions

The manuscript was written through contributions of all authors. All authors have given approval to the final version of the manuscript.

6.2.5.   Aknowledgment

6.2.6.   Abbreviations

ACN, acetonitrile; AMP, antimicrobial peptide; anh, anhydrous; diSC$_2$5, 3,3′-diethylthiadicarbocyanine iodide; DPPC, 1,2-dipalmitoyl-sn-glycero-3-phosphocholine; EYPC, egg yolk phosphatidylcholine; LC-LCQ, liquid chromatography quadrupole; LC-TOF, liquid chromatography-time of flight; MeOH, methanol; mol. %, mole percentage; mV, milivolt; NTf$_2$, bis(trifluoromethanesulfonimide); OTf, trifluoromethanesulfonate.

6.2.7.   References

1. a) Busschaert, N., Gale, P. A., *Angew. Chem. Int. Ed.* **2013**, *52*, 1374. b) Haynes, C. J. E., Gale, P. A., *Chem. Comm.* **2011**, *47*, 8203. c) Davis, J. T., Okunola, O., Quesada, R., *Chem. Soc. Rev.* **2010**, *39*, 3843. d) Davis, A. P., Sheppard, D. N., Smith, B. D. *Chem. Soc. Rev.* **2007**, *36*, 348. e) Gale, P. A., Pérez-Tomás, R., Quesada, R., *Acc. Chem. Res.* **2013**, *46*, 2801.

2. Sessler, J. L., Allen, W. E., *CHEMTECH* **1999**, *9*, 16.

3. Boudreault, P.-L., Arseneault, M., Otis, F., Voyer, N., *Chem. Comm.* **2008**, 2118.

4. Davis, J. T., Gale, P. A., Okunola, O. A., Prados, P., Iglesias-Sánchez, J. C., Torroba, T., Quesada, R., *Nat. Chem.* **2009**, *1*, 138.

5. Hernandez, P. I., Moreno, D., Javier, A. A., Torroba, T., Perez-Tomas, R., Quesada, R., *Chem. Comm.* **2012**, *48*, 1556.

6. LeDell, K., Muto, C. A., Jarvis, W. R., Farr, B. M., *Infect. Contr. Hosp. Epidemiol.* **2003**, *24*, 639.

7. a) Boman, H. G., *Annu. Rev. Immunol.* **1995**, *13*, 61. b) Zasloff, M., *Nature* **2002**, *415*, 389.

8. a) Brogden, N. K., Brogden, K. A., *Int. J. Antimicrob. Agents* **2011**, *38*, 217. b) Gindri, I. M., Siddiqui, D. A., Bhardwaj, P., Rodriguez, L. C., Palmer, K. L., Frizzo, C. P., Martins, M. A. P., Rodrigues, D. C. D. *RSC Adv.* **2014**, *4*, 62594. c) Garcia-Lorenzo, A., Tojo, E., Tojo, J., Teijeira, M., Rodriguez-Berrocal, F. J., Gonzalez, P., Martinez-Zorzano, V. S., *Green Chem*, **2008**, *10*, 508.

9. Elie, C.-R., Noujeim, N., Pardin, C., Schmitzer, A. R., *Chem. Comm.* **2011**, *47*, 1788.

10. Elie, C.-R., Charbonneau, M., Schmitzer, A. R., *Med. Chem. Comm.* **2012**, *3*, 1231.

11. Davis, A. P., Sheppard, D. N., Smith, B. D., *Chem. Soc. Rev.* **2007**, *36*, 348.

12. Sidorov, V., Kotch, F. W., Kuebler, J. L., Lam, Y.-F., Davis, J. T., *J. Am. Chem. Soc.* **2003**, *125*, 2840.

13. Harrell, J. W. A., Bergmeyer, M. L., Zavalij, P. Y., Davis, J. T., *Chem. Comm.* **2010**, *46*, 3950.

14. McNally, B. A., Koulov, A. V., Smith, B. D., Joos, J.-B., Davis, A. P., *Chem. Comm.* **2005**, 1087.

15. a) Koulov, A. V., Lambert, T. N., Shukla, R., Jain, M., Boon, J. M., Smith, B. D., Li, H., Sheppard, D. N., Joos, J.-B., Clare, J. P., Davis, A. P., *Angew. Chem. Int. Ed.* **2003**, *42*, 4931. b) Krasne, S., Eisenman, G., Szabo, G. Freezing and melting of lipid bilayers and the mode of action of nonactin, valinomycin, and gramicidin. *Science* **1971**, *174*, 412. c) Elie, C.-R., Hebert, A., Charbonneau, M., Haiun, A., Schmitzer, A. R., *Org. Biomol. Chem.* **2013**, *11*, 923.

16. Yamnitz, C. R., Negin, S., Carasel, I. A., Winter, R. K., Gokel, G. W., *Chem. Comm.* **2010**, *46*, 2838.

17. a) Litvinchuk, S., Bollot, G., Mareda, J., Som, A., Ronan, D., Shah, M. R., Perrottet, P., Sakai, N., Matile, S., *J. Am. Chem. Soc.* **2004**, *126*, 10067. b) Bhosale, S., Matile, S., *Chirality* **2006**, *18*, 849. c) Mora, F., Tran, D.-H., Oudry, N., Hopfgartner, G., Jeannerat, D., Sakai, N., Matile, S., *Chem. Eur. J.* **2008**, *14*, 1947. d) Hennig, A., Fischer, L., Guichard, G., Matile, S., *J. Am. Chem. Soc.* **2009**, *131*, 16889. e) Butterfield, S. M., Hennig, A., Matile, S., *Org. Biomol. Chem.* **2009**, *7*, 1784. f) Rhee, J. S., Ebihara, S., Akaike, N., *J. Neurophysiol.* **1994**, *72*, 1103.

18. Gravel, J., Schmitzer, A. R., *Supramol. Chem.* **2014**, *27*, 364.

19. Aono, R., Tsukagoshi, N., Yamamoto, M., *J. Bacteriol.* **1998**, *180*, 938.

20. Goldberg, K., Sarig, H., Zaknoon, F., Epand, R. F., Epand, R. M., Mor, A., *FASEB J.* **2013**, *27*, 3818.

21. Vidal, M., Elie, C.-R., Campbell, S., Claing, A., Schmitzer, A. R., *Med. Chem. Comm.* **2014**, *5*, 436.

22. Heritage, J., Evans, E.G.V., Killington, R.A. Microbial Structure and Mode of Life., in Introductory Microbiology, Cambridge university press eds, Cambridge, **1996**

23. Martinac, B., Saimi, Y., Kung, C., *Physiol. Rev.* **2008**, *88*, 1449.

24. a) Strahl, H., Hamoen, L. W., *Proc. Nat. Ac. Sci. U.S.A* **2010**, *107*, 12281. b) Cheng, K., Haspel, H. C., Vallano, M. L., Osotimehin, B., Sonenberg, M., *J. Membr. Biol.* **1980**, *56*, 191.

25. Epand, R. F., Pollard, J. E., Wright, J. O., Savage, P. B., Epand, R. M., *Antimicrob. Agents Chemother.* **2010**, *54*, 3708.

26. Silverman, J. A., Perlmutter, N. G., Shapiro, H. M., *Antimicrob. Agents Chemother.* **2003**, *47*, 2538.

27. Livne, L., Kovachi, T., Sarig, H., Epand, R. F., Zaknoon, F., Epand, R. M., Mor, A., *Chem. Biol.* **2009**, *16*, 1250.

28. Qian, C.-D., Wu, X.-C., Teng, Y., Zhao, W.-P., Li, O., Fang, S.-G., Huang, Z.-H., Gao, H.-C., *Antimicrob. Agents Chemother.* **2012**, *56*, 1458.

29. Stewart, J. C., *Anal Biochem.* **1980,** *104*,10.

Chapitre 7   Conclusions & Perspectives

L'objectif principal du projet de recherche était d'élaborer et d'étudier les propriétés biologiques de différents sels d'imidazolium et benzimidazolium dans des matrices variées, tels que les liposomes, les bactéries et les globules rouges humains. Tout cela pour comprendre et rationaliser comment chaque partie de la molécule gouverne ses interations avec son environnement et influe son activité, aussi bien ionophore qu'antibactérienne.

Pour arriver à ces fins, trois bromures d'imidazolium ont d'abord été analysés, chacun différant de par la nature de la chaîne aromatique ou aliphatique greffée au noyau imidazolium. Il nous est apparu que l'espèce formée de deux bras aromatiques phényléthynylbenzyl, disposés symétriquement de part et d'autre d'un cation imidazolium, induisait le meilleur transport des anions chlorures, au travers d'une membrane de liposomes, à des concentrations de l'ordre du µM. Il a également été démontré qu'en présence d'un macrocycle hydrosoluble, le transporteur formait des complexes d'inclusion, permettant de moduler sa distribution dans les bicouches et donc son activité anionophore.

Par la suite, en effectuant une métathèse du contre-anion bromure en anions tétrafluoroborate (BF_4^-), hexafluorophosphate (PF_6^-) et bis(trifluoromethylsulfonyl)amide (NTf_2^-) il a été possible d'observer que l'espèce NTf_2^- conduisait à un meilleur sel d'imidazolium en terme de transport. Un mécanisme d'auto-assemblage en canaux transmembranaires, appuyé par des tests dans des liposomes de DPPC, a en outre été proposé pour expliquer la translocation des anions. À ces résultats s'est ajoutée une étude de l'efficacité du meilleur transporteur dans des liposomes de EYPC afin de dégager des paramètres cinétiques et thermodynamiques utiles en vue de comparaisons.

Dans une étude similaire, s'inscrivant dans la continuité de la précédente, une nouvelle série de sels de benzimidazolium a été analysée. Au terme des tests de transports suivis par la lucigénine dans des liposomes, il a été possible de confirmer la tendance voulant que les anions NTf_2^- soient associés à un meilleur composé anionophore. Qui plus est, en s'appuyant sur ces résultats, nous avons présenté le premier exemple, à notre connaissance, d'un transporteur d'anions et de cations, contenant le cation benzimidazolium et capable d'agir aussi bien dans des liposomes que dans des bactéries.

Ces conclusions ont ainsi ouvert la porte à des considérations antimicrobiennes pour nos sels de benzimidazolium.

Enfin la structure de nos transporteurs a été davantage modifiée en ajoutant à des espaceurs pyridine et lutidine, deux noyaux benzimidazolium flanqués de la chaîne phényléthynylbenzyl, puis en faisant varier la nature du contre-anion. L'effet de ces modifications a été évalué en mesurant l'efficacité de transport anionique de chaque composé dans des liposomes (EC_{50}), ce qui a permis de sélectionner un candidat s'étant démarqué des autres. Ce dernier fut évalué, en compagnie de ses proches analogues, pour ses propriétés de dépolarisation de la membrane bactérienne ainsi que sous microscopie électronique à balayage (SEM) afin d'observer visuellement les dommages causés à la membrane d'une souche *E. coli*. Fait plus intéressant encore, l'agent antimicrobien **6.8** le plus efficace dans des bactéries (*B. thuringiensis* et *E. coli*) a présenté une toxicité limitée de l'ordre de 10% sur les globules rouges humains à ses concentrations bactéricides. Ces observations encourageantes démontrant une ébauche de sélectivité envers les bactéries plutôt que les globules rouges humains, probablement dues à la composition différente des deux types de membranes.

À la lumière de ces dernières découvertes, le défi principal auquel fait face notre modèle est d'optimiser la sélectivité contre les microorganismes pathogènes multirésistants versus les cellules saines humaines. Des analyses sont présentement en cours afin vérifier si un mécanisme d'acquisition de résistance est dévéloppé dans des bactéries en présence de nos sels de dibenzimidazolium. Par ailleurs, il appert déjà être à notre portée de réduire davantage la toxicité de nos transporteurs en utilisant conjointement et intelligemment les différents leviers qu'offre la chimie supramoléculaire. À titre d'exemple, la formation d'un complexe d'inclusion entre un transporteur imidazolium et une cyclodextrine s'est avéré, dans le cadre de nos recherches, une stratégie efficace pour masquer transitoirement la toxicité d'un agent antibactérien, avant de restaurer son activité par l'ajout d'un compétiteur liant préférentiellement le macrocycle hydrosoluble (Figure 7.1).[1] Ce concept s'inspire d'exemples d'interrupteurs supramoléculaires que nous avions antérieurement présentés dans le groupe, afin de contrôler l'activité ionophore de sels d'imidazolium dans des liposomes (voir notamment chapitre 2).[2,3] Il est donc envisageable que cette stratégie de camouflage, à l'instar d'un

cheval de Troie, puisse également s'appliquer pour nos sels de dibenzimidazolium. En outre, l'ajout de sites de reconnaissance sur le transporteur dibenzimidazolium pourrait aussi être une alternative intéressante afin d'optimiser sa fixation à la surface des cellules malignes surexprimant des récepteurs caractéristiques, qui sont en même temps, moins abondants chez les cellules saines.
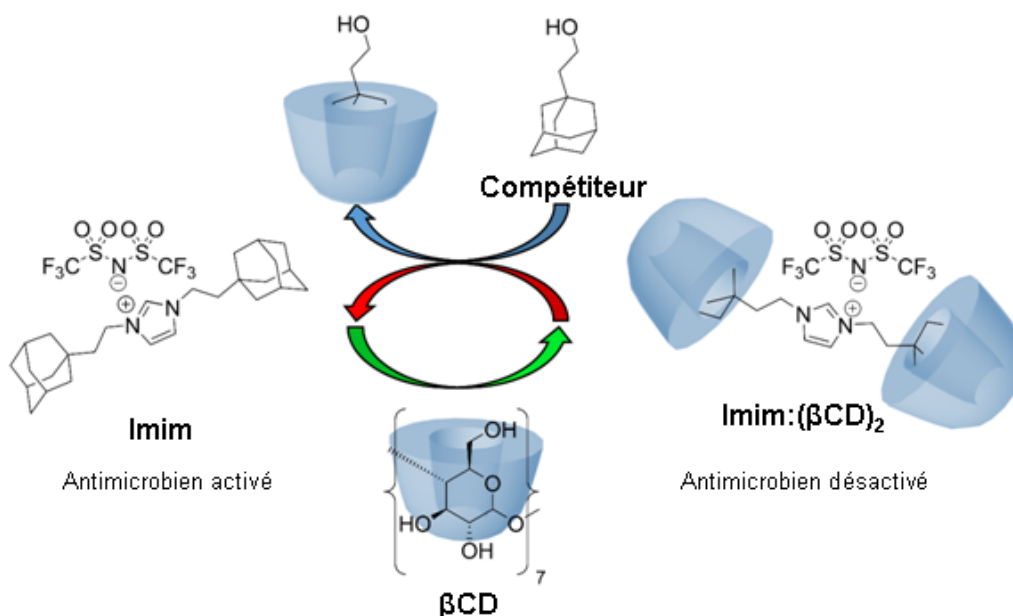

Figure 7.1. Désactivation des propriétés antibactérienne du transporteur **Imim** par la formation du complexe d'inclusion **Imim:(βCD)₂** et réactivation de son activité biologique par l'ajout du compétiteur.[1]

Nous avons enfin imaginé récemment un complexe organométallique, apparenté au meilleur agent antimicrobien présenté dans cette thèse. Ce composé qui se résume en un dibenzimidazole, avec un espaceur *o*-xylène et complexé à un atome de palladium, a démontré dans le cadre des travaux de recherche de mon collègue Mathieu Charbonneau, un potentiel en catalyse. Sachant que la littérature rapporte déjà de nombreux exemples de complexes organométalliques dotés d'un pouvoir antibactérien accru et d'une toxicité suprenamment plus basse que le ligand seul, il n'est donc pas impossible que les analogues organometalliques de nos meilleurs antimicrobiens puissent apporter un avantage en termes d'activité bactéricide et d'innocuité sur les cellules saines.
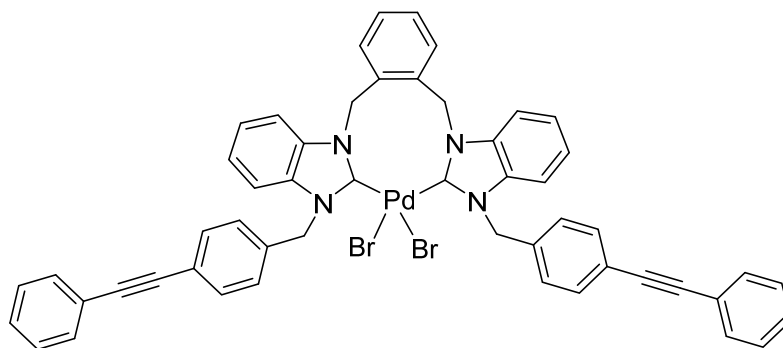
Figure 7.2.   Structure du complexe organométallique avec le palladium.

L'étude des transporteurs synthétiques d'anions, datant d'à peine quelques décennies, n'en est qu'à ses premiers balbutiements. Pourtant déjà, elle s'impose comme un domaine prometteur aux applications variées dans des champs d'expertise tels que l'organocatalyse, la signalisation cellulaire, les biosenseurs ou le transport membranaire. Notre contribution à ce vaste chantier de recherche, présenté dans cette thèse, a su mettre en lumière le grand potentiel des motifs imidazolium et benzimidazolium fonctionnalisés pour leur propriétés anionophores et antibactériennes, ce qui demeure une avancée encourageante. Toutefois, avant de pouvoir les considérer comme étant biocompatibes, nous restons conscients qu'il reste encore bien du chemin à faire pour mieux comprendre nos sels d'imidazolium et benzimidazolium, en termes de voie d'administration et mode de libération dans le corps, mais aussi d'absorption, de distribution, de métabolisme, d'élimination et de réponse sur l'ensemble de l'organisme humain. La voie vers des molécules biologiquement exploitables nécessite encore plusieurs analyses pour souhaiter qu'un jour ces dernières puissent venir renforcer l'arsenal thérapeutique.

7.1.1.   References

1. Elie, C.-R., Gravel, J., Khayat, M., Schmitzer A. R., *Med. Chem. Commun.* **2016**, *7*, 1128.
2. Elie, C.-R., Noujeim, N., Pardin, C., Schmitzer, A. R., *Chem. Commun.* **2011**, *47*, 1788.
3. Gravel, J., Kempf, J., Schmitzer, A. R. *Chem. Eur. J.* **2015**, *21*, 18642.
4. Charbonneau, M., Addoumieh, G., Oguadinma, P., Schmitzer, A. R. *Organometallics* **2014**, *33*, 6544.

Partie expérimentale

Annexe 1 : Partie expérimentale du chapitre 2, article 1 : «Uncovering new properties of imidazolium salts: Cl transport and supramolecular regulation of their transmembrane activity»

General Remarks.

4-iodobenzoïc acid, borane in tetrahydrofuran (BH$_3$ in THF), phosphorus tribromide (PBr$_3$), imidazole, methylimidazole, cucurbit[7]uril, α-cyclodextrin and Sephadex G-25 were obtained from Aldrich. Tetrahydrofuran (THF), dichloromethane (DCM), acetonitrile (CH$_3$CN), hexane and ethyl acetate (EtOAc) were purchased from EMD. ^{1}H- and ^{13}C-NMR spectra were recorded on a Bruker spectrometer at 300 and 75 MHz, respectively, in the indicated solvent. Chemical shifts are reported in ppm with internal reference to TMS. Chemical shifts are given in ppm (δ) and measured relative to residual solvent. High-resolution mass spectra (HRMS) were recorded on a TSQ Quantum Ultra (Thermo Scientific) with accurate mass options instrument (Université de Montréal Mass Spectrometry Facility). Either protonated molecular ions (M+H)$^+$ or silver adducts (M+Ag)$^+$ were used for empirical formula confirmation. L-α-phosphatidylcholine was purchased from Avanti Polar Lipids. Liposome fluorimetric assays were recorded using a Varian Cary Eclipse Fluorescence spectrophotometer. UV spectroscopy was performed using a Cary Bio 100 UV-visible spectrophotometer.

Scheme S1.1. Synthesis of transporters **2.2** and **2.3**
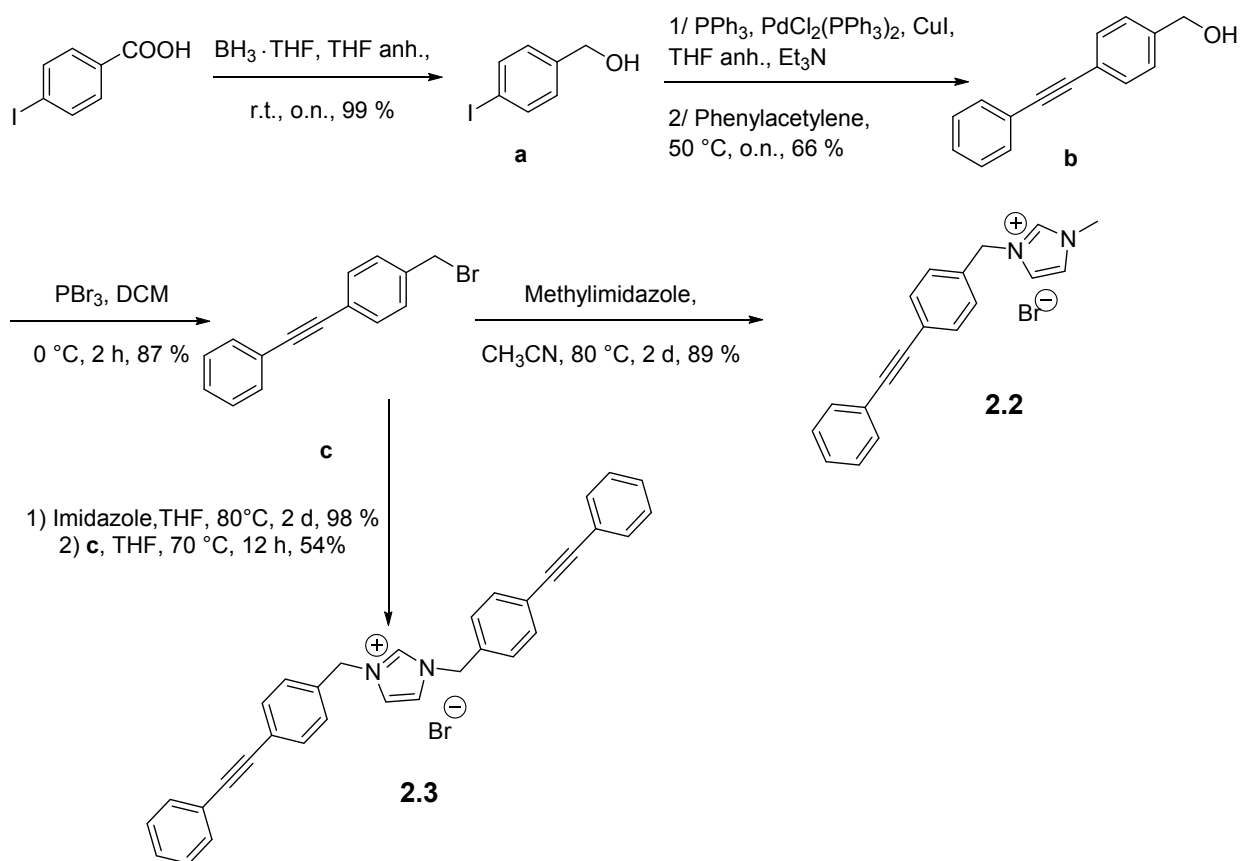
4-Iodobenzyl alcohol (a) : 4-Iodobenzoïc acid (0.02 mol) diluted in 40 mL THF was added to 40 mL of a 1.0 M solution of BH₃ in THF and the mixture was stirred overnight at room temperature. The reaction was quenched with 100 mL of a 2 N HCl solution and extracted with 3 × 140 mL of DCM. The combined organic layers were washed with 2 × 80 mL of saturated $NaHCO_3$ then 2 × 80 mL of brine and dried over $MgSO_4$. The solvent was removed under reduced pressure to give the pure product as a white solid in a 99 % isolated yield. Mp 68 – 70 °C. ¹H NMR (300 MHz, CDCl₃) δ 7.65 (d, 2H, J = 8.2 Hz), 7.06 (d, 2H, J = 8.0 Hz), 4.58 (s, 2H), 2.04 (b, 1H). ¹³C NMR (75 MHz, CDCl₃) δ 140.3, 137.4, 128.7, 92.9, 64.4. HRMS (ESI) calcd for $C_7H_7AgIO^+$ [M+Ag]⁺: 340.8587, found 340.8591.

(4-Phenylethynyl)benzyl alcohol (b) : To a carefully degassed solution of **a** (4.3 mmol), PPh₃ (0.085 mmol) and PdCl₂(PPh₃)₂ (0.026 mmol) in 10 mL of dry THF and 5 mL of

dry triethylamine was added CuI (0.085 mmol). The mixture was degassed for 5 min and a solution of phenylacetylene (4.3 mmol) in 2 mL of dry THF was added dropwise. The reaction was stirred overnight at 50 °C under nitrogen atmosphere. The mixture was added to 50 mL of ice water and the organic phase was recovered, dried over $MgSO_4$. The solvent was removed under reduced pressure to give the pure product as a white solid in 66 % isolated yield. Mp. 118 – 120 °C. ^{1}H NMR (300 MHz, $CDCl_3$) δ 7.54-7.50 (m, 4H), 7.37-7.24 (m, 5H), 4.66 (s, 2H), 2.00 (b, 1H). ^{13}C NMR (75 MHz, $CDCl_3$) δ 140.9, 131.7, 131.5, 128.3, 128.2, 126.7, 123.1, 122.3, 89.3, 89.1, 64.8. HRMS (ESI) calcd for $C_{15}H_{13}O^+$ $[M+H]^+$: 209.0961, found 209.0969.

(4-Phenylethynyl)benzyl bromide (c) : (4-Phenylethynyl)benzyl alcohol **b** (1.44 mmol) was dissolved in 5 mL of DCM. The mixture was kept at 0 °C and phosphorus tribromide was added dropwise. Then the mixture was stirred 2 hours at 0 °C and the solvent was removed under reduced pressure. The product was purified by flash chromatography (Hexane/EtOAc, 60:40) to afford **c** as a white solid in 87 % isolated yield. Mp 94 – 96 °C. ^{1}H NMR (300 MHz, $CDCl_3$) δ 7.54-7.48 (m, 4H), 7.37-7.24 (m, 5H), 4.48 (s, 2H). ^{13}C NMR (75 MHz, $CDCl_3$) δ 137.6, 131.9, 131.5, 129.0, 128.3, 128.2, 123.3, 122.9, 90.2, 88.8, 32.9. HRMS (ESI) calcd for $C_{15}H_{12}Br^+$ $[M+H]^+$: 271.0117, found 271.0109.

1-Methyl-3-(4-phenylethynyl)benzyl imidazolium bromide (2.2)

Methylimidazole (29 μL, 0.36 mmol) was diluted in 10 mL of acetonitrile and (4-phenylethynyl)benzyl bromide **c** (97.6 mg, 0.36 mmol) was added to the solution. The solution was stirred 48 h at 80 °C and the solvent was removed in vacuuo to yield 110 mg of compound **2.2**. Yield 86 %. ^{1}H NMR (CD_3OD, 400MHz): δ=7.66 (d, J=1.9Hz, 1H), 7.63 (s, 1H), 7.61 (d, J=8.4 Hz, 2H), 7.52-7.54 (m, 2H), 7.45 (d, J=8.4Hz, 2H), 7.38-7.42 (m, 2H), 5.46 (s, 2H), 3.96 ppm (s, 3H). ^{13}C NMR (CD_3OD, 75 MHz): δ=134.7, 132.8, 132.0, 129.2, 129.0, 125.1, 124.8, 123.5, 123.2, 53.1, 35.9 ppm. HR-MS (ESI): m/z Calcd for $C_{19}H_{17}N_2$ $[M-Br]^+$: 273.1386, found 273.1387

 (N,N'-diphenylethynylbenzyl)imidazolium bromide (2.3): 27.5 mg (0.40 mmol) of imidazole and 37.8 mg of sodium hydride (1.57 mmol) are diluted in 10 mL of THF.

After 5 minutes at room temperature, 100 mg (0.40 mmol) of (4-phenylethynyl)benzyl bromide **c** is added to the mixture. The solution is stirred at room temperature for 12 h and the solvent is removed in vacuuo. 20 mL of water and 30 mL of DCM are added to the crude product. The organic phase is separated, washed with 2 x 20 mL of water and then dried on $MgSO_4$. The solvent is removed in vacuuo to yield 100 mg of the intermediate (4-phenylethynyl)benzylimidazole. This compound is then used without further purification: 100 mg (0.47 mmol) of (4-phenylethynyl)benzylimidazole and 127 mg (0.47 mmol) of (4-phenylethynyl)benzyl bromide **c** are disolved in 10 mL of THF. The mixture is stirred 12 h at 70 °C and the resulting precipitate is filtered, washed with 10 mL of THF, and dried in vacuuo. 134 mg of **2.3** were obtained. Yield 54 %. ^{1}H NMR (CD_3OD, 400MHz): δ=7.71 (s, 2H), 7.62 (d, *J*=8.3 Hz, 4H), 7.51-7.56 (m, 4H), 7.46 (d, *J*=8.3 Hz, 4H), 7.37-7.42 (m, 6H), 7.38-7.42 (m, 2H), 5.48 ppm (s, 4H). ^{13}C NMR (CD_3OD, 75 MHz): δ=134.6, 132.8, 132.0, 129.3, 129.2, 129.0, 125.2, 123.7, 123.5, 123.2, 90.9, 88.5, 53.3 ppm. HR-MS (ESI): m/z Calcd for $C_{33}H_{25}N_2$ $[M-Br]^+$: 449.2012, found 449.2017

Preparation of liposomes for lucigenin-based assays. A stock solution of egg-yolk phosphatidylcholine (EYPC) in $CHCl_3$ (60 mg) was evaporated under reduced pressure on the water bath at *r.t.* to produce a thin film that was dried *in vaccuo* for 2 h at 35 °C. The lipid film was hydrated with 1 mL of 10 mM sodium phosphate containing 100 mM NaCl and 2 mM lucigenin. Freeze/thaw cycles were repeated at least 10 times until no solid particles were visible. The frozen solution was warmed to 30-35 °C before every freeze cycle. The mixture was placed on a vortex 3 times for 1 min to facilitate hydration. The cloudy solution was extruded with an Avanti High Pressure Mini-Extruder through a 100 nm polycarbonate membrane at least 20 times until the solution became transparent. A Sephadex G-25 column (15 cm x 1 cm) was used to remove the extravesicular dye. Each stock solution of liposomes was used that same day.

Lucigenin-based ion transport assays. A 20 µL aliquot of the stock solution of EYPC liposomes was added to a cuvette containing 2 mL of a 100 mM solution of $NaNO_3$ and 10 mM phosphate buffer to obtain a 0.25-0.3 mM solution of phospholipid. The fluorescence of intravesicular dye was monitored by excitation at 372 nm and the

emission was recorded at 503 nm. A 400 µL aliquot of a 0.25 mM solution of **2.1, 2.2** and **2.3** in MeOH was injected. At the end of the experiment, 10% aqueous Triton-X was injected to lyse the liposomes. The temperature was set to 25 $^{\circ}$C. The resulting Cl^{-} concentration gradient across the lipid membrane was relieved by compound-mediated transmembrane transport of Cl^{-} from the liposomes, resulting in the increase of lucigenin fluorescence. Experiments were repeated in triplicate and all traces reported are the average of the three trials.

Lucigenin-based ion transport assays in the presence of α-CD and CB7. Intravesicular 100 mM NaCl, 10 mM phosphate buffer, extravesicular 100 mM NaNO$_3$, 10 mM phosphate buffer (pH 6.3), 25 $^{\circ}$C. **2.3** (0.25 mM) was injected at $t = 35$ s. **2.3** + 2 eq **CB7**: 100 µL of **CB7** (2 mM) was injected at $t = 10$ s and 400 µL of **2.3** (0.25 mM) was injected at $t = 35$ s. **2.3** + 2 eq **α-CD**: 100 µL of **α-CD** (2 mM) of was injected at $t = 10$s and 400 µL of **2.3** (0.25 mM) was injected at $t = 35$ s.

Molecular modeling. All calculations were performed on a Windows® Vista platform. In order to assess the energy content for various molecules designed, semi-empirical quantum calculations were undertaken using the PM6 method in gas phase or in aqueous solution (MOPAC2009$^{\text{TM}}$, ©Stewart Computational Chemistry). Theoretical calculations were carried out at the restricted Hartree-Fock level (RHF) using the PM6 semi-empirical SCF-MO methods. All structures were optimized to a gradient inferior to 0.1 using the eigenvector following method. The MOPAC Cartesian coordinates were generated with OpenBabel 2.2.0 graphical interface (©Chris Morley) from the geometries obtained with ArgusLab UFF.
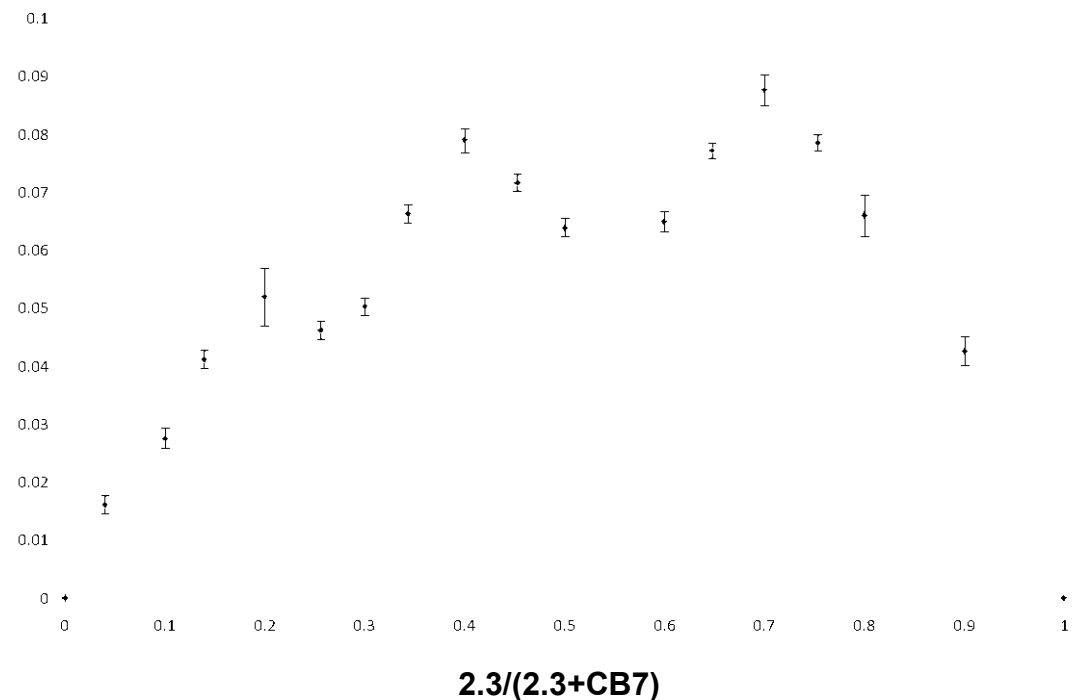
Formation of the inclusion complex of 2.3 with CB7: Job's Plot

Δ Abs

2.3/(2.3+CB7)

Figure S1.1: Continuous variation plot (Job's plot) derived from UV data for **2.3** in H$_2$O/MeOH with **CB7** at 280 nm. The UV study was made in triplicata.

Examination of the Job plot shows several slope changes, indicating the presence of multiple stoechiometry complexes. We previously observed the same behaviour of imidazolium salts when they form multiple complexes with different macrocycles (Noujeim, N., Jouvelet, B., Schmitzer, A. R., *J. Phys. Chem. B.* **2009**, *113*, 16159. Leclercq, L., Schmitzer, A. R., *J. Phys. Chem. B.* **2008**, *112*, 11064).
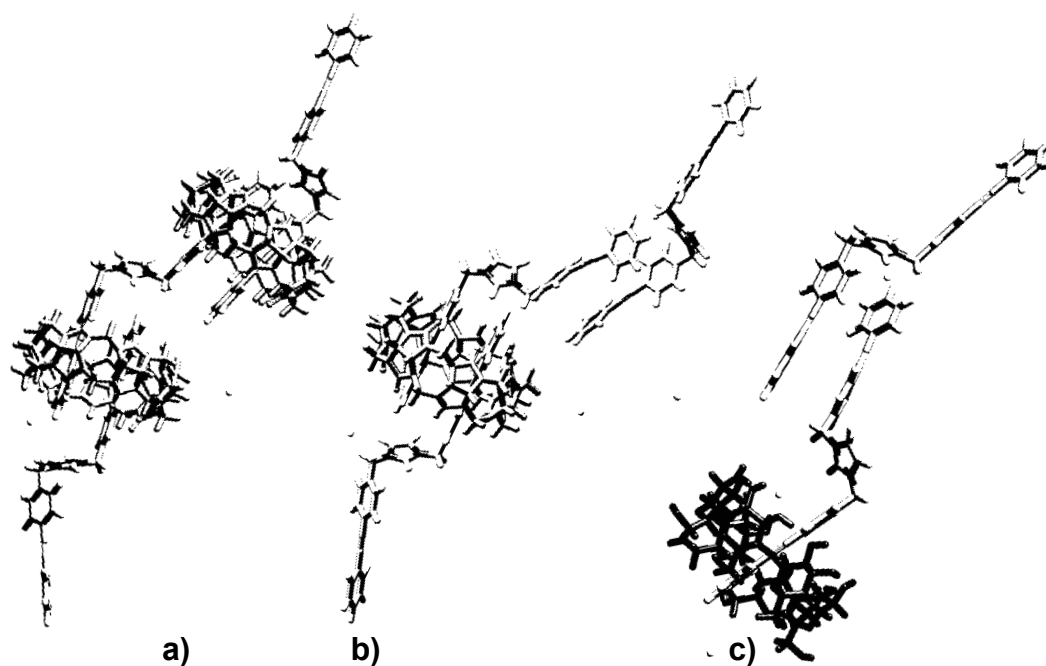
Figure S1.2: PM3 snapshots obtained by PM3 energy minimization: (*a*) **2.3** with two units **CB7** (*b*) **2.3** with **CB7**, c) **2.3** with α-**CD**
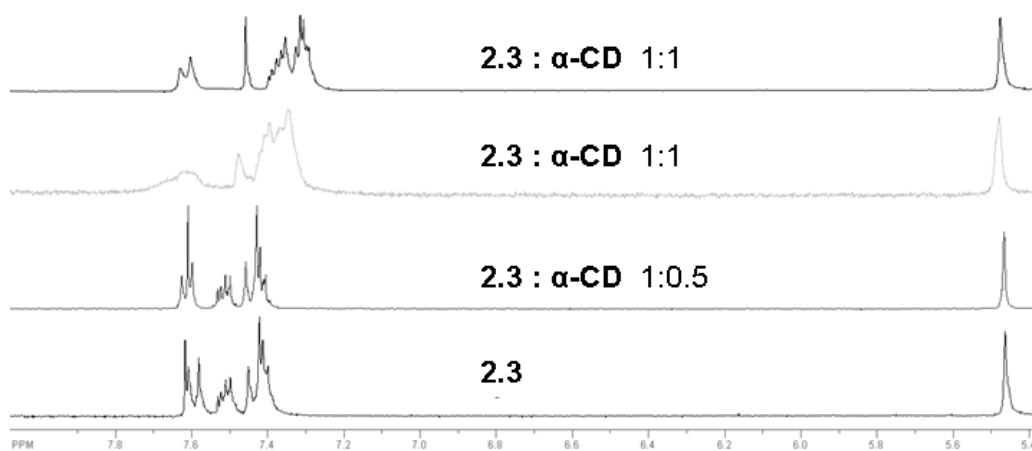

Figure S1.3: Partial NMR ^{1}H spectra of **2.3** in the presence of different amounts of α-CD in D2O/CD3OD (50/50 V/V), [**2.3**] = 0.25 mM.
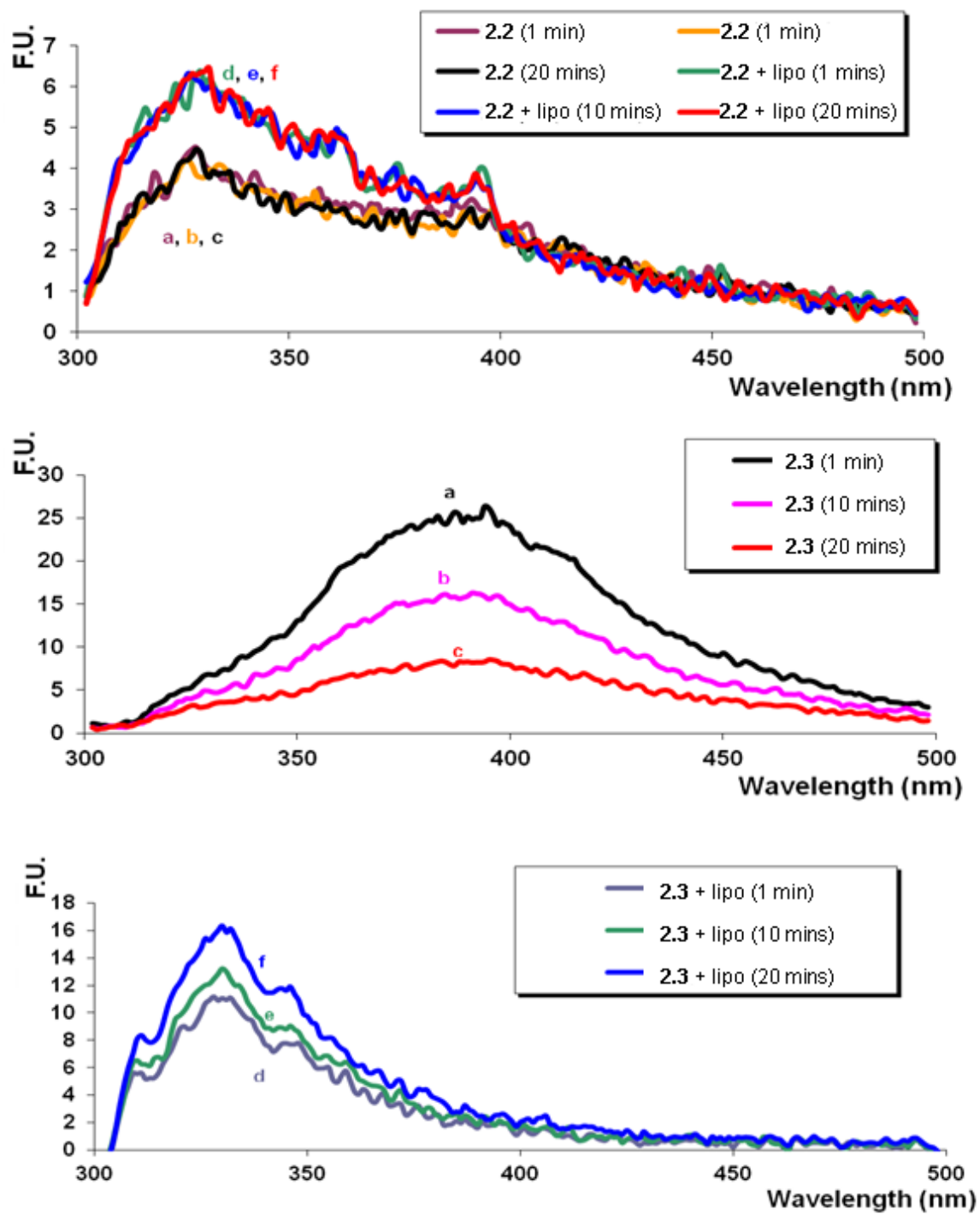
Figure S1.4: Fluorescence spectra of **2.2** and **2.3** in the absence and in the presence of liposomes.

Annexe 2 : Partie expérimentale du chapitre 3, article 2 : « An anion structure-activity relationship of imidazolium-based synthetic transporters »

Experimental section.

General. 4-Iodobenzoic acid, borane in tetrahydrofuran (BH$_3$ in THF) and phosphorus tribromide (PBr$_3$) were obtained from Aldrich. Tetrahydrofuran (THF), dichloromethane (DCM), acetonitrile (CH$_3$CN), hexane and ethyl acetate (EtOAc) were purchased from EMD. ^{1}H- and ^{13}C-NMR spectra were recorded on a Bruker spectrometer at 300 and 75 MHz, respectively, in the indicated solvent. Chemical shifts are reported in ppm with reference to TMS. High-resolution mass spectra (HRMS) were recorded on a LC-MSD-Tof instrument from Agilent technologies in positive electrospray mode in general. Either protonated molecular ions (M+H)$^+$ or silver adducts (M+Ag)$^+$ were used for empirical formula confirmation. NMR spectra, for the complexation studies, were recorded on a Bruker spectrometer at 300 MHz. Phospholipids used to prepare liposomes were purchased from Avanti Polar Lipids. Size-exclusion chromatography was performed using Sephadex G-25. Fluorescent dyes HPTS and lucigenin were purchased from Fluka and Molecular Probes, respectively. Liposome fluorimetric assays were recorded using a Varian Cary Eclipse Fluorescence spectrophotometer.

Synthesis. The synthesis and characterization of compound **3.1** were previously reported (see annexe 1 of this thesis). The compounds **3.2-3.4** have been synthesized by a counter ion change of compound **3.1** (Scheme 2.2). (*N,N'*-diphenylethynylbenzyl)imidazolium bromide salt (**3.1**) has been synthesized from imidazole using (4-phenylethynyl)benzyl bromide (**d**) in THF at 70 °C during 12 hours (Scheme 2.2). The (4-phenylethynyl)benzyl bromide (**c**) has been obtained from 4-iodobenzoic acid (**a**) reduced to 4-iodobenzyl alcohol (**b**) using BH$_3$ in THF overnight at room temperature. It was then mixed with benzylacetylene, PPh$_3$, PdCl$_2$(PPh$_3$)$_2$, CuI in dry THF with Et$_3$N overnight at 50 °C (Scheme 2.1).

4-Iodobenzyl alcohol (b) : 4-Iodobenzoïc acid (0.02 mol) diluted in 40 mL THF was added to 40 mL of a solution of a 1.0 M BH$_3$ in THF solution and the mixture was stirred overnight at room temperature. The reaction was quenched with 100 mL of a 2 N HCl solution and extracted with 3 × 140 mL of DCM. The combined organic layers were washed with 2 × 80 mL of NaHCO$_3$ saturated then 2 × 80 mL of Brine and dried over MgSO$_4$. The solvent was removed under reduced pressure to give the pure product as a white solid in a 99 % isolated yield. Mp 68 – 70 °C. ^{1}H NMR (300 MHz, CDCl$_3$) δ 7.65

(d, 2H, J = 8.2 Hz), 7.06 (d, 2H, J = 8.0 Hz), 4.58 (s, 2H), 2.04 (b, 1H). ^{13}C NMR (75 MHz, CDCl$_3$) δ 140.3, 137.4, 128.7, 92.9, 64.4. HRMS (ESI) calcd for $C_7H_7AgIO^+$ [M+Ag]$^+$: 340.8587, found 340.8591.

(4-Phenylethynyl)benzyl alcohol (c) : To a carefully degassed solution of 4-iodobenzyl alcohol **b** (4.3 mmol), PPh$_3$ (0.085 mmol), and PdCl$_2$(PPh$_3$)$_2$ (0.026 mmol) in 10 mL of dry THF and 5 mL of dry triethylamine was added CuI (0.085 mmol). The mixture was degassed for 5 min and a solution of phenylacetylene (4.3 mmol) in 2 mL of dry THF was added dropwise. The reaction was stirred overnight at 50 °C under nitrogen atmosphere. The mixture was added to 50 mL of ice water and the organic phase was recovered, dried over MgSO$_4$. The solvent was removed under reduced pressure to give the pure product as a white solid in 99 % isolated yield. Mp. 118 – 120 °C. ^{1}H NMR (300 MHz, CDCl$_3$) δ 7.54-7.50 (m, 4H), 7.37-7.24 (m, 5H), 4.66 (s, 2H), 2.00 (b, 1H). ^{13}C NMR (75 MHz, CDCl$_3$) δ 140.9, 131.7, 131.5, 128.3, 128.2, 126.7, 123.1, 122.3, 89.3, 89.1, 64.8. HRMS (ESI) calcd for $C_{15}H_{13}O^+$ [M+H]$^+$: 209.0961, found 209.0969.

(4-Phenylethynyl)benzyl bromide (d) : (4-Phenylethynyl)benzyl alcohol (**c**) (1.44 mmol) was dissolved in 5 mL of DCM. The mixture was put at 0 °C and phosphorus tribromide was added dropwise. Then the mixture was stirred 2 hours at 0 °C and the solvent was removed under reduced pressure. The product was purified by flash chromatography (Hexane/EtOAc, 60:40) to afford the compound **d** as a white solid in 100 % isolated yield. Mp 94 – 96 °C. ^{1}H NMR (300 MHz, CDCl$_3$) δ 7.54-7.48 (m, 4H), 7.37-7.24 (m, 5H), 4.48 (s, 2H). ^{13}C NMR (75 MHz, CDCl$_3$) δ 137.6, 131.9, 131.5, 129.0, 128.3, 128.2, 123.3, 122.9, 90.2, 88.8, 32.9. HRMS (ESI) calcd for $C_{15}H_{12}Br^+$ [M+H]$^+$: 271.0117, found 271.0109.
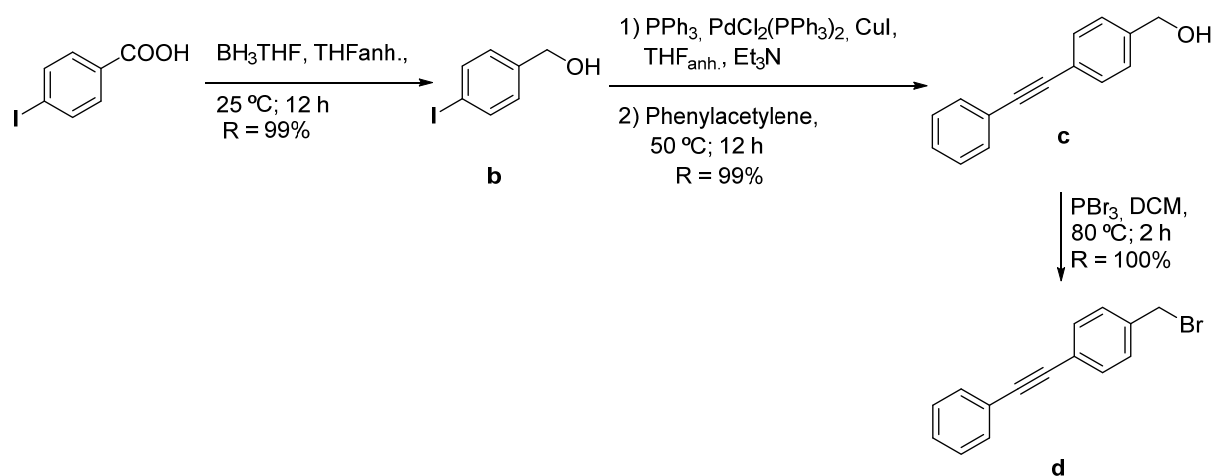
(*N,N'*-Diphenylethynylbenzyl)imidazolium bromide (3.1) : 27.5 mg (0.40 mmol) of imidazole and 37.8 mg of sodium hydride (1.57 mmol) are diluted in 10 mL of THF. After 5 minutes at room temperature, 100 mg (0.40 mmol) of (4-phenylethynyl)benzyl bromide **d** is added to the mixture. The solution is stirred at room temperature for 12 h and the solvent is removed in vacuuo. 20 mL of water and 30 mL of DCM are added to the crude product. The organic phase is separated, washed with 2 x 20 mL of water and then dried on MgSO$_4$. The solvent is removed in vacuuo to yield 100 mg of the intermediate (4-Phényléthynyl)benzylimidazole. This compound is then used without
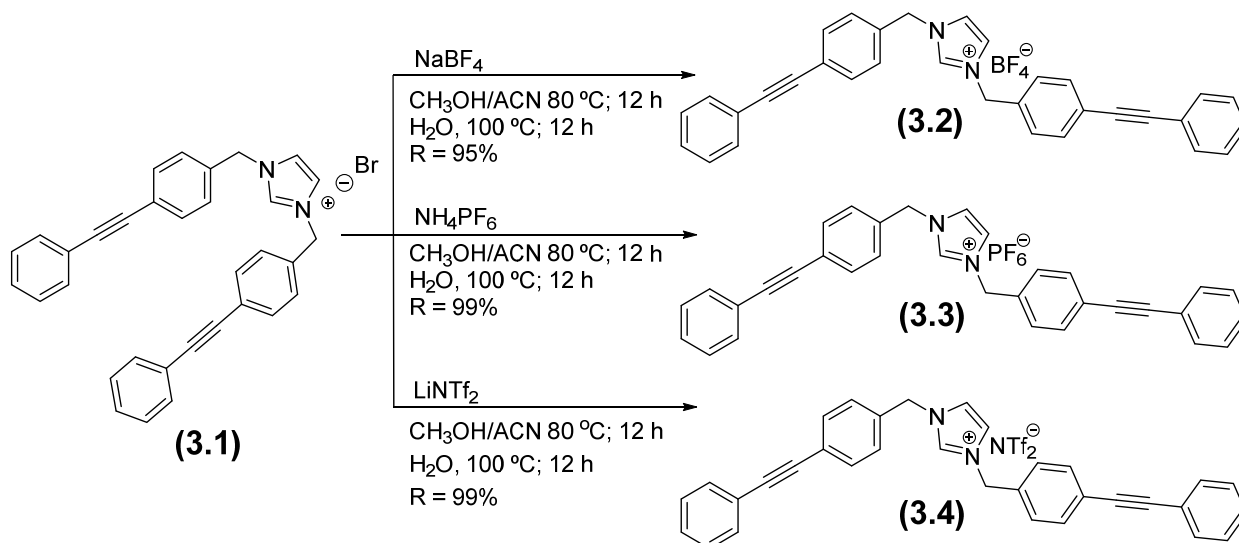
further purification: 100 mg (0.47 mmol) of (4-phenylethynyl)benzylimidazole and 127 mg (0.47 mmol) of (4-phenylethynyl)benzyl bromide **d** are disolved in 10 mL of THF. The mixture is stirred 12 h at 70 °C and the resulting precipitate is filtered, washed with 10 mL of THF, and dried in vacuuo. 134 mg of **3.1** were obtained. Yield 67 %. ^{1}H NMR (CD$_3$OD, 400MHz): δ=7.71 (s, 2H), 7.62 (d, J=8.3 Hz, 4H), 7.51-7.56 (m, 4H), 7.46 (d, J=8.3 Hz, 4H), 7.37-7.42 (m, 6H), 7.38-7.42 (m, 2H), 5.48 ppm (s, 4H). 13C NMR (CD3OD, 75 MHz): δ=134.6, 132.8, 132.0, 129.3, 129.2, 129.0, 125.2, 123.7, 123.5, 123.2, 90.9, 88.5, 53.3 ppm. HR-MS (ESI): m/z Calcd for $C_{33}H_{25}N_2$ [M-Br]+: 449.2012, found 449.2017.

(*N,N'*-Diphenylethynylbenzyl)imidazolium Tetrafluoroborate (3.2) : 0.10 g (0.19 mmoles) of (*N,N'*-diphenylethynylbenzyl)imidazolium bromide are dissolved in a mixture of MeOH/ACN (50 : 50). Then, 32 mg (0.29 mmoles) of NaBF$_4$ are added to 10 mL of methanol before being poured onto the solution containing the imidazolium salt. The resulting mixture is then brought to 80 °C and stirred with a magnetic stir bar during 12 hours. After evaporating the solvent under reduced pressure, 40 mL of distilled water are added to the powder obtained. The mixture is heated to 100 °C for 12 hours under magnetic stirring, and then filtered on a fritted glass. The raw product is then dried at 80 °C for 2 hours, in order to obtain 96 mg of a white powder (95% yield).^{1}H NMR (400 MHz, CDCl$_3$) δ ppm = 9.40 (s, 1 H), 7.87 (d, J=1.41 Hz, 2 H), 7.62 - 7.66 (m, 4 H), 7.53 - 7.59 (m, 4 H), 7.43 - 7.50 (m, 10 H), 5.49 (s, 4 H).

(*N,N'*-Diphenylethynylbenzyl)imidazolium Hexafluorophosphate (3.3) : 100 mg (0.19 mmoles) of (*N,N'*-Diphenylethynylbenzyl)imidazolium bromide are dissolved in a mixture of MeOH/ACN (50 :50). Then, 46 mg (0.29 mmoles) of NH$_4$PF$_6$ are added to 10 mL of methanol before being poured onto the solution containing the imidazolium salt. The resulting mixture is then brought to 80 °C and stirred with a magnetic stir bar during 12 hours. After evaporating the solvent under reduced pressure, 40 mL of distilled water are added to the powder obtained. The mixture is heated to 100 °C for 12 hours under magnetic stirring, and then filtered on a fritted glass. The raw product is then dried at 80 °C for 2 hours, in order to obtain 113 mg of a white powder (99% yield).^{1}H NMR (400 MHz, CDCl$_3$) δ ppm = 9.40 (s, 1 H), 7.87 (d, J=1.41 Hz, 2 H), 7.62 - 7.66 (m, 4 H), 7.53 - 7.59 (m, 4 H), 7.43 - 7.50 (m, 10 H), 5.49 (s, 4 H).

(*N,N'*-Diphenylethynylbenzyl)imidazolium Bistrifluorométhaneesulfonimide (3.4) :
100 mg (0.19 mmoles) of (*N,N'*-Diphenylethynylbenzyl)imidazolium bromide are
dissolved in a mixture of MeOH/ACN (50 :50). Then, 83 mg (0.29 mmoles) of $LiNTf_2$
are added to 10 mL of methanol before being poured onto the solution containing the
imidazolium salt. The resulting mixture is then brought to 80 ºC and stirred with a
magnetic stir bar during 12 hours. After evaporating the solvent under reduced pressure,
40 mL of distilled water are added to the powder obtained. The mixture is heated to 100
ºC for 12 hours under magnetic stirring, and then filtered on a fritted glass. The raw
product is then dried at 80 °C for 2 hours, in order to obtain 138 mg of a white powder
(99% yield).^{1}H NMR (400 MHz, $CDCl_3$) δ ppm = 9.40 (s, 1 H), 7.87 (d, J=1.41 Hz, 2 H),
7.62 - 7.66 (m, 4 H), 7.53 - 7.59 (m, 4 H), 7.43 - 7.50 (m, 10 H), 5.49 (s, 4 H).

Scheme S2.1. : Synthesis of (4-Phenylethynyl)benzyl bromide

Scheme S2.2 : Synthesis of (*N,N'*-Diphenylethynylbenzyl)imidazolium bromide (**3.1**)
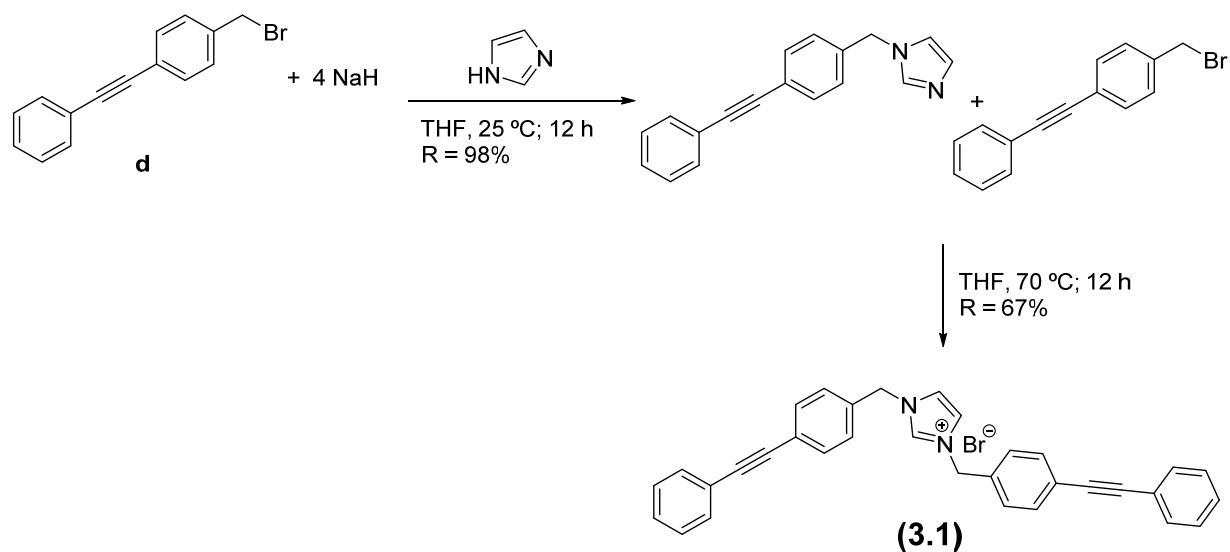
Scheme S2.3. : Counter anion change of **3.1** in order to obtain trasnporters **3.2-3.4**

Preparation of EYPC liposomes for Lucigenin-based assays. A stock solution of egg-yolk phosphatidylcholine (EYPC) in $CHCl_3$ (100 mg) was evaporated under reduced pressure on the water bath rt to produce a thin film that was dried *in vacuo* for 2 h at 35 ºC. This lipid film was hydrated with 1 mL of 10 mM sodium phosphate (pH =6.4) containing sodium chloride, [NaCl] = 100 mM, and 2 mM Lucigenin. Freeze/thaw cycles were repeated at least 10 times until no solid particles were visible. The frozen solution was warmed to 30-35 ºC before every freeze cycle. The mixture was also placed on a vortexer 3 times for 1 min to facilitate hydration. The cloudy solution was extruded through a 100 nm polycarbonate membrane at least 20 times until the solution was transparent. This solution was passed down a Sephadex G-25 column (15 cm x 1 cm) to remove extravesicular lucigenin dye. The eluant was free of lucigenin and contained 10 mM phosphate buffer and 75 mM Na_2SO_4. The 2.6 mL of solution isolated from gel filtration was 50 mM in lipid, assuming all EYPC was incorporated into the liposomes. Each stock solution of liposomes was used that same day for any ion transport assays.

Preparation of DPPC liposomes for Lucigenin-based assays. DPPC lipid (50 mg) was dissolved in 5 mL of a chloroform/methanol mixture (5 % MeOH), and the resulting solution was then evaporated under reduced pressure at 45 ºC to produce a thin film that was then dried *in vacuo* for 2 h. The lipid film was hydrated with 1 mL of 10 mM sodium

phosphate containing sodium chloride, [NaCl] = 100 mM, and 2 mM Lucigenin. After 10 freeze/thaw cycles (thawing, and then warming to 45 °C) the liposomes were extruded through a 100 nm polycarbonate membrane 21 times at temperature between 45-55 °C (fluid state lipid). This solution was passed down a Sephadex G-25 column (15 cm x 1 cm) to remove extravesicular lucigenin dye. The eluant used for the column was free of lucigenin and contained 10 mM phosphate buffer and 75 mM Na_2SO_4. The 2.6 mL of solution isolated from gel filtration was 26.2 mM in lipid, assuming all DPPC was incorporated into the liposomes. A small aliquot of liposomes suspension was taken from time to time, in order to verify the DPPC concentration by Stewart *et al.* method.[*] Each stock solution of liposomes was used that same day for any ion transport assays.

Lucigenin-based ion transport assays. A 20 µL aliquot of the stock solution of liposomes was added to a cuvette containing 2 mL of a 100 mM solution of salt $NaNO_3$ and 10 mM phosphate buffer to give a 0.25 – 0.3 mM solution of phospholipid. The fluorescence of intravesicular dye was monitored by excitation at 372 nm and the emission at 503 nm was recorded. For assays in EYPC liposomes, some time within the first 100 s of the experiment, 400 µL aliquot of a 0.1 mM solution of imidazoliums **3.1-3.4** in MeOH was injected to give a final solution that was ~16 µM in imidazolium. At the end of the experiment, 10% aqueous Triton-X was injected to lyse the liposomes. The temperature was set to 37 °C. For kinetic analysis in EYPC liposomes, some time within the first 100 s of the experiment, 400 µL aliquots of 0.0215 mM to 0.75 mM solutions of imidazolium **3.4** in MeOH was injected to give solutions that were 0.004 mM to 0.123 mM in imidazolium respectively. The temperature was set to 37 °C. For assays in DPPC liposomes, some time within the first 100 s of the experiment, 400 µL aliquot of a 0.25 mM solution of imidazolium **3.4** in MeOH was injected to give a solution that was ~40 µM in imidazolium. The temperature was set to 25 °C, 30 °C, 35 °C, 40 °C, 45 °C successively.

---

[*] Stewart, J. C., *Anal Biochem.* **1980,** *104*, 10

Preparation of liposomes for HPTS-based assays. A stock solution of egg-yolk phosphatidylcholine (EYPC) in CHCl₃ (100 mg) was evaporated on the water bath rt under reduced pressure to produce a thin film that was dried *in vacuo* for 2 h at 35 ℃. This lipid film was hydrated with 1 mL of 10 mM sodium phosphate containing sodium perchlorate, [NaClO₄] = 100 mM, and 0.1 mM HPTS. Freeze/thaw cycles were repeated at least 10 times until no solid particles were visible. The frozen solution was warmed to 30-35 ℃ before every freeze cycle. The mixture was also placed on a vortexer 3 times for 1 min to facilitate hydration. The cloudy solution was extruded through a 100 nm polycarbonate membrane at least 20 times until the solution was transparent. This solution was passed down a Sephadex G-25 column (11 cm x 1 cm) to remove extravesicular HPTS dye. The eluant was identical to the solution used to hydrate the EYPC films except that it was free of HPTS. The 2.6 mL of solution isolated from gel filtration was 50 mM in lipid, assuming all EYPC was incorporated into the liposomes. Each stock solution of liposomes was used that same day for any ion transport assays.

HPTS-based ion transport assays. This procedure describes the typical ion transport assay. A 20 µL aliquot of the stock solution of EYPC liposomes was added to a cuvette containing 2 mL of a 100 mM solution of salt NaNO₃, NaCl or NaSO₄ and 10 mM phosphate buffer to give a 0.25–0.3 mM solution of phospholipid. The fluorescence of intravesicular HPTS was monitored by excitation at both 403 nm and 460 nm and the emission at 510 nm was recorded. Some time within the first 5 min of the experiment, a 70 µL aliquot of a 1.5 mM solution of imidazolium **3.4** was injected to give a solution that contained 0.0525 mM of amphiphile. At the end of the experiment (25 min), 10% aqueous Triton-X was injected to lyse the liposomes. The temperature was set to 37 °C.

Initial rate and rate constant calculations

Fluorescence assays were run at different **3.3**/EYPC ratios: 1.0-30 mol.%. The initial rates were determined at $t = 50$ s when the transporter is injected, following the Stern-Volmer equation.

$$\left(\frac{F_0}{F}\right) = 1 + K_{SV}[Cl^-]$$

with F_0 : maximum fluorescence intensity in absence of quencher

                 F : fluorescence intensity

                 K_{SV} : Stern-Volmer constant[*], here $K_{SV} = 142$ M^{-1}

                 $[Cl^-]$: intravesicular chloride concentration

From this equation, we can deduce:

$$\text{At } t=0, \qquad -\left(\frac{d[Cl^-]}{dt}\right) = \left(\frac{F_0}{K_{SV}}\right) \bullet \left(\frac{1}{F^2}\right) \bullet \left(\frac{dF}{dt}\right)_{t=0} = V_0$$

With V_0 : initial rate

According to equation 4 (see the article), the initial rate of ion flow (V_0) is expected to have a dependence on the pseudo first order constant (k_{obsd}) and $[Cl^-]$ the total initial intravesicular chloride concentration (48 mM).

$V_0 = k_{obsd}\,[Cl^-]_{t=0}$

---

[*] Wissing, F., Smith, J. A. C., *J. Membrane Biol.* **2000**, *177*, 199. (b) Chhun, C. Axe et Rotaxane Parapluie, vers de nouveaux transporteurs transmembranaires de chlorures et de médicaments cycliques. Thèse de doctorat, Université de Montréal, Montréal, **2012**

Table SII-1. Determination of V_0 and k_{obds} at different 3.4/EYPC ratios

mol% 3.4 /EYPC	[3.4] (mM)	(dF/dt) (s^{-1})	V_0 (mM/s)	V_0 average (mM/s)	K_{obsd} (s^{-1})	Standard deviation
1.0	0.004	0.019	0.242	0.192	0.0040	0.0009
		0.014	0.181			
		0.012	0.153			
1.7	0.007	0.024	0.310	0.353	0.007	0.001
		0.034	0.431			
		0.025	0.317			
3.4	0.014	0.040	0.509	0.641	0.013	0.003
		0.047	0.598			
		0.064	0.818			
6.9	0.028	0.158	2.017	1.664	0.035	0.007
		0.122	1.562			
		0.110	1.411			
8.6	0.035	0.105	1.344	1.535	0.032	0.004
		0.136	1.734			
		0.119	1.526			
14.0	0.057	0.178	2.278	2.480	0.052	0.005
		0.212	2.714			
		0.192	2.448			
18.0	0.074	0.299	3.822	3.279	0.07	0.01
		0.233	2.975			
		0.238	3.041			
25.0	0.102	0.540	6.901	5.577	0.12	0.04
		0.281	3.584			
		0.489	6.247			
30.0	0.123	0.442	5.642	5.363	0.11	0.02
		0.493	6.295			
		0.325	4.151			

Table SII-2. Determination of activity of 3.4 at different 3.4 /EYPC ratios

mol% 3.4 /EYPC	Log (mol% 4/EYPC)	% of Rmax at 250 s	Average % of Rmax at 250 s	Standard deviation
1.0	0.0000	23.98	24.3	0.5
		24.87		
		24.12		
1.7	0.2304	35.14	37	3
		40.93		
		36.85		
3.4	0.5315	48.21	51	4
		50.34		
		55.62		
6.9	0.8388	90.14	85	5
		86.60		
		79.91		
8.6	0.9345	87.29	86	3
		83.51		
		88.71		
14.0	1.1461	92.51	90	3
		87.84		
		91.77		
18.0	1.2553	100.20	97	3
		97.11		
		94.94		
25.0	1.3979	100.00	99.2	0.7
		98.60		
		99.09		
30.0	1.4771	97.06	99	3
		102.23		
		98.04		
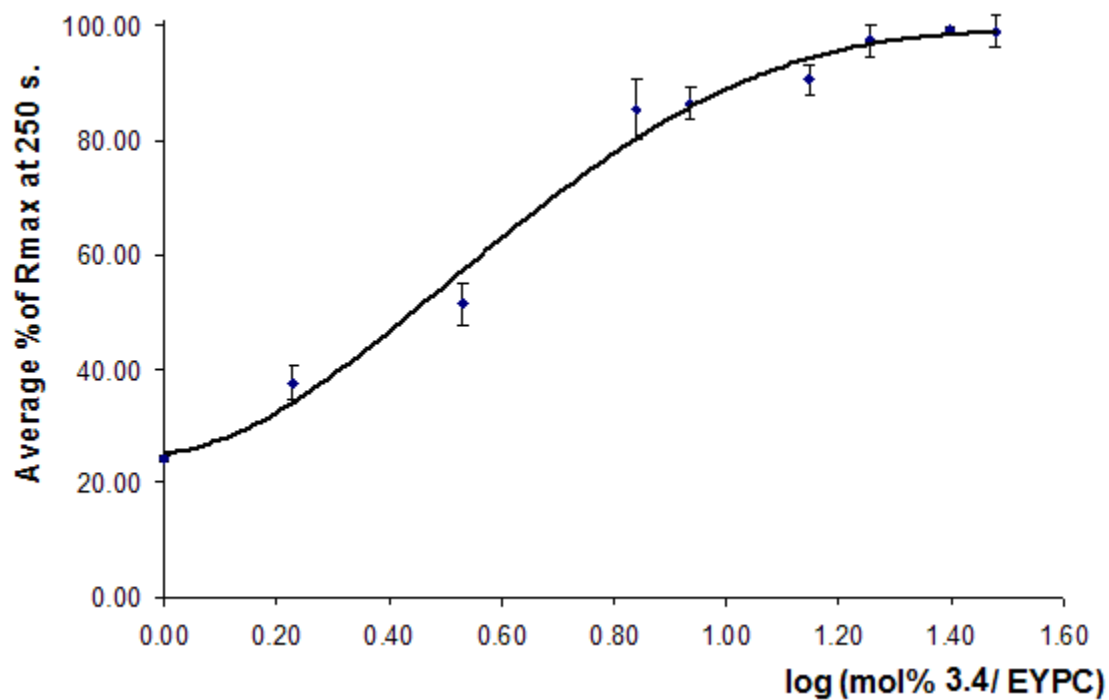
Figure S2.1. Dose response curve for determination of the EC_{50} for imidazolium **3.4**. The data at each mol% is the average of 3 runs, with the standard deviation. %Rmax is the ratio between response induced by **3.4** versus 10% aqueous Triton-X injected at 250 s. The log(mol% **3.4** /EYPC) that provokes a response half way between the baseline (24.2%) and maximum response (99.2%) has a value of 0.750. This corresponds to a mol% **3.4** /EYPC of 5.74%.

Annexe 3 : Partie expérimentale du chapitre 4, article 3 : « Benzimidazolium-based synthetic chloride and calcium transporters in bacterial membranes »

GENERAL INFORMATION

4-Iodobenzoic acid, borane in tetrahydrofuran (BH_3 in THF) and phosphorus tribromide (PBr_3) were obtained from Aldrich. Tetrahydrofuran (THF), dichloromethane (DCM), acetonitrile (CH_3CN), hexane and ethyl acetate (EtOAc) were purchased from EMD. ^{1}H- and ^{13}C-NMR spectra were recorded on a Bruker spectrometer at 300 and 75 MHz, respectively, in the indicated solvent. Chemical shifts are reported in ppm with internal reference to TMS. High-resolution mass spectra (HRMS) were recorded on a LC-MSD-Tof instrument from Agilent technologies in positive electrospray mode in general. Either protonated molecular ions $(M+H)^+$ or silver adducts $(M+Ag)^+$ were used for empirical formula confirmation. Phospholipids used to prepare liposomes were purchased from Avanti Polar Lipids. Size-exclusion chromatography was performed using Sephadex G-25. Fluorescent dyes HPTS and lucigenin were purchased from Fluka and Molecular Probes, respectively. Liposome fluorimetric assays were recorded using a Varian Cary Eclipse Fluorescence spectrophotometer.

GENERAL PROCEDURES

Synthesis. (4-Phenylethynyl)benzyl bromide (**c**) has been obtained from 4-iodobenzoic acid (**a**) reduced to 4-iodobenzyl alcohol (**b**) using BH_3 in THF overnight at room temperature, then to react with benzylacetylene using PPh_3, $PdCl_2(PPh_3)_2$, CuI in dry THF with Et_3N overnight at 50 °C (Scheme 3.1). The (*N,N'*-diphenylethynylbenzyl)benzimidazolium bromide salt (**4.1**) has been synthesized from benzimidazole using (4-phenylethynyl)benzyl bromide (**d**) in THF at 25 ºC during 12 hours and in DMF at 140 ºC during 48 hours (Scheme 3.2). The compounds **4.2-4.4** have been synthesized by a counter ion change of compound **4.1** (Scheme 3.3).

4-Iodobenzyl alcohol (b) : 4-Iodobenzoïc acid (0.02 mol) diluted in 40 mL THF was added to 40 mL of a solution of a 1.0 M BH_3 in THF solution and the mixture was stirred overnight at room temperature. The reaction was quenched with 100 mL of a 2 N HCl solution and extracted with 3×140 mL of DCM. The combined organic layers were washed with 2×80 mL of saturated $NaHCO_3$, then 2×80 mL of Brine and dried over $MgSO_4$. The solvent was removed under reduced pressure to give the pure product as a white solid in a 99 % isolated yield. Mp 68 – 70 °C. ^{1}H NMR (300 MHz, CDCl$_3$) δ 7.65 (d, 2H, J = 8.2 Hz), 7.06 (d, 2H, J =

8.0 Hz), 4.58 (s, 2H), 2.04 (b, 1H). ^{13}C NMR (75 MHz, CDCl$_3$) δ 140.3, 137.4, 128.7, 92.9, 64.4. HRMS (ESI) calcd for C$_7$H$_7$AgIO$^+$ [M+Ag]$^+$: 340.8587, found 340.8591.

(4-Phenylethynyl)benzyl alcohol (c) : To a carefully degassed solution of 4-iodobenzyl alcohol **b** (4.3 mmol), PPh$_3$ (0.085 mmol), and PdCl$_2$(PPh$_3$)$_2$ (0.026 mmol) in 10 mL of dry THF and 5 mL of dry triethylamine was added CuI (0.085 mmol). The mixture was degassed for 5 min and a solution of phenylacetylene (4.3 mmol) in 2 mL of dry THF was added dropwise. The reaction was stirred overnight at 50 °C under nitrogen atmosphere. The mixture was added to 50 mL of ice water and the organic phase was recovered, dried over MgSO$_4$. The solvent was removed under reduced pressure to give the pure product as a white solid in 99 % isolated yield. Mp. 118 – 120 °C. ^{1}H NMR (300 MHz, CDCl$_3$) δ 7.54-7.50 (m, 4H), 7.37-7.24 (m, 5H), 4.66 (s, 2H), 2.00 (b, 1H). ^{13}C NMR (75 MHz, CDCl$_3$) δ 140.9, 131.7, 131.5, 128.3, 128.2, 126.7, 123.1, 122.3, 89.3, 89.1, 64.8. HRMS (ESI) calcd for C$_{15}$H$_{13}$O$^+$ [M+H]$^+$: 209.0961, found 209.0969.

(4-Phenylethynyl)benzyl bromide (d) : (4-Phenylethynyl)benzyl alcohol (**c**) (1.44 mmol) was dissolved in 5 mL of DCM. The mixture was put at 0 °C and phosphorus tribromide was added dropwise. Then the mixture was stirred 2 hours at 0 °C and the solvent was removed under reduced pressure. The product was purified by flash chromatography (Hexane/EtOAc, 60:40) to afford the compound **d** as a white solid in 100 % isolated yield. Mp 94 – 96 °C. ^{1}H NMR (300 MHz, CDCl$_3$) δ 7.54-7.48 (m, 4H), 7.37-7.24 (m, 5H), 4.48 (s, 2H). ^{13}C NMR (75 MHz, CDCl$_3$) δ 137.6, 131.9, 131.5, 129.0, 128.3, 128.2, 123.3, 122.9, 90.2, 88.8, 32.9. HRMS (ESI) calcd for C$_{15}$H$_{12}$Br$^+$ [M+H]$^+$: 271.0117, found 271.0109.

(*N,N*'-Diphenylethynylbenzyl)benzimidazolium bromide (4.1) : 0.50 g (4.3 mmol) of benzimidazole and 464 mg (19.3 mmol) of sodium hydride were diluted in 10 mL of THF. After 5 minutes of stirring at room temperature, 0.127 g (4.68 mmol) of (4-phenylethynyl)benzyl bromide **d** was added to the mixture. The solution was stirred at room temperature for 12 hrs and the solvent was removed in vacuuo. 30 mL of water were added to the crude product and extracted with 3 x 30 mL of DCM. The organic phase was separated, washed with 2 x 30 mL of water, of NaHCO$_3$ and NaCl$_{(sat.)}$ and then dried on MgSO$_4$. The solvent was removed in vacuuo to yield 1060 mg of the intermediate (4-Phenylethynylbenzyl)benzimidazole. This compound was then used without further purification: 745 mg (2.41 mmol) of (4-Phenylethynylbenzyl)benzimidazole and 0.6535 mg

(2.41 mmol) of (4-phenylethynyl)benzyl bromide **d** was dissolved in 30 mL of DMF. The mixture is stirred 48 h at 140 °C and the resulting precipitate is filtered, washed with 10 mL of THF, and dried in vacuuo. 880 mg of **1** were obtained. Yield 63 %. ^{1}H NMR (Chloroform-*d*, 300 MHz): δ ppm = 9.97 (s, 1 H), 7.90 - 7.96 (m, 1 H), 7.52 (m, 14 H), 7.38 - 7.45 (m, 7 H), 5.81 (s, 4 H). MS (ESI): m/z Calcd for $C_{37}H_{27}N_2$ [M-Br]+: 499.22, found 499.22.
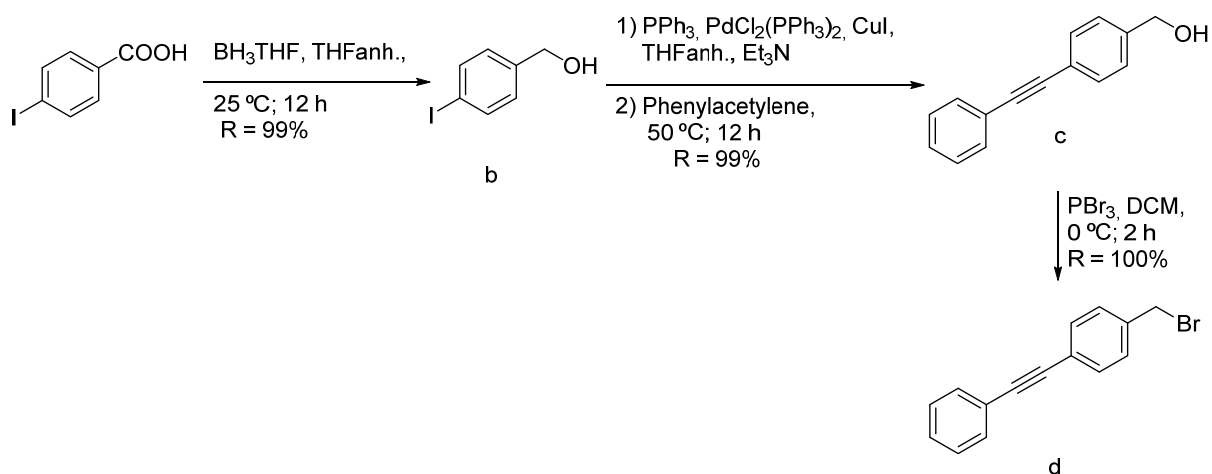
(***N,N'*-Diphenylethynylbenzyl)imidazolium   Tetrafluoroborate   (4.2)   :   150 mg** (0.26 mmoles) of (N,N'-Diphenylethynylbenzyl)imidazolium bromide (**4.1**) were dissolved in a mixture of MeOH/ACN (50 :50). Then, 71 mg (0.65 mmoles) of NaBF$_4$ were added to 10 mL of methanol before being poured onto the solution containing the imidazolium salt. The resulting mixture was then brought to 80 ºC and stirred with a magnetic stir bar during 12 hours. After evaporating the solvent under reduced pressure, 40 mL of distilled water were added to the powder obtained. The mixture was heated to 100 ºC for 12 hours under magnetic stirring, and then filtered on a fritted glass. The raw product is then dried at 80 ºC for 2 hours, in order to obtain 137 mg of a white powder (90% yield). ^{1}H NMR (300 MHz, CHLOROFORM-*d*) δ ppm = 9.97 (s, 1 H), 7.90 - 7.96 (m, 1 H), 7.52 (m, 14 H), 7.38 - 7.45 (m, 7 H), 5.81 (s, 4 H). MS (ESI): m/z Calcd for $C_{37}H_{27}N_2$ [M- BF$_4$]+: 499.22, found 499.22. (ESI): m/z Calcd for BF$_4^-$: 87.00, found 87.00.

(***N,N'*-Diphenylethynylbenzyl)imidazolium   Hexafluorophosphate   (4.3)   :   150 mg** (0.26 mmoles) of (N,N'-Diphenylethynylbenzyl)imidazolium bromide were dissolved in a mixture of MeOH/ACN (50 :50). Then, 106 mg (0.65 mmoles) of NH$_4$PF$_6$ were added to 10 mL of methanol before being poured onto the solution containing the imidazolium salt. The resulting mixture was then brought to 80°C and stirred with a magnetic stir bar during 12 hours. After evaporating the solvent under reduced pressure, 40 mL of distilled water were added to the powder obtained. The mixture was heated to 100 ºC for 12 hours under magnetic stirring, and then filtered on a fritted glass. The raw product was then dried at 80 ºC for 2 hours, in order to obtain 167 mg of a white powder (99% yield). ^{1}H NMR (300 MHz, CHLOROFORM-*d*) δ ppm = 9.97 (s, 1 H), 7.90 - 7.96 (m, 1 H), 7.52 (m, 14 H), 7.38 - 7.45 (m, 7 H), 5.81 (s, 4 H). MS (ESI): m/z Calcd for $C_{37}H_{27}N_2$ [M- PF$_6$]+: 499.22, found 499.22. (ESI): m/z Calcd for PF$_6^-$: 144.96, found 144.96.

(***N,N'*-Diphenylethynylbenzyl)imidazolium Bis(trifluoromethane)sulfonimide (4.4) :** 150 mg (0,19 mmoles) of (N,N'-Diphenylethynylbenzyl)imidazolium bromide are dissolved in a

mixture of MeOH/ACN (50 :50). Then, 187 mg (0.65 mmoles) of LiNTf$_2$ was added to 10 mL of methanol before being poured onto the solution containing the imidazolium salt. The resulting mixture was then brought to 80 ºC and stirred with a magnetic stir bar during 12 hours. After evaporating the solvent under reduced pressure, 40 mL of distilled water are added to the powder obtained. The mixture was heated to 100 ºC for 12 hours under magnetic stirring, and then filtered on a fritted glass. The raw product is then dried at 80 ºC for 2 hours, in order to obtain 182 mg of a white powder (90% yield). ^{1}H NMR (300 MHz, CHLOROFORM-d) δ ppm = 9.97 (s, 1 H), 7.90 - 7.96 (m, 1 H), 7.52 (m, 14 H), 7.38 - 7.45 (m, 7 H), 5.81 (s, 4 H). MS (ESI): m/z Calcd for C$_{37}$H$_{27}$N$_2$ [M- NTf$_2$]+: 499.22, found 499.22. (ESI): m/z Calcd for NTf$_2$$^-$: 279.92, found 279.92.

Scheme 3.1. : Synthesis of (4-Phenylethynyl)benzyl bromide

Scheme 3.2 : Synthesis of (*N,N'*-diphenylethynylbenzyl)imidazolium bromide (**4.1**)

Scheme 3.3. : Counter anion change of **4.1** in order to obtain compounds **4.2-4.4**

Preparation of EYPC liposomes for Lucigenin-based assays. A stock solution of egg-yolk phosphatidylcholine (EYPC) in CHCl₃ (100 mg) was evaporated under reduced pressure on the water bath at room temperature to produce a thin film that was dried *in vacuo* for 2 h at 35 °C. This lipid film was hydrated with 1 mL of 10 mM sodium phosphate (pH = 6.4)

containing sodium chloride, [NaCl] = 100 mM, and 2 mM lucigenin. Freeze/thaw cycles were repeated at least 30 times until no solid particles were visible. The frozen solution was warmed to 37 °C before every freeze cycle. The mixture was also placed on a vortexer 10 times for 1 min to facilitate hydration. The cloudy solution was extruded through a 100 nm polycarbonate membrane at least 20 times until the solution was transparent. This solution was passed down a Sephadex G-25 column (15 cm x 1 cm) to remove extravesicular lucigenin dye. The eluant used for the column was free of lucigenin and contained 10 mM phosphate buffer and 100 mM NaCl. The 2.6 mL of solution isolated from gel filtration was 50 mM in lipid, assuming all EYPC was incorporated into the liposomes. Each stock solution of liposomes was used that same day for any ion transport assays.

Preparation of DPPC liposomes for Lucigenin-based assays. DPPC lipid (50 mg) was dissolved in 5 mL of a chloroform/methanol mixture (5 % MeOH), and the resulting solution was then evaporated under reduced pressure at 45 °C to produce a thin film that was then dried *in vacuo* for 2 h. The lipid film was hydrated with 1mL of 10 mM sodium phosphate containing sodium chloride, [NaCl] = 100 mM, and 2 mM Lucigenin. After 15 freeze/thaw cycles (thawing, and then warming to 45 °C) the liposomes were extruded through a 100 nm polycarbonate membrane 21 times at temperature between 45-55 °C (fluid state lipid). This solution was passed down a Sephadex G-25 column (15 cm x 1 cm) to remove extravesicular lucigenin dye. The eluant used for the column was free of lucigenin and contained 10 mM phosphate buffer and 100 mM NaCl. The 2.6 mL of solution isolated from gel filtration was 26.2 mM in lipid, assuming all DPPC was incorporated into the liposomes. A small aliquot of liposomes suspension was taken from time to time, in order to verify the DPPC concentration by Stewart *et al.* method.* Each stock solution of liposomes was used that same day for ion transport assays.

---

* Stewart, J. C., *Anal Biochem.* **1980,** *104*, 10

Lucigenin-based ion transport assays. A 20 µL aliquot of the stock solution of liposomes was added to a cuvette containing 2.5 mL of a solution of salt $NaNO_3$ (100 mM) in phosphate buffer (10 mM) to give a 0.4 mM solution of phospholipid. The fluorescence of intravesicular dye was monitored by excitation at 372 nm and the emission at 503 nm was recorded. For assays in EYPC liposomes, some time within the first 100 s of the experiment, 400 µL aliquot of a 0.25 mM solution of molecules **4.1-4.4** in MeOH was injected to give a final solution that was 34.2 µM in benzimidazolium. At the end of the experiment, 10% aqueous Triton-X was injected to lyse the liposomes. The temperature was set to 37 °C. For kinetic analysis in EYPC liposomes, some time within the first 100 s of the experiment, 400 µL aliquots of 0.025 mM to 0.31 mM solutions of benzimidazolium **4.4** in MeOH were injected to give solutions that were 3 µM to 43 µM in benzimidazolium respectively. The temperature was set to 37 °C. For assays in DPPC liposomes, some time within the first 100 s of the experiment, 400 µL aliquot of a 0.25 mM solution of benzimidazolium **4.4** in MeOH was injected to give a solution that was 34.2 µM in benzimidazolium. The temperature was set to 20 °C, 25 °C, 30 °C, 35 °C, 40 °C, 45 °C successively.

Initial rate and the rate constant calculations

Fluorescence assays were run at different **4.4**/EYPC ratios: 1.0-12.5. The initial rate were determined at t = 50 s when the transporter is injected, following the Stern-Volmer equation.

$$\left(\frac{F_0}{F}\right)=1+K_{SV}[Cl^-]$$

with

F$_0$: maximum fluorescence intensity in absence of quencher

F : fluorescence intensity

K$_{SV}$: Stern-Volmer constant*, here K$_{SV}$ = 142 M^{-1}

[Cl$^-$] : intravesicular chloride concentration

From this equation, we can deduce:

At t = 0,

$$-\left(\frac{d[Cl^-]}{dt}\right)=\left(\frac{F_0}{K_{SV}}\right)\bullet\left(\frac{1}{F^2}\right)\bullet\left(\frac{dF}{dt}\right)_{t=0}=V_0$$

With V$_0$: initial rate

According to equation 1 (see the article), the initial rate of ion flow (V_0) is expected to have a dependence on the pseudo first ordre constant (k_{obsd}) and [Cl$^-$] the total initial intravesicular chloride concentration (77 mM).

$V_0 = k_{obsd}[Cl^-]_{t=0}$

---

* Wissing, F., Smith, J. A. C., *J. Membrane Biol.* **2000**, *177*, 199. (b) Chhun, C. Axe et Rotaxane Parapluie, vers de nouveaux transporteurs transmembranaires de chlorures et de médicaments cycliques. Thèse de doctorat, Université de Montréal, Montréal, **2012**.

Table SIII-1. Determination of V_0 and k_{obds} at different 4.4/EYPC ratios

mol% 4.4/EYPC	[4.4] (mM)	(dF/dt) (s^{-1})	V_0 (mM/s)	V_0 average (mM/s)	K_{obsd} (s^{-1})	Standard deviation
1.0	0.003	0.067	1.075	0.419	0.006	0.004
		0.006	0.095			
		0.005	0.087			
1.6	0.005	0.131	2.103	1.389	0.019	0.005
		0.038	0.607			
		0.091	1.458			
2.5	0.009	0.047	0.750	1.278	0.018	0.005
		0.139	2.231			
		0.053	0.854			
5.0	0.017	0.118	1.900	2.376	0.033	0.003
		0.154	2.472			
		0.172	2.757			
7.0	0.024	0.397	6.373	5.506	0.075	0.007
		0.364	5.849			
		0.268	4.297			
10.0	0.034	0.517	8.300	10.232	0.14	0.01
		0.634	10.177			
		0.761	12.218			
12.5	0.043	0.767	12.309	13.756	0.19	0.01
		0.994	15.957			
		0.810	13.003			

Table SIII-2. Determination of activity of 4.4 at different 4.4/EYPC ratios

mol% 4.4/EYPC	Log(mol% 4.4/EYPC)	% of Rmax at 250 s	Average % of Rmax at 250 s	Standard deviation
1.0	0.0000	29.52	32	4
		30.57		
		37.24		
1.6	0.1987	42.30	47	6
		44.23		
		53.61		
2.5	0.3979	55.07	56	1
		56.45		
		57.69		
5.0	0.6990	87.34	87	3
		83.81		
		88.80		
7.0	0.8451	100.30	102	6
		109.25		
		97.07		
10.0	1.0000	104.33	102	2
		99.98		
		102.21		
12.5	1.0969	104.58	101	1×10^{1}
		86.97		
		112.43		

Figure S3.1. Dose response curve for determination of the EC$_{50}$ for imidazolium **4.4**. The data at each mol% is the average of 3 runs, with the standard deviation. %Rmax is the ratio between response induced by **3.4** versus 10% aqueous Triton-X injected at 250 s. The log(mol% **4.4**/EYPC) that provokes a response half way between the baseline (32.44%) and maximum response (102.21%) has a value of 0.475. This corresponds to a mol% **4.4**/EYPC of 2.99%. Hill coefficient n was also estimated with a curve fitting from the GraphPad Prism 6.00 for Windows (GraphPad Software, Inc.) at 2.092.

Activation of citrine-pBAD. Single colony of *E. coli* (*DH5α*) containing the pBAD plasmid from frozen stocks were picked and used to inoculate 2 mL of Luria-Bertani (LB) media supplemented with ampicillin (100 mg/ml). The priming culture was grown with shaking overnight at 37 °C and resuspended in 75 mL of a fresh LB medium. The new culture was grown at 37 °C until the O.D.$_{600}$ = 0.5-0.7 and induced at 37 °C for 16 hours with 0.02% (w/v) of arabinose (final concentration). Citrine-pBAD was a gift from Robert Campbell & Michael Davidson & Olivier Griesbeck & Roger Tsien (Addgene plasmid 54772).

Ion transport assays with *E. coli*. A 1.6 mL aliquot of the stock solution of *E. coli* culture was added to a cuvette containing 1.082 mL of a solution of salt $CaCl_2$ (1 mM). The fluorescence of intracellular citrine non-ratiometric indicator was monitored by excitation at 516 nm and the emission at 529 nm was recorded. Some time within the first two minutes of the experiment, an 150 µL aliquot of a 4.5 mM solution of benzimidazoliums **4.4** in MeOH was injected to give a solution of 0.24 mM in benzimidazolium in the cuvette. For the blank, at t = 2 minutes, an 150 µL aliquot of MeOH was injected in the cuvette containing 1.6 mL of *E. coli* and 1.082 mL of $CaCl_2$ (1 mM). The temperature was set to 37 °C.

Destruction of YFP-Citrine-pBAD *E. coli* membranes. Bacterial growth solution of *E. coli* is stirred at 100 °C for 3 h. An ultrasonic probe was used on the bacterial solution to destroy the remaining membranes with four cycles of sonication (30 seconds) and relaxation (1 minute).

Optic Density (O.D.) assay. 800 µL of a bacterial growth solution of *E. coli* is added to a cuvette containing 800 µL of a $CaCl_2$ 1mM solution and 150 µL of transporter **4.4** or MeOH. The absorbance of the solution is monitored at a 600 nm wavelength. The absorbance of compound **4.4** at this wavelength is subtracted out.

Université de Montréal

CRYSTAL AND MOLECULAR STRUCTURE OF

C37 H27 Br N2 COMPOUND (SCHM55)

Equipe Schmitzer

Département de chimie, Université de Montréal,

C.P. 6128, Succ. Centre-Ville, Montréal, Québec, H3C 3J7 (Canada)

Table SIII-3. Crystal data and structure refinement for C37 H27 Br N2.

Identification code   SCHM55

Empirical formula   C37 H27 Br N2

Formula weight   579.52

Temperature   100K

Wavelength   1.54178 Å

Crystal system   Triclinic

Space group   P-1

Unit cell dimensions   a = 9.5643(2) Å α = 89.925(1)^{o}
                                      b = 9.7254(2) Å β = 80.209(1)^{o}
                                      c = 17.4889(4) Å γ = 62.908(1)^{o}

Volume   1421.79(5)Å^3

Z   2

Density (calculated)   1.354 g/cm^3

Absorption coefficient   2.179 mm^{-1}

F(000)   596

Crystal size   0.16 x 0.08 x 0.04 mm

Theta range for data collection   2.57 to 70.95^{o}

Index ranges $-11 \leq h \leq 11$, $-11 \leq k \leq 11$, $-21 \leq \ell \leq 21$

Reflections collected   27726

Independent reflections   5290 [R_{int} = 0.042]

Absorption correction   Semi-empirical from equivalents

Max. and min. transmission   0.9165 and 0.6232

Refinement method   Full-matrix least-squares on F^2

Data / restraints / parameters   5290 / 0 / 361

Goodness-of-fit on F^2 1.058

Final R indices [I>2sigma(I)] R_1 = 0.0525, wR_2 = 0.1437

```
R indices (all data)              R₁ = 0.0568, wR₂ = 0.1526

Largest diff. peak and hole       1.562 and -1.166 e/Å³
```

Table SIII-4. Atomic coordinates (x 10^4) and equivalent isotropic displacement parameters ($Å^2$ x 10^3) for C37 H27 Br N2.

U_{eq} is defined as one third of the trace of the orthogonalized Uij tensor.

	x	y	z	U_{eq}
Br(1)	9271(1)	3164(1)	4208(1)	30(1)
N(1)	3764(3)	3171(3)	4839(1)	27(1)
C(2)	2437(4)	3025(4)	5027(2)	28(1)
N(3)	2585(3)	2031(3)	5563(1)	26(1)
C(4)	4100(3)	1490(3)	5750(2)	25(1)
C(5)	4865(4)	429(3)	6260(2)	27(1)
C(6)	6427(4)	111(4)	6271(2)	30(1)
C(7)	7184(4)	846(4)	5803(2)	30(1)
C(8)	6423(4)	1913(3)	5304(2)	28(1)
C(9)	4860(4)	2219(3)	5282(2)	25(1)
C(10)	4015(4)	4182(4)	4257(2)	30(1)
C(11)	4673(4)	3372(3)	3450(2)	26(1)
C(12)	6322(4)	2592(4)	3171(2)	30(1)
C(13)	6918(4)	1807(4)	2434(2)	30(1)
C(14)	5888(4)	1821(4)	1951(2)	29(1)
C(15)	4226(4)	2628(4)	2232(2)	29(1)
C(16)	3640(4)	3375(4)	2972(2)	29(1)
C(17)	6531(4)	1067(4)	1157(2)	33(1)
C(18)	7057(4)	511(4)	537(2)	35(1)
C(19)	7728(4)	-196(4)	-264(2)	30(1)
C(20)	9320(4)	-1380(4)	-481(2)	33(1)
C(21)	9902(4)	-2044(4)	-1238(2)	33(1)
C(22)	8956(4)	-1536(4)	-1801(2)	33(1)
C(23)	7374(4)	-356(4)	-1590(2)	35(1)
C(24)	6770(4)	290(4)	-833(2)	33(1)
C(25)	1336(3)	1614(4)	5916(2)	28(1)
C(26)	563(3)	2350(4)	6738(2)	26(1)
C(27)	-232(4)	1685(4)	7230(2)	32(1)
C(28)	-976(4)	2327(4)	7983(2)	33(1)
C(29)	-939(3)	3651(4)	8264(2)	29(1)
C(30)	-157(4)	4321(4)	7771(2)	29(1)
C(31)	591(4)	3673(4)	7015(2)	28(1)
C(32)	-1707(4)	4340(4)	9059(2)	33(1)
C(33)	-2275(3)	4881(3)	9673(2)	31(1)
C(34)	-2999(4)	5522(4)	10494(2)	28(1)
C(35)	-4081(4)	5099(4)	10941(2)	33(1)
C(36)	-4716(4)	5686(4)	11706(2)	35(1)
C(37)	-4304(4)	6720(4)	12045(2)	35(1)
C(38)	-3249(4)	7171(4)	11600(2)	35(1)
C(39)	-2594(4)	6567(4)	10835(2)	32(1)

Table SIII-5. Hydrogen coordinates (x 10^4) and isotropic displacement parameters ($Å^2$ x 10^3) for C37 H27 Br N2.

	x	y	z	U_{eq}
H(2)	1508	3560	4807	34
H(5)	4345	-51	6585	32
H(6)	7003	-625	6603	36
H(7)	8255	599	5832	36
H(8)	6937	2413	4991	33
H(10A)	4766	4527	4406	36
H(10B)	2984	5115	4258	36
H(12)	7036	2597	3487	36
H(13)	8042	1253	2255	37
H(15)	3506	2657	1912	35
H(16)	2518	3899	3160	35
H(20)	9991	-1720	-105	40
H(21)	10964	-2859	-1376	40
H(22)	9374	-1982	-2323	40
H(23)	6718	-2	-1971	42
H(24)	5692	1074	-694	39
H(25A)	1814	473	5922	33
H(25B)	504	1943	5592	33
H(27)	-260	782	7044	38
H(28)	-1514	1866	8311	40
H(30)	-135	5228	7956	35
H(31)	1123	4137	6686	33
H(35)	-4378	4407	10716	39
H(36)	-5440	5387	12007	42
H(37)	-4739	7112	12575	42
H(38)	-2982	7890	11822	42
H(39)	-1863	6861	10536	38

Table SIII-6. Anisotropic parameters ($Å^2$ x 10^3) for C37 H27 Br N2.

The anisotropic displacement factor exponent takes the form:

$$-2 \pi^2 [h^2 a^{*2} U_{11} + ... + 2 h k a^* b^* U_{12}]$$

	U11	U22	U33	U23	U13	U12
Br(1)	26(1)	38(1)	32(1)	5(1)	-4(1)	-20(1)
N(1)	29(1)	30(1)	23(1)	0(1)	0(1)	-17(1)
C(2)	29(1)	30(2)	25(1)	0(1)	-2(1)	-16(1)
N(3)	25(1)	34(1)	24(1)	1(1)	0(1)	-18(1)
C(4)	25(1)	29(1)	23(1)	-3(1)	1(1)	-17(1)
C(5)	30(2)	30(2)	23(1)	-1(1)	1(1)	-18(1)
C(6)	30(2)	33(2)	26(1)	0(1)	-5(1)	-14(1)
C(7)	25(1)	35(2)	31(2)	-3(1)	-2(1)	-16(1)
C(8)	29(1)	32(2)	26(1)	-4(1)	4(1)	-20(1)
C(9)	27(1)	27(1)	22(1)	-2(1)	0(1)	-15(1)
C(10)	36(2)	31(2)	27(1)	3(1)	0(1)	-20(1)
C(11)	30(2)	30(2)	24(1)	5(1)	-3(1)	-19(1)
C(12)	30(2)	43(2)	27(1)	6(1)	-5(1)	-26(1)
C(13)	25(1)	38(2)	31(2)	8(1)	-2(1)	-17(1)
C(14)	35(2)	33(2)	24(1)	4(1)	-1(1)	-22(1)
C(15)	31(2)	34(2)	28(1)	6(1)	-8(1)	-20(1)
C(16)	26(1)	33(2)	32(2)	8(1)	-4(1)	-15(1)
C(17)	28(2)	27(2)	44(2)	8(1)	-2(1)	-16(1)
C(18)	45(2)	40(2)	37(2)	16(1)	-16(2)	-31(2)
C(19)	34(2)	32(2)	28(1)	2(1)	-1(1)	-21(1)
C(20)	32(2)	35(2)	37(2)	10(1)	-10(1)	-18(1)
C(21)	30(2)	31(2)	37(2)	4(1)	2(1)	-16(1)
C(22)	41(2)	31(2)	32(2)	1(1)	0(1)	-23(1)
C(23)	40(2)	35(2)	36(2)	4(1)	-10(1)	-21(2)
C(24)	28(2)	34(2)	36(2)	1(1)	-3(1)	-16(1)
C(25)	26(1)	34(2)	27(1)	0(1)	0(1)	-20(1)
C(26)	21(1)	32(2)	26(1)	4(1)	-2(1)	-14(1)
C(27)	30(2)	34(2)	36(2)	1(1)	0(1)	-21(1)
C(28)	31(2)	40(2)	32(2)	4(1)	3(1)	-22(1)
C(29)	22(1)	35(2)	28(1)	2(1)	-2(1)	-12(1)
C(30)	28(1)	30(2)	29(2)	1(1)	-4(1)	-15(1)
C(31)	28(1)	32(2)	26(1)	5(1)	-1(1)	-18(1)
C(32)	26(1)	38(2)	38(2)	11(1)	-6(1)	-18(1)
C(33)	21(1)	26(2)	47(2)	2(1)	-9(1)	-10(1)
C(34)	25(1)	32(2)	25(1)	2(1)	-2(1)	-12(1)
C(35)	32(2)	34(2)	38(2)	4(1)	-5(1)	-20(1)
C(36)	32(2)	35(2)	35(2)	5(1)	4(1)	-16(1)
C(37)	36(2)	33(2)	29(2)	0(1)	-2(1)	-12(1)
C(38)	33(2)	38(2)	34(2)	2(1)	-10(1)	-16(1)
C(39)	28(2)	32(2)	38(2)	8(1)	-5(1)	-16(1)

Table SIII-7. Bond lengths [Å] and angles [°] for C37 H27 Br N2

N(1)-C(2)	1.328(4)	C(5)-C(4)-C(9)	121.7(3)
N(1)-C(9)	1.395(4)	N(3)-C(4)-C(9)	106.2(3)
N(1)-C(10)	1.480(4)	C(6)-C(5)-C(4)	116.3(3)
C(2)-N(3)	1.323(4)	C(5)-C(6)-C(7)	121.8(3)
N(3)-C(4)	1.396(4)	C(8)-C(7)-C(6)	122.1(3)
N(3)-C(25)	1.471(3)	C(7)-C(8)-C(9)	116.4(3)
C(4)-C(5)	1.390(4)	C(8)-C(9)-N(1)	132.1(3)
C(4)-C(9)	1.401(4)	C(8)-C(9)-C(4)	121.7(3)
C(5)-C(6)	1.384(4)	N(1)-C(9)-C(4)	106.2(2)
C(6)-C(7)	1.405(4)	N(1)-C(10)-C(11)	112.3(2)
C(7)-C(8)	1.376(5)	C(16)-C(11)-C(12)	119.2(3)
C(8)-C(9)	1.393(4)	C(16)-C(11)-C(10)	120.3(3)
C(10)-C(11)	1.503(4)	C(12)-C(11)-C(10)	120.5(3)
C(11)-C(16)	1.396(4)	C(13)-C(12)-C(11)	120.0(3)
C(11)-C(12)	1.396(4)	C(12)-C(13)-C(14)	121.0(3)
C(12)-C(13)	1.387(4)	C(13)-C(14)-C(15)	118.6(3)
C(13)-C(14)	1.399(4)	C(13)-C(14)-C(17)	120.4(3)
C(14)-C(15)	1.409(4)	C(15)-C(14)-C(17)	120.9(3)
C(14)-C(17)	1.464(4)	C(16)-C(15)-C(14)	120.2(3)
C(15)-C(16)	1.379(4)	C(15)-C(16)-C(11)	121.0(3)
C(17)-C(18)	1.136(5)	C(18)-C(17)-C(14)	177.6(3)
C(18)-C(19)	1.463(4)	C(17)-C(18)-C(19)	179.7(5)
C(19)-C(24)	1.404(5)	C(24)-C(19)-C(20)	118.6(3)
C(19)-C(20)	1.413(5)	C(24)-C(19)-C(18)	119.6(3)
C(20)-C(21)	1.380(5)	C(20)-C(19)-C(18)	121.7(3)
C(21)-C(22)	1.388(5)	C(21)-C(20)-C(19)	120.1(3)
C(22)-C(23)	1.404(5)	C(20)-C(21)-C(22)	120.8(3)
C(23)-C(24)	1.375(5)	C(21)-C(22)-C(23)	119.4(3)
C(25)-C(26)	1.510(4)	C(24)-C(23)-C(22)	120.3(3)
C(26)-C(31)	1.388(4)	C(23)-C(24)-C(19)	120.7(3)
C(26)-C(27)	1.401(4)	N(3)-C(25)-C(26)	112.7(2)
C(27)-C(28)	1.382(4)	C(31)-C(26)-C(27)	119.1(3)
C(28)-C(29)	1.397(4)	C(31)-C(26)-C(25)	122.4(3)
C(29)-C(30)	1.396(4)	C(27)-C(26)-C(25)	118.6(3)
C(29)-C(32)	1.458(4)	C(28)-C(27)-C(26)	120.8(3)
C(30)-C(31)	1.389(4)	C(27)-C(28)-C(29)	120.1(3)
C(32)-C(33)	1.127(5)	C(30)-C(29)-C(28)	119.1(3)
C(33)-C(34)	1.483(4)	C(30)-C(29)-C(32)	119.9(3)
C(34)-C(35)	1.401(4)	C(28)-C(29)-C(32)	121.0(3)
C(34)-C(39)	1.406(4)	C(31)-C(30)-C(29)	120.6(3)
C(35)-C(36)	1.377(5)	C(26)-C(31)-C(30)	120.3(3)
C(36)-C(37)	1.399(5)	C(33)-C(32)-C(29)	178.5(3)
C(37)-C(38)	1.398(5)	C(32)-C(33)-C(34)	177.4(3)
C(38)-C(39)	1.382(5)	C(35)-C(34)-C(39)	119.1(3)
C(2)-N(1)-C(9)	108.4(2)	C(35)-C(34)-C(33)	121.1(3)
C(2)-N(1)-C(10)	125.1(3)	C(39)-C(34)-C(33)	119.8(3)
C(9)-N(1)-C(10)	126.5(2)	C(36)-C(35)-C(34)	120.1(3)
N(3)-C(2)-N(1)	110.7(3)	C(35)-C(36)-C(37)	120.7(3)
C(2)-N(3)-C(4)	108.5(2)	C(38)-C(37)-C(36)	119.6(3)
C(2)-N(3)-C(25)	125.3(3)	C(39)-C(38)-C(37)	119.8(3)
C(4)-N(3)-C(25)	126.2(2)	C(38)-C(39)-C(34)	120.7(3)
C(5)-C(4)-N(3)	132.0(3)		

Table SIII-8. Torsion angles [°] for C37 H27 Br N2.

C(9)-N(1)-C(2)-N(3)	-0.3(3)
C(10)-N(1)-C(2)-N(3)	179.8(2)
N(1)-C(2)-N(3)-C(4)	0.5(3)
N(1)-C(2)-N(3)-C(25)	178.8(2)
C(2)-N(3)-C(4)-C(5)	-178.9(3)
C(25)-N(3)-C(4)-C(5)	2.9(5)
C(2)-N(3)-C(4)-C(9)	-0.5(3)
C(25)-N(3)-C(4)-C(9)	-178.7(2)
N(3)-C(4)-C(5)-C(6)	177.0(3)
C(9)-C(4)-C(5)-C(6)	-1.2(4)
C(4)-C(5)-C(6)-C(7)	1.3(4)
C(5)-C(6)-C(7)-C(8)	-0.6(5)
C(6)-C(7)-C(8)-C(9)	-0.5(4)
C(7)-C(8)-C(9)-N(1)	-177.7(3)
C(7)-C(8)-C(9)-C(4)	0.6(4)
C(2)-N(1)-C(9)-C(8)	178.5(3)
C(10)-N(1)-C(9)-C(8)	-1.6(5)
C(2)-N(1)-C(9)-C(4)	0.0(3)
C(10)-N(1)-C(9)-C(4)	179.9(2)
C(5)-C(4)-C(9)-C(8)	0.2(4)
N(3)-C(4)-C(9)-C(8)	-178.4(3)
C(5)-C(4)-C(9)-N(1)	178.9(3)
N(3)-C(4)-C(9)-N(1)	0.3(3)
C(2)-N(1)-C(10)-C(11)	-88.5(3)
C(9)-N(1)-C(10)-C(11)	91.6(3)
N(1)-C(10)-C(11)-C(16)	87.0(4)
N(1)-C(10)-C(11)-C(12)	-92.1(3)
C(16)-C(11)-C(12)-C(13)	-1.1(5)
C(10)-C(11)-C(12)-C(13)	178.0(3)
C(11)-C(12)-C(13)-C(14)	1.9(5)
C(12)-C(13)-C(14)-C(15)	-1.1(5)
C(12)-C(13)-C(14)-C(17)	176.4(3)
C(13)-C(14)-C(15)-C(16)	-0.4(4)
C(17)-C(14)-C(15)-C(16)	-177.9(3)
C(14)-C(15)-C(16)-C(11)	1.2(5)
C(12)-C(11)-C(16)-C(15)	-0.4(5)
C(10)-C(11)-C(16)-C(15)	-179.5(3)
C(13)-C(14)-C(17)-C(18)	-55(9)
C(15)-C(14)-C(17)-C(18)	122(9)
C(14)-C(17)-C(18)-C(19)	-73(81)
C(17)-C(18)-C(19)-C(24)	-29(80)
C(17)-C(18)-C(19)-C(20)	152(100)
C(24)-C(19)-C(20)-C(21)	-0.5(4)
C(18)-C(19)-C(20)-C(21)	178.6(3)
C(19)-C(20)-C(21)-C(22)	1.7(4)
C(20)-C(21)-C(22)-C(23)	-1.5(4)
C(21)-C(22)-C(23)-C(24)	0.0(5)
C(22)-C(23)-C(24)-C(19)	1.2(5)
C(20)-C(19)-C(24)-C(23)	-1.0(4)
C(18)-C(19)-C(24)-C(23)	179.9(3)
C(2)-N(3)-C(25)-C(26)	-105.1(3)
C(4)-N(3)-C(25)-C(26)	72.9(4)
N(3)-C(25)-C(26)-C(31)	22.0(4)
N(3)-C(25)-C(26)-C(27)	-159.1(3)
C(31)-C(26)-C(27)-C(28)	-0.3(5)

C(25)-C(26)-C(27)-C(28)	-179.2(3)
C(26)-C(27)-C(28)-C(29)	-0.2(5)
C(27)-C(28)-C(29)-C(30)	0.6(5)
C(27)-C(28)-C(29)-C(32)	-179.5(3)
C(28)-C(29)-C(30)-C(31)	-0.7(5)
C(32)-C(29)-C(30)-C(31)	179.5(3)
C(27)-C(26)-C(31)-C(30)	0.2(5)
C(25)-C(26)-C(31)-C(30)	179.1(3)
C(29)-C(30)-C(31)-C(26)	0.2(5)
C(30)-C(29)-C(32)-C(33)	-34(14)
C(28)-C(29)-C(32)-C(33)	146(14)
C(29)-C(32)-C(33)-C(34)	-108(15)
C(32)-C(33)-C(34)-C(35)	-54(7)
C(32)-C(33)-C(34)-C(39)	126(7)
C(39)-C(34)-C(35)-C(36)	-1.0(5)
C(33)-C(34)-C(35)-C(36)	178.8(3)
C(34)-C(35)-C(36)-C(37)	0.6(5)
C(35)-C(36)-C(37)-C(38)	0.6(5)
C(36)-C(37)-C(38)-C(39)	-1.4(5)
C(37)-C(38)-C(39)-C(34)	1.1(5)
C(35)-C(34)-C(39)-C(38)	0.1(5)
C(33)-C(34)-C(39)-C(38)	-179.7(3)

ORTEP view of the C37 H27 Br N2 compound with the numbering scheme adopted. Ellipsoids drawn at 30% probability level. Hydrogen atoms are represented by sphere of arbitrary size.

REFERENCES

SAINT Release 7.34A, Integration Software for Single Crystal Data, 2006, Bruker AXS Inc., Madison, WI 53719-1173.

G.M. Sheldrick, SADABS, Bruker Area Detector Absorption Corrections, 2008, Bruker AXS Inc., Madison, WI 53719-1173.

G.M. Sheldrick, *Acta Cryst*., 2008, **A64**, 112-122.

SHELXTL version 6.12, 2001, Bruker AXS Inc., Madison, WI 53719-1173.

APEX2, Bruker Molecular Analysis Research Tool, 2009, Bruker AXS Inc., Madison, WI 53719-1173.

A.L. Spek, PLATON, A Multipurpose Crystallographic Tool, 2008, Utrecht University, Utrecht, The Netherlands.

T. Maris, UdMX, 2004, University of Montréal, Montréal, QC, Canada.

XPREP Version 2008/2, X-ray data Preparation and Reciprocal space Exploration Program, 2008, Bruker AXS Inc., Madison, WI 53719-1173.

Annexe 4 : Partie expérimentale du chapitre 6, article 5: « Stong properties of anion transporters: a result of depolarization and weakening of membrane »

NMR and MS spectra
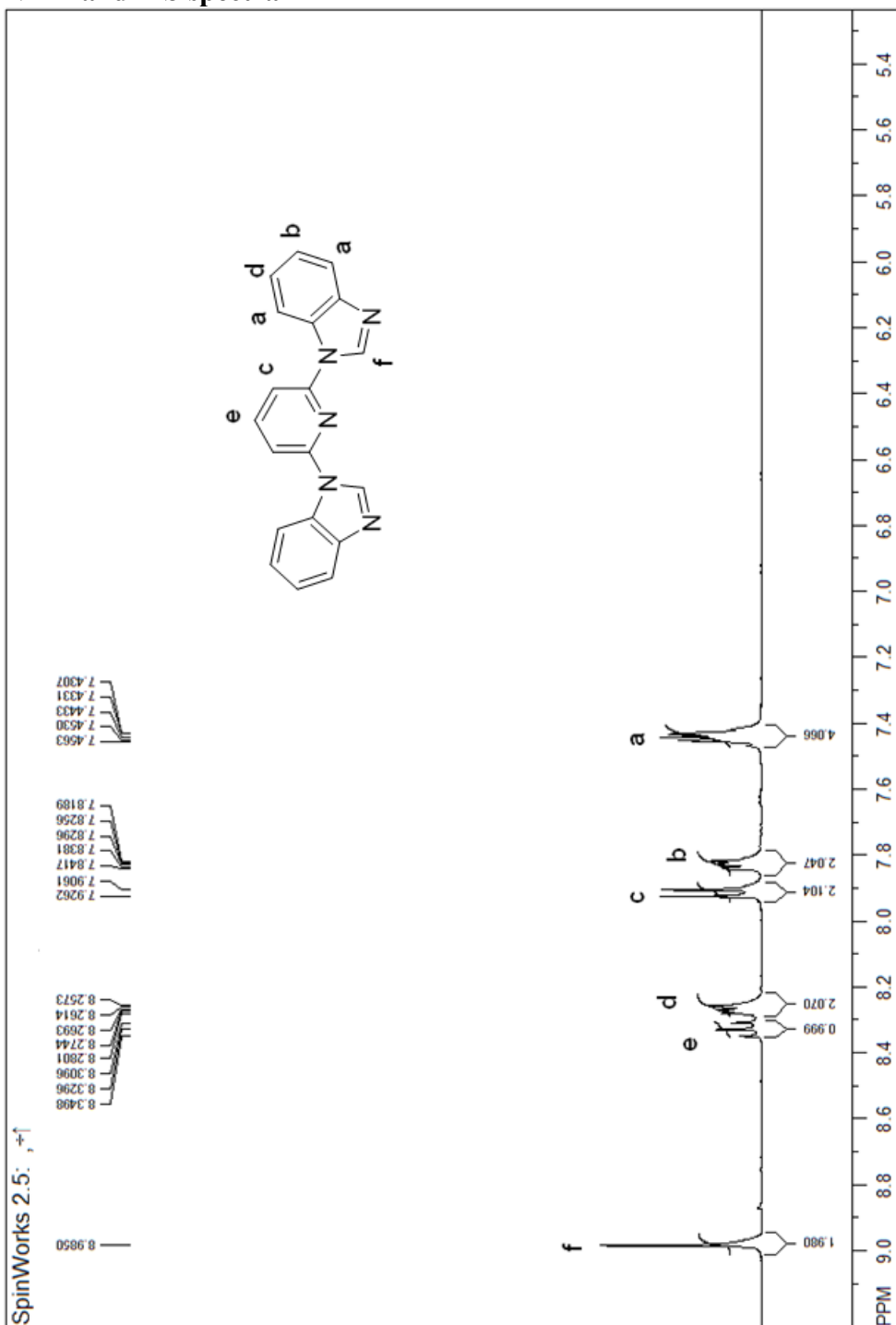
Supplementary figure S4.1. ^{1}H NMR (CD$_3$OD) spectrum of 2,6-bis(1H-benzo[d]imidazol-1-yl)pyridine.
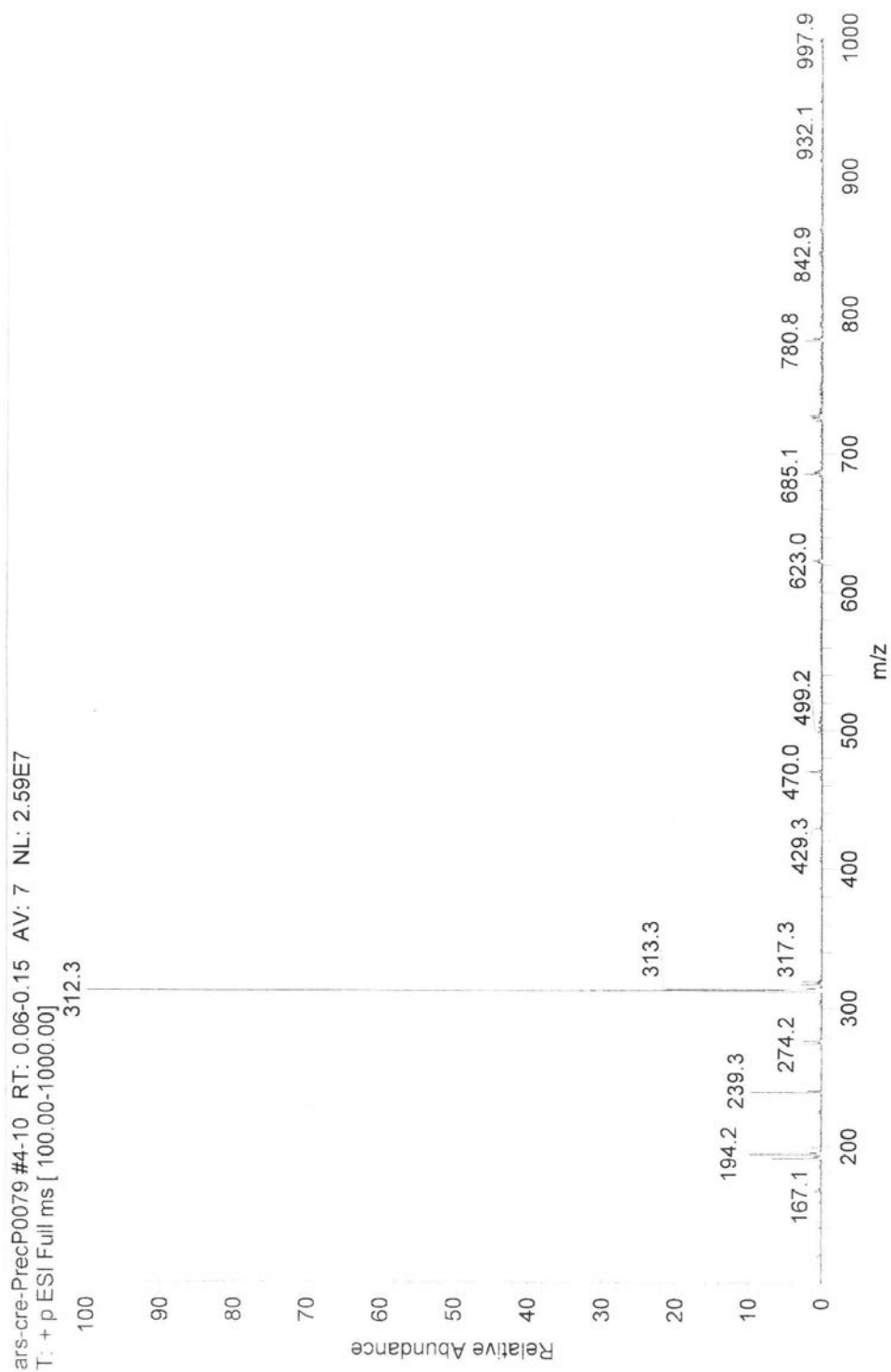
Supplementary figure S4.2. ESI mass spectrum (positive ionization) of 2,6-bis(1H-benzo[d]imidazol-1-yl)pyridine.
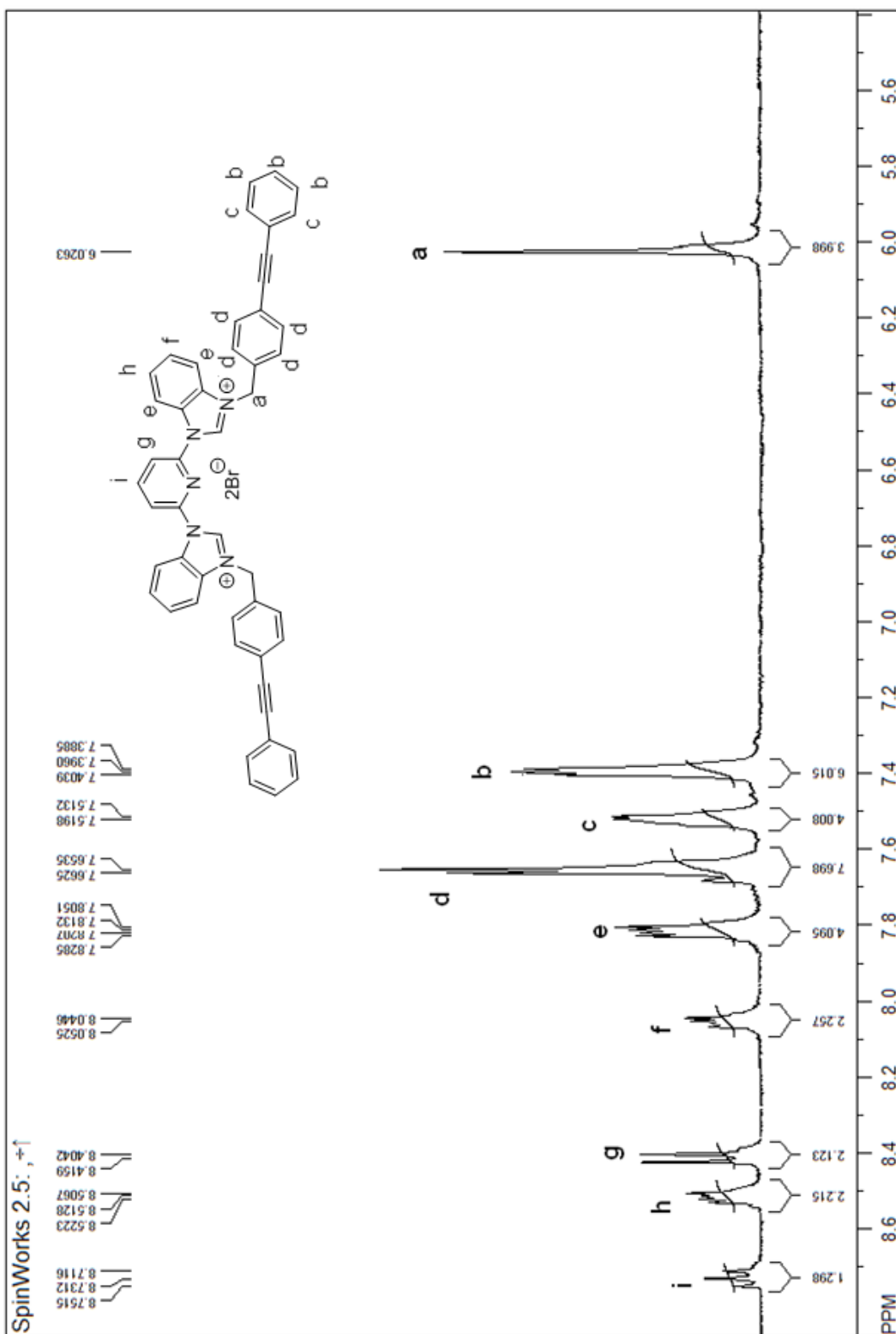
Supplementary figure S4.3. ^{1}H NMR (CD$_3$OD) spectrum of **6.3**.
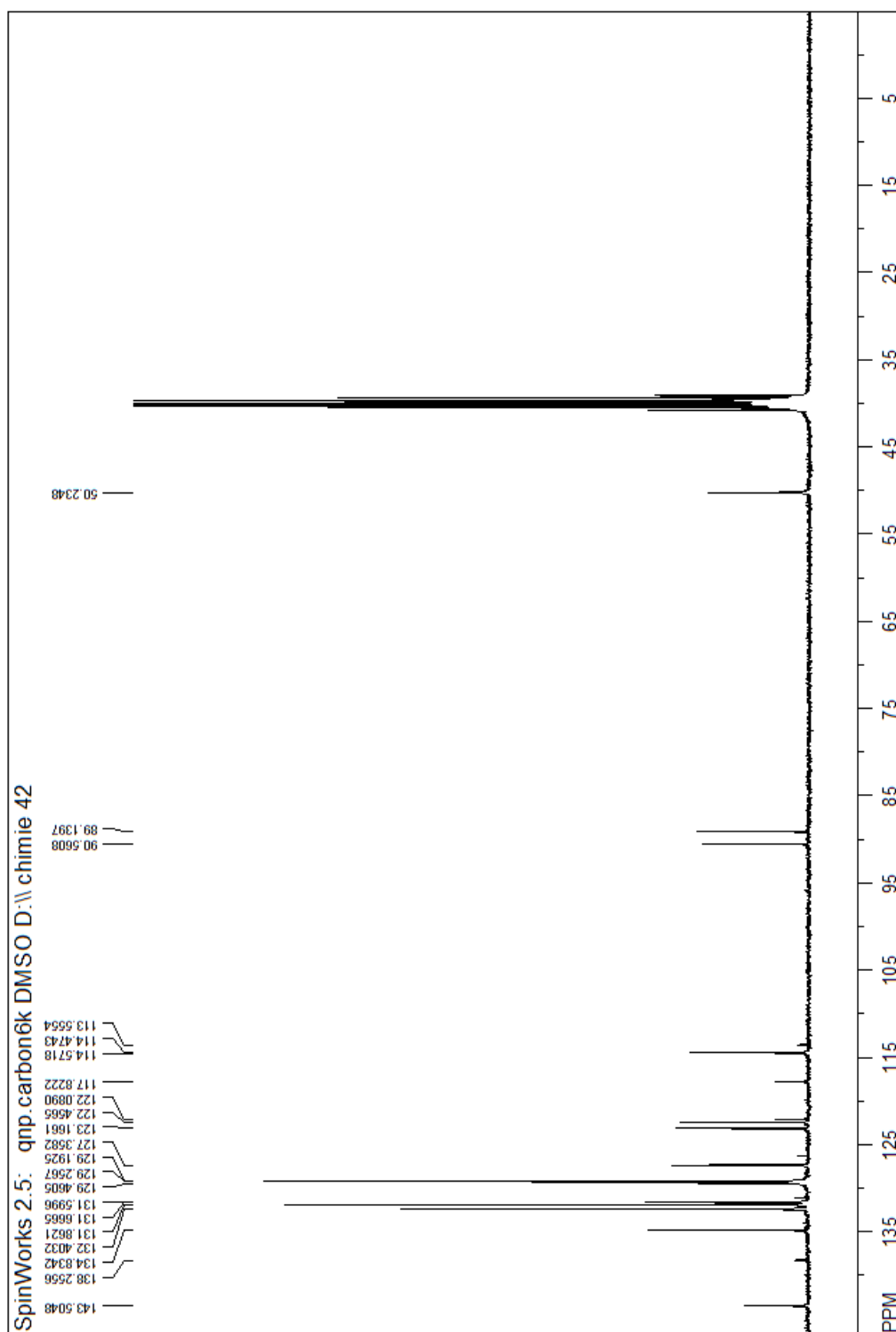
Supplementary figure S4.4. ^{13}C NMR (DMSO-d$_6$) spectrum of **6.3**.
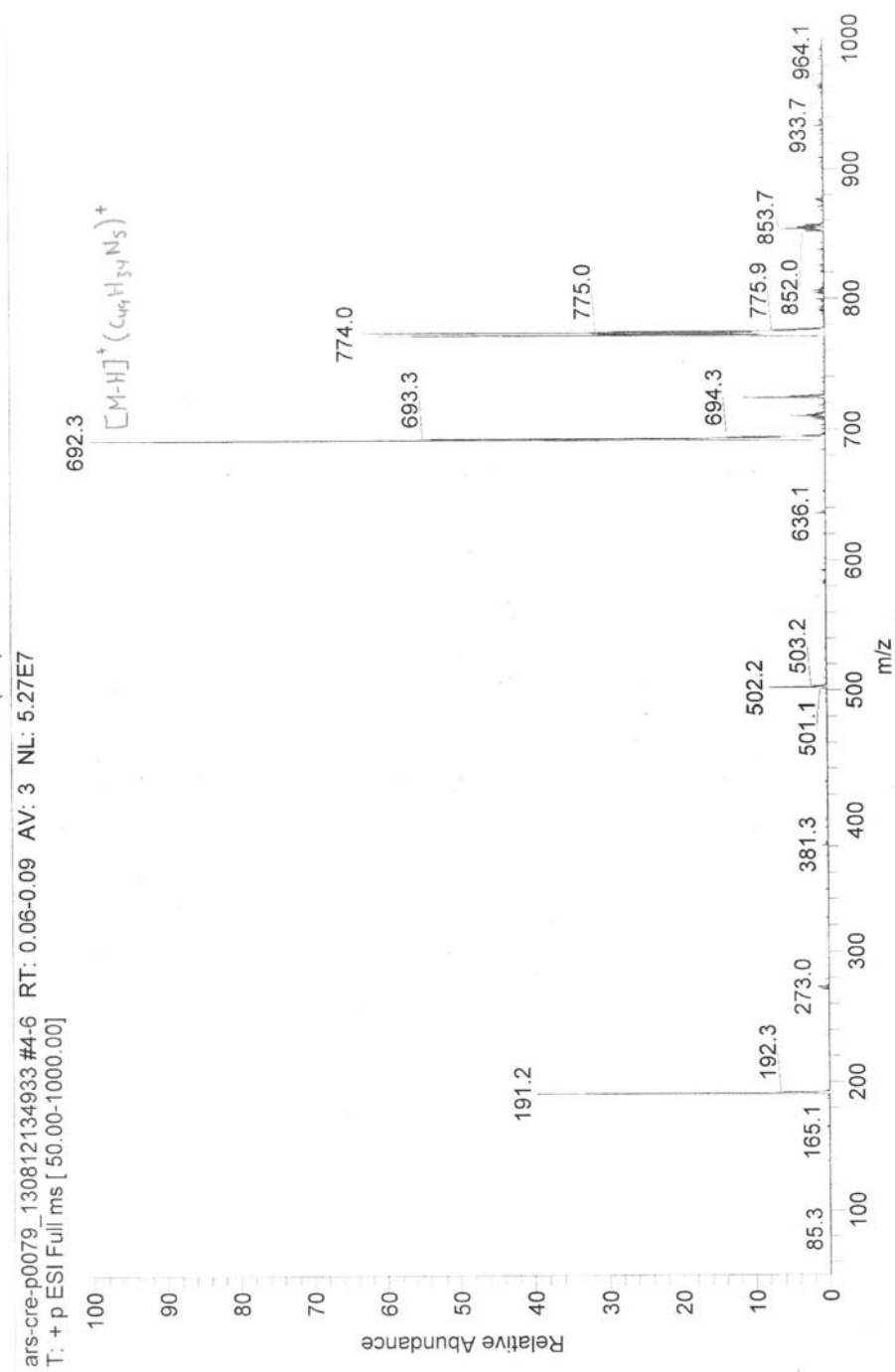
Supplementary figure S4.5. ESI mass spectrum (positive ionization) of **6.3**.
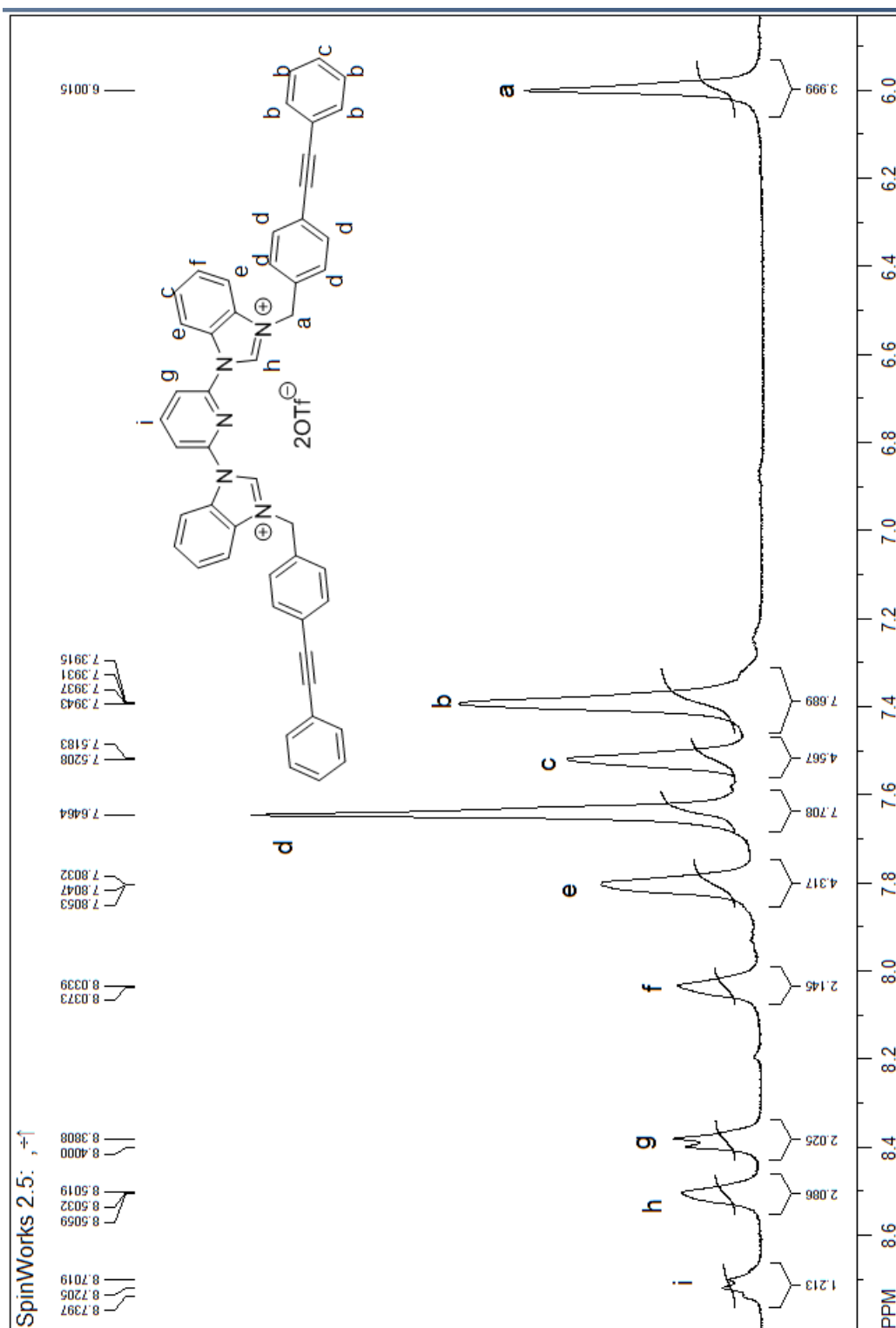
Supplementary figure S4.6. ^{1}H NMR (CD$_3$OD) spectrum of **6.5**.
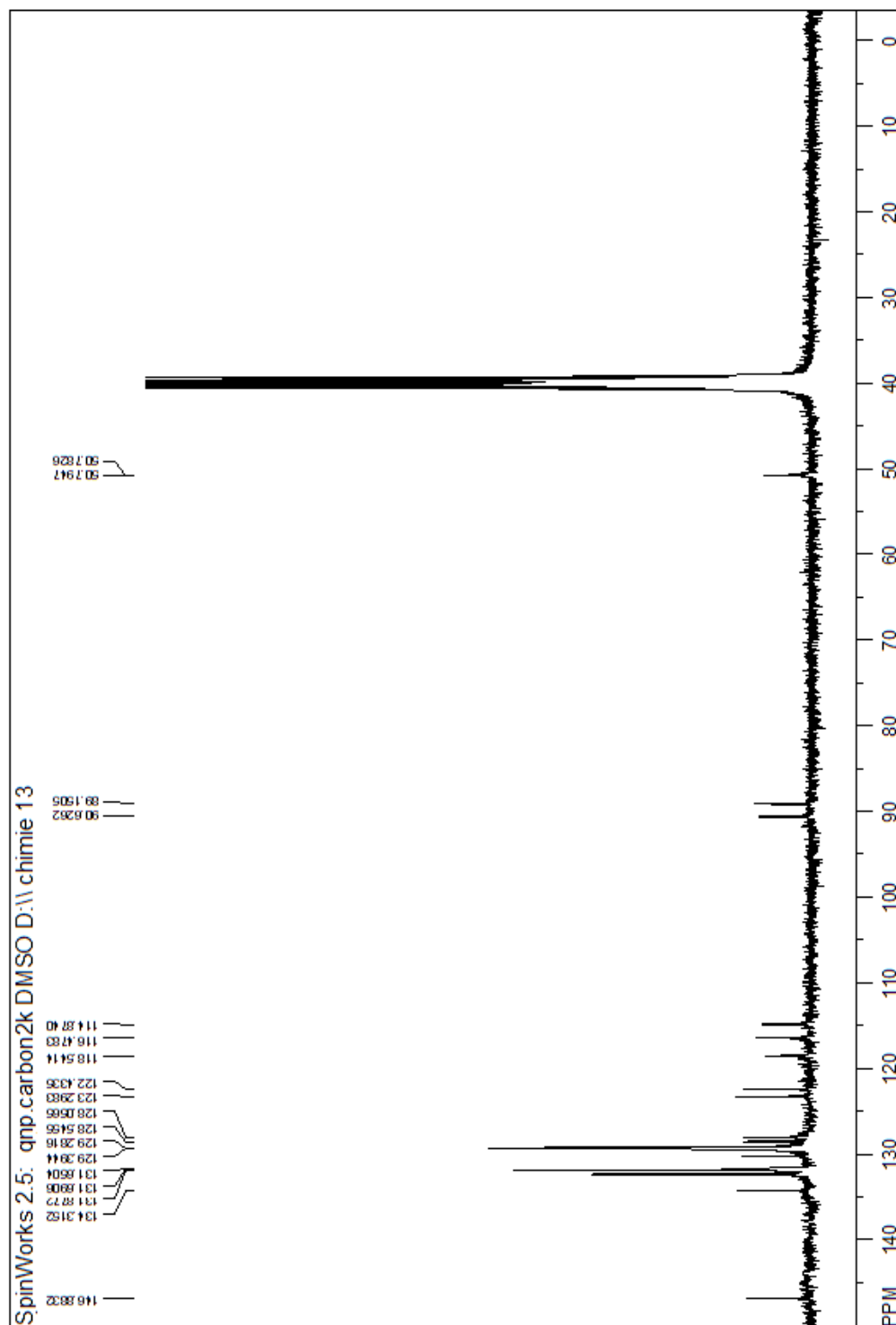
Supplementary figure S4.7. ^{13}C NMR (DMSO-d$_6$) spectrum of **6.5**.
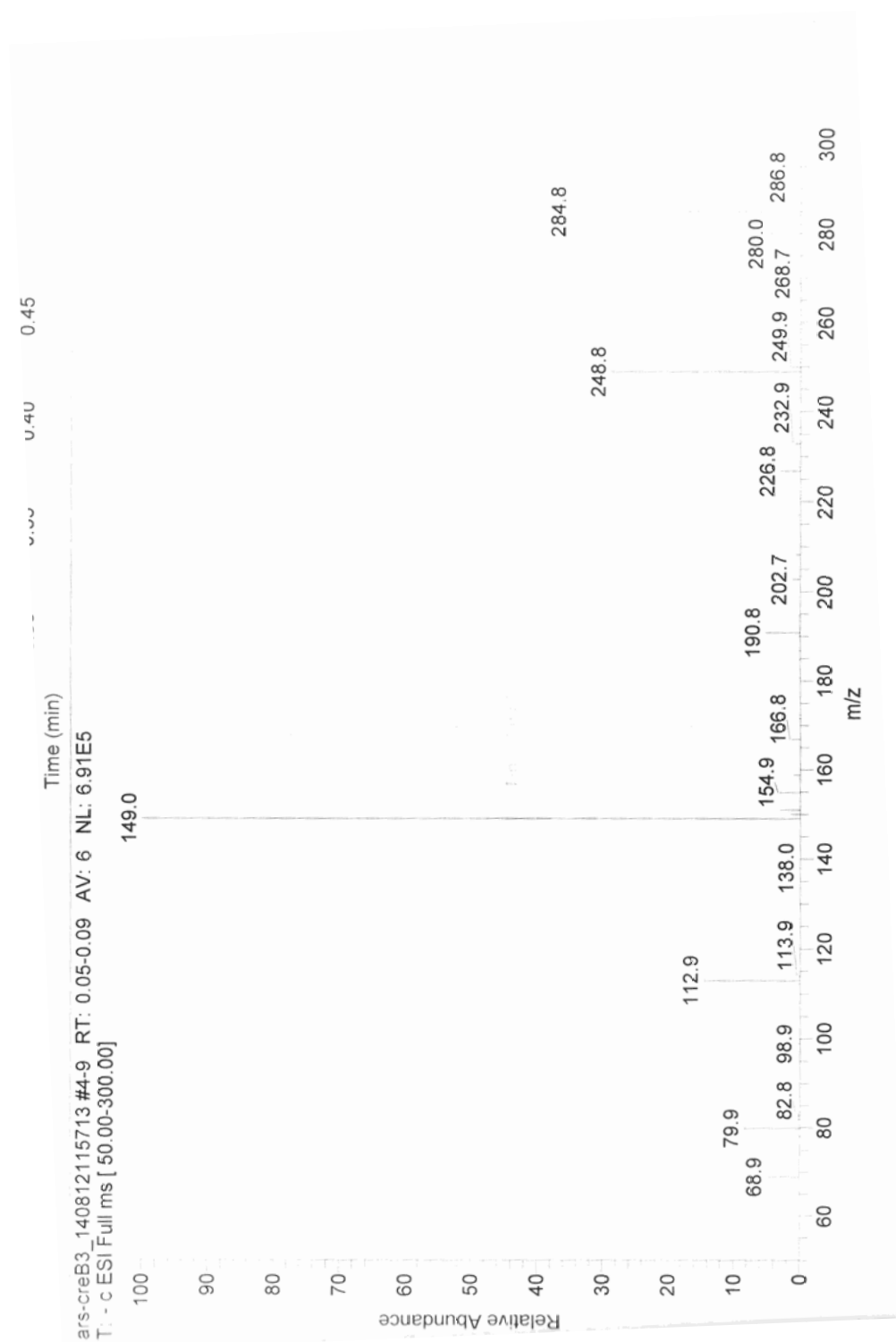
Supplementary figure S4.8. ESI mass spectrum (negative ionization) of **6.5**.
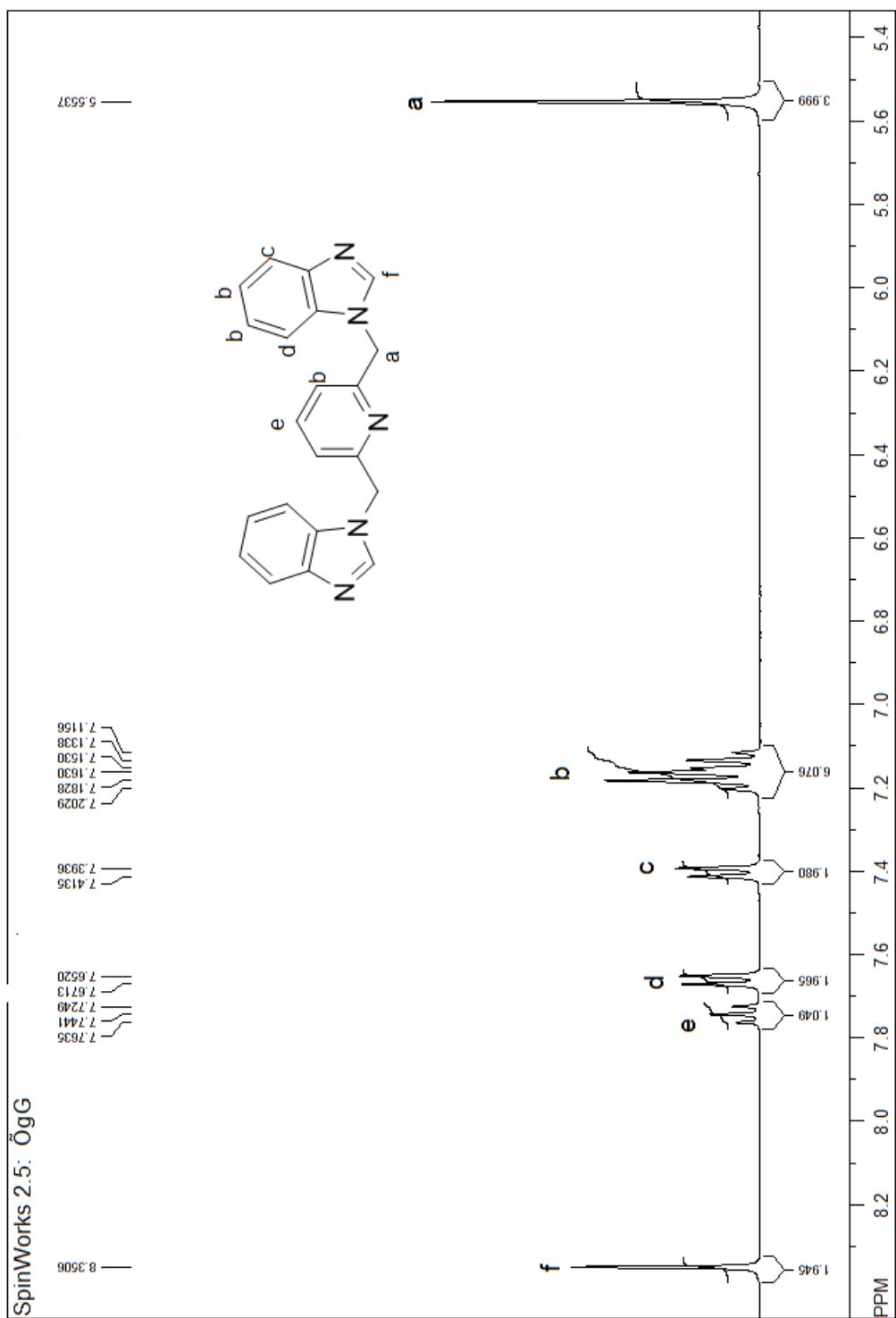
Supplementary figure S4.9. ^{1}H NMR (CD₃OD) spectrum of 2,6-bis((1H-benzo[d]imidazol-1-yl)methyl)pyridine.
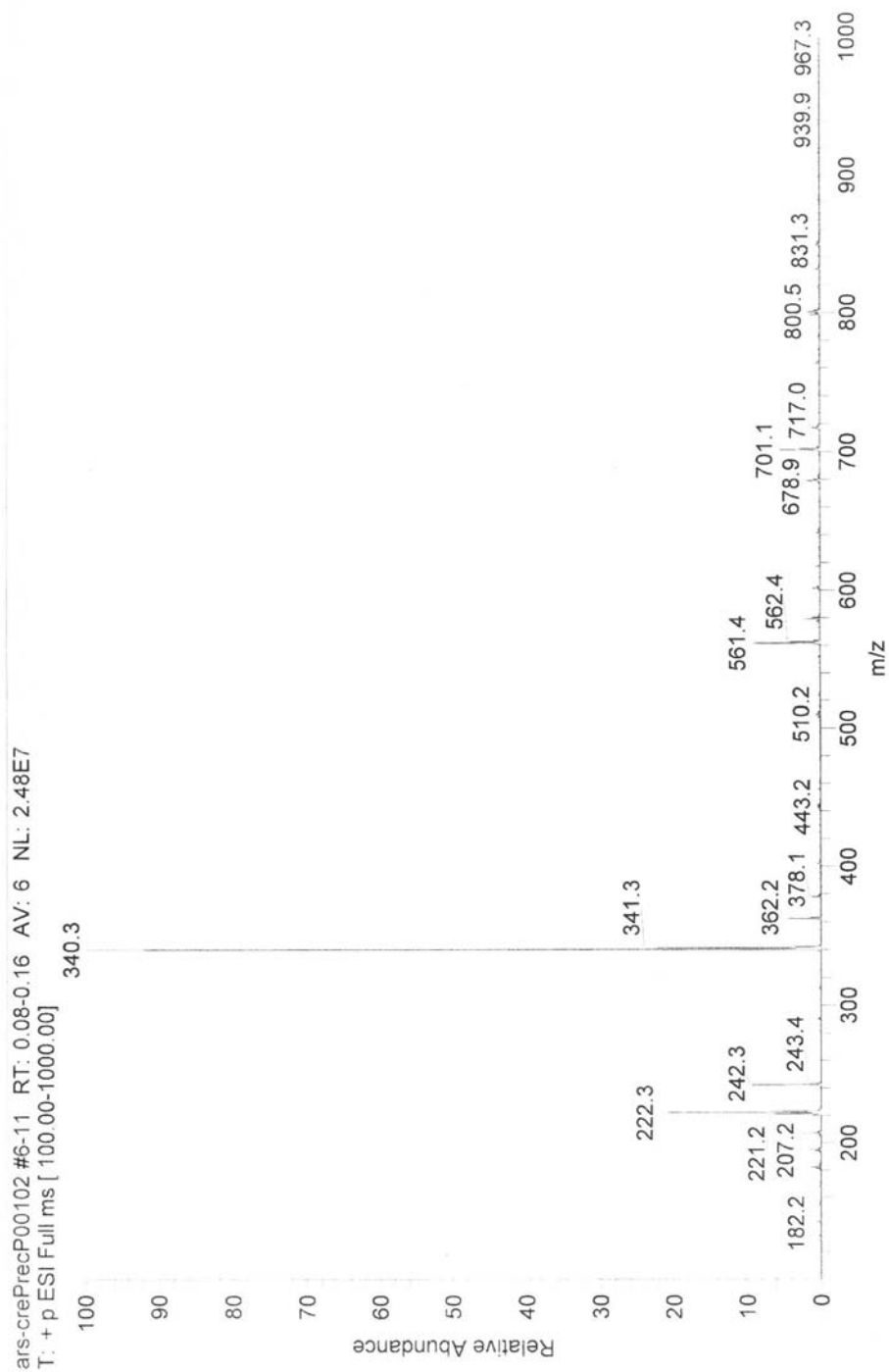
Supplementary figure S4.10. ESI mass spectrum (positive ionization) of 2,6-bis((1H-benzo[d]imidazol-1-yl)methyl)pyridine.
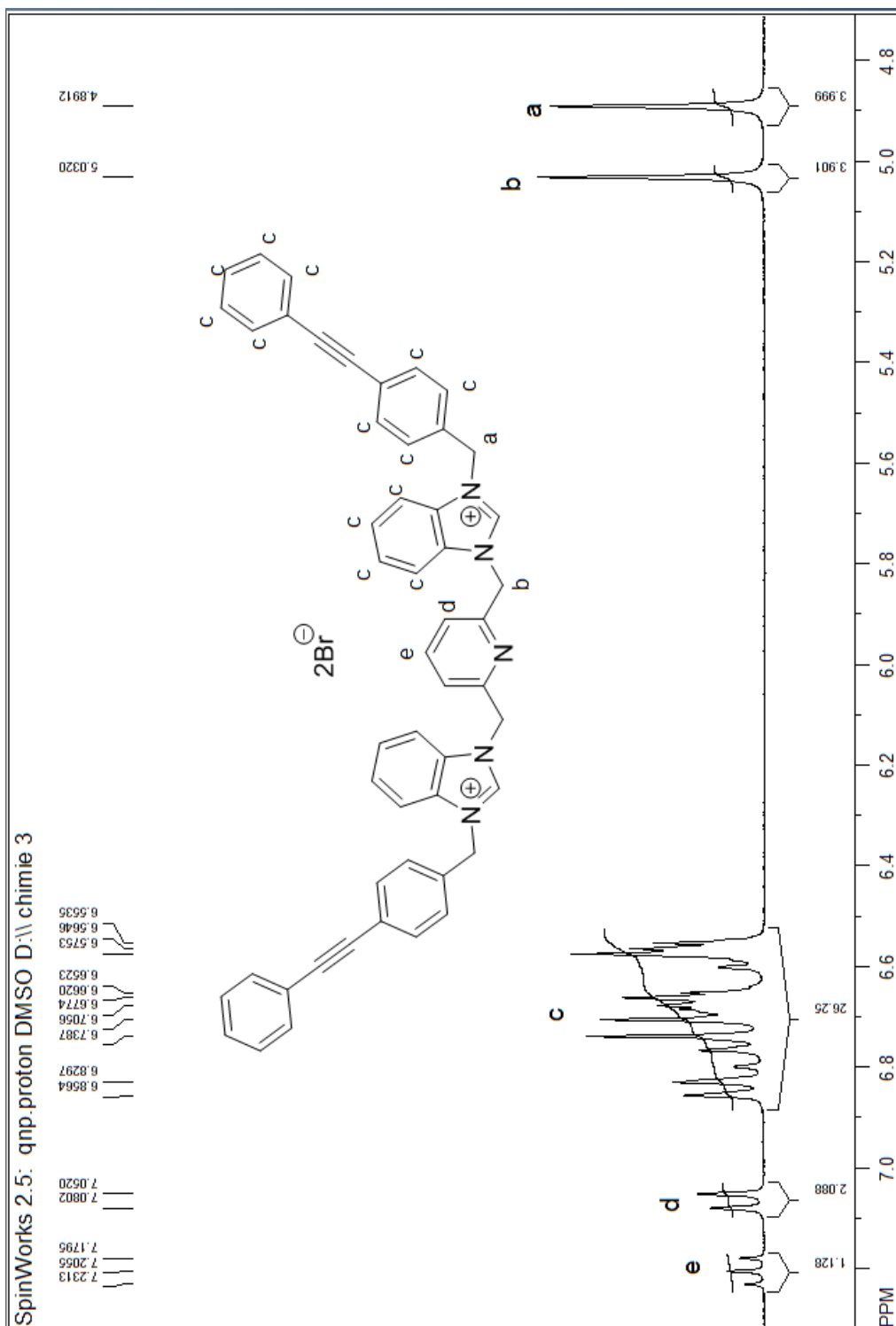
Supplementary figure S4.11. ^{1}H NMR (CD3OD) spectrum of **6.6**.
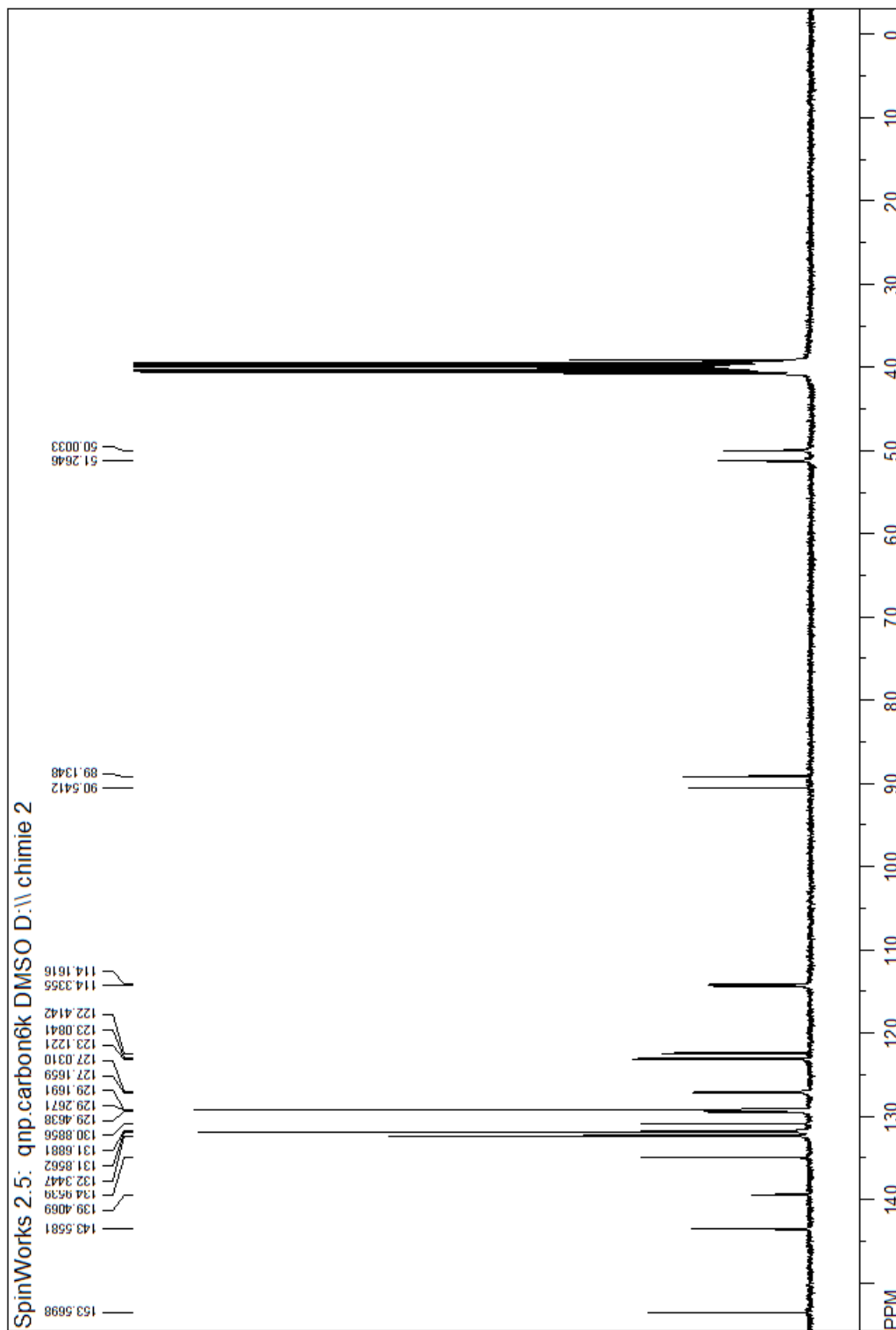
Supplementary figure S4.12. ^{13}C NMR (DMSO-d$_6$) spectrum of **6.6**
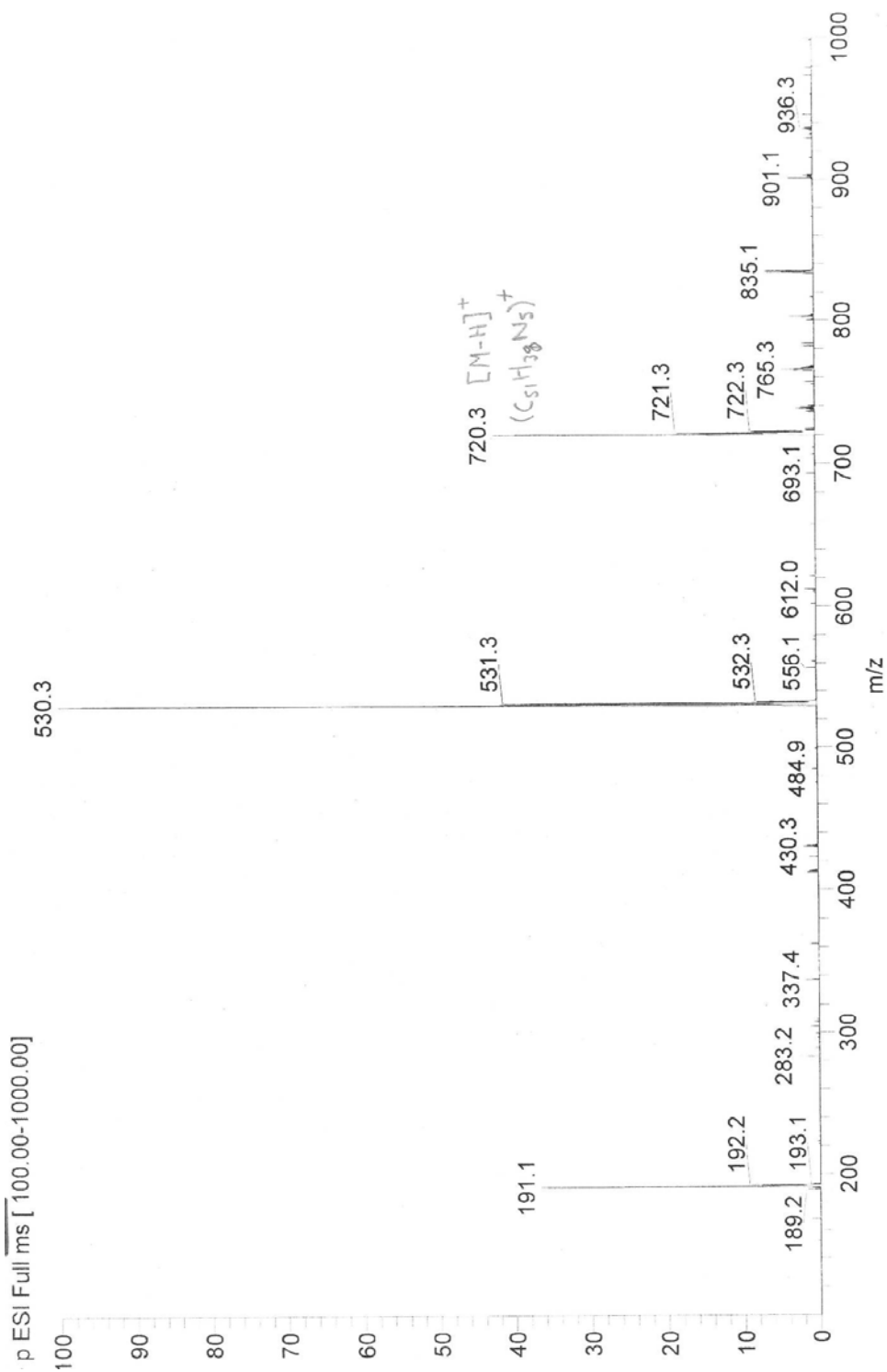
Supplementary figure S4.13. ESI mass spectrum (positive ionization) of **6.6**.
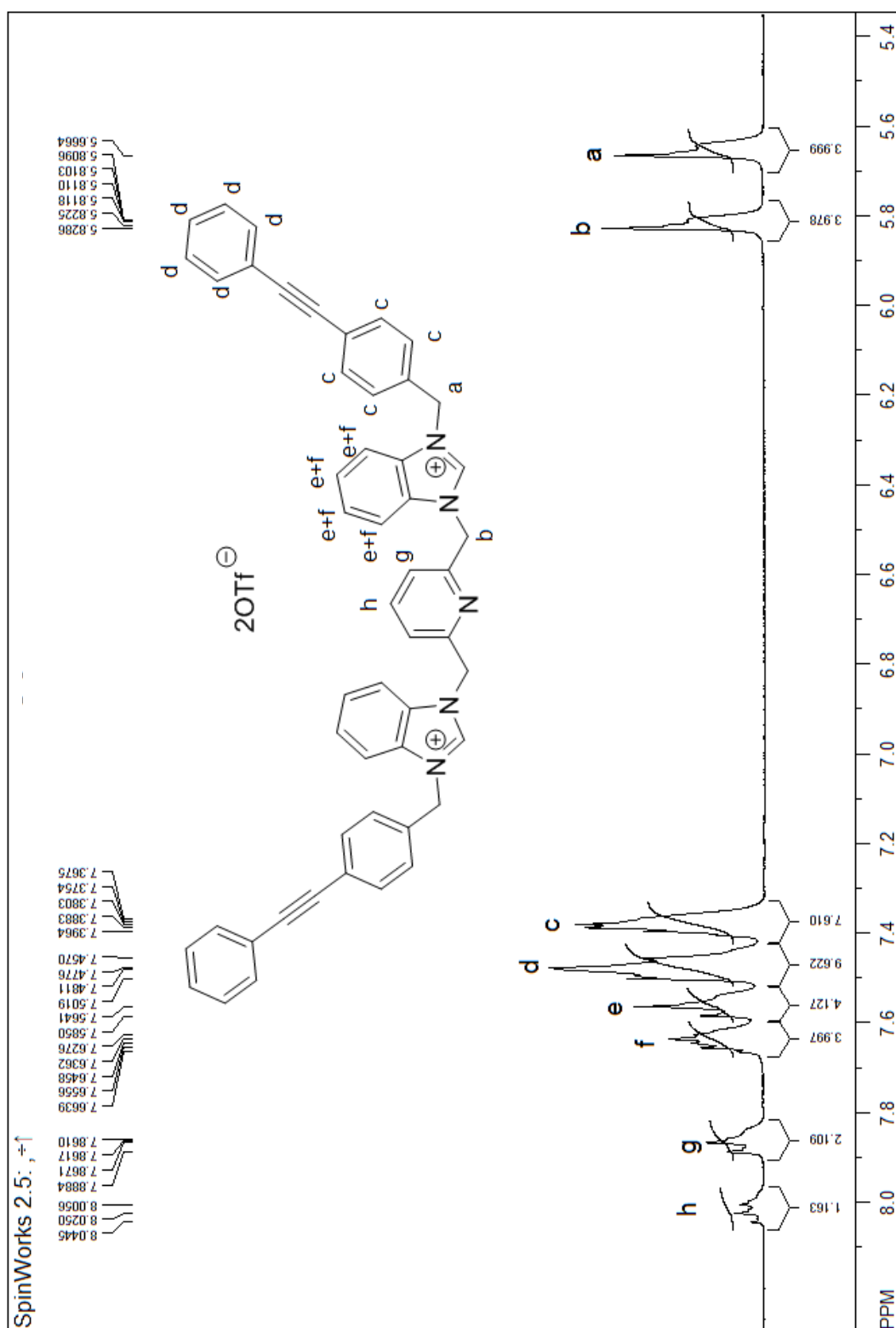
Supplementary figure S4.14. ^{1}H NMR (CD$_3$OD) spectrum of **6.8**.
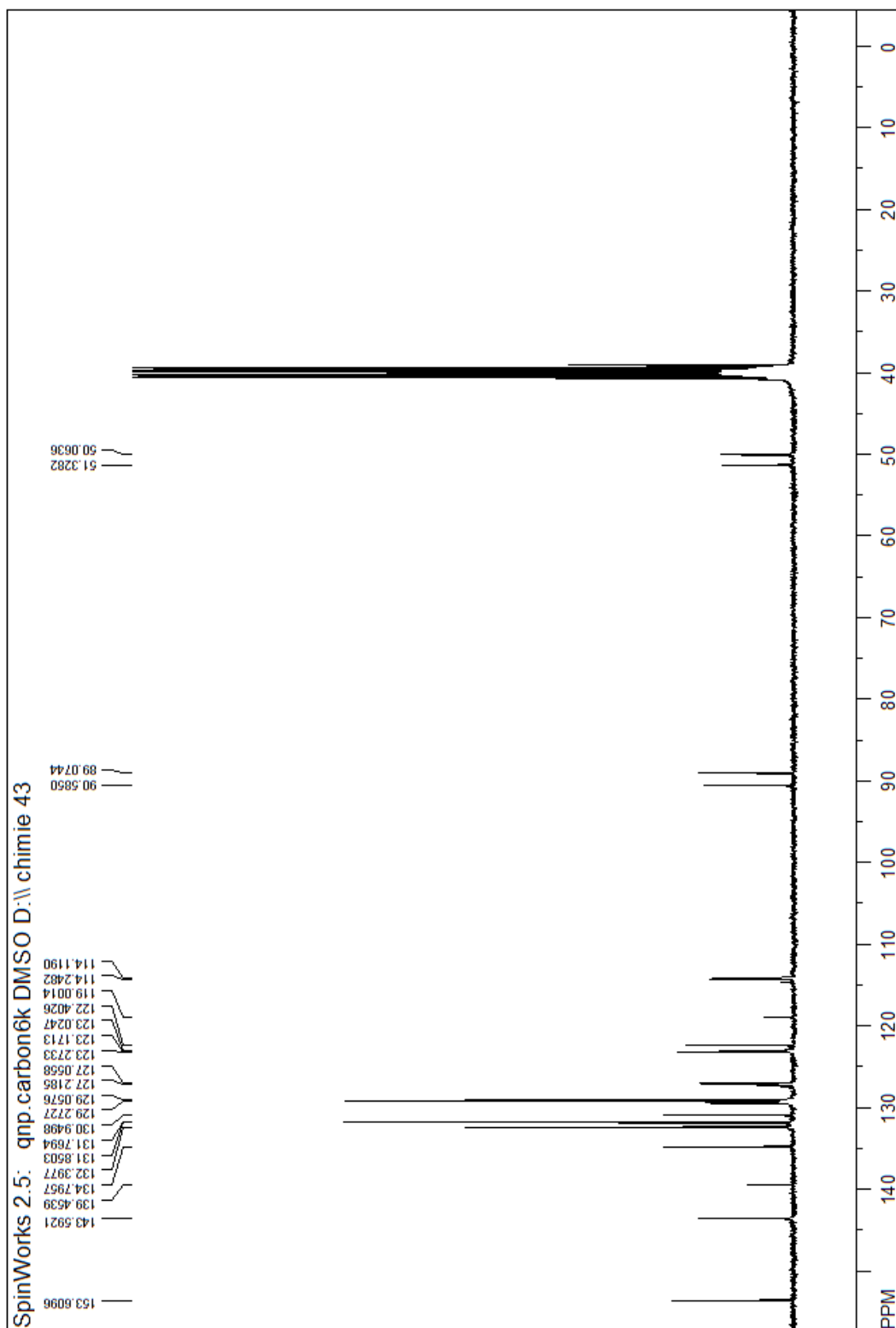
Supplementary figure S4.15. ^{13}C NMR (DMSO-d_6) spectrum of **6.8**.
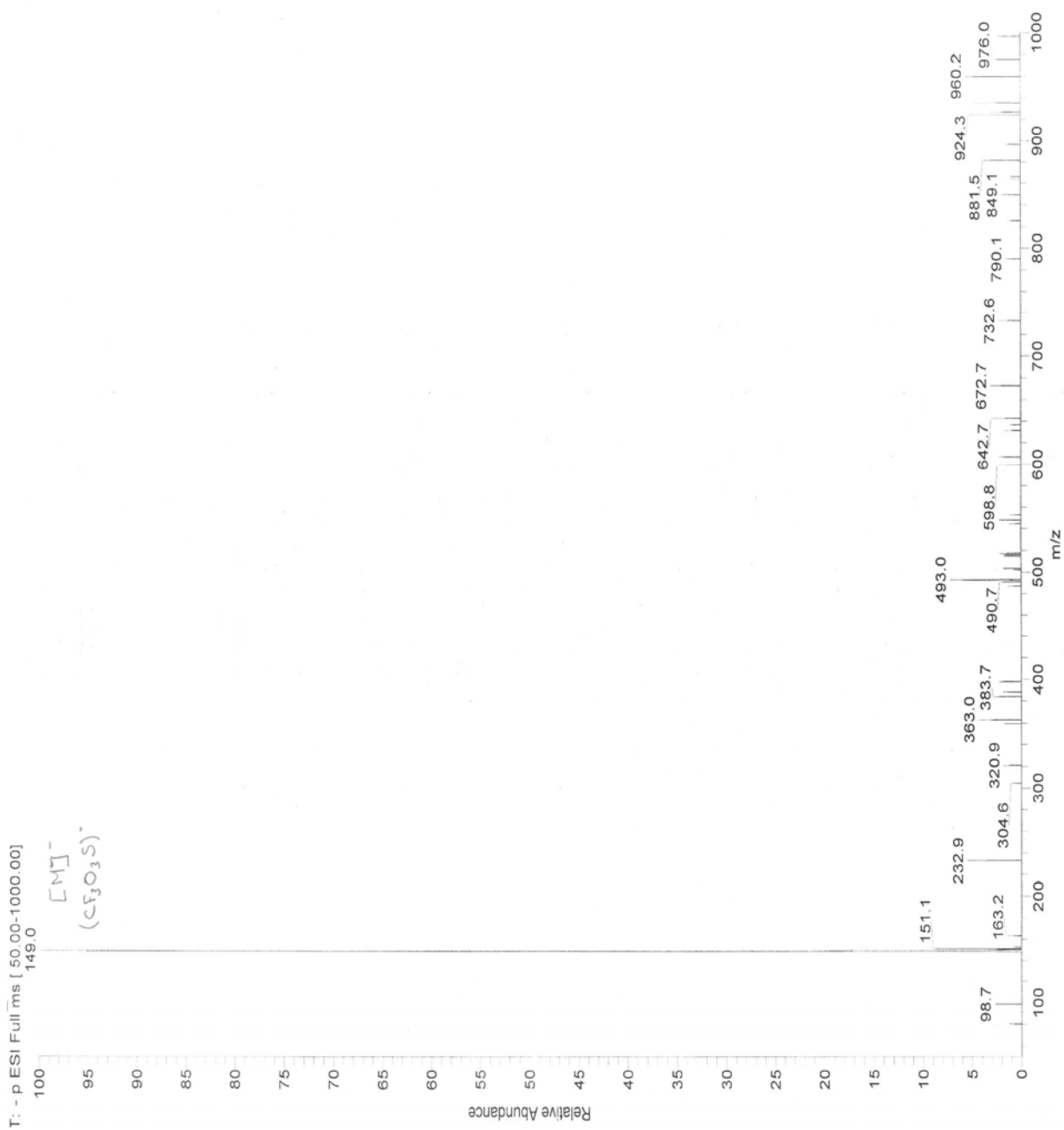
Supplementary figure S4.16. ESI mass spectrum (negative ionization) of **6.8**.
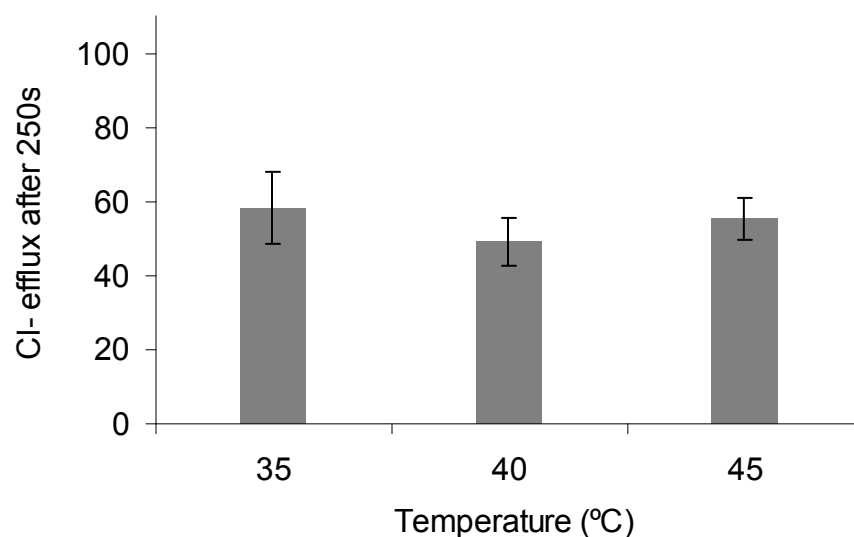
Supplementary figure S4.17. Chloride efflux out of DPPC liposomes at 35 °C, 40 °C and 45 °C. The data at each temperature are obtained by using 10 mol% of benzimidazolium salt 6.1 (relative to DPPC concentrations). The data at each temperature are the average of three series of measurements.
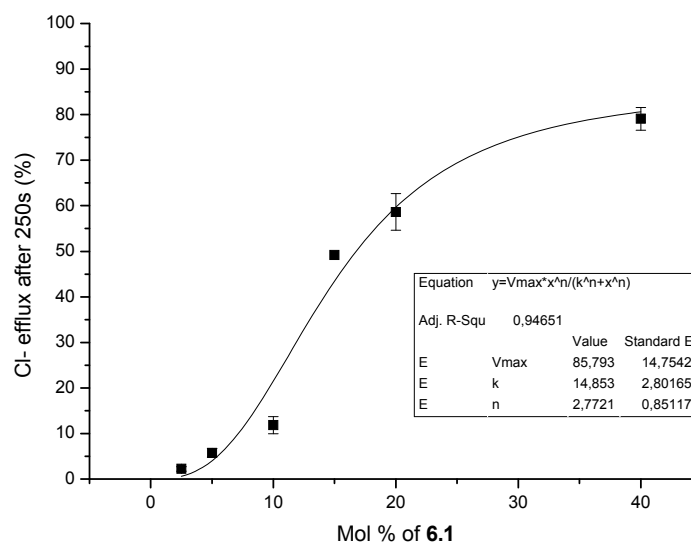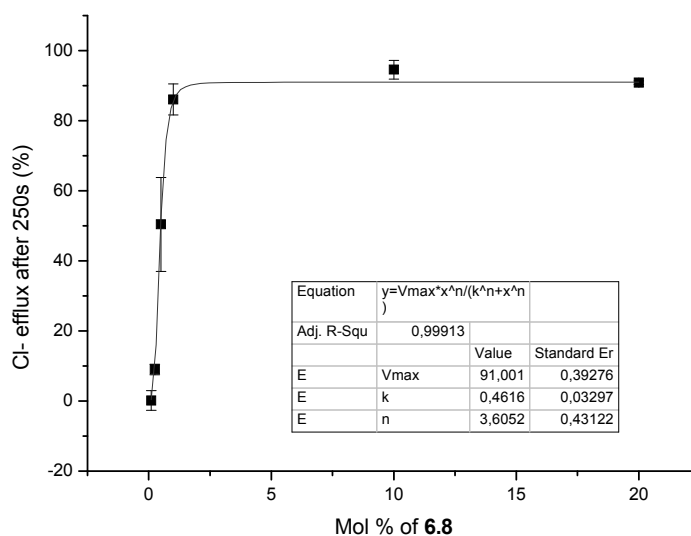

Supplementary figure S4.18. Hill plot for chloride release mediated by compound **6.1** from EYPC LUVs loaded with 100 mM NaCl buffered to pH 6.4 with 10 mM phosphate buffer. The vesicles were dispersed in 100 mM $NaNO_3$ buffered to pH 6.4 with 10 mM phosphate buffer. Chloride efflux was measured 250 s after injection.
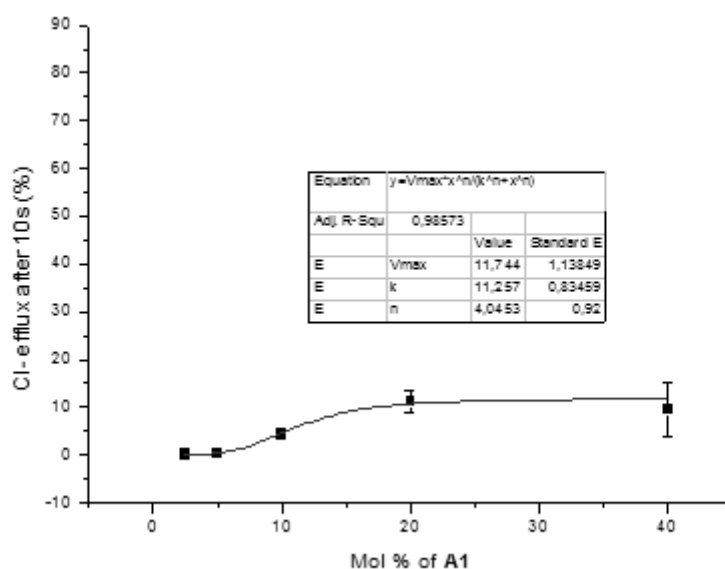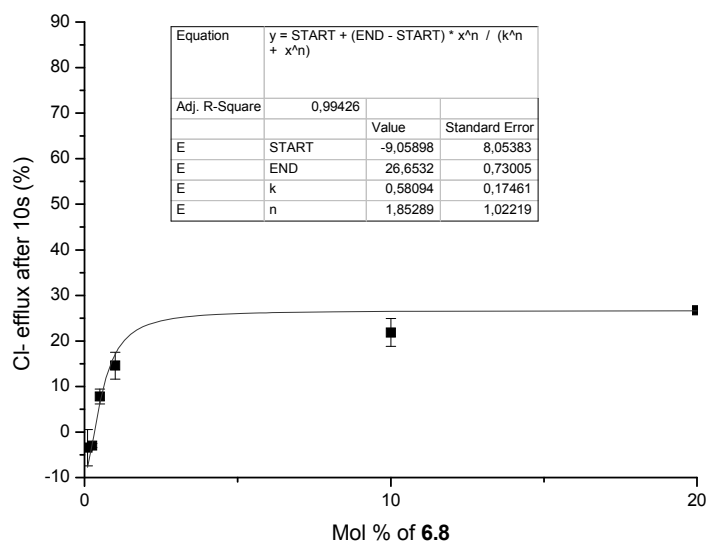
Supplementary figure S4.19. Hill plot for chloride release mediated by compound **6.1** from EYPC LUVs loaded with 100 mM NaCl buffered to pH 6.4 with 10 mM phosphate buffer. The vesicles were dispersed in 100 mM NaNO₃ buffered to pH 6.4 with 10 mM phosphate buffer. Chloride efflux was measured 10 s after injection.
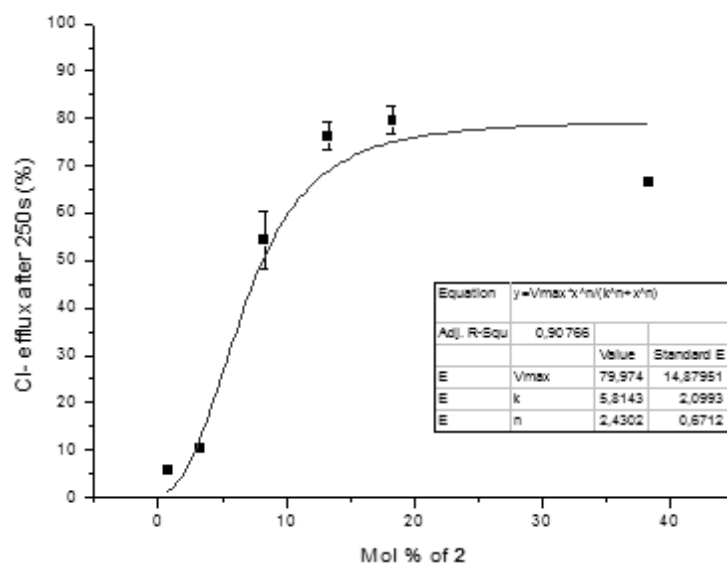
Supplementary figure S4.20. Hill plot for chloride release mediated by compound **6.2** from EYPC LUVs loaded with 100 mM NaCl buffered to pH 6.4 with 10 mM phosphate buffer. The vesicles were dispersed in 100 mM NaNO₃ buffered to pH 6.4 with 10 mM phosphate buffer. Chloride efflux was measured 10 s after injection.
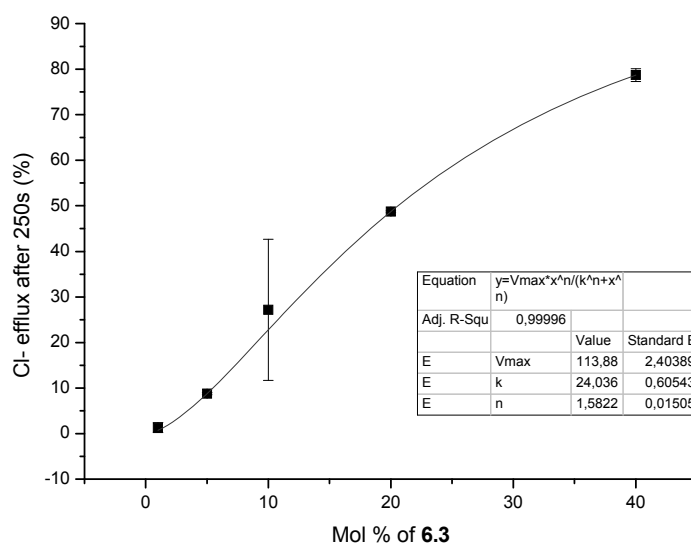
Supplementary figure S4.21. Hill plot for chloride release mediated by compound **6.3** from EYPC LUVs loaded with 100 mM NaCl buffered to pH 6.4 with 10 mM phosphate buffer. The vesicles were dispersed in 100 mM NaNO$_3$ buffered to pH 6.4 with 10 mM phosphate buffer. Chloride efflux was measured 250 s after injection.
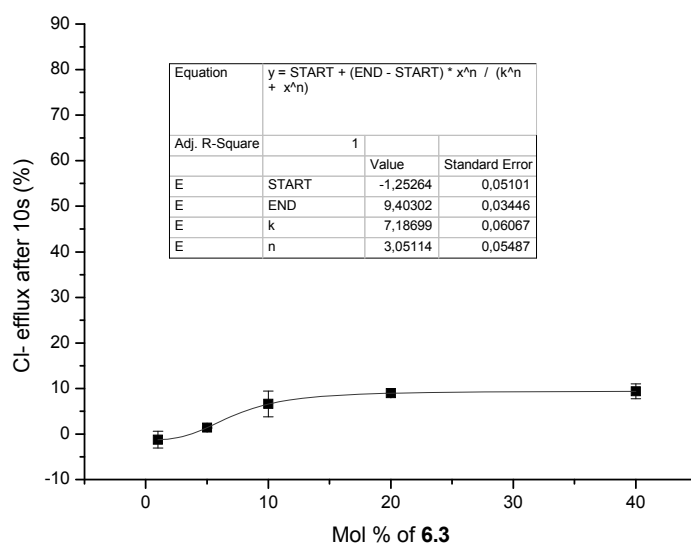

Supplementary figure S4.22. Hill plot for chloride release mediated by compound **6.3** from EYPC LUVs loaded with 100 mM NaCl buffered to pH 6.4 with 10 mM phosphate buffer. The vesicles were dispersed in 100 mM NaNO$_3$ buffered to pH 6.4 with 10 mM phosphate buffer. Chloride efflux was measured 10 s after injection.

Equation	y=Vmax*x^n/(k^n+x^n)	
Adj. R-Squa	0,988	
	Value	Standard Err
E	Vmax	95,4863	4,65033
E	k	6,90665	1,53346
E	n	1,94646	0,47761
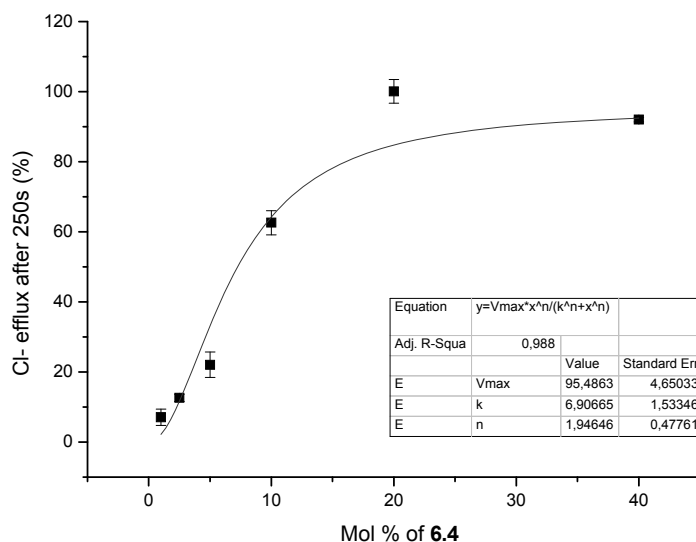
Supplementary figure S4.23. Hill plot for chloride release mediated by compound **6.4** from EYPC LUVs loaded with 100 mM NaCl buffered to pH 6.4 with 10 mM phosphate buffer. The vesicles were dispersed in 100 mM NaNO$_3$ buffered to pH 6.4 with 10 mM phosphate buffer. Chloride efflux was measured 250 s after injection.


Equation	y=Vmax*x^n/(k^n+x^n)	
Adj. R-Squ	0,9972	
	Value	Standard E
E	Vmax	68,081	13,75655
E	k	30,136	11,36843
E	n	1	0,09583
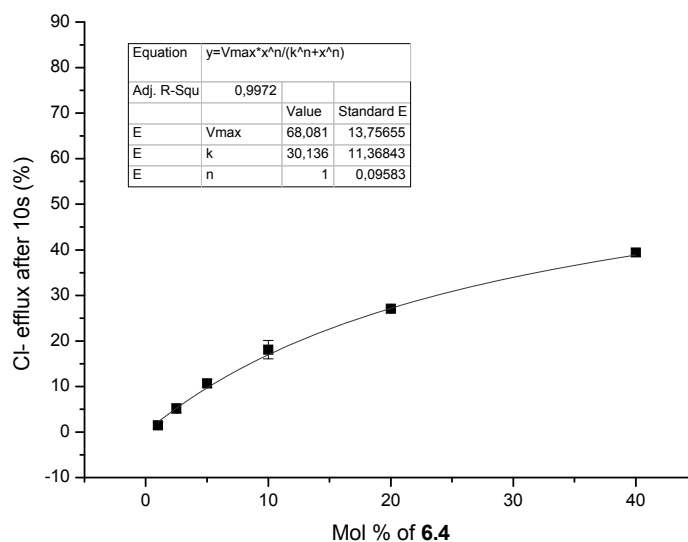
Supplementary figure S4.24. Hill plot for chloride release mediated by compound **6.4** from EYPC LUVs loaded with 100 mM NaCl buffered to pH 6.4 with 10 mM phosphate buffer. The vesicles were dispersed in 100 mM NaNO$_3$ buffered to pH 6.4 with 10 mM phosphate buffer. Chloride efflux was measured 10 s after injection.
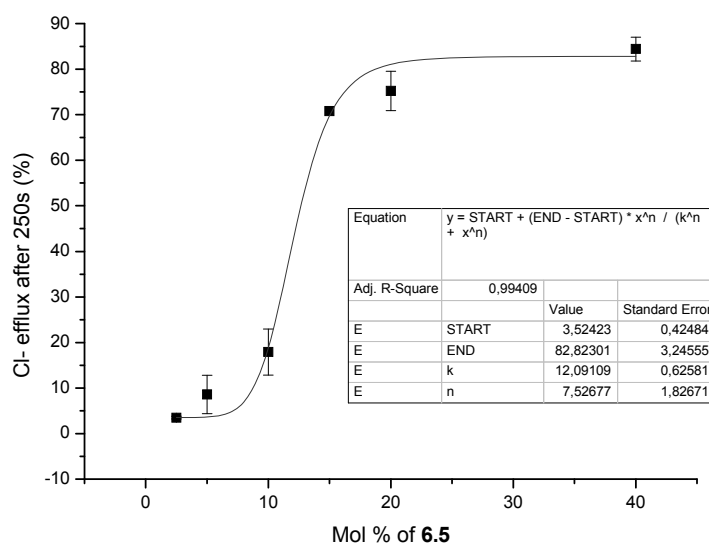
Supplementary figure S4.25. Hill plot for chloride release mediated by compound **6.5** from EYPC LUVs loaded with 100 mM NaCl buffered to pH 6.4 with 10 mM phosphate buffer. The vesicles were dispersed in 100 mM NaNO$_3$ buffered to pH 6.4 with 10 mM phosphate buffer. Chloride efflux was measured 250 s after injection.
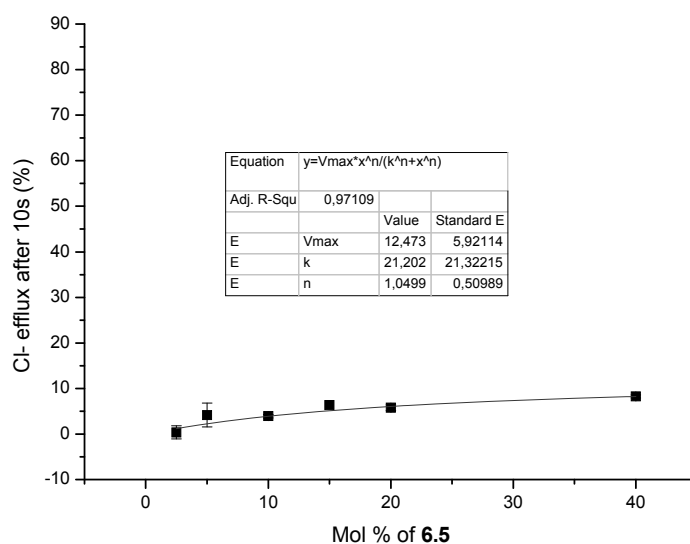
Supplementary figure S4.26. Hill plot for chloride release mediated by compound **6.5** from EYPC LUVs loaded with 100 mM NaCl buffered to pH 6.4 with 10 mM phosphate buffer. The vesicles were dispersed in 100 mM NaNO$_3$ buffered to pH 6.4 with 10 mM phosphate buffer. Chloride efflux was measured 10 s after injection.
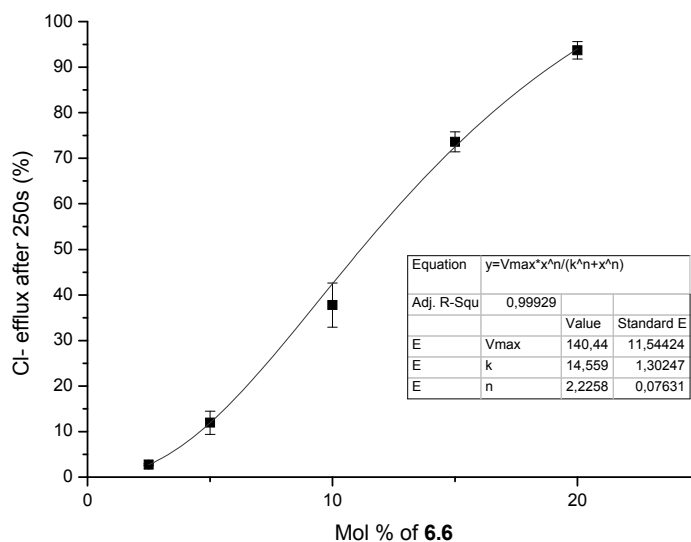
Supplementary figure S4.27. Hill plot for chloride release mediated by compound **6.6** from EYPC LUVs loaded with 100 mM NaCl buffered to pH 6.4 with 10 mM phosphate buffer. The vesicles were dispersed in 100 mM NaNO$_3$ buffered to pH 6.4 with 10 mM phosphate buffer. Chloride efflux was measured 250 s after injection.
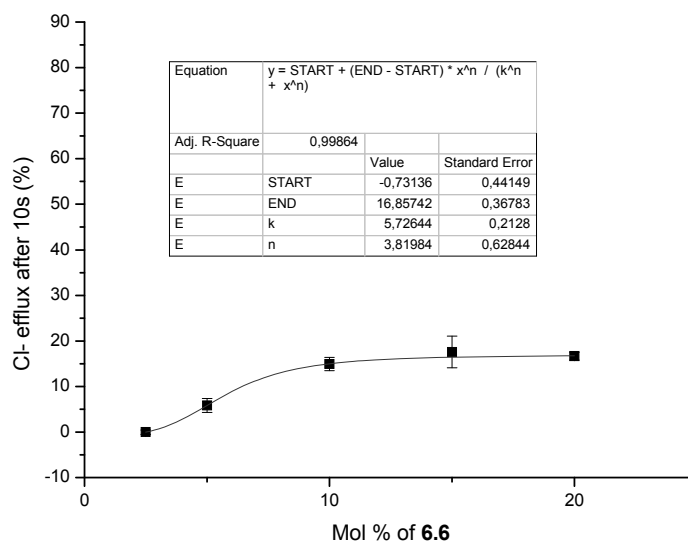
Supplementary figure S4.28. Hill plot for chloride release mediated by compound **6.6** from EYPC LUVs loaded with 100 mM NaCl buffered to pH 6.4 with 10 mM phosphate buffer. The vesicles were dispersed in 100 mM NaNO$_3$ buffered to pH 6.4 with 10 mM phosphate buffer. Chloride efflux was measured 10 s after injection.
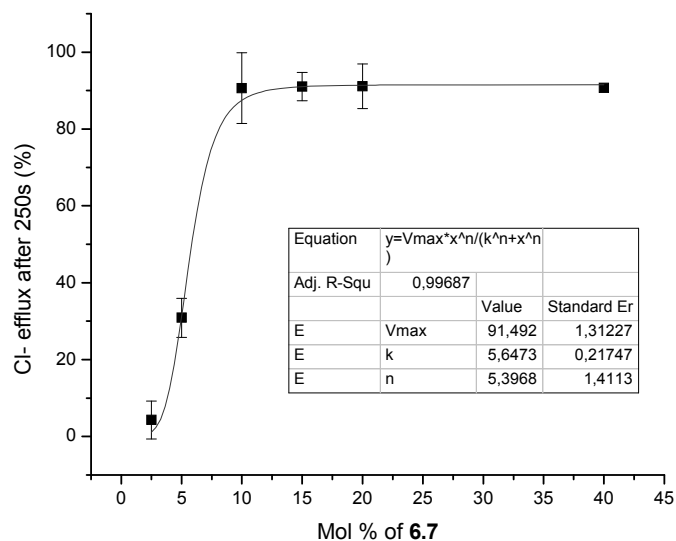
Supplementary figure S4.29. Hill plot for chloride release mediated by compound **6.7** from EYPC LUVs loaded with 100 mM NaCl buffered to pH 6.4 with 10 mM phosphate buffer. The vesicles were dispersed in 100 mM NaNO$_3$ buffered to pH 6.4 with 10 mM phosphate buffer. Chloride efflux was measured 250 s after injection.
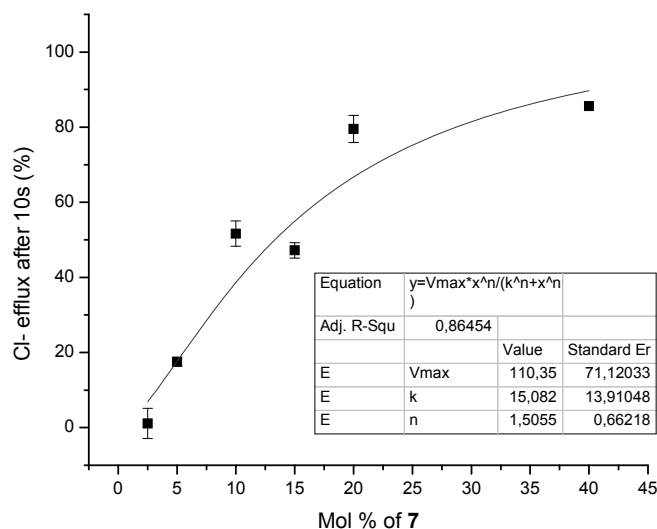
Supplementary figure S4.30. Hill plot for chloride release mediated by compound **6.7** from EYPC LUVs loaded with 100 mM NaCl buffered to pH 6.4 with 10 mM phosphate buffer. The vesicles were dispersed in 100 mM NaNO$_3$ buffered to pH 6.4 with 10 mM phosphate buffer. Chloride efflux was measured 250 s after injection.

Supplementary figure S4.31. Hill plot for chloride release mediated by compound **6.8** from EYPC LUVs loaded with 100 mM NaCl buffered to pH 6.4 with 10 mM phosphate buffer. The vesicles were dispersed in 100 mM $NaNO_3$ buffered to pH 6.4 with 10 mM phosphate buffer. Chloride efflux was measured 250 s after injection.

Supplementary figure S4.32. Hill plot for chloride release mediated by compound **6.8** from EYPC LUVs loaded with 100 mM NaCl buffered to pH 6.4 with 10 mM phosphate buffer. The vesicles were dispersed in 100 mM $NaNO_3$ buffered to pH 6.4 with 10 mM phosphate buffer. Chloride efflux was measured 10 s after injection.

U-tube experiment
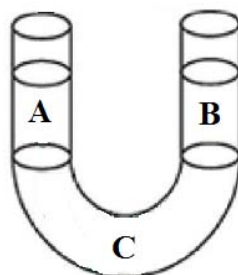
Supplementary figure S4.33. U-tube experiment scheme. A: Aqueous donating phase containing 0.1 mM Lucigenin (water, 5 mL). B: Receiving phase (water, 5 mL). C: Bulk organic phase ($CHCl_3$, 10 mL) with ionophore (1mM) or without.
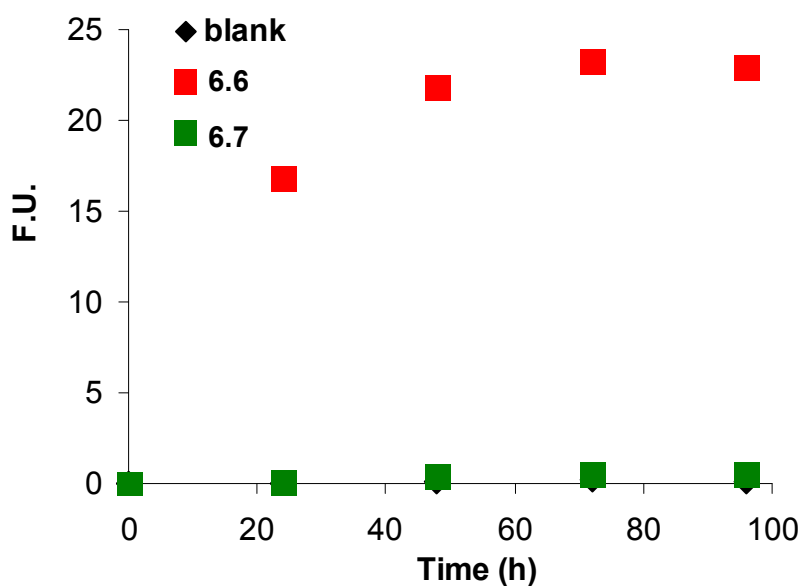
Supplementary figure S4.34. Increase of the lucigenin's fluorescence in U-tube tests in the presence of compounds **6.6**, **6.7** and the blank.
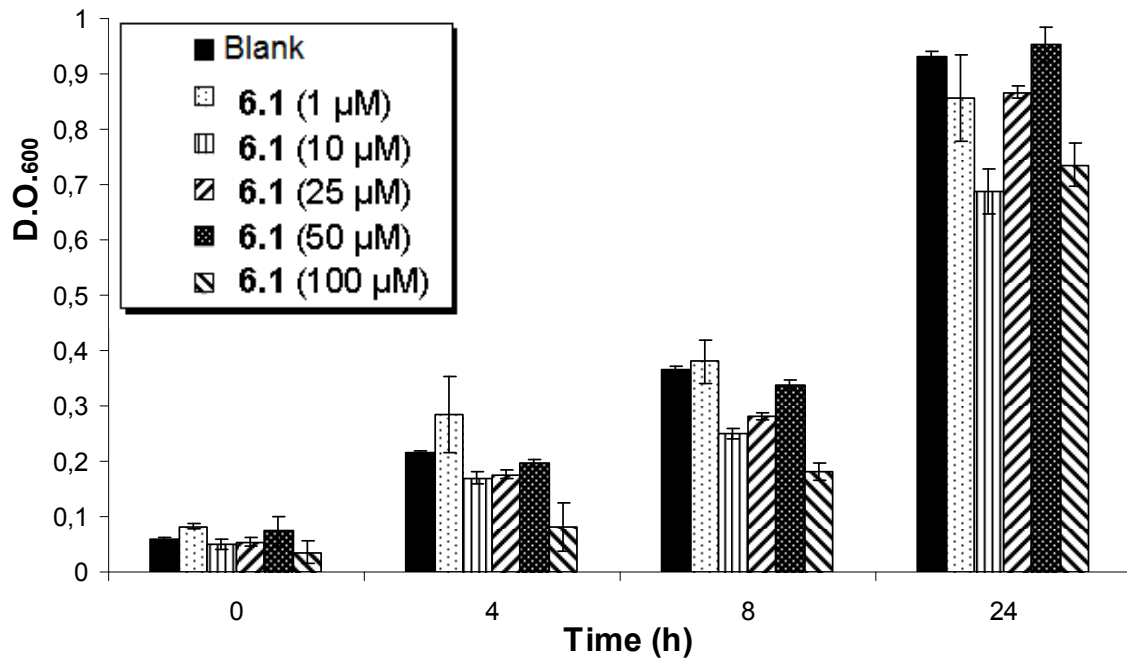
Supplementary figure S4.35. Dose-dependent growth inhibition of *E. coli (DH5α)* by **6.1**.
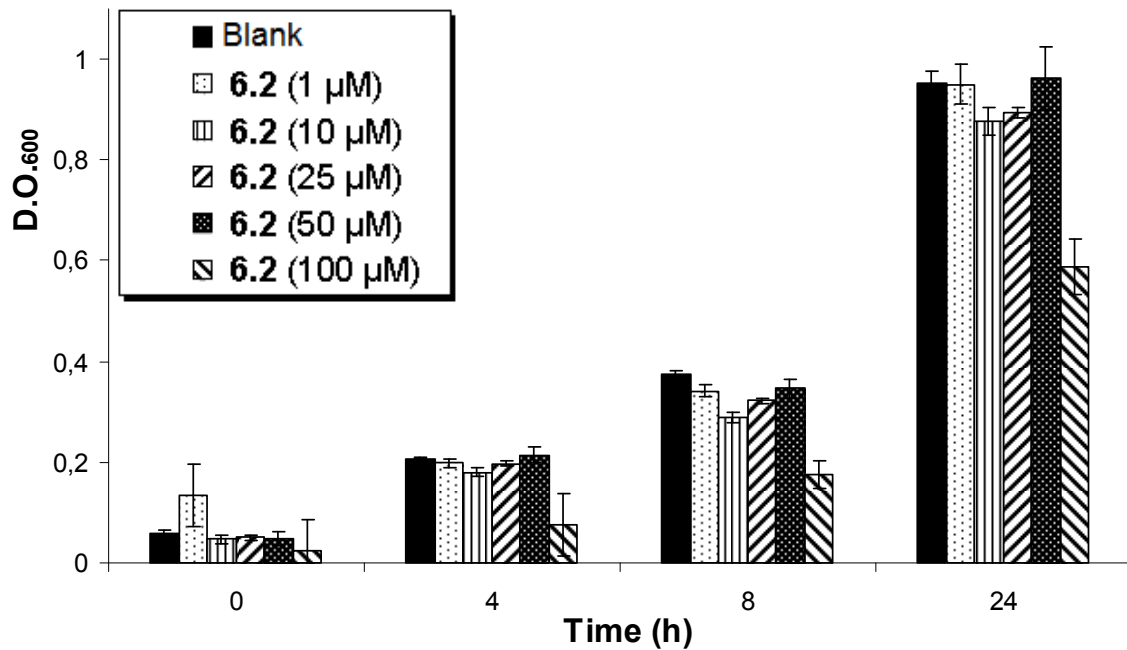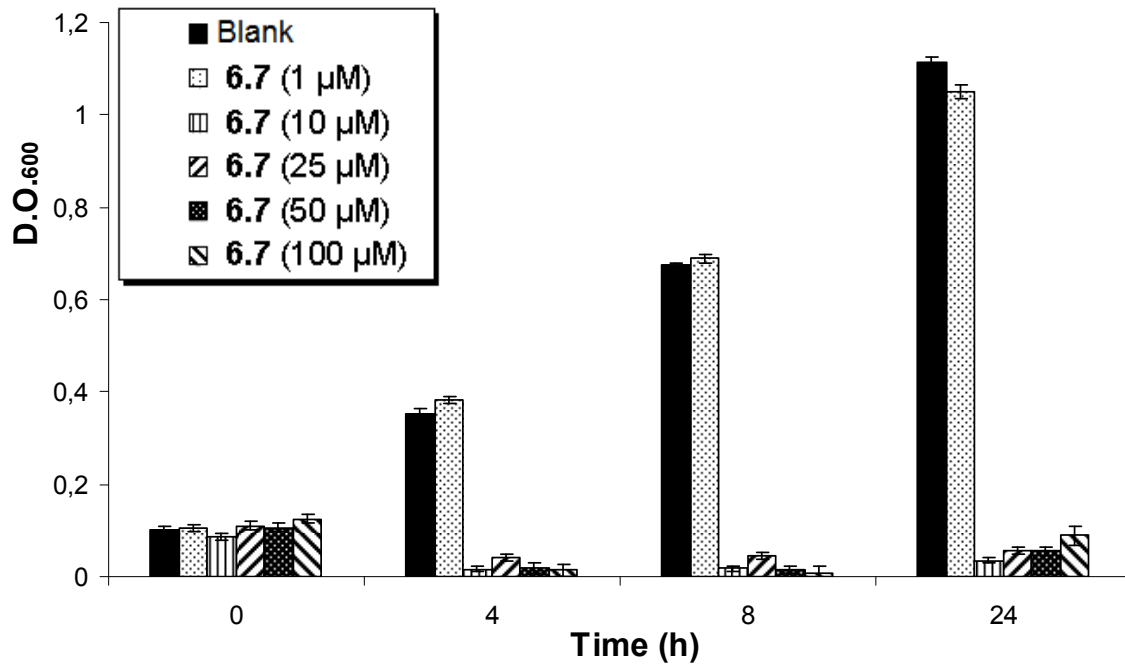

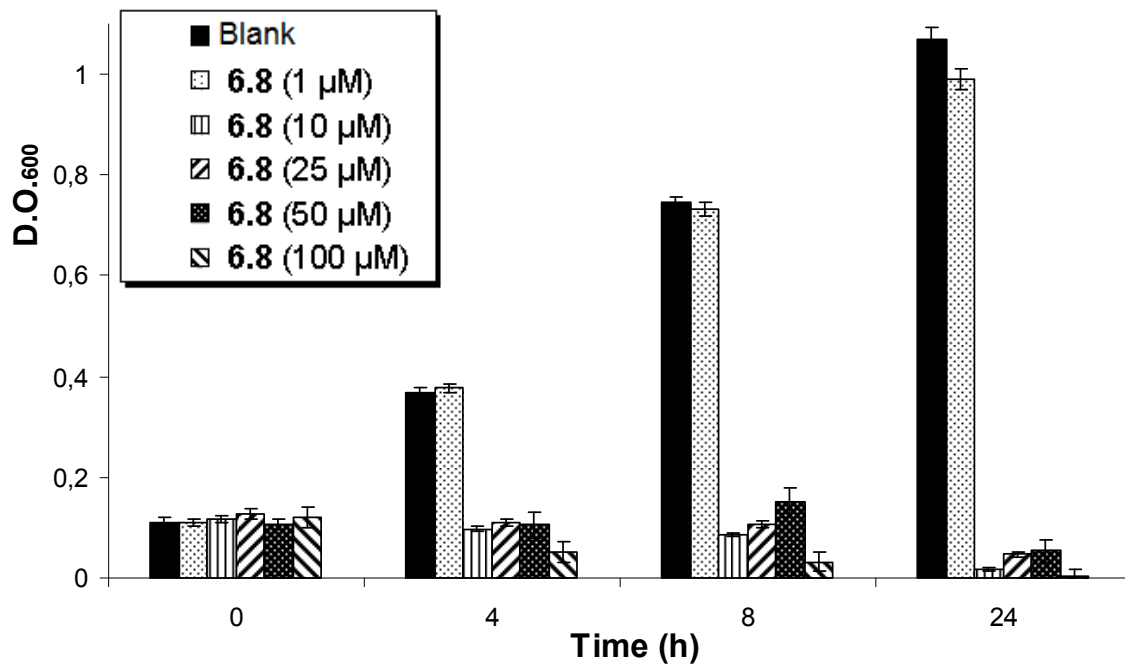**Supplementary figure S4.36.** Dose-dependent growth inhibition of *E. coli (DH5α)* by **6.2**.
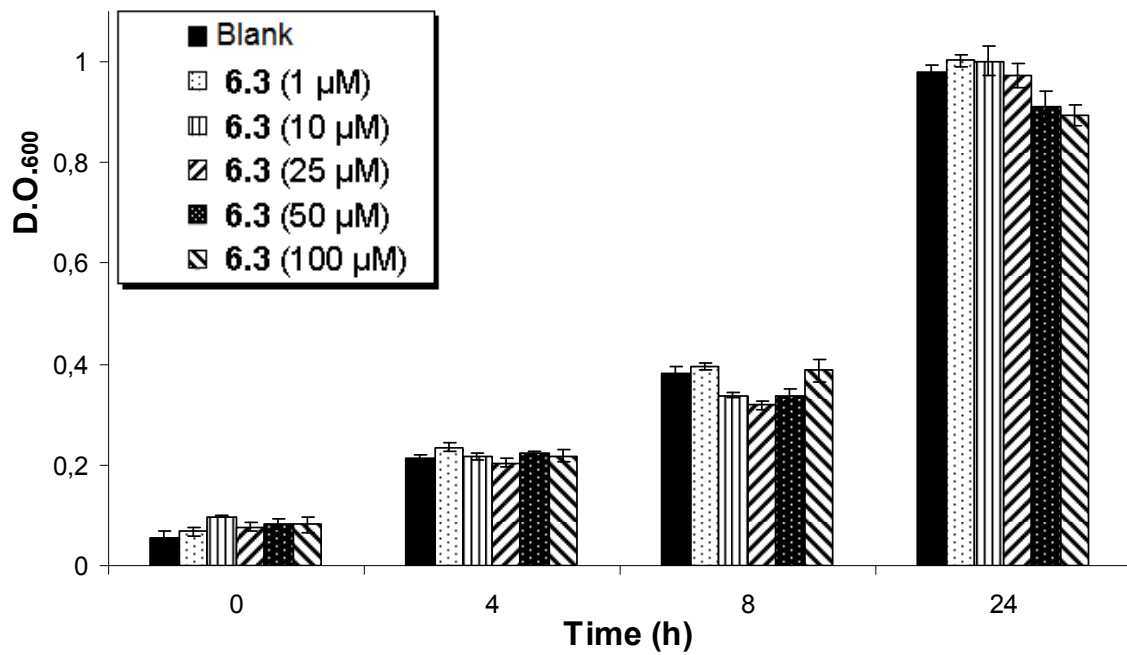
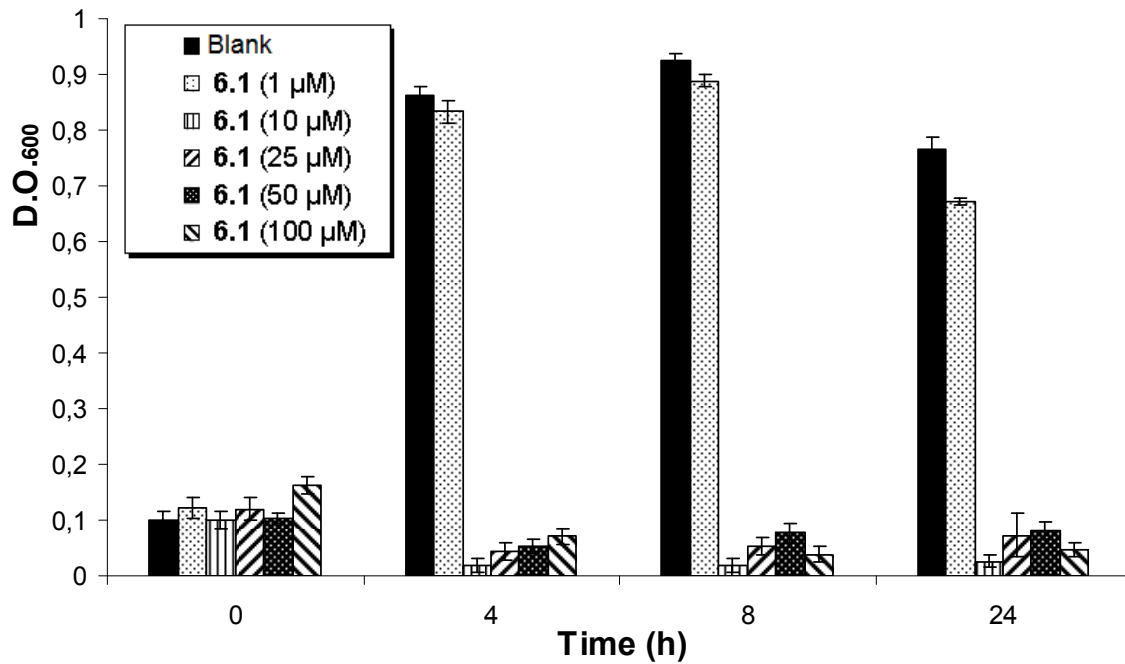**Supplementary figure S4.37.** Dose-dependent growth inhibition of *E. coli (DH5α)* by **6.3**.
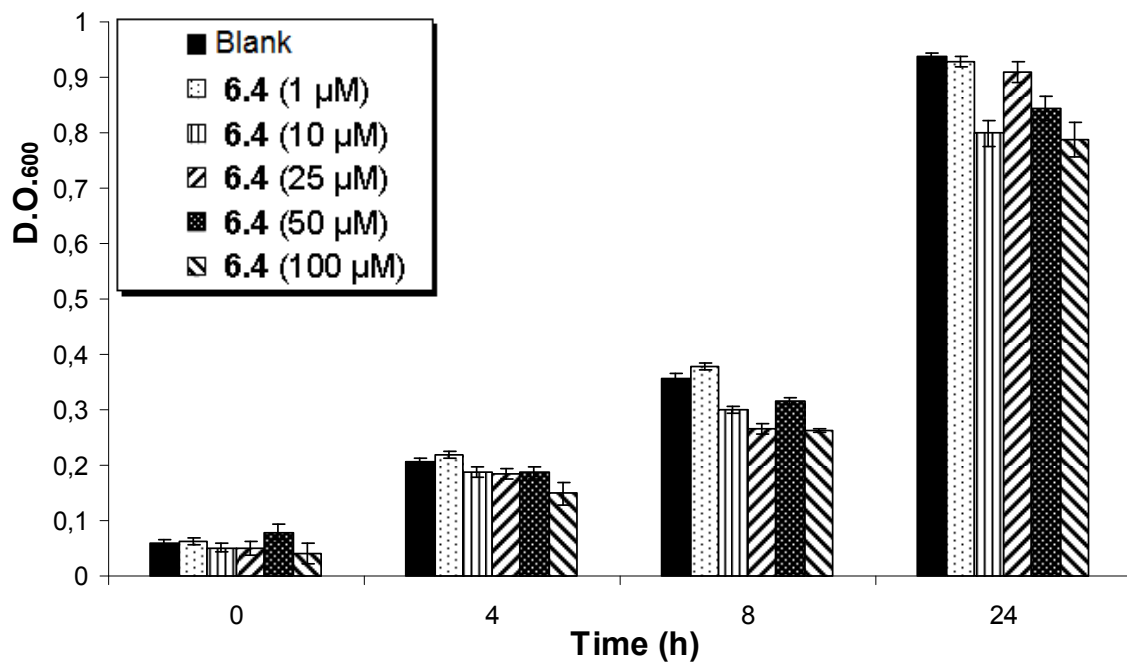
Supplementary figure S4.38. Dose-dependent growth inhibition of *E. coli (DH5α)* by **6.4**.
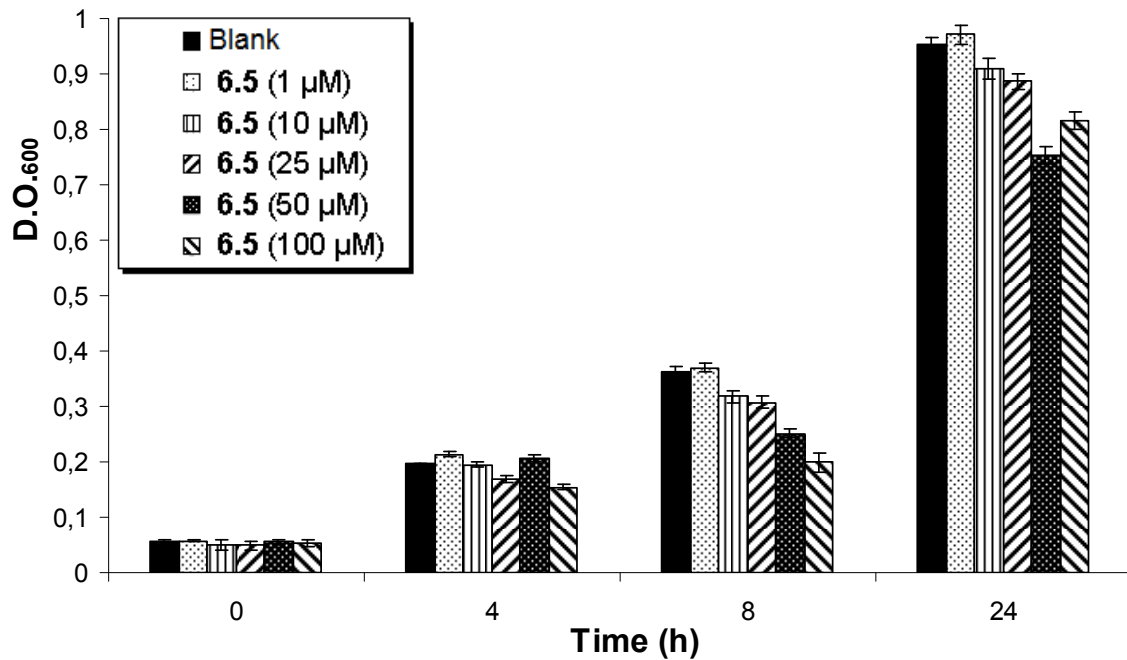
Supplementary figure S4.39. Dose-dependent growth inhibition of *E. coli (DH5α)* by **6.5**.
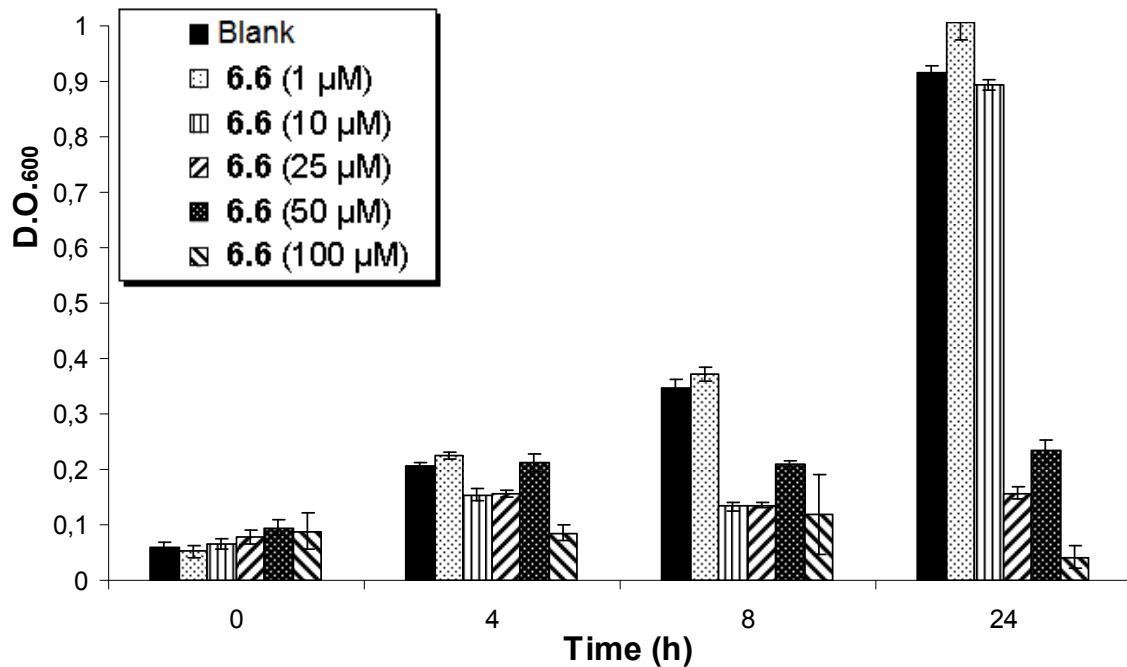
Supplementary figure S4.40. Dose-dependent growth inhibition of *E. coli (DH5α)* by **6.6**.
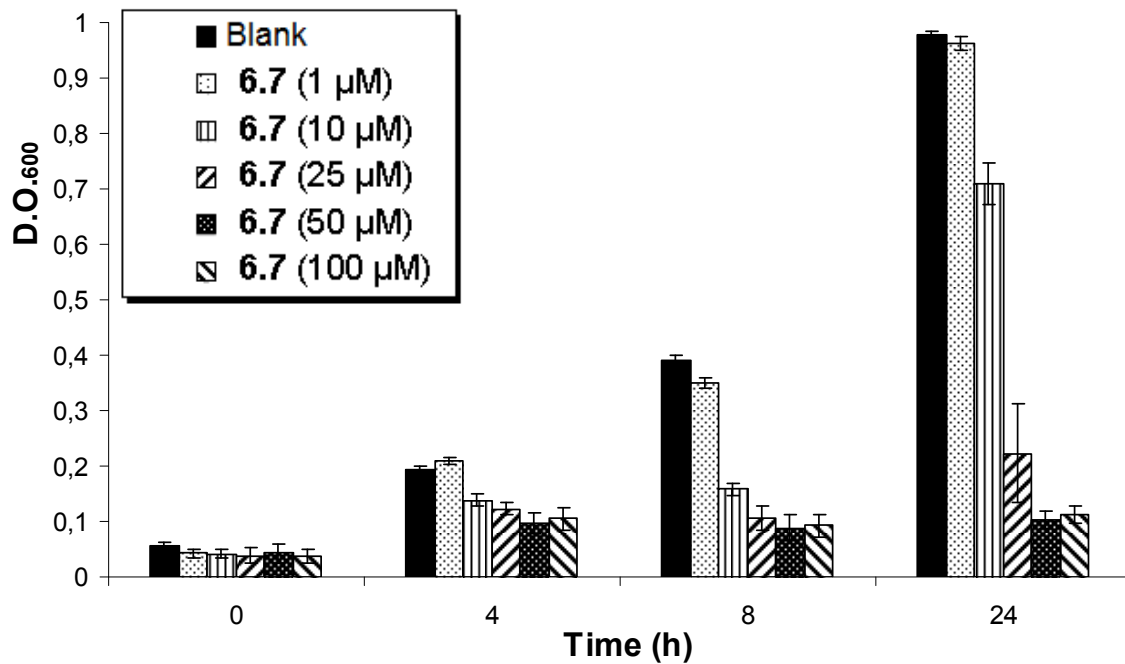
Supplementary figure S4.41. Dose-dependent growth inhibition of *E. coli (DH5α)* by **6.7**.
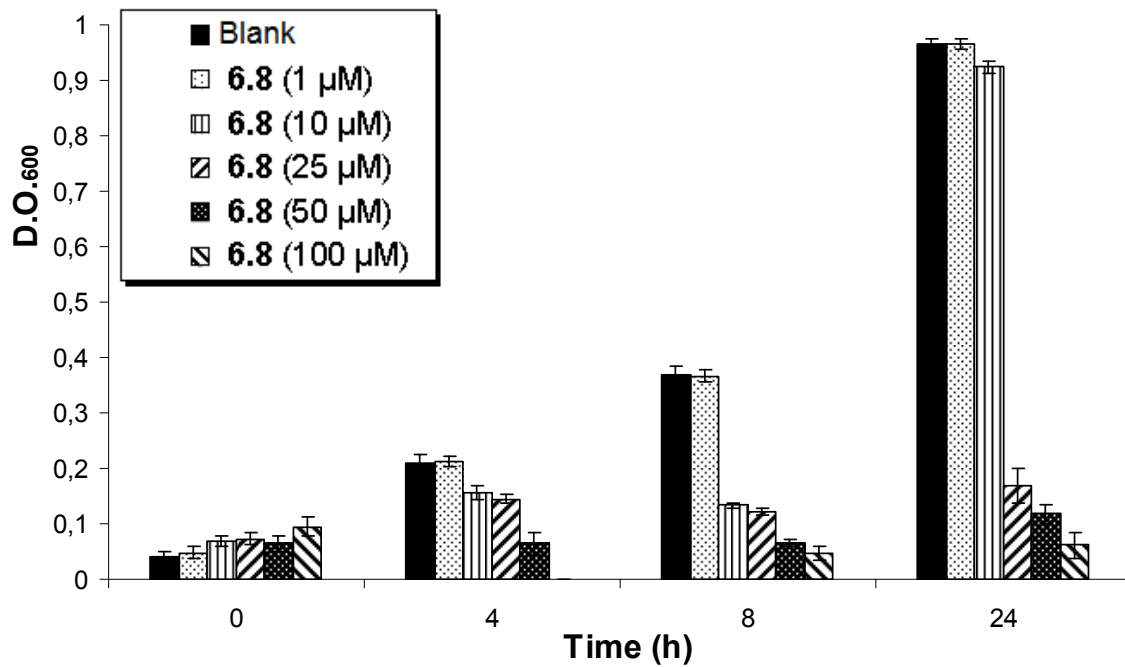
Supplementary figure S4.42. Dose-dependent growth inhibition of *E. coli (DH5α)* by **6.8**.
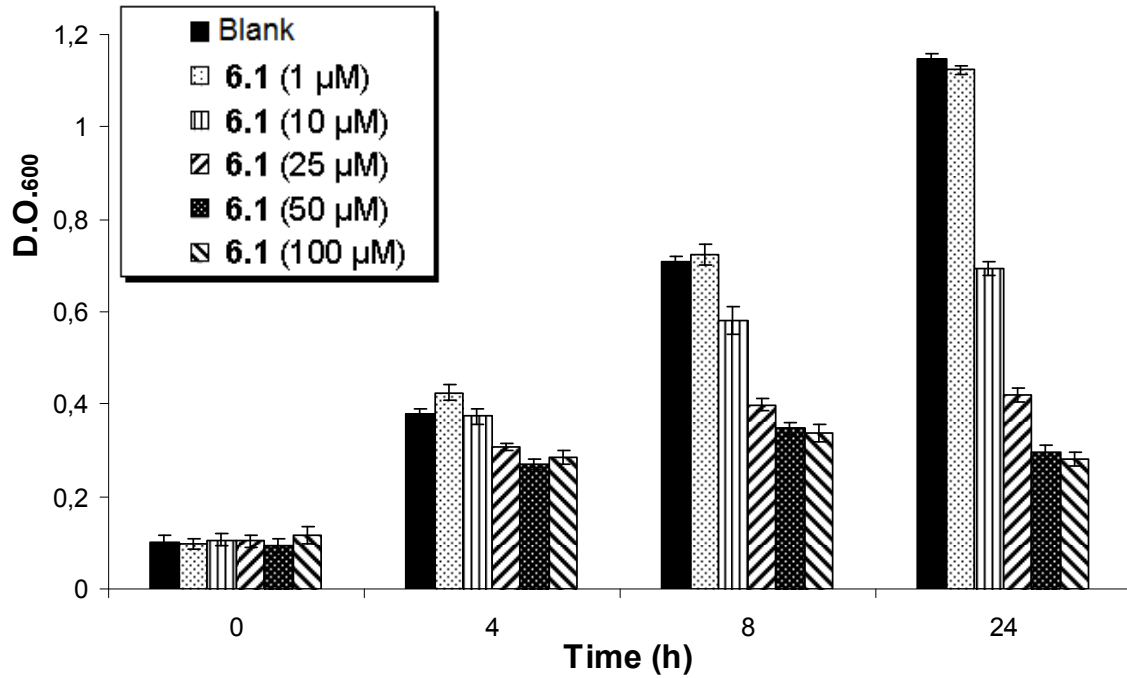
Supplementary figure S4.43. Dose-dependent growth inhibition of *E. coli (SK037)* by **6.1**.
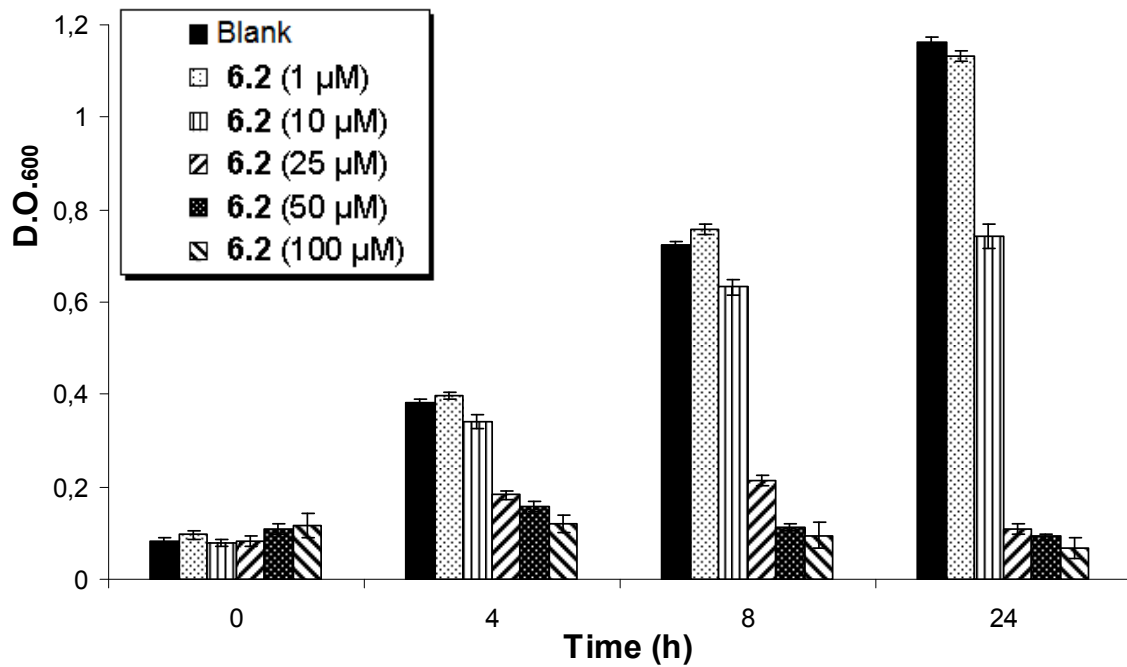
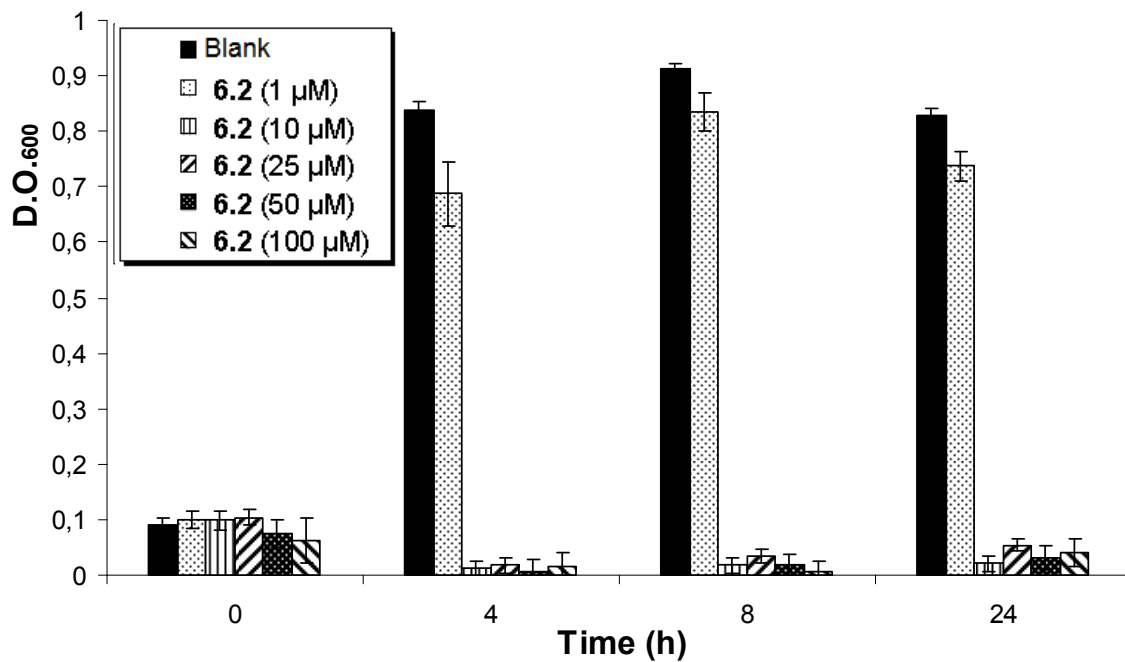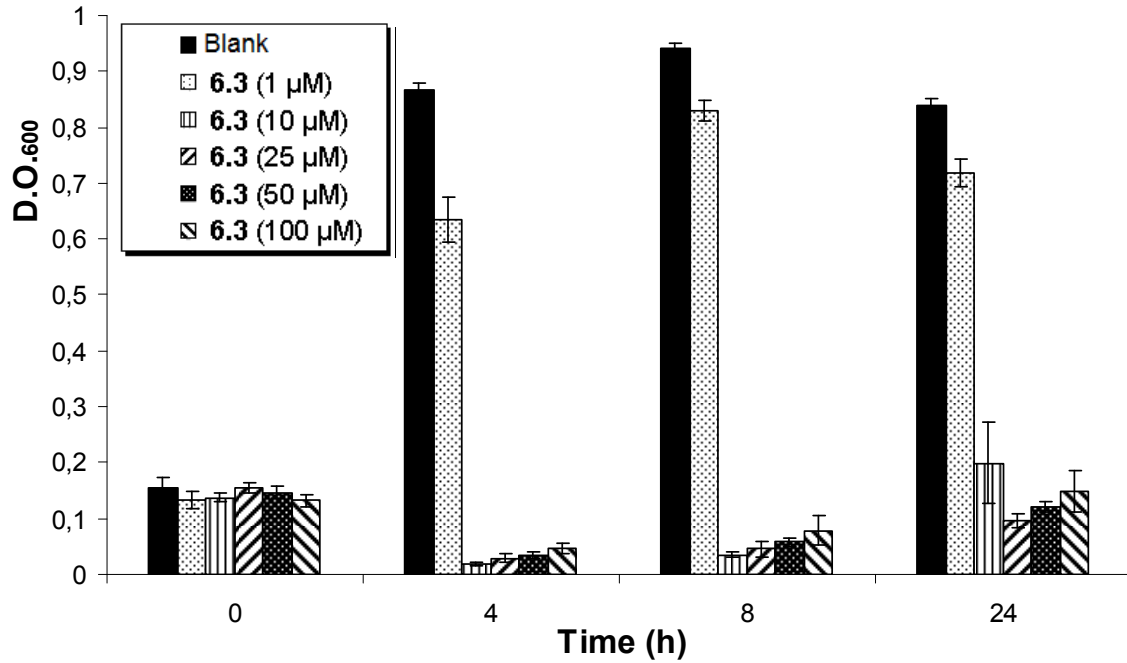**Supplementary figure S4.44.** Dose-dependent growth inhibition of *E. coli (SK037)* by **6.2**.
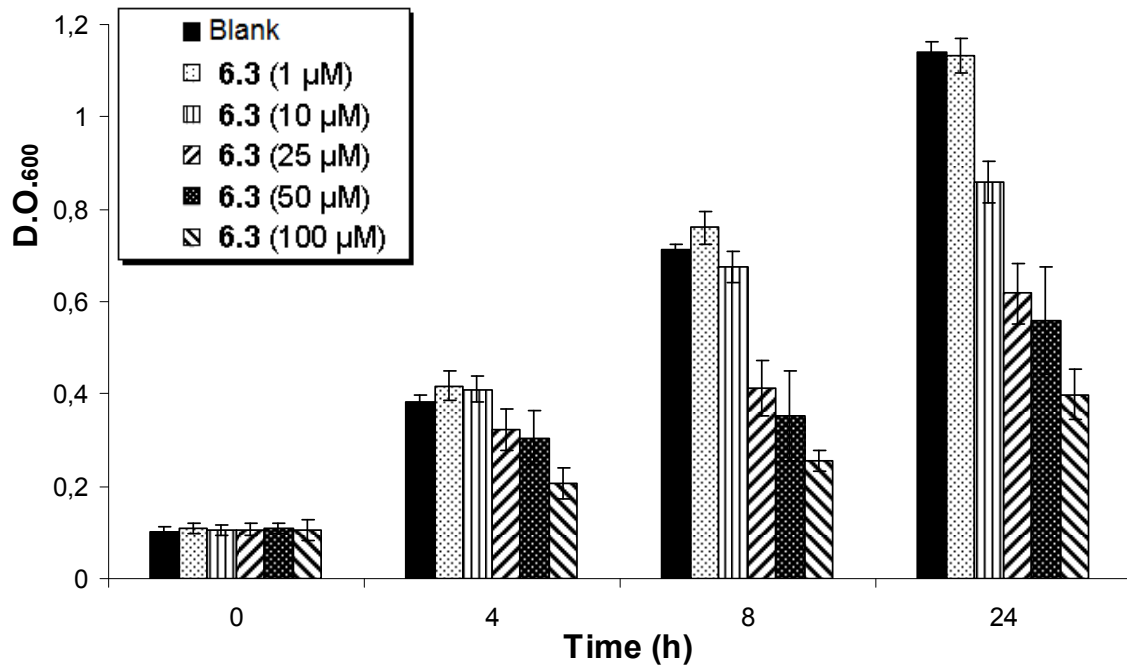
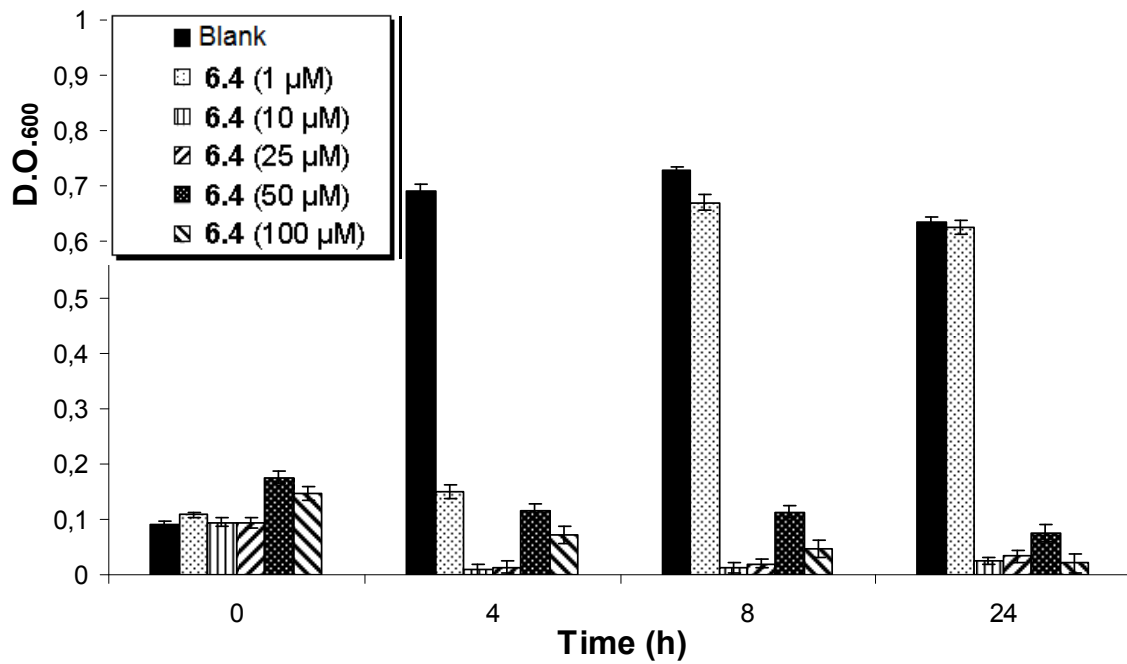**Supplementary figure S4.45.** Dose-dependent growth inhibition of *E. coli (SK037)* by **6.3**.
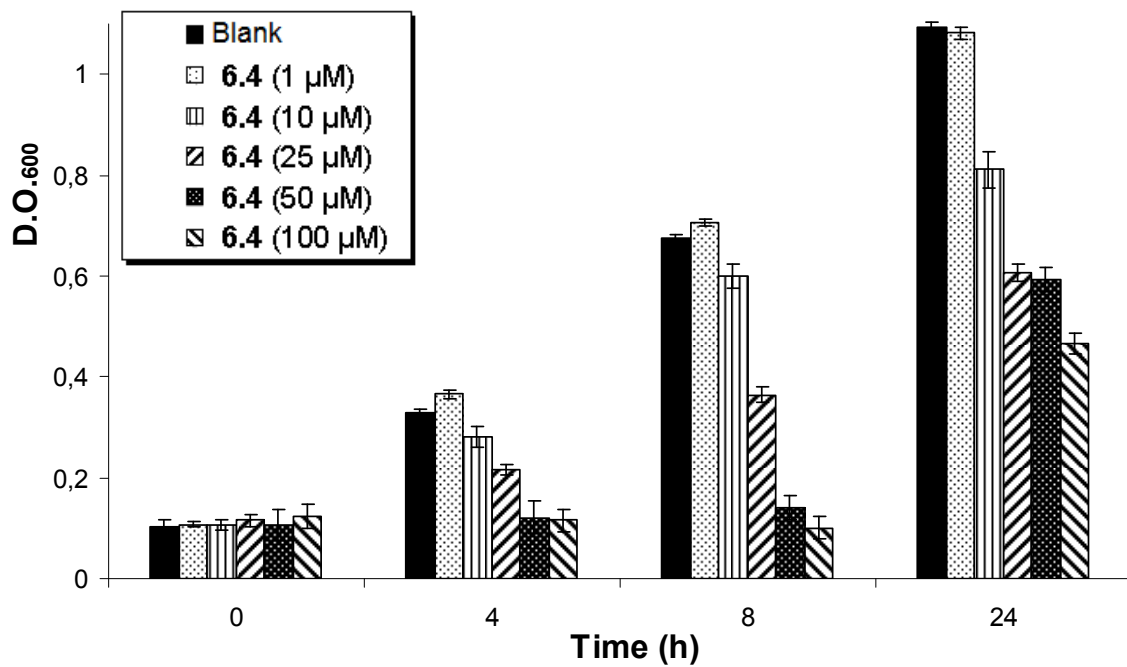
Supplementary figure S4.46. Dose-dependent growth inhibition of *E. coli (SK037)* by **6.4**.
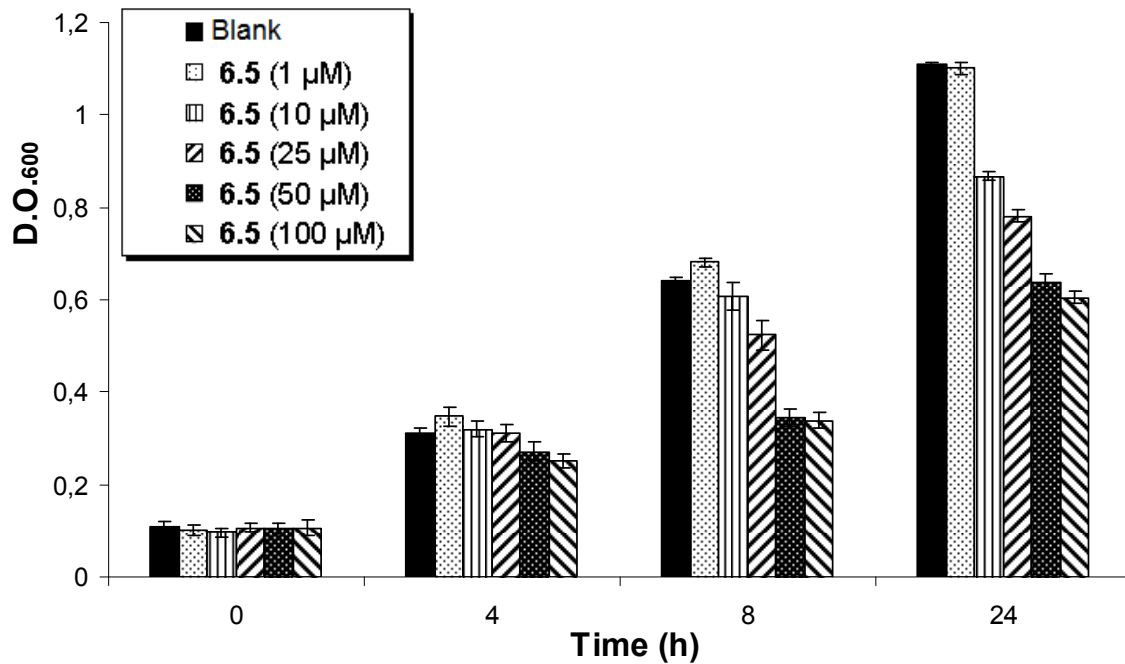
Supplementary figure S4.47. Dose-dependent growth inhibition of *E. coli (SK037)* by **6.5**.
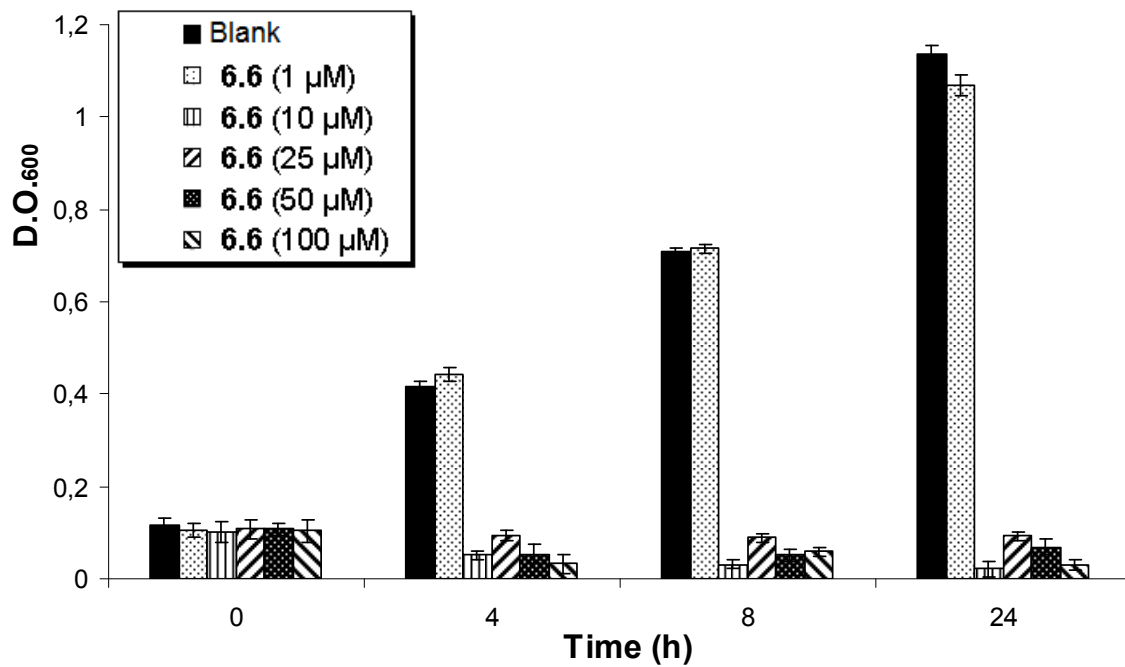
Supplementary figure S4.48. Dose-dependent growth inhibition of *E. coli (SK037)* by **6.6**.

Supplementary figure S4.49. Dose-dependent growth inhibition of *E. coli (SK037)* by **6.7**.

Supplementary figure S4.50. Dose-dependent growth inhibition of *E. coli (SK037)* by **6.8**.

Supplementary figure S4.51. Dose-dependent growth inhibition of *B. thuringiensis (HD73)* by **6.1**.

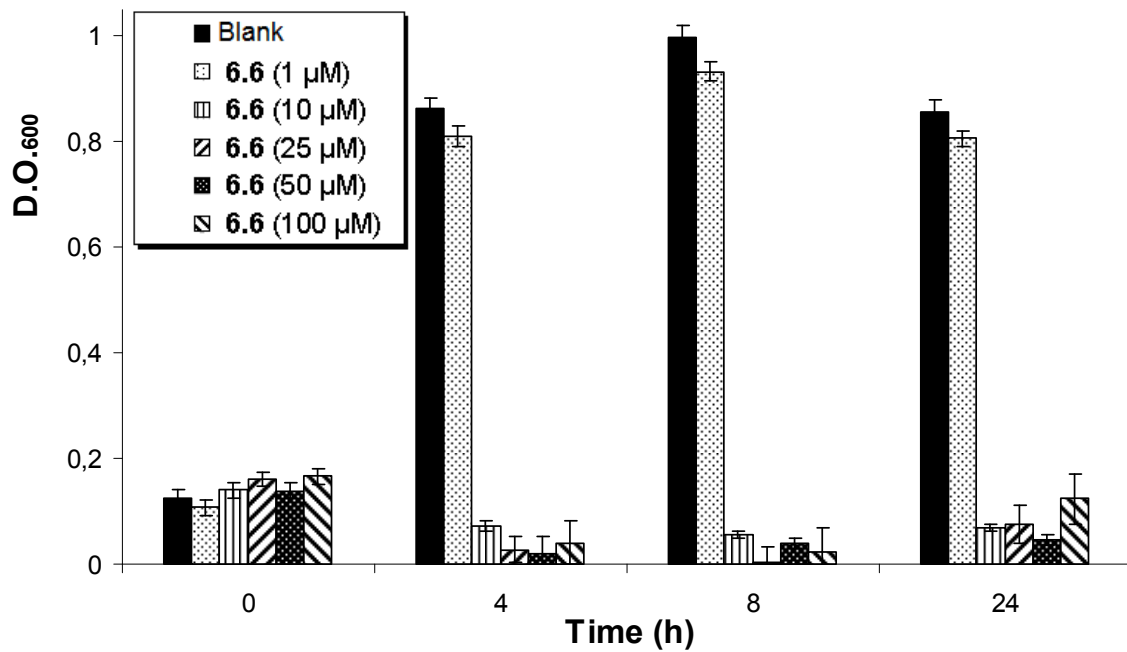**Supplementary figure S4.52.** Dose-dependent growth inhibition of *B. thuringiensis (HD73)* by **6.2**.

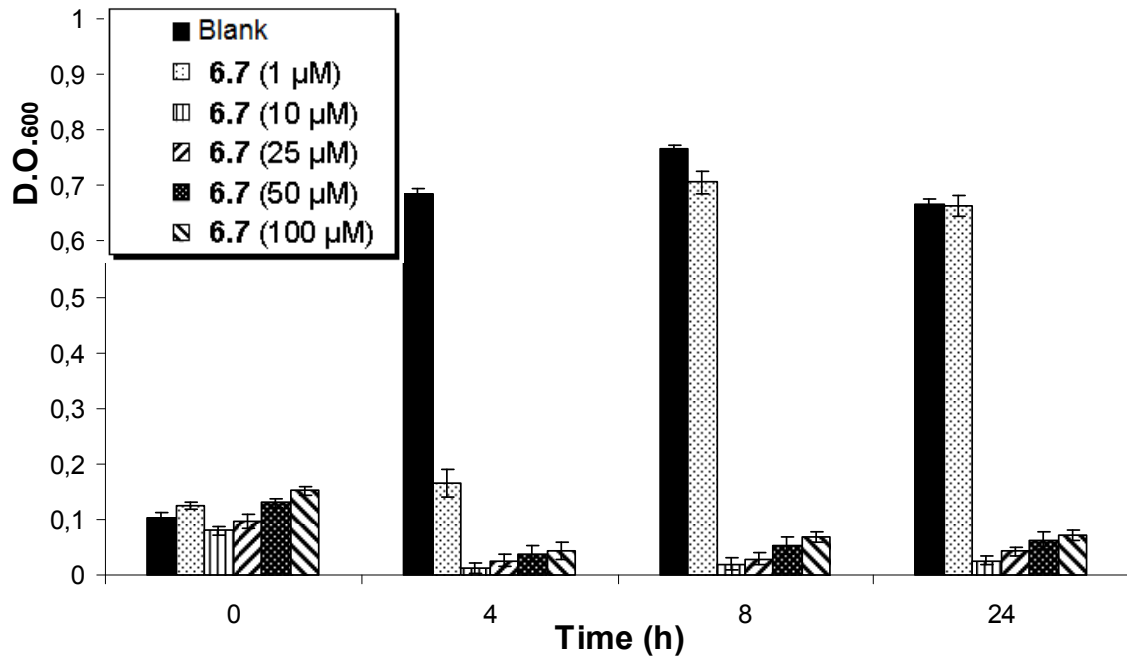**Supplementary figure S4.53.** Dose-dependent growth inhibition of *B. thuringiensis (HD73)* by **6.3**.

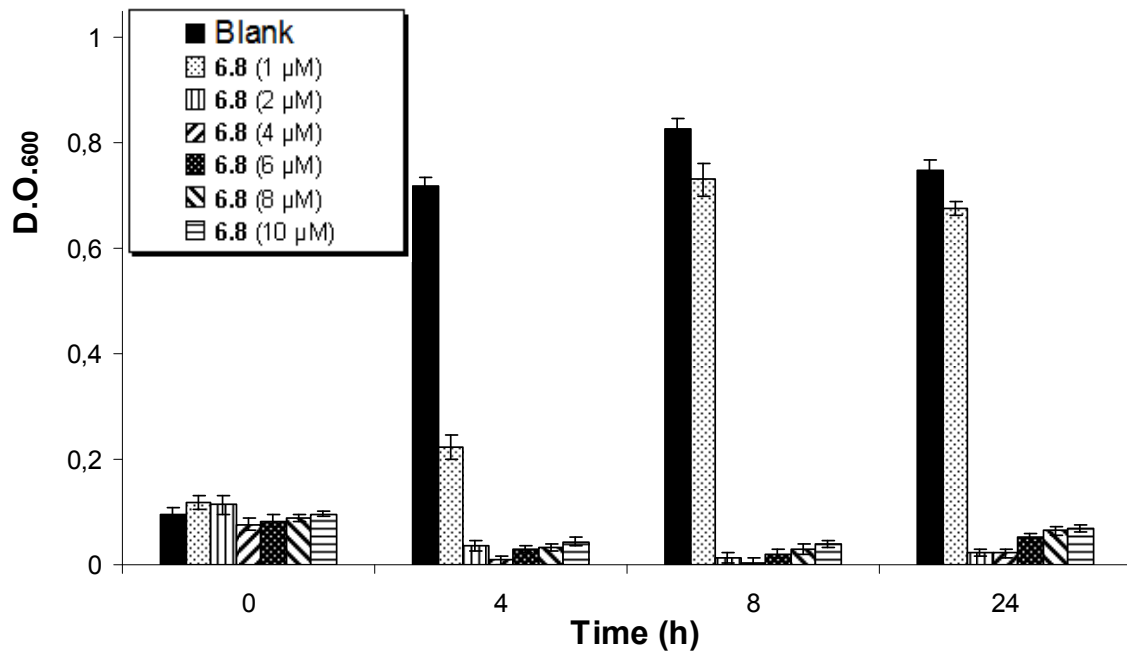**Supplementary figure S4.54.** Dose-dependent growth inhibition of *B. thuringiensis (HD73)* by **6.4**.
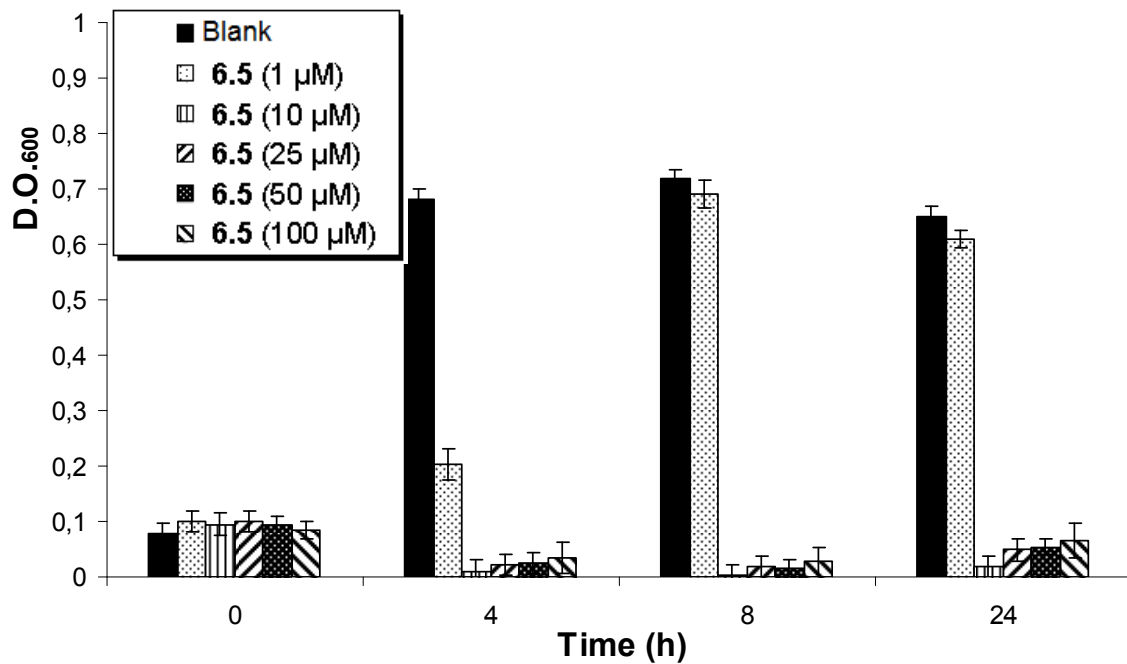
Supplementary figure S4.55. Dose-dependent growth inhibition of *B. thuringiensis (HD73)* by **6.5**.

Supplementary figure S4.56. Dose-dependent growth inhibition of *B. thuringiensis (HD73)* by **6.6**.

Supplementary figure S4.57. Dose-dependent growth inhibition of *B. thuringiensis (HD73)* by **6.7**.

Supplementary figure S4.58. Dose-dependent growth inhibition of *B. thuringiensis (HD73)* by **6.8**